

University of Alberta

The Discovery and Characterization of Rigid Amphipathic Fusion
Inhibitors (RAFIs), a Novel Class of Broad-Spectrum Antiviral Compounds

by

Mireille Renée Marie St.Vincent

A thesis submitted to the Faculty of Graduate Studies and Research
in partial fulfillment of the requirements for the degree of

Doctor of Philosophy

Department of Biochemistry

©Mireille Renée Marie St.Vincent

Spring 2012
Edmonton, Alberta

Permission is hereby granted to the University of Alberta Libraries to reproduce single copies of this thesis and to lend or sell such copies for private, scholarly or scientific research purposes only. Where the thesis is converted to, or otherwise made available in digital form, the University of Alberta will advise potential users of the thesis of these terms.

The author reserves all other publication and other rights in association with the copyright in the thesis and, except as herein before provided, neither the thesis nor any substantial portion thereof may be printed or otherwise reproduced in any material form whatsoever without the author's prior written permission.

This thesis is dedicated to my son, Maksim.

Merci mon grand, qui a tant sacrifié afin que maman puisse rédiger ce texte!

Je t'aime.

ABSTRACT

Antiviral drugs targeting viral proteins or their interactions with cellular proteins lead to rapid selection for resistance. Moreover, the number of viral targets is limited. Novel antiviral targets are needed. The unique characteristics of fusion between virion envelopes and cell membranes may provide such targets. Like all fusing bilayers, virion envelopes must locally convert to negative curvature to form hourglass-shaped hemifusion stalks. Unlike cellular vesicles, virion envelopes fuse to the outer leaflets of cell membranes without lipid redistribution between leaflets, and using only the energy released by glycoprotein binding and rearrangement. Enrichment in inverted-cone shaped lysophospholipids in the outer leaflet of vesicles disfavors negative curvature, inhibiting fusion. Such lipids, however, are toxic and not pharmacologically useful.

My hypothesis is that pharmacologically useful small amphipathic molecules of appropriate shape (hydrophilic region of larger crosssection than the hydrophobic one) can intercalate within virion lipids, inhibiting the formation of the negative curvature required for fusion of all enveloped viruses.

Herein, I report the discovery and characterization of the novel antiviral mechanisms of a novel family of rigid amphipathic nucleosides. One such compound, dUY11, disfavors the formation of the required negative curvature. Exposure to dUY11 inhibits the infectivity of several otherwise unrelated enveloped viruses (IC_{50} , 50 nM), including hepatitis C and genital herpes virus. dUY11 has no major cytotoxic/static effects ($SI > 1,800$). dUY11 does not inhibit viral DNA replication, but inhibits infectivity produced by cells treated after

infection, even with acyclovir or phosphonoacetic acid resistant strains. The targets of dUY11 are not encoded in the viral genomes. Consistently, resistance to dUY11 has not been detected.

This thesis serves as proof-of-concept that small molecule fusion inhibitors targeting envelope bilayer curvature are viable antiviral strategies. These strategies may help in overcoming the limitations of clinical antivirals, including narrow specificity and rapid resistance selection. dUY11 inhibits infection and acts extracellularly, highly desirable properties for microbicides. dUY11 has therapeutic potential, too, targeting and inhibiting functions conserved among all otherwise unrelated enveloped viruses. The novel antiviral mechanisms of action presented herein may impact future development of prophylactic and therapeutic antivirals.

ACKNOWLEDGEMENTS

I would first like to thank my supervisor, Dr. Luis M. Schang, for being an exceptional mentor, as well as the members of my supervisory committee, Dr. Charles Holmes and Dr. David Evans, who monitored my progress throughout the years and provided helpful discussions along the way. I would also like to sincerely thank my external examiners, Dr. François Jean and Dr. Lorne Tyrrell.

The work described in this thesis would not have been possible without the expertise of our collaborators, in particular Dr. Alexey Ustinov, Dr. Richard Epanand and Dr. Rachel Epanand, as well as many others who provided reagents for these studies.

I would also like to acknowledge the generous support I have received from the Natural Sciences and Engineering Research Council of Canada (Alexander Graham Bell Canada Graduate Scholarship), as well as my family, friends and co-workers.

TABLE OF CONTENTS

CHAPTER 1: INTRODUCTION	1
1.1 Antiviral strategies.....	1
1.1.1 Antiviral drugs.....	1
1.1.1.1 Clinical antiviral chemotherapies	2
1.1.1.1.1 Drugs targeting viral-encoded functions.....	2
1.1.1.1.1.1 Drugs targeting viral genome replication.....	2
1.1.1.1.1.2 Drugs targeting viral integration.....	6
1.1.1.1.1.3 Drugs targeting viral gene expression.....	7
1.1.1.1.1.4 Drugs targeting viral assembly, maturation and release	7
1.1.1.1.1.4.1 Viral protease.....	7
1.1.1.1.1.4.2 Viral neuraminidase	8
1.1.1.1.1.5 Drugs targeting viral entry.....	9
1.1.1.1.2 Drugs targeting cellular proteins	9
1.1.1.1.2.1 Drugs targeting cellular entry proteins.....	9
1.1.1.1.2.2 Drugs targeting other cellular proteins.....	10
1.1.1.2 Select drugs under development.....	10
1.1.1.3 Challenges of current antiviral chemotherapies and strategies	14
1.1.1.3.1 Resistance	16
1.1.1.3.2 Specificity.....	22
1.1.1.3.3 Intracellular metabolism.....	24
1.2 Viral entry	27
1.2.1 Entry of enveloped viruses.....	28
1.2.1.1 Hepatitis C virus entry	29
1.2.1.2 Sindbis virus entry	30
1.2.1.3 Vesicular stomatitis virus entry	31
1.2.1.4 Vaccinia virus entry	32
1.2.2 Entry of nonenveloped viruses	32
1.2.2.1 Poliovirus entry.....	32
1.2.2.2 Adenovirus entry	33
1.3 Membrane fusion.....	33
1.3.1 Viral fusion.....	34
1.3.1.1 Viral fusion proteins	35
1.3.1.1.1 Class I fusion proteins.....	36
1.3.1.1.2 Class II fusion proteins.....	39
1.3.1.1.3 Class III fusion proteins	41
1.3.1.2 Lipids in viral fusion and replication.....	43
1.3.2 Cellular membrane fusion.....	49
1.3.2.1 Cellular fusion proteins.....	49
1.3.2.2 Lipids in cell fusion	52
1.3.3 Lipid fusion	54
1.3.3.1 General model of lipid fusion.....	54
1.3.3.2 Modulation of membrane fusion by targeting lipids	59
1.4 Herpes simplex virus	62
1.4.1 Classification and virion organization.....	62

1.4.2 Replication	63
1.4.2.1 Entry.....	63
1.4.2.1.1 Primary attachment.....	64
1.4.2.1.2 Secondary binding.....	65
1.4.2.1.3 Envelope fusion.....	66
1.4.2.3 Gene expression and DNA replication.....	69
1.4.2.4 Egress.....	70
1.5 Rationale and hypothesis.....	72
1.6 References.....	75
CHAPTER 2: MATERIALS AND METHODS	118
2.1 Introduction.....	118
2.2 Cells and virus.....	118
2.3 Drugs.....	120
2.4 Cytotoxicity assays.....	121
2.5 Virus infections.....	122
2.5.1 Virus stocks.....	122
2.5.1.1 Herpes simplex virus types 1 and 2 stock preparation.....	122
2.5.1.2 Poliovirus stock preparation.....	124
2.5.2 Herpes simplex virus type-1 infection.....	126
2.5.3 Sindbis virus infection.....	127
2.5.4 Virus harvest.....	127
2.6 Virus titrations.....	128
2.7 Viral infectivity assays.....	129
2.7.1 Virion infectivity assay.....	129
2.7.2 Hepatitis C virus infectivity assay.....	130
2.7.3 Infectivity of green fluorescent protein-expressing viruses.....	132
2.7.4 Cell protection assay.....	133
2.8 Temperature dependence assay.....	134
2.9 Cellular localization.....	135
2.10 Analysis of progeny virions.....	136
2.10.1 Herpes simplex virus type-1 DNA replication and progeny infectivity	136
2.10.2 Progeny Sindbis virus infectivity.....	139
2.11 Virion integrity analysis.....	139
2.12 Western blot analyses.....	140
2.12.1 Virion and cell lysate preparations.....	140
2.12.2 Protein separation.....	141
2.12.3 Protein transfer.....	142
2.12.4 Western blot.....	142
2.13 Southern blot analyses.....	143
2.13.1 DNA purification.....	143
2.13.2 DNA separation.....	144
2.13.3 DNA transfer.....	145
2.13.4. Hybridization analyses.....	146
2.13.4.1 Random-primed DNA labeling.....	146

2.13.4.2 Hybridization	147
2.14 Binding assays	148
2.14.1 Production of radiolabeled herpes simplex virus type-1 virions	148
2.14.2 Total binding assay	149
2.14.3 High-affinity binding assay	151
2.15 Herpes simplex virus type-1 entry assay	154
2.15.1 UV inactivation of herpes simplex virus type-1	154
2.15.2 VP16 entry assay	155
2.16 Differential scanning calorimetry	156
2.17 Drug-selective pressure	157
2.17.1 Plaque purification	157
2.17.2 Standard serial passage selection	158
2.17.2.1 Infections and harvest	158
2.17.2.2 Percent resistance analyses	159
2.18 <i>In vivo</i> studies	160
2.18.1 Oestrus synchronization	160
2.18.2 Animal infections	161
2.18.2.1 Anesthesia	161
2.18.2.2 Herpes simplex virus type-2 infection	161
2.18.2.3 Animal monitoring	162
2.18.2.3.1 Clinical monitoring of infection	162
2.18.2.3.2 Virus shedding	163
2.19 Statistical analyses	164
2.20 References	165

CHAPTER 3: THE CHARACTERIZATION OF THE ANTIVIRAL ACTIVITIES OF RIGID AMPHIPATHIC FUSION INHIBITORS	167
3.1 Introduction	167
3.2 Results	170
3.2.1 Structure activity relationship studies	170
3.2.1.1 Effects of different hydrophilic heads	171
3.2.1.2 Effects of polarity of the hydrophobic moiety	173
3.2.1.3 Effects of aryl size of the hydrophobic moiety	174
3.2.1.4 Effects of planarity and flexibility of the hydrophobic moiety	174
3.2.2 dUY11 localizes to Vero cell membranes	176
3.2.3 dUY11 is not cytotoxic and is only mildly cytostatic	177
3.2.4 Rigid amphipathic fusion inhibitors inhibit infectivity	178
3.2.4.1 Virion exposure to dUY11 before adsorption inhibits infectivity	178
3.2.4.2 dUY11 does not lyse virions	179
3.2.4.3 dUY11 does not inhibit primary herpes simplex virus type-1 attachment	181
3.2.4.4 dUY11 does not inhibit high-affinity herpes simplex virus type-1 virion binding	182
3.2.4.5 dUY11 inhibits herpes simplex virus type-1 entry	184
3.2.4.6 Rigid amphipathic fusion inhibitors inhibit lamellar to inverted- hexagonal phase transitions	185

3.2.4.6.1 dUY11 inhibits lamellar to inverted-hexagonal phase transitions..	187
3.2.4.6.2 Other rigid amphipathic fusion inhibitors inhibit lamellar to inverted-hexagonal phase transitions	188
3.2.5 Rigid amphipathic fusion inhibitors target virion envelope bilayers ...	189
3.2.5.1 The antiviral activities of dUY11 are cell-type independent	189
3.2.5.2 dUY11 primarily targets virion envelopes.....	190
3.2.5.3 dUY11 inhibits herpes simplex virus type-1 infectivity as a result of its interactions with fluid envelopes.....	191
3.3 Discussion	192
3.4 References.....	199

CHAPTER 4: THE CHARACTERIZATION OF THE SPECIFICITY OF RIGID AMPHIPATHIC FUSION INHIBITORS	224
4.1 Introduction.....	224
4.2 Results.....	227
4.2.1 dUY11 inhibits the infectivity of closely related viruses.....	227
4.2.2 dUY11 inhibits the infectivity of otherwise unrelated enveloped viruses	228
4.2.3 dUY11 inhibits the infectivity of hepatitis C virus.....	229
4.2.4 Treatment of infected cells with dUY11 inhibits the levels of Sindbis virus infectivity	231
4.2.5 dUY11 does not inhibit the infectivity of nonenveloped viruses	232
4.3 Discussion	234
4.4 References.....	237

CHAPTER 5: RIGID AMPHIPATHIC FUSION INHIBITORS DO NOT ACT BY CLASSIC NUCLEOSIDIC ANTIVIRAL MECHANISMS.....	246
5.1 Introduction.....	246
5.2 Results.....	248
5.2.1 dUY11 does not target viral proteins to inhibit herpes simplex virus type-1 replication.....	248
5.2.1.1 dUY11 inhibits herpes simplex virus type-1 yields.....	249
5.2.1.2 dUY11 does not inhibit herpes simplex virus type-1 DNA replication	249
5.2.1.3 dUY11 is active against drug-resistant herpes simplex virus type-1 strains.....	251
5.2.1.4 The antiviral activities of dUY11 are not attenuated by increasing multiplicity of infection.....	253
5.2.2 Treatment of infected cells with dUY11 inhibits the levels of herpes simplex virus type-1 infectivity	254
5.2.2.1 Treatment of herpes simplex virus type-1 infected cells with dUY11 inhibits the levels of cell-associated and cell-free progeny infectivity	254
5.2.2.2 dUY11 inhibits the release of progeny herpes simplex virus type-1 virions by 2.8-fold.....	256
5.2.3 dUY11 does not readily select for resistant variants	258

5.2.3.1 Standard passages in the presence of an increasing concentration of dUY11 did not readily select for resistant variants	259
5.3 Discussion	263
5.4 References	268

CHAPTER 6: HERPES SIMPLEX VIRUS TYPE-2 VIRIONS PRE-EXPOSED TO RIGID AMPHIPATHIC FUSION INHIBITORS ARE NOT INFECTIOUS TO MICE.....		279
6.1 Introduction		279
6.2 Results		282
6.2.1 Evaluation of the infectivity to mice of herpes simplex virus type-2 exposed to dUY11 before infection.....		282
6.2.1.1 One lethal dose for 50% of mice of herpes simplex virus type-2 exposed to dUY11 is not infectious to mice		283
6.2.1.1.1 Evaluation of herpes simplex virus type-2 infection		284
6.2.1.2 Three lethal doses for 50% of mice of herpes simplex virus type-2 exposed to dUY11 are not infectious to mice.....		286
6.2.1.2.1 Evaluation of herpes simplex virus type-2 infection		286
6.3 Discussion		288
6.4 References		291

CHAPTER 7: DISCUSSION.....	297
7.1 Mechanisms of action of rigid amphipathic fusion inhibitors	298
7.2 Selectivity of rigid amphipathic fusion inhibitors for viral fusion.....	307
7.3 Broad-spectrum activities of rigid amphipathic fusion inhibitors.....	312
7.4 Other potential small molecules targeting envelope lipids	320
7.5 Future considerations.....	329
7.6 Perspective	337
7.7 References	338

APPENDICES	349
Appendix 1 The lipid composition of virion envelopes and cell membranes	349
Appendix 2 The fatty acid composition of virion envelopes and cell membranes	358
Table legends and references	379

LIST OF TABLES

Table 1.1 Clinically approved antiviral drugs.....	104
Table 1.2 Select antivirals under development.....	106
Table 1.3 Clinical human vaccines	107
Table 1.4 Viral fusion protein classification.....	108
Table 1.5 Budding sites of enveloped viruses	109
Table 1.6 Molecular shapes and polymorphic phases exhibited by natural lipids	110
Table 2.1 Clinical scoring of vaginal HSV-2 infection.....	166
Table 3.1 IC ₅₀ of RAFIs against HSV-1 infectivity.....	204
Table 3.2 Effects of dUY11 on cell doubling.....	205
Table 3.3 Effects of dUY11 on cell viability.....	206
Table 3.4 IC ₅₀ of dUY11 on HSV-1 infectivity to different cell lines	207
Table 3.5 IC ₅₀ of dUY11 against HSV-1 infectivity by direct virion exposure or by cell pretreatment.....	208
Table 4.1 IC ₅₀ of dUY11 against enveloped and nonenveloped viruses.....	240
Table 4.2 IC ₅₀ of dUY11 against SIN infectivity by direct exposure of infecting virions or by treating cells for 1- or 23-hours after infection	241
Table 5.1 IC ₅₀ of dUY11 against HSV-1 infectivity by direct exposure of infecting virions or by treating cells for 1- or 23-hours after infection.....	270
Table 5.2 Viral titers did not recover under dUY11 selection pressure	271
Table 7.1 Virion properties of some enveloped and nonenveloped viruses	347
Appendix 1. The lipid composition of virion envelopes and cell membranes ...	349
Appendix 2. The fatty acid composition of virion envelopes and cell membranes	358

LIST OF FIGURES

Figure 1.1 Clinically approved antiviral drugs	111
Figure 1.2 Natural membrane phospholipids.....	115
Figure 1.3 Lipid reorganizations during fusion	116
Figure 1.4 Extracellular exposure of vesicles to synthetic rigid amphiphiles	117
Figure 3.1 Structures of rigid amphipathic fusion inhibitors.....	209
Figure 3.2 RAFIs inhibit HSV-1 infectivity.....	210
Figure 3.3 dUY11 inhibits HSV-1 infectivity with an IC ₅₀ of 38 nM and an IC ₉₉ of 2.16 μM	211
Figure 3.4 dUY11 localizes to cell membranes	212
Figure 3.5 dUY11 has no cytotoxic effects and is only mildly cytostatic.....	213
Figure 3.6 dUY11 exposure in semi-solid media after adsorption of HSV-1 virions does not inhibit plaquing.....	214
Figure 3.7 dUY11 does not lyse HSV-1 virions.....	215
Figure 3.8 dUY11 does not inhibit total HSV-1 binding	216
Figure 3.9 dUY11 does not inhibit high-affinity HSV-1 binding.....	217
Figure 3.10 dUY11 inhibits HSV-1 entry	218
Figure 3.11 dUY11 inhibits lamellar to inverted-hexagonal phase transitions ..	219
Figure 3.12 dUY2 and dUY4 inhibit lamellar to inverted-hexagonal phase transitions.....	220
Figure 3.13 dUY11-mediated inhibition of HSV-1 infectivity is independent of cell type.....	221
Figure 3.14 dUY11 primarily targets virion envelopes.....	222
Figure 3.15 dUY11 inhibits HSV-1 infectivity only when virions with fluid envelopes are exposed to it	223

Figure 4.1 dUY11 inhibits the infectivity of otherwise unrelated enveloped viruses	242
Figure 4.2 dUY11 inhibits HCV infectivity	243
Figure 4.3 Treatment of SIN-infected cells with dUY11 inhibits the levels of progeny infectivity	244
Figure 4.4 dUY11 does not inhibit the infectivity of nonenveloped viruses.....	245
Figure 5.1 dUY11 inhibits HSV-1 yield with an apparent IC ₅₀ of 0.906 μM	272
Figure 5.2 dUY11 does not inhibit HSV-1 DNA replication	273
Figure 5.3 dUY11 inhibits the levels of infectivity in cells infected by HSV-1 strains resistant to drugs that target viral DNA replication	274
Figure 5.4 The antiviral effects of dUY11 are not attenuated by increasing multiplicity of infection.....	275
Figure 5.5 Treatment of HSV-1-infected cells with dUY11 inhibits the levels of cell-free and cell-associated progeny infectivity.....	276
Figure 5.6 dUY11 inhibits the release of progeny virions by only 2.8-fold.....	277
Figure 5.7 No dUY11-resistant variants were detected after 10 passages in selective media.....	278
Figure 6.1 One LD ₅₀ of HSV-2 virions pre-exposed to a high dose of dUY11 is not infectious to mice	294
Figure 6.2 Three LD ₅₀ of HSV-2 virions pre-exposed to a high dose of dUY11 are not infectious to mice	295
Figure 6.3 Mice infected with 3xLD ₅₀ of HSV-2 virions pre-exposed to a high dose of dUY11 show no clinical signs	296
Figure 7.1 Small molecules targeting virions envelopes.....	348

LIST OF ABBREVIATIONS

ACV: acyclovir
AdV: adenovirus
AIDS: acquired immunodeficiency syndrome
ALV: avian leucosis virus
ANA: acyclic nucleoside analogue
ANP: acyclic nucleoside phosphonate
AP-2: adaptor protein complex 2
APS: ammonium persulfate
APT/2: adult pig thyroid cells
ART: antiretroviral therapy
ASV: avian sarcoma virus
ATP: adenosine triphosphate
AZT: 3'-azidothymidine
A3G: apolipoprotein B mRNA-editing enzyme-catalytic polypeptide-like 3G

BAR: Bin/Amphiphysin-Rvs
BCNA: bicyclic furanopyrimidine nucleoside analogue
BHK-21: baby hamster kidney-21

CAR: Coxsackievirus and adenovirus receptor
CCR5: cellular chemokine receptor 5
CD₅₀: concentration causing death to 50%
CD4: cluster of differentiation 4
CD81: cluster of differentiation 81
CD155: cluster of differentiation 155
cDNA: complimentary deoxyribonucleic acid
CEs: cholesterol esters
CEC: chicken embryo cell
CEF: chicken embryo fibroblast
Cer: ceramide
CEV: cell-associated enveloped virus
CFC: chicken fibroblast cell
CH: cholesterol
CI: confidence interval
CKC: calf kidney cell
CL: cardiolipin
CNT: concentrative nucleoside transporter
CPE: cytopathic effect
cpm: counts per minute
Cs: cyclosporine
CV: crystal violet
CXCR4: C-X-C chemokine receptor type 4
CypA: cyclophilin A

dCK: deoxycytidine kinase
DEAE: diethylaminoethyl cellulose
DEPC: diethylpyrocarbonate
DEPE: dielaidoylphosphatidylethanolamine
dGTP: deoxyguanosine triphosphate
dhSM: dihydrosphingomyelin
DNA: deoxyribonucleic acid
DMEM: Dulbecco's modified Minimum Eagle's Medium
DMSO: dimethyl sulfoxide
dNTP: deoxyribonucleotide triphosphate
dpi: days post-infection
ds: double stranded
DSA: 5-docyl stearic acid
DSC: differential scanning calorimetry
dTMP: deoxythymidine monophosphate
DTT: dithiothreitol
dUMP: deoxyuridine monophosphate

E: early
EAV: equine arteritis virus
EBV: Epstein-Barr virus
EC₅₀: 50% effective concentration
ECE: embryonated chicken egg
EDTA: ethylenediaminetetraacetic acid
ENT: equilibrative nucleoside transporter
ER: endoplasmic reticulum
EV: extracellular enveloped virus

FBS: fetal bovine serum
FDA: Food and Drug Administration
FL: fusion loop
FLV: feline leukemia virus
FP: fusion peptide
FPV: fowl plague virus

GAG: glycosaminoglycan
gB: glycoprotein B
gC: glycoprotein C
gD: glycoprotein D
GFP: green fluorescent protein
gH: glycoprotein H
gL: glycoprotein L
gp: glycoprotein
GP: glycerophosphate
gp41: glycoprotein 41
gp120: glycoprotein 120

gp160: glycoprotein 160
GPI: glycosylphosphatidylinositol
GTPase: guanosine triphosphatase

HA: hemagglutinin
HaK: hamster kidney
HAART: highly active antiretroviral therapy
HBSS: Hanks balanced salt solution
HBV: hepatitis B virus
HCMV: human cytomegalovirus
HCV: hepatitis C virus
HCVpp: hepatitis C virus pseudoparticle
HEK293: human embryonic kidney 293
Hep: heparin
HEP: high egg passage
HFF: human foreskin fibroblast
HIgR: herpesvirus immunoglobulin-like receptor
HIV: human immunodeficiency virus
HIV-1: human immunodeficiency virus type-1
HIV-2: human immunodeficiency virus type-2
hpi: hours post-infection
HPV: human papillomavirus
HRs: heptad repeats
HR1: heptad repeat 1
HR2: heptad repeat 2
HS: heparan sulphate
HSV: herpes simplex virus
HSV-1: herpes simplex virus type-1
HSV-2: herpes simplex virus type-2
HTLV-1: human T-lymphotrophic virus type-1
HveA: herpes virus entry A
HVEM: herpes virus entry mediator

IC₅₀: 50% inhibitory concentration
IC₉₅: 95% inhibitory concentration
IC₉₉: 99% inhibitory concentration
ID₅₀: 50% inhibitory dose
ID₉₅: 95% inhibitory dose
IE: immediate-early
IFN: interferon
Ig: immunoglobulin
IgV: immunoglobulin-variable
InfA: influenza virus type A
IN: integrase
JEV: Japanese encephalitis virus

L: late
LBA: lysobisphosphatidic acid
LD₅₀: 50% lethal dose
LEDGF/p75: lens epithelium-derived growth factor
LPA: lysophosphatidic acid
LPC: lysophosphatidylcholine
LPE: lysophosphatidylethanolamine

MC: methylcellulose
MDBK: Madin-Darby bovine kidney
MDCK: Madin-Darby canine kidney
MDM: monocyte-derived macrophage
Met: methionine
MHV: mouse hepatitis virus
min: minute
MK: monkey kidney
MLV: murine leukemia virus
MOI: multiplicity of infection
mRNA: messenger ribonucleic acid
MRP: multidrug resistance protein
MRP4: multidrug resistance protein related protein 4
MV: mature virus
N-9: nonoxynol-9
NA: neuraminidase
nc: not classified
nd: not determined
ND: no drug
NDP: nucleoside diphosphate
NDV: Newcastle disease virus
Nef: negative factor
NLs: neutral lipids
NMP: nucleoside monophosphate
NNRTI: non-nucleoside reverse transcriptase inhibitor
NRTI: nucleoside reverse transcriptase inhibitor
NS3: non-structural protein 3
NS5A: non-structural protein 5A
NSF: N-ethylmaleimide-sensitive factor
NTP: nucleoside triphosphate

OA: oleic acid
OAT: organic anion transporter
OCT: organic cation transporter

PA: phosphatidic acid
PAA: phosphonoacetic acid
PBS: phosphate-buffered saline

PC: phosphatidylcholine
p.e.: presented elsewhere as a mixture
PE: phosphatidylethanolamine
pegIFN: pegylated interferon
PEPT: peptide transporter 1
PFA: phosphonoformic acid
PFD: profusion domain
PFU: plaque-forming units
P-gp: P-glycoprotein
PI: phosphatidylinositol
PIP: phosphatidylinositol phosphate
PIP₂: phosphatidylinositol bisphosphate
PIs: protease inhibitors
PK/1: primary pig kidney
pLs: polar lipids
PL: phospholipid
pl-PE: plasmalogen phosphatidylethanolamine
PM: plasma membrane
PR: protease
Prr: poliovirus-related receptors
PRV: pseudorabies virus
PS: phosphatidylserine
PV: poliovirus
PVDF: polyvinylidene fluoride

QC: quail cell

RAFI: rigid amphipathic fusion inhibitor
RAV: resistance-associated variant
REF: rat embryo fibroblast
RFP: red fluorescent protein
RK: rabbit kidney
RLV: Rauscher leukemia virus
RNA: ribonucleic acid
RNase: ribonuclease
rpm: revolutions per minute
RSV: respiratory syncytial virus
RT: reverse transcriptase

SAR: structure activity relationship
SDS: sodium dodecyl sulphate
SDS-PAGE: sodium dodecyl sulphate polyacrylamide gel electrophoresis
sec: seconds
SEM: standard error of the mean
SFM: serum-free media
SFV: Semliki forest virus

SI: selectivity index
SIN: Sindbis virus
SM: sphingomyelin
SNAP-25: synaptosome-associated protein-25
SNARE: *N*-ethylmaleimide-sensitive factor attachment protein receptor
SR-BI: Scavenger receptor class B, type I
SSC: saline sodium citrate
ssRNA: single stranded ribonucleic acid
SSV: simian sarcoma virus
STE: sodium-Tris-ethylenediaminetetraacetic acid
STD: sexually transmitted disease
STI: sexually transmitted infection
SV5: simian virus 5
SVR: sustained virological response

TAE: Tris-acetate-ethylenediaminetetraacetic acid
TAM: thymidine-associated mutation
TBEV: tick-borne encephalitis virus
TE: Tris-ethylenediaminetetraacetic acid
TEMED: N,N,N,N-tetramethylethylenediamine
TGEV: transmissible gastroenteritis virus
TK: thymidine kinase
TK-: thymidine kinase null
TK1: thymidine kinase 1
TK2: thymidine kinase 2
TM: transmembrane
TNF: tumor necrosis factor
t-SNARE: target *N*-ethylmaleimide-sensitive factor attachment protein receptor

UGT: uridine diphosphate glucuronosyltransferase
UV: ultraviolet

VAMP: vesicle-associated membrane protein
VEE: Venezuelan equine encephalitis
VP: virion protein
VP16: virion protein 16
v-SNARE: vesicle *N*-ethylmaleimide-sensitive factor attachment protein receptor
VSV: vesicular stomatitis virus
VV: vaccinia virus
VZV: varicella-zoster virus

YFV: yellow fever virus

6HB: six helix-bundle
 α -H: alpha helix

CHAPTER 1: INTRODUCTION

1.1 Antiviral strategies

1.1.1 Antiviral drugs

Despite the existence of several vaccines, antiviral chemotherapy is still critical. The discovery that 9-(2-hydroxyethoxymethyl) (or acycloguanosine) inhibited the replication of herpes simplex virus (HSV) (Elion et al., 1977) by targeting the virally encoded thymidine kinase (TK) (Schaeffer et al., 1978) set the foundation for further antiviral drug development. Antiviral research then exploded with the discovery in 1983 that human immunodeficiency virus (HIV) (Barre-Sinoussi et al., 1983; Popovic et al., 1983) was the etiological agent of the acquired immunodeficiency syndrome, AIDS (Gallo et al., 1984; Popovic et al., 1984). Only two years after the discovery of HIV, 3'-azidothymidine (AZT) was approved for clinical use to treat HIV/AIDS (Mitsuya et al., 1985).

There are currently 48 approved antiviral drugs, used either as monotherapy (**Table 1.1**) or in combination. Nearly half of these approved antivirals (23 approved monotherapies; all but three combinations) are specific against HIV. Clinical antivirals also target HSV type-1 and -2 (HSV-1 and HSV-2; 8 drugs), hepatitis B virus (HBV; 6 drugs), human cytomegalovirus (HCMV; 6 drugs), Varicella-zoster virus (VZV; 4 drugs), influenza virus (4 drugs), hepatitis C virus (HCV; 3 combinations), Epstein Barr virus (EBV; 1 drug), and respiratory syncytial virus (RSV; 1 drug). Thousands of other compounds are at various stages of clinical or preclinical development.

1.1.1.1 Clinical antiviral chemotherapies

Antivirals can be classified according to the viral replication functions they target. All but two (discussed in **section 1.1.1.1.2**) target viral proteins, and most target viral polymerases or integrase to inhibit different stages during viral genome replication (reviewed in (De Clercq, 2001), updated in (De Clercq, 2004) and (De Clercq, 2008a). The second most common targets are the enzymes required for virion maturation (protease or neuraminidase). The third most common target is entry and fusion. In the discussion below, the clinical antivirals are classified based on the origin of their target (viral or cellular), the step they target, and their chemical structure.

1.1.1.1.1 Drugs targeting viral-encoded functions

1.1.1.1.1.1 Drugs targeting viral genome replication

The largest class of antiviral drugs is composed of compounds that target viral polymerases. There are twenty-eight approved antiviral drugs targeting viral ribonucleic acid (RNA) or deoxyribonucleic acid (DNA) polymerases. Twenty-two are nucleoside or nucleotide derivatives, structural analogues of natural substrates of the target enzyme. The other six are non-nucleosidic.

Acycloguanosine (acyclovir) was one of the first described antiviral nucleoside analogues targeting viral DNA polymerases. It is an acyclic nucleoside analogue (ANA), a sub-class that includes five other antivirals (**Figure 1.1A1**): guanine-derived acyclovir and ganciclovir, as well as their respective prodrugs valaciclovir and valganciclovir, and the guanine analogue penciclovir and its

prodrug, famciclovir. As a defining characteristic, all ANAs have an acyclic substituent replacing the ribose ring. ANAs are specific for infected cells because the first of the three successive phosphorylations required for their activation is catalyzed by a virally encoded kinase (HSV or VZV TK; HCMV UL97; or EBV protein kinase) (reviewed in Deville-Bonne, 2010). Once monophosphorylated, they are further phosphorylated by cellular kinases into their triphosphate active forms. ANA triphosphates target the viral DNA-dependent polymerase, which incorporates them at the 3'-end of nascent viral DNA. Incorporated ANAs are obligatory chain terminators (immediate or delayed), depending on the presence of a 3'-hydroxyl group necessary for DNA elongation (reviewed in Deval, 2009). The principal indications of ANAs are for herpesvirus disease caused by HSV-1, HSV-2, VZV, EBV or HCMV.

Cyclic nucleoside derivatives can also inhibit viral genome replication. Five drugs are classified in this category (**Figure 1.1AII**): the pyrimidine analogues brivudine, idoxuridine, trifluridine and telbivudine, as well as the purine-derived entecavir. A sixth drug, the ribosyl purine analogue ribavirin, can also be classified in this category by its structure. Most triphosphorylated cyclic nucleoside analogues compete with natural nucleotides for viral polymerases to inhibit DNA replication. As an exception, intracellularly monophosphorylated trifluridine inhibits thymidylate synthetase, thus preventing the conversion of deoxyuridine monophosphate (dUMP) to deoxythymidine monophosphate (dTMP) (De Clercq, 2004). Ribavirin is also proposed to have several other antiviral mechanisms and can thus be mechanistically classified as a drug

targeting cellular proteins (discussed in **section 1.1.1.1.2.2**) (Tam, Lau, and Hong, 2001). Brivudine, idoxuridine and trifluridine are approved against HSV-1, HSV-2 or VZV, whereas entecavir and telbivudine are used against HBV. Ribavirin is used to treat infections by RSV, most usually in children, and, in combination with pegylated interferon (pegIFN) (and boceprevir or telaprevir), against HCV. Pegylated interferon α -2a is also used to treat patients chronically infected with Hepatitis B (Soriano et al., 2010).

Another class of antivirals targeting viral DNA polymerases is the 2',3'-dideoxynucleosides. The drugs in this class are didanosine, abacavir, zidovudine, stavudine, zalcitabine, emtricitabine and lamivudine (**Figure 1.1AIII**), commonly referred to as nucleoside reverse transcriptase inhibitors (NRTIs). They are used in combination treatments against HIV (reviewed in Cihlar and Ray, 2010). Didanosine and abacavir are purine-base derivatives, whereas the thymidine-derived zidovudine and stavudine, or the cytosine-derived zalcitabine, emtricitabine and lamivudine, are pyrimidine-base analogues. Most NRTIs have unmodified purine or pyrimidine bases, the exceptions being emtricitabine (which contains a fluorine at the 5-position) and abacavir (which has a 6-modified diaminopurine ring that serves as a prodrug to a guanine base). All NRTIs lack 2'- and 3'-hydroxyl groups, and they contain diversely modified ribose rings. The simplest are didanosine and zalcitabine, which closely resemble natural deoxynucleosides, except for the absence of the 3'-hydroxyl. Among those with the most significant ribose modifications is abacavir, which contains a 2',3'-unsaturated bond within a carbocyclic ring. Lamivudine and emtricitabine have an

unnatural L-enantiomeric ribose configuration in addition to an oxathiolane ring. NRTIs are activated by host cell kinases and phosphotransferases into 5'-triphosphate nucleotides, and they act as obligatory chain-terminators of DNA elongation. The principal indication of all seven drugs is against HIV, with the exception of lamivudine and emtricitabine, which are used to treat HBV infections. Zidovudine is administered to pregnant women as a pre-exposure prophylaxis to reduce the risk of HIV transmission to the unborn child (Connor et al., 1994).

The next sub-class are drugs that directly mimic nucleotides, the so-called acyclic nucleoside phosphonates, or ANPs (**Figure 1.1AIV**) (Cihlar and Ray, 2010). ANPs are characterized by a replacement of the normal nucleotide phosphate link by a phosphonate link, which resists attack by esterases or other catabolic enzymes (De Clercq, 2007a). ANPs do not require the first activating phosphorylation, which is often the rate-limiting step for the activation of nucleoside analogues (Van Rompay, Johansson, and Karlsson, 2000). Cidofovir, an acyclic cytosine-based analogue, was the first ANP introduced into the clinic. It was approved in 1996 for the treatment of HCMV retinitis in AIDS patients. The acyclic adenosine phosphonate analogues tenofovir disoproxil fumarate and adefovir dipivoxil are approved against HBV. Adefovir dipivoxil is also approved against HIV.

The last category of viral polymerase inhibitors are non-nucleosidic compounds (reviewed in de Bethune, 2010). Five members of this category, nevirapine, delavirdine, efavirenz, etravirine and rilpivirine (**Figure 1.1AV**), form

the non-nucleoside reverse transcriptase inhibitors (NNRTIs). They are used in combination therapies to treat HIV-1. Non-nucleosidic compounds target elongation without competing with the natural substrates of the polymerase. Instead, NNRTIs bind allosteric pockets of the target polymerase to induce conformational changes that inhibit the catalytic activities of the reverse transcriptase (RT) (Sluis-Cremer, Temiz, and Bahar, 2004). Nevirapine is among the nonteratogenic anti-HIV drugs (which also includes the NRTIs zidovudine and lamivudine), and thus is administered (alone or in combination) during pregnancy or prophylactically to newborns to reduce the risk of HIV transmission from infected mothers. The sixth non-nucleosidic polymerase inhibitor is foscarnet, a base conjugate of phosphonic acid (phosphonoformate) that binds to the pyrophosphate binding site of the viral DNA polymerase (Mao and Robishaw, 1975). Foscarnet is approved for clinical use against HCMV, HSV-1 and HSV-2.

1.1.1.1.2 Drugs targeting viral integration

The newest class of drugs targeting viral proteins inhibit viral integrase (IN; reviewed in McColl and Chen, 2010). There is only one drug in this sub-class, raltegravir (**Figure 1.1B**). Raltegravir binds the catalytic core domain of IN to inhibit the strand transfer reaction required for integration of proviral DNA into host cell chromosomes. Raltegravir was approved in 2007 by the Food and Drug Administration (FDA) to treat HIV-1 infections.

newest addition to the class of HIV PIs, tipranavir (approved in 2005; boosted with ritonavir to increase its plasma levels), is a non-peptidomimetic small molecule (Turner et al., 1998b). Tipranavir is also used against HIV-2. The production of infectious HCV is similarly dependent on polypeptide cleavage to produce mature functional virus proteins (Moradpour, Penin, and Rice, 2007). In 2011, two PIs were approved against HCV; boceprevir and telaprevir target the NS3/NS4A PR (reviewed in Soriano et al., 2010). Results from three phase 3 efficacy studies (two evaluating boceprevir and one, telaprevir) showed that the addition of a PI (boceprevir or telaprevir) to the standard treatment of ribavirin and pegIFN increased the number of patients who achieved a sustained virological response (SVR; no detectable HCV six months after treatment is terminated) by up to 75% (Kwo et al., 2010).

1.1.1.1.4.2 Viral neuraminidase

Another class of antivirals targets a viral enzyme that participates in late stages of replication. These are the inhibitors of influenza virus neuraminidase (NA): oseltamivir and zanamavir (**Figure 1.1E**). Influenza NA promotes progeny virion release by cleaving the terminal *N*-acetylneuraminic acid residues of cell surface glycoproteins bound by virion hemagglutinin (HA). Oseltamivir and zanamavir bind the NA active site and prevent this cleavage of sialic acid moieties (Moscona, 2005). The lack of NA activity inhibits the release of progeny virions from infected cells (Liu et al., 1995). It also causes virion aggregation (Liu et al.,

1995) and reduces viral infectivity (Suzuki et al., 2005). Both drugs are approved against influenza A and B.

1.1.1.1.5 Drugs targeting viral entry

Recently, significant efforts have been focused on developing inhibitors of viral infectivity (reviewed in Tilton and Doms, 2010). Such drugs block the first events in viral replication and may therefore also be used prophylactically. There are currently three clinical inhibitors of infectivity targeting viral proteins. The first two are adamantane derivatives, amantadine and rimantadine (**Figure 1.1F**). Both bind the influenza M2 pH-activated proton channel to inhibit viral uncoating (Davies et al., 1964). The FDA approved amantadine and rimantadine in 1966 and 1993, respectively, against influenza A virus.

A more recently approved entry inhibitor targets structural refolding events of HIV fusion glycoprotein 41 (gp41). The FDA approved enfuvirtide (FUZEON, T-20) in 2003. It is a linear 36 amino acid synthetic peptide (peptidomimetic; **Figure 1.1F**) that prevents the gp41 rearrangements necessary for envelope fusion, and consequently, entry (Wild et al., 1994).

1.1.1.1.2 Drugs targeting cellular proteins

1.1.1.1.2.1 Drugs targeting cellular entry proteins

Maraviroc is the first small molecule antiviral specifically designed to target the interaction of a viral entry protein with a cellular protein. It was FDA-approved in 2007 against HIV-1. Following the primary attachment of HIV glycoprotein 120

(gp120) to its receptor, cluster of differentiation 4 (CD4), one of two cellular proteins acts as co-receptor for viral entry. These are C-C motif chemokine receptor 5 (CCR5) and C-X-C motif chemokine receptor 4 (CXCR4) (Feng et al., 1996; Wu et al., 1996). Maraviroc binds the CCR5 co-receptor allosterically, inducing conformational changes that prevent HIV gp120 binding to CCR5 (Dorr et al., 2005). Maraviroc is therefore a non-competitive inhibitor specific to HIV-1 variants that engage only CCR5 as co-receptor.

1.1.1.1.2.2 Drugs targeting other cellular proteins

Maraviroc is the first clinically approved antiviral specifically designed to target an interaction with a cellular (entry) protein. However, ribavirin was approved in 1985 to treat RSV, and in 1998 it was approved in combination with pegIFN-2 α to treat HCV. Among the several antiviral mechanisms proposed for ribavirin is its ability to inhibit inosine-5'-monophosphate dehydrogenase, a cellular enzyme required for purine nucleotide biosynthesis (Feld and Hoofnagle, 2005). In combination with interferon, the current standard chemotherapy against HCV also regulates cellular immune responses to infection (Chung et al., 2008).

1.1.1.2 Select drugs under development

Drug approval requires evaluation in three clinical phases, and thousands of compounds are at various stages in development, from drug discovery to phase 3. The drugs under development include many with classic antiviral targets (viral

proteins required for replication), and others that target new viral or cellular molecules. A select few (**Table 1.2**) are described below.

Many derivatives of already approved drugs targeting viral proteins are under development. Second-generation drugs typically have higher potency, longer half-life, or reduced side-effect profiles compared to first-generation drugs of the same class (De Clercq, 2008b). One such example is CMX157, under development by Chimerix, Inc., a prodrug lipid conjugate of the ANP tenofovir. CMX157 was generated by coupling tenofovir to a long aliphatic side chain (hexadecyloxypropyl) (Hostetler, 2009). CMX157 associates directly with virion envelopes through its aliphatic side chain. Following viral fusion and entry, CMX157 is converted into the parent compound tenofovir and inhibits viral replication via chain termination. CMX157 is >300 times more potent than tenofovir against HIV (Lanier et al., 2009). The increased potency is proposed to result from facilitated delivery by HIV virions into infected cells. Phase-1 clinical trials were completed in 2010, and CMX157 demonstrated a favorable safety, tolerability and distribution profile.

Other new investigational strategies are directed against novel viral or cellular proteins, and may thus lead to new drug classes. One such example is cyclosporine (Cs), used to prevent the rejection of transplants. Cs binds cyclophilin A (CypA), a cellular enzyme possessing peptidylprolyl isomerase activity. Cs-CypA complexes inhibit calcineurin, a protein phosphatase that normally activates T cell response by upregulating the expression of interleukin 2. Cs thus acts as an immunosuppressant by inhibiting the production of pro-

inflammatory cytokines. CypA also reduces HCV viral loads by mechanisms that are not fully understood, but that may include the disruption of CypA interactions with the replication complex of HCV or the proper folding of viral proteins (Yang et al., 2008). Synthetic non-immunosuppressive Cs derivatives are under development, such as alisporivir (formerly Debio 025) (Coelmont et al., 2010). Alisporivir is the first non-immunosuppressive, cell-specific inhibitor that results in a substantial reduction in HCV viral loads (Coelmont et al., 2009a; Coelmont et al., 2009b). Phase-3 clinical trials evaluating alisporivir are currently underway, with results from ESSENTIAL-2 expected in March 2013.

An alternate approach to developing antivirals is the potential to screen compounds that are already marketed to treat other disorders for antiviral activities (Schang, 2006). For example, artemisinin and ivermectin are more commonly known as antimalarial agents, but they reportedly have broad-spectrum antiviral activities against a number of important flaviviruses, including yellow fever virus (YFV), Japanese encephalitis virus (JEV), and tick-borne encephalitis viruses (TBEV), by mechanisms that are not yet fully defined (Efferth et al., 2008; Hodge, 2011).

Preventing viral infection altogether is the ideal strategy, with vaccines available against a number of important human diseases (**Table 1.3**). In the absence of effective vaccines, microbicides are a good choice to prevent or decrease transmission of sexually transmitted infections (STIs) (Haase, 2010). Topical microbicides act on cellular or viral targets to prevent infection of, or viral replication in, the primary target cells. They are grouped into five classes: (i)

surfactants, (ii) membrane disruptors, (iii) vaginal milieu protectors, and (iv-v) molecules that inhibit virus entry into cells by (iv) non-specific or (v) specific mechanisms.

The earliest microbicides tested (against HIV) were surfactants and membrane disruptors, for example nonoxynol 9 (N-9). Unfortunately, one study found an increase in HIV seroincidence when N-9 was used more than 3 times daily (Van Damme et al., 2002). In another study, no difference in the rate of HIV infection was associated with N-9, and N-9 increased the incidence of genital ulcers (Roddy et al., 1998). In retrospect, the increase in susceptibility to infection by non-specific surfactants and membrane disruptors could perhaps have been anticipated (Beer et al., 2006).

Moderately specific microbicides are also being developed (against HIV). These interact with virion envelope proteins through their negative charge, interfering with HIV attachment to CD4 cell surface receptors (Schols et al., 1990). PRO2000, a naphthalene sulfonate polymer, targets HIV gp120 to prevent attachment to CD4 (Keller et al., 2006). One phase 3 trial of a 0.5% PRO 2000 gel demonstrated a 30% reduction in transmission rates (2009, HPTN 035 trial; 3087 participants), while another showed that 0.5% PRO 2000 gel offered no protection against HIV acquisition (2009, MDP301; 9385 women). It has since been revealed that postcoital lavages and seminal plasma interfere with the antiviral activities of PRO 2000 (Keller et al., 2010). Another agent of interest is cellulose sulfate (Ushercell), which binds the V3 loop of HIV gp120 to inhibit CXCR4 or CCR5 tropic viruses (Scordi-Bello et al., 2005). However, its phase 3 trial was

halted because of higher HIV seroincidence in the cellulose sulfate arm (Van Damme et al., 2008).

The success of antiretroviral therapy (ART) in preventing mother-to-child transmission has generated interest in developing therapeutic drugs as prophylactic microbicides. Tenofovir was the first antiretroviral drug evaluated as pre-exposure prophylaxis, as a proof-of-concept (Tsai et al., 1995).

Pharmacokinetic data indicated low levels of systemic tenofovir absorption in women enrolled in phase 2 studies (Hillier, 2008). For the first time in a phase 3 trial, a vaginal gel formulation (1% tenofovir) has shown promise, with an estimated overall reduction of HIV acquisition by 39% (Karim et al., 2010).

1.1.1.3 Challenges of current antiviral chemotherapies and strategies

Vaccination is arguably the strategy of choice to prevent viral infections.

However, the challenges of worldwide vaccination strategies, coupled with the duration of protective immunity, have sometimes limited attempts to successfully eradicate viral diseases, such as hepatitis B or polio. To control HBV infection, the World Health Organization recommends the introduction of hepatitis B immunization at birth yet HBV chronically infects 400 million people worldwide.

The influenza virus vaccine must be updated every season (due to genetic reassortments), to protect against the most recent and commonly circulating viruses. No effective vaccine is yet available to protect against diseases caused by other important human pathogens, such as HCV (Yu and Chiang, 2010) or HIV (Virgin and Walker, 2010). Some important challenges for structure-based HIV

vaccine design, for example, include the rapidly mutating variable regions of exposed type-specific epitopes and the shielding of conserved glycoprotein epitopes by steric barriers such as glycans, which ultimately hinder the access of neutralizing antibodies (Schief, 2009). As efforts to develop effective vaccines continue, so too does the continued reliance on anti-infective drugs.

Anti-infective drugs target differences between infectious agents and hosts (De Clercq, 2004). Targeting viral proteins, for example, confers specificity for infected cells. Unfortunately, antivirals targeting viral proteins suffer several limitations. They promptly select for resistant variants that render the drug ineffective and thus require constant surveillance (Pillay, 2007). The number of “drugable” viral targets is also limited, with most clinical antivirals acting on only two classes of enzymes: polymerases or PRs (De Clercq, 2007b). Many are specific or efficient against only one species, strain, or even genotype. Drugs targeting cellular proteins required for viral replication may help to overcome these and related limitations (Schang, 2006). Inhibition of cellular proteins required for multiple viral functions could minimize the potential for selection for resistance. A large number of cellular proteins are required for the replication of viruses that encode only a few proteins. Moreover, many cellular proteins are required for the replication of even distantly related viruses. Drugs targeting cellular proteins thus have the potential to have activities against a broad spectrum of viruses. However, targeting cellular proteins can also generate negative side effects. Understanding the limitations of current antiviral strategies is critical for developing more effective antiviral agents and therapies.

1.1.1.3.1 Resistance

Selection for resistance is the major clinical limitation to antiviral chemotherapies. Viral polymerases are low fidelity, with viral RNA polymerases even lacking proof-reading 3'-5' exonuclease activity (Lauring and Andino, 2010). Consequently, the viral polymerases have high mutation rates. The distribution of genomes in any virus population is therefore continuously variable (quasispecies diversity). Viral quasispecies are defined by a dominant sequence and a spectrum of mutants. A previously minor population may become the dominant sequence following a change in the environment. The initiation of antiviral chemotherapy, for example, often promptly selects for drug-resistant species.

The genetic barrier to resistance is defined by the number and location of mutations required to confer resistance. Resistance can occur following a single mutation. A single nucleotide point mutation, for example, leads to an amino acid substitution (e.g. methionine 184 to valine or isoleucine, or M184V/I), which confers resistance to lamivudine (Fischer and Tyrrell, 1996). Mutations that confer drug resistance can have a detrimental effect on viral fitness in comparison to wild-type virus (with wild-type virus being defined as the most frequent genome). Consequently, primary drug resistance mutations are often followed by compensatory mutations to improve replicative fitness. In other cases, therefore, resistance to a drug requires multiple mutations. Moreover, multiple resistance mechanisms can exist for a single drug. The selection for HSV variants that are resistant to ACV, for example, is associated with mutations occurring either in the viral TK gene or promoter region, or in the viral DNA polymerase gene (Coen

and Schaffer, 1980). Three mechanisms of selection for ACV-resistance are common: a loss of TK activity (TK-deficient virus), an alteration of TK substrate specificity (TK-altered virus), or alteration of DNA polymerase sensitivity to ACV-triphosphate (Larder, Cheng, and Darby, 1983).

Resistance has been identified against every clinical antiviral, but it is particularly well analyzed in ART (Menendez-Arias, 2010). Two general modes of resistance to NRTIs have been elucidated (McColl et al., 2008). The first are mutations that primarily involve residues in direct contact with the incoming NRTI triphosphate. These mutations affect the binding and incorporation of the incoming nucleotide analogue. A classic example is M184V/I resistance to lamivudine. This substitution of hydrophobic amino acids causes steric hindrance and prevents lamivudine binding to the active site of the HIV RT (Sarafianos et al., 1999). A second mode of NRTI resistance results from mutations in proximity to the triphosphate binding site, which increases the rate of excision of chain-terminating NRTI. Such mutations were originally named thymidine-associated mutations (TAMs) due to their frequent selection by thymidine analogues such as zidovudine or stavudine.

Resistance to NNRTI is also well documented. NNRTIs are characterized by low genetic barriers to resistance. Consequently, NNRTIs are recommended only in combination with at least two other non-NNRTIs. The prevalent NNRTI resistance substitutions are lysine to asparagine at position 103 (K103N) and tyrosine to cysteine at residue 181 (Y181C) (Tambuyzer et al., 2009). NNRTI binding to RT depends on hydrophobic ring stacking interactions with tyrosine

181. Substitutions by non-aromatic amino acids at position 181 therefore reduce the binding affinity. The other prevalent NNRTI resistance mutation, K103N, also inhibits effective binding of the NNRTI. However, the mechanism is as yet unknown. The K103N mutation has little impact on HIV-1 viral fitness.

Resistance to all the PIs against HIV has been well documented (Wensing, van Maarseveen, and Nijhuis, 2010). First, a substitution in the substrate-binding cleft is selected for. This mutation typically enlarges the catalytic site of the enzyme, causing a decrease in binding avidity for the protease inhibitor. These mutations also tend to impair the binding of the natural polyprotein substrate. Minor or secondary mutations are later selected for, and they improve and restore replicative fitness. These have no substantial effects on inhibitor binding, but do improve the proteolytic efficiency of the resistant enzyme, thus increasing replication of the resistant variant (Nijhuis et al., 1999). Compensatory mutations can occur in the genes encoding for the polyprotein substrate too, typically near the protease cleavage site. It is proposed that they adapt the virus to the altered substrate-binding cleft of the mutant drug-resistant viral protease (Mammano, Petit, and Clavel, 1998). Major PI-resistance mutations have been identified at 15 protease codons, and minor ones at an additional 19 (Johnson et al., 2009).

The barrier to resistance to the HIV fusion inhibitor enfuvirtide has also been characterized (Lu et al., 2006). Resistance is conferred by primary mutations that cluster within the gp41 heptad repeat 1 (HR1) domain bound by enfuvirtide (Sista et al., 2004; Wei et al., 2002). Primary mutations in HR1 decrease the efficiency of fusion, but compensatory mutations in a complementing domain

(heptad repeat 2; HR2) restore it (Ray, Blackburn, and Doms, 2009). Resistance against newer anti-HIV drugs has also been characterized. Even resistance to the IN inhibitor raltegravir has already been selected for. Both primary and compensatory mutations map to the catalytic core domain near the binding site (McColl and Chen, 2010).

Resistance has also been described against the lone small molecule antiviral (maraviroc) specific for the interactions between a viral entry protein and its cellular receptor. Resistance to maraviroc can occur by selecting for variants that utilize CCR5 for entry despite the presence of the drug (Westby et al., 2007). Variants that use inhibitor-receptor complexes for entry have mutations in gp120 (Ogert et al., 2008) or in gp41 (Anastassopoulou et al., 2009). A second mechanism of maraviroc-resistance is the outgrowth of X4-tropic virus (Scarlati et al., 1997).

Despite the introduction of HAART, even triple combination therapies eventually select for drug resistance (Phillips et al., 2007). The role of transmitted resistance in the failure of a first-line therapy has become apparent with the growing number of patients on therapy. Transmitted resistance to at least one antiviral drug was established in 6-16% of patients in one study (Ross et al., 2007). Genotypic analysis prior to selecting initial treatment regimens in naïve patients has consequently been recommended.

Resistance to drugs used against other viruses is also common. Resistance to the anti-influenza agents targeting the homotetrameric M2 hydrogen ion channel has been characterized. The four transmembrane domains that form the

four-helix bundle act as a pH-activated proton channel. Histidine 37 (H37) is the pH sensor in the channel and tryptophan 41 (W41) forms the gate (Sharma et al., 2010). The crystal structure of the transmembrane-spanning region of the homotetrameric M2 protein has been solved (Stouffer et al., 2008). Both H37 and W41 lie near the channel exit, or gate, consistent with their functions.

Rimantadine and amantadine are both allosteric inhibitors that bind near the gate. Their binding stabilizes the closed conformation of the channel. In this conformation, the four transmembrane helices are tightly packed. Resistance mutations perturb the helix-helix interface to facilitate channel opening.

The resistance mutation leading to a substitution of histidine 274 to tyrosine (H274Y) in influenza NA is a common cause of resistance against oseltamivir. H274 is located near the substrate-binding pocket of NA (Russell et al., 2006). The H274Y mutation causes subtle structural alterations that weaken oseltamivir binding affinity (Collins et al., 2008). The severity of impairment of viral growth and infectivity of H274Y mutants led to the assumption that this was not a clinically relevant variant (Herlocher et al., 2004). However, the H274Y mutation emerged (apparently spontaneously) during the worldwide H1N1 outbreak of 2008/2009 (Moscona, 2009). Bloom et al. characterized another mutation that resulted in a decreased expression of NA at the virion membrane, and that conferred resistance to oseltamivir (Bloom, Gong, and Baltimore, 2010).

The mechanisms of resistance to the standard treatment against HCV (ribavirin and pegIFN) are not as well characterized as those of specific agents targeting proteins. It is proposed that failure to clear HCV infection is likely a

consequence of several factors, including treatment regimen (initiation, duration), patient characteristics and viral-related factors (Pawlotsky, 2000). The mechanisms of resistance to the two new anti-HCV drugs, boceprevir and telaprevir, which target the NS3/4A serine protease are also emerging. Several factors appear to contribute to the selection for resistance-associated variants (RAVs), such as genotype and ethnicity. For example, a higher rate of development of RAVs in patients infected with genotype 1a compared to genotype 1b was observed in two phase 3 trials (SPRINT-2; 1a: 58%, 1b: 48%; RESPOND-2; 1a: 48%, 1b: 41%) (Hazuda et al., 2011). Also, RAVs V36M and R155K (located in the binding pocket) were more common in patients infected with genotype 1a, while T54A/S, A156S, and V170A were more common in genotype 1b patients (Welsch et al., 2008). Such RAVs also occur in telaprevir treatment (Hiraga et al., 2011). RAVs were also more frequent (68%) in patients with poor (<1 log viral load decline at treatment week 4) IFN response compared to patients (31%) with good (≥ 1 log viral load decline at treatment week 4) IFN response (Hazuda et al., 2011).

Resistance profiles are more complex in patients co-infected with multiple viruses, for example HBV and HIV. Agents such as emtricitabine, tenofovir and lamivudine have activity against both viruses. In some cases, only one infection requires treatment. For example, when only HBV infection requires treatment (CD4 counts >350 cells/mm³), agents with little or no anti-HIV activity are recommended so as to avoid the introduction of drug-selective pressures against HIV (which could compromise subsequent ART) (Soriano et al., 2010). However,

following this principle can sometimes be difficult. For example, entecavir was reported to have no relevant anti-HIV-1 activity (Innaimo et al., 1997), but entecavir treatment of HIV and HBV co-infected patients lead to the selection for HIV-1 variants with the entecavir-, lamivudine- and emtricitabine-resistant M184V mutation (McMahon et al., 2007). Such resistance profiles argue against treating HBV/HIV-1 co-infected patients who are not receiving fully suppressive anti-HIV drug regimens.

1.1.1.3.2 Specificity

Most current antiviral drugs inhibit virus-encoded enzymes that are essential for viral replication. Despite their success, many of these drugs are specific to only one type of any given virus. For example, all NNRTIs and nine of eleven PIs are highly specific to HIV-1 (Balzarini, 2004). Other drugs are only effective against specific genotypes. Ribavirin (with pegIFN) is efficacious in approximately 80% of individuals infected with HCV genotype 2 or 3. Unfortunately, this treatment regimen results in SVR in less than 50% of patients infected with genotype 1 (the most prevalent in America, Europe, China and Japan) (Schinazi, Bassit, and Gavegnano, 2010). Drug specificity is also further limited for viruses that display a high prevalence of intra-patient variants or heterogeneity, such as HCV (Gonzalez-Candelas and Lopez-Labrador, 2010). HCV replicates very rapidly, with approximately 10^{12} virions produced in an infected patient per day, and it has six main genotypes and more than 50 subtypes (Suzuki et al., 2007).

The specificity of the anti-HIV drug maraviroc is even further limited by disease progression and treatment experience. Maraviroc is effective against only R5-tropic HIV, and is limited to treatment-naïve patients (Moyle et al., 2005). In treatment-experienced patients, there is an increase in variants that use CXCR4 as co-receptor (X4- or R5/X4 HIV dual tropic) (Melby, 2007). The percentage of persons infected with R5-exclusive tropic virus also decreases with disease progression (Hoffmann, 2007), rendering maraviroc ineffective in patients in advanced stages of the disease. The narrow spectrum of action of current antivirals targeting proteins, or their interaction with cellular ones, is a major limitation to their use.

The number of potential viral targets is also limited. Some viruses have small genomes and encode only a few enzymes with known binding pockets for small molecules considered “drugable”. Human papillomavirus (HPV), for example, encodes two tumor-promoting proteins (E6 and E7), but it does not encode polymerases or other enzymes necessary for viral replication (Moody and Laimins, 2010). Only four known genes are encoded by the HBV genome: C (core protein), P (DNA polymerase), S (surface antigen) and X (putative transcriptional transactivator). The deadly filoviruses Ebola and Marburg also have only limited genome sizes which encode only 7 structural proteins (Dolnik, Kolesnikova, and Becker, 2008).

Other viruses, such as influenza, constantly undergo genetic reassortments. The envelope binding and fusion glycoproteins required for entry are typically among the most variable virus-encoded proteins, and thus they pose

additional challenges for the development of drugs specific for proteins (and for vaccines).

1.1.1.3.3 Intracellular metabolism

Most currently approved antivirals act intracellularly to inhibit viral enzymes. Many of these drugs are hydrophilic molecules with limited membrane permeability. Their activities are thus dependent on their cellular entry, which may occur by passive diffusion or carrier-mediated transport. Others require intracellular metabolism to be converted into their active form. The same molecules are also subject to catabolism and are eliminated from the infected cell or host.

Many antiviral drugs are transported across the plasma membrane and also mobilized from intracellular compartments. Multiple members of the solute carrier superfamily transport nucleoside and nucleotide analogues, and consequently, function in their uptake, efflux and elimination (Izzedine, Launay-Vacher, and Deray, 2005b). The most important of these are the concentrative nucleoside transporter (CNT), equilibrative nucleoside transporter (ENT), organic anion transporter (OAT), organic cation transporter (OCT), peptide transporter (PEPT) and multidrug resistance protein (MRP) (Pastor-Anglada et al., 2005). Many of these exist as multiple isoforms, each with varying substrate preference and tissue distribution, which influence intracellular drug concentrations in different cells, compartmentalization, plasma levels and excretion. For example, the extracellular transport of antivirals by adenosine triphosphate (ATP)-binding

cassette family proteins (efflux pumps) contributes to reduced drug susceptibility. The MDR related protein 4 (MRP4) is a resistance factor for adefovir (Schuetz et al., 1999). Tenofovir is also a substrate for MRP4 that is expressed on renal proximal tubule epithelial cells (Ray et al., 2006), and its metabolism thus leads to high EC₅₀ values against HIV and renal toxicity (Szczech, 2008). In clinical formulations, the two negative charges of ANPs are masked with dipivoxil or disoproxil fumarate, which improve oral absorption but not toxic limitations (De Clercq and Holy, 2005). The related transporters MRP5 and MRP8 transport several NRTIs (Guo et al., 2003).

All nucleoside analogues that target viral polymerases require anabolic multi-step phosphorylation for activation. The cellular kinases that most commonly catalyze the first and activating phosphorylation of nucleoside analogues are those involved in nucleoside salvage pathways. These are cytosolic deoxycytidine kinase (dCK) and thymidine kinase 1 (TK1), mitochondrial TK2, and deoxyguanosine kinase (Deville-Bonne et al., 2010). The addition of the second phosphate group is most commonly catalyzed by the nucleoside monophosphate (NMP) kinases thymidylate kinase, uridylate-cytidylate kinase, adenylate kinases 1-5 and guanylate kinase (Van Rompay, Johansson, and Karlsson, 2000). The third activating phosphorylation can be catalyzed by various enzymes, including nucleoside diphosphate (NDP) kinase, phosphoglycerate kinase, pyruvate kinase and creatine kinase (Bourdais et al., 1996). Some nucleoside analogues must be even further modified before they are active.

Abacavir, for example, is converted by deamination to the 5'-triphosphate of the corresponding guanosine analogue (carbovir).

The activities of nucleoside kinases are counterbalanced by those of 5'-nucleotidases, which dephosphorylate nucleoside monophosphates (Hunsucker, Mitchell, and Sychala, 2005). In addition to dephosphorylation, some nucleoside analogues are subject to other catabolism. Cellular nucleoside degradation pathways by depurination and depyrimidation, or by glucuronidation, also reduce the levels of active antivirals. The integrase inhibitor raltegravir, and NRTIs such as zidovudine, didanosine, stavudine and abacavir, are excreted as metabolites (Cihlar and Ray, 2010). For example, zidovudine is metabolized by uridine diphosphate glucuronosyltransferase (UGT) and excreted in the urine as its 5'-O-glucuronide (Resetar and Spector, 1989).

Another major challenge is to develop compounds that are not metabolized by cytochrome P450 enzymes, a metabolism that contributes to both drug toxicity and drug elimination. PIs, such as saquinavir and indinavir and some NRTIs (zidovudine) have extensive first-pass metabolism by the hepatic and intestinal cytochrome P450 3A system, thus greatly reducing their bioavailability in systemic circulation (Fitzsimmons and Collins, 1997). To circumvent elimination, most PIs are boosted with ritonavir, which inhibits cytochrome P450 3A (Koudriakova et al., 1998). Ritonavir consequently acts as an enhancer that improves the bioavailability and half-life of PIs (Zeldin and Petruschke, 2004).

Drug metabolism also influences combination therapies. Some combinations are contraindicated due to reduced efficacy or increased toxicities.

Drugs activated by the same kinase are contraindicated, for example, as they compete for the kinase. The two NRTIs zidovudine and stavudine are both monophosphorylated by TK1 and TK2. Zidovudine and zidovudine monophosphate have a stronger affinity for TK1 and TK2, which results in reduced levels of stavudine triphosphate when the two NRTIs are combined (Ho and Hitchcock, 1989). Likewise, lamivudine and zalcitabine are also contraindicated because both are dependent on dCK for activation (Veal et al., 1997). Drugs that modulate CYP450s, either by inducing or inhibiting their activities, or that block transporters of antiviral drugs (e.g. PIs), require dosing adjustments in combination therapies to avoid related toxicities (Izzedine, Launay-Vacher, and Deray, 2005a). For example, maraviroc is principally metabolized by CYP3A4 to inactive metabolites, and it is also a substrate for the efflux transport protein P-glycoprotein (P-gp). Maraviroc dosing must therefore be doubled when it is co-administered with CYP3A4 inducers such as efavirenz, or reduced by 50% when co-administered with P-gp inhibitors such as saquinavir and elvitegravir (Abel, Back, and Vourvahis, 2009).

1.2 Viral entry

Viral entry is an attractive antiviral target, as drugs targeting entry can prevent infection altogether. Entry of all viruses depends on interactions between virion glycoproteins and cell receptors. The mechanisms whereby viruses enter host cells also depend on whether they have a host-cell derived lipid bilayer (envelope).

1.2.1 Entry of enveloped viruses

Several enveloped viruses are important human pathogens, including HIV, HCV, influenza virus and HSV. HIV is a 180-nm diameter, spherical retrovirus. The HIV virion contains two copies of the single-stranded (ss) positive-sense 9.8 kb RNA. Hepatitis C virus is a 50-nm diameter, spherical flavivirus. The HCV virion contains one copy of the ss positive-sense 9.6 kb RNA. Influenza virus is an 80- to 120-nm diameter, spherical orthomyxovirus. The influenza virion contains segmented negative-sense ssRNA of 14 kb. HSV is a 200-nm diameter, spherical herpesvirus. The HSV virion contains a double-stranded (ds) 150 kb DNA genome. Some enveloped viruses, such as HIV and HSV, enter by pH-independent fusion with the plasma membrane, whereas others, such as influenza viruses, rhabdoviruses and flaviruses, enter by pH-dependent fusion with endocytic vesicles.

Despite differences in pH-dependence, virion morphology, protein composition and cell receptors, entry of all enveloped viruses share some common features. Following attachment and receptor binding, virion glycoproteins undergo conformational changes that expose their fusion peptides (FPs), bring virus and cell membranes into close apposition, and trigger membrane fusion. The mechanisms of entry of a select few viruses are presented below.

1.2.1.1 Hepatitis C virus entry

The HCV envelope glycoproteins E1 and E2 mediate HCV entry. E1 and E2 form non-covalent heterodimer complexes at the virion surface (De Beeck et al., 2004). HCV E2 is thought to be primarily responsible for receptor binding to cellular receptors and co-receptors, while HCV E1 is proposed to be the fusion protein. Sequence analysis of E1 suggests that it may contain a putative FP in its ectodomain (Garry and Dash, 2003). However, structural homology of E2 with fusion proteins of other viruses suggests E2 is the fusion protein (Yagnik et al., 2000). Many details of HCV entry, including the identity of the fusion protein and the characterization of the route of entry, remain to be fully elucidated (von Hahn and Rice, 2008).

Several putative HCV receptors or co-receptors have been identified, including scavenger receptor class B type I (SR-BI) (Scarselli et al., 2002), the surface receptor cluster of differentiation 81 (CD81) (Pileri et al., 1998) and tight junction components claudin 1 (Evans et al., 2007) and occludin (Ploss et al., 2009). SR-BI is best characterized for its role in facilitating the uptake of cholesterol esters from high-density lipoproteins in the liver, whereas CD81 is a member of the tetraspanin superfamily. Plasma-derived HCV infectivity is enhanced by interactions with low- and very-low density lipoproteins, although the mechanisms whereby lipoproteins enhance infectivity are not well understood (von Hahn and McKeating, 2007).

Following attachment, HCV virions are internalized by clathrin-dependent endocytosis (Meertens, Bertaux, and Dragic, 2006). Studies using HCV

pseudoparticles (HCVpp; retroviral particles pseudotyped with HCV E1/E2) revealed that endocytic uptake is slow. Only 50% of HCVpp reach a proteinase K-protected compartment (indicative of internalization) 53 minutes after the initiation of entry, suggesting additional interactions or trafficking are required for fusion and entry (Meertens, Bertaux, and Dragic, 2006). Low endosomal pH triggers fusion between the viral envelope and the endosomal membrane (Tscherne et al., 2006). Low pH treatment of HCV prior to cell binding does not inactivate virions, suggesting the glycoproteins must be primed first to then become pH-sensitive only after binding (Tscherne et al., 2006). Recent evidence indicates that virion binding to CD81 may be necessary and sufficient to render E1E2 competent for fusion with acidic intracellular compartments (Sharma et al., 2011).

1.2.1.2 Sindbis virus entry

Sindbis virus enters cells by clathrin-mediated endocytosis. The Sindbis virion envelope contains two transmembrane glycoproteins, E1 and E2. E1 and E2 heterodimers assemble into trimers during maturation and form the spikes that protrude at the virion surface. E2 mediates virus binding to cellular receptors, whereas E1 is primarily responsible for virus-cell fusion.

Sindbis virion binding is mediated by E2, which binds to the high-affinity laminin receptor (Wang et al., 1992). Receptor binding and low endosomal pH induce the disassociation of E1/E2, thus exposing E1 trimers and the FP. Insertion of the FP into the target membrane then triggers energetically favorable

rearrangements (that release free energy), which ultimately bring the two membranes into close apposition for fusion and entry into the host (Glomb-Reinmund and Kielian, 1998).

1.2.1.3 Vesicular stomatitis virus entry

Vesicular stomatitis virus (VSV) also enters cells by clathrin-mediated endocytosis (Sun et al., 2005). A single protein, the G protein, mediates VSV entry. VSV G protein functions in viral entry by attachment to the as-yet-unknown host cell receptor. Virus entry is enhanced by the presence of phosphatidylserine in the target membrane, which is proposed to function at a postbinding step (Carneiro et al., 2006; Coil and Miller, 2005).

VSV enters by clathrin-mediated and adaptor-protein complex 2 (AP-2)-independent mechanisms (Johannsdottir et al., 2009). Although AP-2 has long been considered a core component of clathrin-coated vesicles, alternative adaptor proteins have been identified (Conner and Schmid, 2003; Robinson, 2004). VSV entry is dynamin-dependent. Internalization and penetration occur in less than 5 minutes (Johannsdottir et al., 2009). The G protein then mediates fusion of the virion envelope with the endosomal membrane by undergoing sequential conformational changes that bring the two membranes into close apposition and triggers their fusion. The structural rearrangements and insertion of the FP into the cell membrane ultimately creates a fusion pore (by a process discussed in **section 1.3.3.1**), through which the viral core enters the cell.

1.2.1.4 Vaccinia virus entry

The mechanisms whereby vaccinia virus (VV), and other poxviruses, enters cells are as yet unclear. Two infectious enveloped forms of VV are produced in infected cells. The intracellular mature virion (MV), which contains a DNA-protein core surrounded by a lipoprotein membrane, can be released by cell lysis (Condit, Moussatche, and Traktman, 2006). In addition, a subset of MVs are wrapped in additional membranes, are transported to the periphery of the cell and are released as double-enveloped virions (extracellular enveloped virion, or EV) (Doms, Blumenthal, and Moss, 1990). Approximately 20 proteins are associated with the MV membrane and six with the EV membrane. At least eight proteins have been proposed to mediate or regulate VV entry and membrane fusion (Moss, 2006). The cellular receptors and membranes to which vaccinia virions bind and fuse, respectively, also appear to differ depending on the infectious form, strain or even cell type (Roberts and Smith, 2008; Whitbeck et al., 2009).

1.2.2 Entry of nonenveloped viruses

1.2.2.1 Poliovirus entry

The poliovirus (PV) receptor is cluster of differentiation 155 (CD155), a type I transmembrane glycoprotein important for the establishment of intercellular tight junctions between epithelial cells (Mendelsohn, Wimmer, and Racaniello, 1989). The precise mechanism and site of PV entry remain unclear. Two entry pathways have been suggested (Tsai, 2007). Entry of the viral nucleic acid may occur via the formation of a pore in the plasma membrane through which the viral RNA is

injected into the host cell cytoplasm, or the virus may be taken up by receptor-mediated endocytosis (Brandenburg et al., 2007; Hogle, 2002). Under the second model, the viral RNA is released immediately following internalization, which is proposed to occur by actin-dependent and clathrin-independent mechanisms (Brandenburg et al., 2007).

1.2.2.2 Adenovirus entry

Adenovirus (AdV) entry is mediated by the trimeric fiber proteins projecting from the icosahedral capsid, which is composed of 252 capsomers (12 of which are pentons, 240 of which are hexons). The initial attachment of AdV to host cells is mediated by a high-affinity interaction between the capsid fiber knob to its receptor, which in most cells is the Coxsackie's and adenovirus receptor (CAR) (Bergelson et al., 1997). Secondary interactions between the penton base (non-covalently associated with the fiber protein) with α_v integrins facilitate virion uptake (Wickham et al., 1993). Subsequent AdV internalization occurs by clathrin-mediated endocytosis. The precise molecular events involved in AdV disassembly are not well known (Nemerow et al., 2009), but they are proposed to require the release of the internal capsid protein VI and the lysis of endosomes (Wiethoff et al., 2005).

1.3 Membrane fusion

Most cellular compartments are delimited by membranes. The movement of contents between such compartments is in part dependent on membrane fusion,

whereby two separate lipid bilayers merge to become one continuous bilayer. Biological fusions occur between cells, between different intracellular compartments, or between intracellular compartments and the plasma membrane. Synaptic release of neurotransmitters, fertilization, and intracellular membrane trafficking, for example, all require the fusion of lipid bilayers (reviewed in Martens and McMahon, 2008). Entry of enveloped viruses is also dependent on fusion of their envelope with cell membranes.

Lipid bilayers do not fuse spontaneously. Specific proteins control the events leading to the merger of two separate lipid bilayers. Moreover, a source of energy to overcome the energy barrier is required. Biomembrane fusion is therefore dependent on the interactions between proteins and lipids located within, or that interact with, fusing membranes (Chernomordik and Kozlov, 2003).

1.3.1 Viral fusion

The roles of virion glycoproteins in fusion are well characterized. The subcellular location of viral fusion varies, and each fusion protein class has distinct properties. Nonetheless, viral fusion proteins all share the common feature of driving the membrane fusion reaction leading to entry. Fusion between the virion envelope and cell membrane is triggered by specific glycoproteins in the virion envelope, which undergo structural rearrangements and provide the energy to merge lipid bilayers. Viral fusion is dependent on virion fusion proteins, cellular receptors, and the lipids of the fusing bilayers. Viral fusion has historically been a

most useful model in the study of biomembrane fusion (Weissenhorn, Hinz, and Gaudin, 2007).

1.3.1.1 Viral fusion proteins

Viral fusion proteins on the surface of mature virions are in fusion-competent states. Upon their activation, these glycoproteins undergo extensive structural refolding that ultimately leads to membrane fusion. Fusion proteins are proposed to drive fusion by coupling protein-refolding events to juxtaposition of the virion envelope and cell membrane (White et al., 2008).

Fusion proteins are anchored into the virion envelope by C-terminal transmembrane helices and contain FP segments (at or near the N-terminus) that insert into the target membrane. Fusion peptides are typically short stretches of small apolar residues, usually rich in glycine, leucine, isoleucine and alanine. Fusion peptides have a high propensity to insert into membranes (Epanand, 2003). Fusion proteins also contain complementary heptad repeats (HRs) important for their refolding during the fusion process.

The structural rearrangements of virion glycoproteins are activated by receptor binding or low pH protonation (Kielian and Rey, 2006). An activated fusion protein undergoes structural refolding to form a so-called pre-hairpin intermediate, a homotrimer of the fusion subunit. Pre-hairpin formation exposes and relocates the FP, which inserts into the target membrane. The insertion of the FP into target membranes results in pre-hairpin intermediates simultaneously anchored to the virion envelope and target cell membrane. Then, the HR domains

of the fusion subunits fold back onto themselves to form highly reorganized and thermodynamically stable coiled-coils, the so-called six-helix bundle (6HB), or stable hairpins. The final structure of all viral fusion proteins is the stable hairpin, a compact rod-like trimer-of-hairpin with the two critical hydrophobic elements (TM domain and FP) at the same end. These structures bring the two fusing membranes into close juxtaposition (White et al., 2008). All viral fusion proteins transition from a pre-fusion conformation to a post-fusion state as trimers-of-hairpins, releasing some of the free energy required for fusion (Jelesarov and Lu, 2001).

The viral fusion proteins are classified into class I, II or III by their oligomeric form at the virion surface, their three-dimensional structure and the location of the FP (reviewed in Backovic and Jardetzky, 2009, White et al., 2008).

1.3.1.1.1 Class I fusion proteins

Class I fusion proteins undergo proteolytic processing (priming) during virion maturation. These cleavages produce a primed fusion subunit, which is clamped by the binding subunit in the pre-fusion state. Both subunits together form heterotrimers at the virion surface. Trimeric organization in the pre- and post-fusion states is a characteristic of the class I fusion proteins. Class I fusion proteins consist mainly of helical structures, and their FP is located at or near the N-terminus of the fusion subunit. They are activated by low pH, receptor binding or both. The *orthomyxoviridae* (e.g. the influenza viruses), *retroviridae* (e.g.

HIV), *paramyxoviridae* (e.g. RSV), and *filoviridae* (e.g. ebola virus), for example, all encode class I fusion glycoproteins (**Table 1.4**).

The prototype class I fusion protein is the influenza HA protein, the structure of which was first determined in 1981 (Wilson, Skehel, and Wiley, 1981). HA is overall the best-characterized fusion protein. HA is synthesized as a precursor (HA0), which is then cleaved during virion assembly to produce two chains, HA1 and HA2. HA1 and HA2 remain linked by disulfide bonds at the virion surface. The HA1 globular head contains the receptor-binding domain, responsible for binding to sialic acid moieties. HA2 is the fusion subunit, containing the FP at its N-terminus.

Several pre- and post-fusion structures of HA have been determined by X-ray crystallography. These include the ectodomain of HA0 (Chen et al., 1998), the mature HA, the neutral pH conformation of HA2 (Wilson, Skehel, and Wiley, 1981), and the fusogenic form of HA2 (Bullough et al., 1994; Skehel et al., 1982). The fusion protein exists in two conformations, a fusion-competent conformation in complex with the receptor binding domain (Wilson, Skehel, and Wiley, 1981), and a stable fusion conformation (Bullough et al., 1994; Chen et al., 1998). The HA trimer is held together by coiled-coil interactions between long helices in the HA2 (fusion) subunit. The globular head of the trimer is formed by the HA1 chains (Bullough et al., 1994). These heads contain the receptor-binding site. The FP is contained in an exposed loop in HA0, or buried between helices at the base of the molecule near the site of attachment into the envelope in HA1-HA2 mature heterotrimers.

Protonation of key residues, likely implicating several histidines, has been reported for several fusion proteins activated by low pH, including those of influenza (Stiasny et al., 2009). The protonation of histidine residues is proposed to affect the salt bridges in HA1 and HA2, thus resulting in significant conformational rearrangements. These rearrangements move both the FP and the C-terminus of the ectodomain of HA2, which is otherwise anchored into the virion envelope, to near the top of the molecule at the cell-proximal end. The movement of HA1 is often referred to as “unclamping” of the HA2 fusion subunit. The two major HA2 rearrangements are “the FP extension” and “C-terminal inversion”, to form the 6HB (White et al., 2008). Formation of the 6HB brings into close proximity the FP, which is now anchored into the cell membrane, and the C-terminus of HA2, still anchored into the virion envelope. These two membranes are thus brought into close proximity by the formation of the 6HB, allowing their fusion.

The precise mechanisms by which these structural re-arrangements induce the merger of the two lipid bilayers are still poorly understood. FP must insert into the target membrane and the 6HB must form. Moreover, the TM domain is important, too. Truncation mutants with shorter cytoplasmic tails, or substitution of the TM domain with a glycosylphosphatidylinositol (GPI) anchor, block fusion (Armstrong, Kushnir, and White, 2000; Melikyan et al., 1997). Some steps in the refolding of HA upon activation also appear to be at least partially reversible (Leikina et al., 2002).

HIV also encodes a class I fusion protein. Like all class I fusion proteins, it is synthesized as a single polypeptide precursor (gp160) that is subsequently cleaved to generate two subunits, gp120 and gp41. The gp120 subunit consists of five conserved and five variable domains (Starcich et al., 1986), and it is responsible for receptor binding. HIV gp41 contains an N-terminal FP, two HR domains (HR1 and HR2) and a TM anchor. Glycoprotein 41 acts during fusion. Non-covalent gp120 and gp41 are assembled as trimers on the virion surface. In this prefusion complex, gp41 is largely occluded by gp120 and is primed for fusion, which is triggered upon receptor binding (Wyatt et al., 1998).

Receptor binding of gp120 to CD4 induces significant structural rearrangements. Receptor binding exposes a bridging sheet (consisting of 4 beta sheets) which, with variable loops V1/V2 and V3 of gp120, forms a co-receptor binding site (Kwong et al., 1998). Co-receptor binding induces additional rearrangements that fully expose HR1, HR2 and the gp41 FP, which is subsequently inserted into the host bilayer (Brasseur et al., 1988). Regions at the distal ends of the HR1 and HR2 domains are buried in the cellular and viral membranes, respectively. The two complementary HR1 and HR2 regions of gp41 then fold back onto each other, forming the thermostable six-helix coiled-coil bundle (Tan et al., 1997).

1.3.1.1.2 Class II fusion proteins

The crystal structure of fusion protein E of TBEV was solved in 1995 (Rey et al., 1995), revealing the existence of a second class of fusion proteins. Class II fusion

proteins often fold with a chaperone protein. The chaperone protein is cleaved during or after viral assembly, priming the fusion protein. In mature virions, the fusion protein ectodomains are organized as anti-parallel homo- or hetero-dimers, themselves in a parallel orientation relative to the virion surface. After low-pH triggering, class II fusion proteins realign as trimers that project perpendicularly from the virion envelope. The conformational rearrangements following activation of class II fusion proteins therefore involves a change in an irreversible oligomeric state, from dimers to trimers (Kielian and Rey, 2006). Further differing from class I, class II fusion proteins consist mostly of β -sheet structures. Their FP segments are composed entirely of a stretch of hydrophobic residues, and are internal, at the tip of a loop formed by anti-parallel β -strands.

The TBEV E protein is the prototype class II fusion protein (**Table 1.4**). The TBEV E protein is associated with the prM chaperone, which is cleaved during maturation. Pre-fusion E protein is an antiparallel homodimer (Rey et al., 1995). Its almost entirely β -sheet structure shields the FP of its partner E subunit. The dimer contacts between the subunits break during acidification. E subunits are then reorganized into trimers, with rotation of almost the entire protein around the C-terminal stem region. The three fusion loops (FLs) are in close contact, in a so-called “closed” conformation (Gibbons et al., 2004). The rearrangements then move the ectodomains toward the target membrane, into which the FLs insert. During the final stage of fusion, a flexible linker folds back at the side of each E protein, bringing together the C-terminal stem regions and the tip of the structures containing the FLs, driving lipid fusion.

1.3.1.1.3 Class III fusion proteins

The newest identified class of fusion proteins is class III. It was identified when the high-resolution crystal structures of both VSV G protein (at low pH) and HSV glycoprotein B (gB) were solved (Heldwein et al., 2006; Roche, 2006). Despite the lack of sequence homology, the secondary structures and putative FL locations of HSV gB and the post-fusion state of the VSV G protein were essentially the same. The HSV gB structure solved was therefore proposed to also be in a post-fusion state. Class III fusion proteins are encoded by members of the *rhabdoviridae*, *herpesviridae* and *baculoviridae* families (**Table 1.4**).

Class III fusion proteins share certain characteristics with class I fusion proteins, and others with class II. They contain a central α -helical trimeric coiled-coil core, which is reminiscent of the class I proteins in post-fusion states. However, the domains of class III fusion proteins are predominantly made of β -sheets, similarly to those of class II fusion proteins. They also contain an internal bipartite FP segment composed of two rigid loops that are part of an elongated β -hairpin formed by anti-parallel β -strands (Backovic and Jardetzky, 2009). Class III FP segments also contain charged residues and at least one aromatic polar residue, usually tryptophane (W) or tyrosine (Y).

The VSV G protein is the only class III protein for which the structures of both the pre- and post-fusion states have been solved (Roche, 2006; Roche et al., 2007). The VSV G FP segment is composed of two exposed loops, WY⁷²⁻⁷³ and YA¹¹⁶⁻¹¹⁷, at the tip of the molecule, with W⁷²⁻⁷³ being the most important (Sun, Belouzard, and Whittaker, 2008). The conformational changes of VSV G induced

by low pH are reversible, and fusogenicity can be fully recovered by neutralization (Gaudin et al., 1991).

The crystal structure of the trypsin-cleaved ectodomain of HSV-1 gB (which removed ~80 residues from the N terminus) was solved at 2.1 angstrom resolution by Heldwein et al. (2006). It revealed a trimeric structure with a coiled-coil core suggestive of a fusion protein (Heldwein et al., 2006). Its structural similarities to the VSV G protein (Roche, 2006) indicates that gB is the HSV-1 fusion protein. Two analogous loops in HSV-1 gB, VWFGHRY¹⁷³⁻¹⁷⁹ (FL1) and RVEAFHRY²⁵⁸⁻²⁶⁵ (FL2), were proposed to form a bipartite FP, but were also suggested to be suboptimal for membrane insertion (Heldwein et al., 2006). Mutational studies with gB have confirmed the importance of residues W¹⁷⁴, Y¹⁷⁹ and A²⁶¹ (Hannah et al., 2007) and its association with target membranes (Hannah et al., 2009). Mutation of any of these three residues within the putative FL segments reduces or abolishes gB binding to liposomes (Hannah et al., 2009). Moreover, the crystal structures of uncleaved wild-type HSV-1 gB and W174R and Y179S mutant gB indicate that the FL2 undergoes important conformational changes for fusion (Stampfer et al., 2010). The EBV gB crystal structure also displays structural similarities to HSV-1 gB (Backovic, Longnecker, and Jardetzky, 2009). VSV G or baculovirus gp64 are the only proteins required to induce fusion of their respective viruses. In contrast, HSV-1 fusion requires several additional viral proteins (discussed in **section 1.4.2.1.3**).

1.3.1.2 Lipids in viral fusion and replication

Ultimately, the fusion of virion envelopes with cell membranes, and therefore viral infection and replication, are dependent on the merger of the two lipid bilayers. The roles of lipids in these processes, however, are less characterized than those of their protein or nucleic acid counterparts (Teissier and Pecheur, 2007).

All enveloped viruses acquire their lipid envelopes from host membranes. Plasma membranes and intracellular membranes of different organelles differ in their lipid composition (van Meer, Voelker, and Feigenson, 2008). It is thus proposed that the lipid composition of virion envelopes should resemble that of the host membrane from which they bud.

The major structural lipids in mammalian cell membranes are glycerophospholipids, sphingolipids and sterols (van Meer, Voelker, and Feigenson, 2008). Glycerophospholipids consist of one or two saturated or *cis*-unsaturated fatty acyl chains covalently ester-linked to a glycerol. According to their hydrophilic headgroups, they are classified as phosphatidylcholine (PC), phosphatidylethanolamine (PE), phosphatidylserine (PS), phosphatidylinositol (PI) and phosphatidic acid (PA) (**Figure 1.2**), among others. The hydrophobic backbone of sphingolipids consists of a ceramide core sphingosine amide-linked to two fatty acids chains. Animal sphingolipids generally have one saturated and one *trans*-unsaturated acyl chain. Structural sphingolipids commonly contain a phosphocholine or phosphoethanolamine polar headgroup. Phosphocholine is the

most common of the two, producing sphingomyelin (SM). Cholesterol is the most abundant sterol in mammalian cells.

Earlier work aimed at comparing the lipid compositions of virions grown in different cells types, or that of otherwise unrelated enveloped viruses grown in the same cell type. Such studies used conventional analytical methods (such as thin-layer chromatography) to provide semiquantitative estimates of the total abundance of major lipid and fatty acid classes. General patterns of envelope lipid and fatty acid composition have emerged from these studies (**Appendices 1 and 2**), despite the fact that otherwise unrelated enveloped viruses bud from different membranes (**Table 1.5**). Virion envelopes are composed of three main classes of amphipathic lipids; the glycerophospholipids PC, PE, PI, PS and PA; the sphingolipid SM; and the sterol cholesterol (**Appendix 1**). However, the lipid species enriched in virion envelopes are different from those enriched in cell membranes. The envelopes of several otherwise unrelated viruses are enriched in SM in comparison to host membranes, typically at the expense of PC (**Appendix 1**). In mammalian cells, in contrast, PC accounts for ~50% of the total phospholipid content. The lipidome of retroviral membranes, for example, is strikingly different from that of the host cell plasma membrane (Aloia, Tian, and Jensen, 1993; Brugger et al., 2006; Chan et al., 2008). PC is reduced by ~2-fold (Brugger et al., 2006; Chan et al., 2008), whereas SM, PS and plasmalogen PE (pl-PE) are all enriched by ~2-3 fold (Brugger et al., 2006; Chan et al., 2008).

Virion envelopes also have high cholesterol content. Cholesterol modulates membrane fluidity by increasing the ordering of phospholipid acyl

chain packing and by reducing permeability (Lande, Donovan, and Zeidel, 1995). In virion envelopes, the cholesterol-to-phospholipid (CH/PL) ratio is typically at least double that of cell membranes, even approaching 1 mol mol⁻¹ in some cases (**Appendix 1**). For example, CH/PL ratios approached 1 in all eight group 1 HIV isolates examined by Aloia et al. and Brugger et al. (Aloia, Tian, and Jensen, 1993; Brugger et al., 2006). Chan et al. also observed that cholesterol was enriched in the HIV envelope by a factor of ~2 (Chan et al., 2008).

The high cholesterol content in virion envelopes is perhaps not surprising, considering the enrichment in SM (Rawat et al., 2003). SM and cholesterol clustering in membranes is well-characterized (Ramstedt and Slotte, 2002). This clustering is considered among the features of so-called lipid raft microdomains in plasma membranes (Brown and London, 1998). These small, heterogeneous and dynamic sterol- and sphingolipid-enriched domains are proposed to compartmentalize cellular membrane processes (Brown and Rose, 1992).

Recent advances in lipid mass spectrometry have enabled the determination of virus lipodomies, including the lipid species and their acyl chains. A strong enrichment of the raft lipids SM, dihydrosphingomyelin (dhSM), glucosylceramide, ceramide, cholesterol, and pl-PE are reported for HIV (Brugger et al., 2006; Chan et al., 2008). An increase in long (up to 32 carbon atoms) saturated lipid species was balanced by a reduction of diunsaturated and polyunsaturated species (Brugger et al., 2006; Chan et al., 2008). Chan et al. also reported an enrichment in phosphatidylinositol 4,5-bisphosphate, a lipid species bound by Bin/Amphiphysin/Rvs (BAR) domain-containing proteins to bend

membranes (further discussed in **section 1.3.2.1**) (Chan et al., 2008; Zimmerberg and Kozlov, 2006). Similar lipidome profiles were also reported for SFV and VSV, again with an enrichment in cholesterol, SM and dhSM, as well as phospholipid species with long acyl chains (30 and 32 carbon atoms) (Kalvodova et al., 2009). Such enrichments lend further support to the hypothesis that viruses bud from specialized domains.

HCV and HCMV virus liposomes are distinct from those reported above. HCV particles produced in Huh7.5 cells revealed an enrichment in cholesterol esters (CE; ~45% of total lipid content), indicating that the lipidome of infectious HCV particles is dissimilar to that of the cells used to generate them but strikingly similar to the lipid composition of low-density and very low-density lipoproteins (Merz et al., 2011). Moreover, the fatty acid compositions of the major HCV lipids CE and PC (~30% of total viral lipidome) were distinct from Huh7.5 cells, with a shift toward saturated lipid species (Merz et al., 2011). Liu et al. recently reported that HCMV virions are enriched in PE and pl-PE, their composition most closely resembling synaptic vesicle lipodomies (2011).

Few studies using semiquantitative approaches to evaluate the asymmetric distribution of lipids within virion bilayers have been reported. Choline-containing phospholipids were reported to reside predominantly in the outer leaflet of VSV, along with a greater amount of saturated fatty acids, whereas the inner leaflet is predominantly composed of aminophospholipids and virtually all of the polyunsaturated fatty acids (Patzner et al., 1978). Shaw et al. similarly reported an enrichment of PC on the outer monolayer of VSV envelopes (1979),

while Pal et al. reported that PE is located predominantly on the outer monolayer of VSV envelopes (1980). Conflicting studies by Fong et al. reported an enrichment of (unsaturated) PE in the inner leaflet of VSV envelopes (64% of total PE), while 36% is present in the outer lipid leaflet (Fong and Brown, 1978; Fong, Hunt, and Brown, 1976). Yet another group reported that PE is equally distributed between the two leaflets of VSV envelopes (Westby et al., 2007). The choline-containing phospholipids PC and SM reportedly reside in the outer leaflet of influenza (Tsai and Lenard, 1975) and Newcastle disease virus (NDV) (Munoz-Barroso et al., 1997). However, the aminophospholipids PE and PI reportedly reside primarily in the inner leaflet of influenza virions (Tsai and Lenard, 1975), whereas they are distributed about equally between the inner and outer leaflets of NDV envelopes (Munoz-Barroso et al., 1997). Therefore, virion envelopes have asymmetric bilayers, but no consensus has yet been reached on the relative enrichment of lipids in each leaflet.

The similarities in lipid enrichments of otherwise unrelated enveloped viruses that bud from different cellular compartments is perhaps surprising. The advancements in membrane purification techniques and quantitative lipid analysis will undoubtedly prove useful in the elucidation of the precise lipid composition of virion envelopes, including their relative enrichment in lipid species compared to cell membranes, as well as their transbilayer asymmetry. The mechanisms whereby virion envelopes are acquired from host cells are not yet characterized, but these quantitative analyses of virion lipidomes may provide some insight into the sorting of cellular lipids into virions. Despite the recent advances in

understanding the chemical composition of virion envelopes, much remains to be elucidated regarding the role of virion lipids in viral replication, particularly in viral fusion.

The studies on the roles of lipids in viral replication have focused on host membrane lipids (Lorizate and Krausslich, 2011). One area of major focus is the role of lipid rafts in viral replication, including entry, assembly, egress and cell-to-cell transmission (Waheed and Freed, 2010). It has been proposed that HIV, among others, uses lipid rafts as a site for both viral entry and for the assembly of progeny virions (Fantini et al., 2002). These associations appear to be at least in part mediated by specific interactions between virion proteins, for example HIV nef, with membrane microdomains (Brugger et al., 2007a). The requirement of lipid rafts for entry or assembly is supported by the observations that sterol depleting agents such as methyl-beta-cyclodextrin inhibit the release of progeny HIV virions (Ono and Freed, 2001) and also their infectivity (Graham et al., 2003). The dependency of viral infectivity on envelope cholesterol has also been reported for a number of other viruses, for example influenza virus (Sun and Whittaker, 2003), HHV-6 (Huang et al., 2006), and HBV (Bremer et al., 2009). High CH/PL ratios and SM enrichments are interpreted as selective lipid sequestration during budding of HIV (Chan et al., 2008) or pseudorabies virus (PRV) (Desplanques et al., 2008) and by extrapolation, other enveloped viruses. It has been proposed that lipid sorting results from preferential interactions of viral proteins with these specific lipids (Brugger et al., 2007b; Chan et al., 2008).

1.3.2 Cellular membrane fusion

Like viral fusion, fusion proteins mediate the merger of two cellular lipid bilayers. However, cellular fusion reactions have fundamental differences in kinetic and functional requirements compared to viral fusion, as well as in the molecular architecture of the fusion site. For example, viral fusion occurs in the time-scale of seconds or minutes, and it requires only a small number of proteins. HIV fusion, for example, is dependent on gp41, and occurs in several seconds or minutes (Koch et al., 2009). In contrast, cellular fusion processes such as synaptic secretion occur in millisecond timescale and involve numerous and diverse proteins distributed between both fusing biomembranes (Guzman et al., 2010). Cellular fusion depends on proteins, lipids, and the interactions between them.

1.3.2.1 Cellular fusion proteins

Cellular compartments communicate in part by fusing vesicles. Cellular proteins are essential in generating and maintaining these vesicles. Numerous proteins that modulate membrane curvature to induce fission (budding off) and fusion participate in physiological membrane fusion (Zimmerberg and Kozlov, 2006).

Intracellular fusion reactions are mediated through the formation of complexes between soluble *N*-ethylmaleimide-sensitive factor attachment protein receptors (SNAREs). SNAREs are membrane-associated proteins that contain so-called SNARE motifs, which are approximately 60 residues long and consist of heptad repeats. SNAREs are anchored in both vesicle (v-) and target (t-) membranes. During cellular fusion, v-SNAREs associate with t-SNAREs to form

coiled-coils, whereby the v- or t-SNARES contribute arginine or glutamine residues, respectively, to the ionic zero layer (and are thus classified as R- or Q-SNARES, respectively) (Fasshauer et al., 1998). These associations position the membrane anchors of the R- and Q-SNARES at the same end of a rod-like complex (Weber et al., 1998).

Neuronal SNARES are among the best-characterized mediators of cellular fusion. Synaptic vesicles containing neurotransmitters fuse with the presynaptic membrane in response to Ca^{2+} influx. Vesicle content is then released into the synaptic cleft, and the neurotransmitters diffuse to the postsynaptic cell to transmit the impulse (Lin and Scheller, 2000). Three SNARE proteins are involved in synaptic vesicle fusion. The vesicle-associated membrane protein (VAMP)-2 is located in the vesicular membrane. The synaptosome-associated protein 25 (SNAP-25) contains two SNARE domains that flank palmitoylated cysteines and is associated with the plasma membrane. Syntaxin 1A is a single-pass transmembrane protein that resides primarily in the plasma membrane (Lin and Scheller, 2000). During synaptic vesicle fusion, the single SNARE motif of VAMP-2 associates into a four-helical bundle with syntaxin 1 and SNAP-25. The four SNARE motifs (one each from VAMP and syntaxin, and two from SNAP-25) assume a parallel orientation in the complex. SNARE complexes are proposed to assemble in a N- to C- terminal progression by a process referred to as “zippering”. After fusion, the SNARE complexes recruit α -SNARE and N-ethylmaleimide-sensitive factor (NSF), which then disassemble the SNARE complex for the recycling of individual SNAREs (Sollner et al., 1993).

SNAREs form the core intracellular fusion machinery, driving fusion by an ATP-dependent cycle of SNARE association and dissociation (Sudhof and Rothman, 2009). However, the list of proteins that interact with SNAREs and function in fusion is continuously growing. Energy-dependent proteins, such as the ATP-driven motor protein myosin V (Ohyama et al., 2002), the Ca²⁺-regulated ATPase Hrs2 (Bean et al., 1997), Rab3 GTPases, and tethering proteins or lipids (Quetglas et al., 2002) all function particularly in fusion. Calcium-binding proteins such as calmodulin and complexin are proposed to regulate fusion pore closure (discussed in **section 1.3.3.1**) (Hu et al., 2002; Pabst et al., 2002). Negative regulators of complex formation, synaptophysin (Edelmann et al., 1995), and several synaptotagmins (which regulate synaptophysin) (Zhang et al., 2002) are other examples of cellular proteins required for physiological fusion.

Intracellular protein scaffolds or coats also function to curve or bend membranes towards one another for cellular fusion and fission. The clathrin coats were the first identified and characterized (Pearse, 1975). COPI and COPII proteins also assemble at membrane surfaces to promote spherical budding during intracellular trafficking. COPII mediates trafficking from the endoplasmic reticulum (ER) to the Golgi, and COPI functions in intra-Golgi transport and retrograde transport from the Golgi to the ER (Bonifacino and Glick, 2004). Clathrin coats function at post-Golgi locations, including the plasma membrane, the *trans*-Golgi network (TGN) and endosomes. These protein scaffolds also contain numerous other proteins and enzymes that function in cargo selection (e.g. AP-2), regulation of assembly or disassembly (e.g. epsin, Dab2), and vesicle

budding (Bonifacino and Glick, 2004). Other accessory proteins are involved in later stages of fusion, including dynamin (GTPase), amphiphysin and endophilin. Proteins of the amphiphysin family bind to inositol lipids and bend membranes, either alone or with sphere-forming coats. Amphiphysin proteins contain so-called banana-shaped BAR domains, which are proposed to stabilize curved membranes (Suetsugu, 2010).

Actin cytoskeleton remodeling and coat proteins such as clathrin, COPI and COPII, and membrane-associated proteins such as caveolin and SNARES, all function in fusion by altering membrane curvature by binding lipids, bringing the membranes into close apposition and providing the energy for fusion (Zimmerberg and Kozlov, 2006).

1.3.2.2 Lipids in cell fusion

Lipids also participate in biological fusion. The lipid composition and their asymmetric distribution across leaflets of different membranes are well characterized. For example, most sphingolipids and PC are distributed predominantly in the outer leaflet of the membrane, whereas PE, PS and PI are primarily in the inner leaflet (Devaux and Morris, 2004). This asymmetric distribution of lipids across leaflets participates in fusion by modulating membrane curvature (discussed in **section 1.3.3.2**).

Energy-driven lipid translocases function in membrane bending (Menon, 1995). Cellular translocases, for example the ATP-dependent aminophospholipid translocase transport PE and PS from the outer to the inner leaflet of membranes

to induce a transbilayer asymmetry which favors endocytosis (Devaux et al., 2008; Farge et al., 1999).

The modulation of acyl chain or headgroup components of membrane lipids alters their geometry. Such changes in the lipid composition of membranes impacts their curvature, and consequently, fusion or fission. Enzymatic remodeling of lipids is proposed to facilitate membrane deformations by generating lipids of particular geometries, thus influencing the spontaneous curvature of membranes and favoring (or disfavoring) the curvature required for fusion (McMahon and Gallop, 2005; Zimmerberg and Kozlov, 2006). For example, lysophosphatidic acid (LPA) and PA are interconverted by lysophosphatidic acid acyl transferase and phospholipase A₂ activities, respectively, which favor opposite spontaneous curvatures (Brown, Chambers, and Doody, 2003; Kooijman et al., 2003). The remodeling of lipids by cellular enzymes is important for a number of physiological events that depend on fusion and fission. For example, phospholipases, lysolipid acyltransferases, sphingomyelinase and ceramidase all contribute to the modulation of synaptic vesicle cycling (exocytosis and endocytosis) and thus, in the transmission of chemicals between neurons (Davletov and Montecucco, 2010).

Lipid remodeling and translocation therefore modify the relative depletion in lipids that favor the membrane curvature needed for fusion and thus minimize the energy needed for fusion (Burger, 2000).

1.3.3 Lipid fusion

1.3.3.1 General model of lipid fusion

Biological membrane fusions occur through intermediate structures according to the principles of the widely accepted “hemifusion stalk” model (Chernomordik and Kozlov, 2005). In 1981, Hui et al. first proposed that after an initial bilayer contact, specific sequential processes lead to fusion (Hui et al., 1981; Markin, Kozlov, and Borovjagin, 1984). Several modifications of the original model have since been proposed, based on theoretical and experimental arguments (Chernomordik and Kozlov, 2005; Chernomordik, Melikyan, and Chizmadzhev, 1987; Kozlovsky and Kozlov, 2002; Kuzmin et al., 2001; Markin and Albanesi, 2002; Siegel, 1999). Despite the different particular modifications proposed in each of these works, the general principles are consistent in all of them.

Following close apposition of two membranes, the proximal (contacting) leaflets merge to form one continuous monolayer, whereas the two distal leaflets remain separate (**Figure 1.3**). This results in the formation of an hourglass shaped intermediate, called the hemifusion stalk (**Figure 1.3I**) (Markin, Kozlov, and Borovjagin, 1984; Siegel, 1993; Siegel, 1999). For the formation of the hemifusion stalk, the outer leaflets of fusion vesicles must transition from a positive curvature (where the lipid headgroups are bent away from each other) to a negative curvature (where the lipid headgroups bend towards each other) (inset A, **Figure 1.3**). Next, the two distal leaflets fuse to produce one continuous bilayer, and the fusion pore (inset B, **Figure 1.3II**) (Chernomordik et al., 1985). Pore expansion (**Figure 1.3III**) then leads to the mixing of content between two

previously separated compartments (Kozlov et al., 1989). Several predictions of the hemifusion stalk model have been verified experimentally in protein-free systems. The transient nature of early fusion intermediates, however, hindered the direct experimental validation of hemifusion as a precursor for a fusion pore. The hemifusion stalk was not observed until 2002, when Yang and Huang reported the observation of hourglass-shaped stalks by X-ray diffraction (Yang and Huang, 2002). Point contacts between separated parallel lipid bilayers were observed to develop into hourglass-like interbilayer structures, or hemifusion stalks, when the hydration layers separating the parallel bilayers were reduced. Such fusion intermediates have now also been validated in biological fusion systems, for example using cryo-electron tomography to capture the fusion of HSV-1 virions to plasma membranes (Maurer, Sodeik, and Grunewald, 2008).

The formation of fusion intermediates requires apposing membranes to overcome the hydration repulsion that separates them, and the elastic deformation of membrane leaflets (bending). Fusion is therefore an energetically costly process. The theoretical kinetics for each step has been analyzed, including those of membrane bending energies for hemifusion intermediates, fusion stalks and fusion pores. The energy barriers to fusion have been estimated theoretically using elastic models of membranes, or computer simulations (Chernomordik and Kozlov, 2008; Cohen and Melikyan, 2004; Katsov, Muller, and Schick, 2004; Kozlovsky and Kozlov, 2002; Markin and Albanesi, 2002; Markin, Kozlov, and Borovjagin, 1984; Siegel, 1999).

The first major energy barrier for fusion is the intermembrane hydration repulsive force between two bilayers. The close apposition of two bilayers thus requires the removal of any water between them. Membrane hydration repulsive forces increase with decreasing membrane spacing (Parsegian, Fuller, and Rand, 1979). Experimentally, repulsion can be overcome by multivalent ions (Bentz et al., 1988), direct dehydration (Yang and Huang, 2002), or by polyethylene glycol to force the membranes into close apposition (Lentz, 2007). X-ray scattering experiments on protein-free bilayers with biologically relevant lipid compositions suggest that membrane contacts with intermembrane distances of 1 nm are sufficient to drive the formation of a fusion stalk (Yang, Ding, and Huang, 2003). Hemifusion stalk formation occurs if the resulting release of hydration energy compensates for the elastic energy of the stalk (Kozlovsky et al., 2004). In such systems, very close membrane apposition is sufficient to trigger hemifusion. In biological systems, however, fusion proteins such as SNARES are responsible for triggering fusion (Kozlov, McMahon, and Chernomordik, 2010). The effects of fusion proteins on membrane distances were considered in a more recent model aimed at calculating the effects of membrane separation on the energy barriers to fusion. A hypothetical mathematical model predicted that fusion pore formation requires $43\text{-}65 k_B T$ with a bilayer separation >6 nm (the closest distance determined by repulsive hydration forces) (Jackson, 2009). Jackson suggested that increases in membrane separation created by fusion protein scaffolding allow membranes a greater freedom to assume shapes with lower energy (Jackson, 2009).

The energetics of stalk formation have also been subject to numerous studies (Cohen and Melikyan, 2004; Kozlov et al., 1989; Markin and Albanesi, 2002; Siegel, 1993). The high kinetic barriers ($\sim 40 k_B T$) for membrane leaflet bending required for stalk formation originally presented significant arguments against the hemifusion stalk model. Another strong argument against the hemifusion stalk model was the formation of “voids” in the hydrophobic regions where the portions of differently curved lipid monolayers contact each other. The arguments against the likelihood of such energetically unstable events were addressed by considering the abilities of lipids to tilt, and acyl chains to splay and stretch (Siegel 1993; Siegel, 1999). These reorganizations reduce the kinetic barriers. During the bending of the distal membrane leaflets for stalk formation, the packing of the hydrocarbon chains around the hydrophobic regions at the stalk is proposed to minimize the interstices between them (Turner and Gruner, 1992). The deformation of tilt results in the stretching of the hydrocarbon chains with respect to their initial length. The stretch of the chains accompanying the tilt fills the hydrophobic void of the stalk intermediate (Kozlovsky and Kozlov, 2002). When acyl chains stretch to their near-fully extended length, their configurational entropy decreases, and the free energy increases. Coarse-grain molecular dynamics simulation models also suggested that tilting and splaying of lipid tails around the edges prevent the formation of the biologically and energetically unlikely voids (Marrink and Mark, 2004). It is proposed that lipid leaflet bending and splaying of the hydrocarbon chains mutually compensate the deformations of membranes at the stalk (May, 2002). A mathematical analysis of a “stress-free

stalk” lowered the energy cost of stalk formation from $+37.8 k_B T$ to $-1.2 k_B T$ (depending on curvature), a biologically relevant kinetic barrier (Markin and Albanesi, 2002). The role of the fatty acid hydrocarbon chains in reducing kinetic barriers to fusion may suffice to solve the “energy crisis” of the hemifusion stalk model (Kozlovsky and Kozlov, 2002). Tilting and rearrangements of hydrocarbon chains during membrane bending (Hamm and Kozlov, 2000), at interfaces between bilayers of different composition such as rafts (Kuzmin et al., 2005) and during stalk formation (Kuzmin et al., 2001) have all now been documented. Mathematical models also predict that the high kinetic barriers for fusion are reduced by diffusion of the neutral lipids within the hydrophobic membrane as well (Kozlovsky and Kozlov, 2002; Markin and Albanesi, 2002). Cholesterol is also proposed to reduce the energy barrier to fusion by clustering fusion proteins such as SNAREs to stimulate a fusogenic state, and by promoting negative curvature (Churchward et al., 2005).

Posthemifusion stages are often considered rate limiting. Pore formation and expansion are not well understood. The number of proteins required for each step does suggest a high kinetic barrier for pore formation (Chernomordik and Kozlov, 2003). For example, one to three HA trimers are estimated to be required for hemifusion, but up to six are required for fusion pore expansion (Blumenthal et al., 1996; Danieli et al., 1996; Imai, Mizuno, and Kawasaki, 2006). For HIV, in contrast, a single gp120-gp41 heterotrimer is proposed to be required for fusion (Yang et al., 2005). Studies reported by Markosyan et al. revealed that the formation of the 6HB in HIV-1 Env occurs only after pore creation, thus

suggesting that the free energy released by 6HB formation may be used directly to promote pore enlargement in viral fusion (Markosyan, Leung, and Cohen, 2009). Fusion pore bending energies depend strongly on the predicted shape of the fusion pore and the mechanisms of pore expansion, for which there is as yet no consensus (Chen et al., 2008; Gao, Lipowsky, and Shillcock, 2008; Jackson, 2009; Zhang and Jackson, 2010).

Membrane fusion is accepted as requiring constant energy input. Experimental evidence indicates that hemifusion connections dissociate if they are not supported by persistent energy input (Chernomordik and Kozlov, 2003). For example, the arrest of viral fusion by lowering the temperature or surface density of fusion proteins results in the dissociation of hemifusion structures or restricted hemifusion, detectable by only partial lipid mixing (Mittal et al., 2003; Zavorotinskaya et al., 2004). Virions arrested at this hemifusion stage by lowering the temperature then complete fusion if the temperature is raised again (Chernomordik et al., 1999).

Despite significant advances in understanding biomembrane fusion over the last several decades, the mechanistic details of the processes whereby lipid intermediates progress to pore expansion remain to be fully characterized.

1.3.3.2 Modulation of membrane fusion by targeting lipids

The functions of lipids in fusion are an attractive antiviral target. The high cholesterol content in virion envelopes has been targeted with cholesterol-like or -binding molecules, or cholesterol regulating drugs, or with detergents such as N-9

(Brugh, 1977; Harada, 2005; Hicks et al., 1985; Kim et al., 1978; Moore et al., 1978; Pal, Barenholz, and Wagner, 1981; Schaffner et al., 1986). Cholesterol binding agents such as amphotericin B methyl ester inhibit HIV particle production (Waheed et al., 2008) and virion infectivity (Waheed et al., 2007). Such attempts have not been successful from an antiviral perspective, however, because cholesterol-mediated membrane fluidity and integrity are also required for the stability of cell membranes. In addition, the depletion of host cell membrane cholesterol by methyl- β -cyclodextrin enhanced the release of progeny Sendai (Fujita et al., 2011) and influenza (Barman and Nayak, 2007) virions, reportedly by disrupting lipid rafts to facilitate virion budding from cell membranes. The role of other virion lipids is even less well characterized.

The hemifusion stalk model implies that fusion is dependent on the propensity of membranes to bend. Consistently, fusion can be modulated by changing the lipid composition of the merging membranes (Cooke and Deserno, 2006; Teissier and Pecheur, 2007). Membrane curvature is partly determined by the polymorphic phases adopted by the lipid constituents of those membranes. Cylindrical lipids, with hydrophobic tails and hydrophilic heads of similar cross-sections, tend to form stable bilayers with no net curvature (lamellar phase; **Table 1.6**). Cone shaped lipids have hydrophobic tails of larger cross-section than their hydrophilic heads, and adopt a spontaneous negative curvature, in configurations where the headgroups bend towards each other (inverted-hexagonal phase; **Table 1.6**) (Chernomordik, 1996). Inverted-cone shaped lipids, such as lysophospholipids, have hydrophilic heads of larger cross-section than their

hydrophobic tail, and tend to adopt configurations with the headgroups bent away from each other (positive curvature; micellar phase; **Table 1.6**) (Basanez, Goni, and Alonso, 1998). Glycolipids also have hydrophilic heads of larger cross-section than their hydrophobic moieties, and also favor positive curvature (**Table 1.6**). In contrast to micellar-forming inverted-cone shaped lipids, however, glycolipids do not form micelles.

The effects of lipid geometry on membrane bending and fusion have been well analyzed in experimental systems. Lamellar lipids such as PC, one of the major lipids of mammalian membranes, are cylindrical shaped lipids that form stable bilayers, for example (Leikin et al., 1993). Non-lamellar lipids inserted into contacting monolayers promote or inhibit fusion by favoring or disfavoring the negative membrane curvature (Gruner, 1985).

Consistent with the hemifusion stalk model, exogenous natural lipids can modulate fusion in model systems. Natural cone-shaped fatty acids such as oleic acid (OA), or PE, promote negative curvature and stalk formation, thus facilitating fusion when added into the outer leaflet of fusing vesicles. Conversely, the exogenous addition of inverted-cone shaped lipids, which adopt spontaneous positive membrane curvatures, into the outer leaflet inhibits fusion. Natural lipid fusion inhibitors include lysophosphatidylcholine (LPC) and LPA (Chernomordik, Kozlov, and Zimmerberg, 1995; Vogel, Leikina, and Chernomordik, 1993; Yeagle et al., 1994).

Exogenous molecules that promote or inhibit negative curvature formation promote or inhibit viral fusion, too. Insertion of cone-shaped lipids such as OA

into the outer leaflet of envelopes favors viral fusion (Chernomordik and Kozlov, 2003). Conversely, targeting lipids of inverted-cone shape such as LPC to the same leaflet inhibits fusion of several enveloped viruses, including influenza (Chernomordik et al., 1999; Gunther-Ausborn, Praetor, and Stegmann, 1995), rabies virus (Gaudin, 2000), TBEV (Stiasny and Heinz, 2004), Sendai virus (Yeagle et al., 1994) and baculovirus (Vogel, Leikina, and Chernomordik, 1993). The inhibitory effects of LPC could be rescued by the addition of cone-shaped OA, indicating that the inhibitory effects of LPC on fusion result from the modulation of membrane curvature (Gaudin, 2000; Stiasny and Heinz, 2004).

1.4 Herpes simplex virus

1.4.1 Classification and virion organization

Herpes simplex virus type-1 and -2 are members of the *alphaherpesvirinae* subfamily of *herpesvirales* order (Davison et al., 2009). All herpesviruses are characterized by several common biological properties, such as nuclear DNA replication and capsid assembly, and final virion processing in the cytoplasm.

Virion morphology is the primary criterion for inclusion in the *herpesvirales* order (Pellet and Roizman, 2007). Herpes virions are spherical and approximately 200 nm in diameter, depending on the species. They have four components: core, capsid, tegument and envelope. Innermost in the HSV virion is a single copy of the linear, double stranded (ds) DNA genome (Honest, 1984). Surrounding the genome is an icosahedral capsid shell (nucleocapsid). The

nucleocapsid is composed of five virion proteins (VP), the major one being VP5 (UL19), which forms the capsomers (Mettenleiter, Klupp, and Granzow, 2006).

Surrounding the nucleocapsid is a proteinaceous layer composed of over twenty proteins, collectively termed tegument (Schrag et al., 1989). The tegument is delimited by a lipid bilayer, or envelope. Like all enveloped viruses, HSV acquires pre-existing cellular lipids from the membranes of the infected cells (Simons and Garoff, 1980). In comparison to host cell membranes, the HSV virion envelope is enriched in SM and PS, at the expense of PC (van Genderen et al., 1994) (**Appendix 1**). This enrichment is independent of the infected cell type.

Embedded within the envelope are the virion proteins. The virion envelope contains sixteen membrane proteins, of which five glycoproteins (gB, gC, gD, gH and gL) participate in entry, as discussed below.

1.4.2 Replication

1.4.2.1 Entry

The entry of extracellular HSV virions into host cells can be divided into three sequential steps. The first is primary attachment of specific virion glycoproteins to cell surface molecules. Attachment is followed by secondary binding of HSV virion glycoproteins to cell surface receptors. Last, virion envelopes fuse with cell membranes. Each of these three sequential steps is detailed below, with particular emphasis on the virion proteins that regulate them. Five glycoproteins (gB, gC, gD, gH and gL) participate in entry; all but gC are essential (reviewed in Akhtar and Shukla, 2009).

1.4.2.1.1 Primary attachment

The initial interaction between virions and cell surface receptors is primarily mediated by the reversible attachment of gC to heparan sulphate (HS)-containing cell surface glycosaminoglycan (GAG) moieties (Wudunn and Spear, 1989; Shieh et al., 1992). Heparinase treatment of cells or exposure of virions to heparin before infection reduces virion binding by approximately 10-fold, depending on the treatment and cell type (Wudunn and Spear, 1989). HSV-1 and HSV-2 attach to HS-containing GAG, showing only minor differences in HS-GAG preference (Lycke et al., 1991).

The interaction with HS is mediated primarily by virion gC (Campadelli-Fiume et al., 1990; Herold et al., 1991). Previous studies by Langeland et al. had revealed that the addition of polylysine during exposure of cells to virus at 4°C effectively inhibited plaque formation by HSV-1, but not by HSV-2 (1988). Studies by Campadelli-Fiume et al. provided the first genetic evidence for the involvement of gC in HSV-1 attachment (1990). Marker rescue studies using HSV-1 x HSV-2 recombinants identified the HSV-2 gene encoding for gC conferred to HSV-1 the capacity to attach to cells in the presence of polycations (Campadelli-Fiume et al., 1990). Evidence for a physical interaction between gC and cell surface heparan sulfate was provided by Herold et al., who reported gC bound to heparin-Sepharose columns (1991). Herold et al. also showed that in gC-null HSV mutants, primary attachment is mediated by gB, although it is ~10-fold less efficient (Herold et al., 1994). Additional studies performed by Herold et al. also revealed that primary attachment is not strictly required for infectivity. gC

and gB-null mutants still bind cells, albeit with severely impaired ability (~3% binding) (Herold et al., 1991; Herold et al., 1994).

1.4.2.1.2 Secondary binding

Primary attachment is dispensable for HSV infectivity, whereas the secondary binding is required. The virion glycoprotein responsible for this secondary binding is gD. Cells constitutively expressing gD interfere with HSV infection by saturating cell surface receptors (Campadelli-Fiume et al., 1988; Johnson and Spear, 1989). Exposure of cells to soluble gD prevents infection (Johnson, Burke, and Gregory, 1990). Anti-idiotypic antibodies mimicking gD also prevent infection (Huang and Campadelli-Fiume, 1996). Several strains containing mutations in gD overcome gD-mediated restriction to infection in gD-expressing cells (Brandimarti et al., 1994; Dean et al., 1994).

Three classes of gD cell surface receptors have been identified. One is a member of the tumor necrosis factor (TNF) receptor family, originally named herpes virus entry mediator (HVEM) (Montgomery et al., 1996), and later re-named “herpes virus entry A” (HveA) (Warner et al., 1998). The second class of gD receptor belongs to the immunoglobulin (Ig) superfamily and is related to the PV receptor CD155. The family was initially named “PV-related receptors” (Prr) (Geraghty et al., 1998), but were later re-named according to their cellular functions as nectins. Nectins form adherence junctions and tight junctions, certain neuronal synapses, and cell junctions in spermatogenesis (Takahashi et al., 1999; Takai and Nakanishi, 2003). The list of nectins continues to grow, but not all are

HSV receptors (Akhtar and Shukla, 2009). Of the nectin-1 isoforms, two splice variants nectin-1 δ (HveC, Prr1) and nectin-1 α (herpesvirus Ig-like receptor, or HIgR) mediate entry of HSV-1 and HSV-2 (Geraghty et al., 1998) by interactions with gD (Cocchi et al., 1998; Krummenacher et al., 1998). Nectin-1 δ and -1 α are broadly expressed in cells infected by HSV, including cells in skin, brain and ganglia (Cocchi et al., 1998). Two other splice variant isoforms, nectin-2 α (HveB, Prr2 α) and nectin-2 δ (Prr2 δ), mediate the entry of HSV-2, but not HSV-1 (Lopez et al., 2000; Warner et al., 1998).

The third family of HSV receptors has only one member. This receptor consists of certain HS modifications catalyzed by specific isoforms of 3-*O*-sulfotransferase (Shukla et al., 1999). The 3-*O*-sulfated heparan sulfates are distributed on a variety of human cells and tissues and efficiently mediate entry of HSV-1, but not HSV-2 (Shukla et al., 1999).

1.4.2.1.3 Envelope fusion

The last step of HSV entry is fusion of the virion envelope with the plasma membrane of the host cell (Morgan, Rose, and Mednis, 1968). In most cell types, including neurons, HSV fusion is pH-independent (Nicola et al., 2005; Wittels and Spear, 1991). Other reports indicate that HSV can enter some cell types by pH-dependent or independent endocytosis (Milne et al., 2005; Nicola et al., 2005). Fusion is the least well-understood step of entry.

Glycoproteins B, D, H and L are all necessary and sufficient to induce HSV-1 or -2 fusion to cells (Muggeridge, 2000; Turner et al., 1998a).

Glycoprotein B (Cai, Gu, and Person, 1988), gD (Ligas and Johnson, 1988), gH (Forrester et al., 1992) or gL (Roop, Hutchinson, and Johnson, 1993) deleted mutant HSV-1 do not enter cells.

The current models for HSV entry propose that all four required proteins form a heterocomplex essential for fusion (Campadelli-Fiume et al., 2007). Complex assembly strictly requires a gD receptor (either nectin-1 or HveA) and gD is considered the trigger for fusion (Cocchi et al., 2004). Evidence for gD receptor-mediated activation is provided by the crystal structures of unbound and bound gD. The gD protein is 369 residues long and contains a transmembrane domain, a C-terminal cytoplasmic tail of 30 residues and an ectodomain. The crystal structures solved by Carfi et al., both alone and in complex with soluble HveA, revealed that gD folded as an Ig-variable (IgV) domain, with N-terminal and C-terminal extensions (2001). Crystals were also obtained using a longer truncated form of gD (residues 23-306), with an added cysteine residue at position 307 to promote dimerization (Krummenacher et al., 2005). The crystal structure of gD in a pre-fusion conformation shows the gD ectodomain organized in two distinct regions. The N-terminus includes the receptor binding sites (residues 1-260), and the C-terminus (residues 260-310) carries a so-called profusion domain (PFD) required to trigger fusion, but not for receptor binding (Cocchi et al., 2004). Unbound gD adopts a closed conformation, in which the flexible C-terminal ectodomain (which carries the PFD) folds back towards the N-terminus, masking the receptor-binding sites. Upon receptor binding, gD adopts an open conformation, where the PFD is displaced from its binding site on the N-terminus

and the latter becomes part of the receptor binding site (Fusco, Forghieri, and Campadelli-Fiume, 2005).

The conformational changes in gD enable the sequential recruitment of a gB homotrimer and a gH/gL heterodimer. Using bimolecular complementation assays, Avitabile et al. showed that gB and gH/gL interactions are triggered by binding of gD to its receptors (2007). Bimolecular complementation assays used by Anatasiu et al. further showed that gB and gH/gL interact with each other concomitantly with fusion (2007).

Glycoproteins H and L function in fusion but their roles are less well understood than those of gD. A hydrophobic α -helix (α -H) is positionally conserved (residues 377 to 397) in all the gH orthologs across the *herpesviridae* family (Cairns et al., 2006). HSV-1 gH α -helix (α -H1), for example, interacts with membranes and converts soluble gD (residues 1-260) into membrane-bound gD (Gianni et al., 2006).

Glycoprotein L is a soluble, 224-residue glycoprotein that forms a noncovalent heterodimer with gH. Using truncation mutants, Peng et al. determined that the first 323 residues of gH and the first 161 residues of gL are required to form stable (secreted) hetero-oligomers (Peng et al., 1998). gL is required for proper folding and trafficking of gH (Hutchinson et al., 1992), and for promoting fusion (Klyachkin, Stoops, and Geraghty, 2006). In addition, the *UL1* gene (encoding gL) is a locus of syncytia mutations, and gH/gL are capable of inducing lipid mixing in the absence of other viral proteins (Subramanian and Geraghty, 2007), further supporting a role for gH/gL complexes in fusion. The

crystal structure of the gH ectodomain bound to gL from HSV-2 was recently solved (Chowdary et al., 2010). Neither gH nor gL have stable cores, supporting the idea that each is required for the proper folding its partner (Chowdary et al., 2010). Moreover, it does not resemble any known viral fusogen. For example, no N-terminal helical FP or internal FP loop characteristic of class I or II fusogens, respectively, was identified (Chowdary et al., 2010). Consistent with previous models, therefore, Chowdary et al. proposed that gH/gL do not directly participate in fusion, but rather may function as a trigger for the fusogenic conformational changes in gB (2010).

The structural similarities of gB to the fusogenic G protein of VSV (discussed in **section 1.3.1.1.3**) indicate that gB is the fusogenic protein (Heldwein et al., 2006; Roche, 2006). Phenotypic studies of deleted and temperature sensitive gB mutants that reduce the rate of HSV entry also indicate that gB is the viral fusogen (Galdiero et al., 2008). The syncytial phenotypes of certain gB mutants further support its role as a fusion effector (Chowdary and Heldwein, 2010).

1.4.2.3 Gene expression and DNA replication

After entering the cytoplasm, HSV-1 capsids are transported to the nucleus by microtubule-dependent mechanisms (Sodeik, Ebersold, and Helenius, 1997). The nucleocapsid docks at nuclear pore complexes and the viral genome is extruded from the capsid into the nucleus (Ojala et al., 2000). Some tegument proteins, such as virion (tegument) protein 16 (VP16), are also transported to the nuclear

membrane. Some are transported in association with capsids, whereas others (such as VP16) are transported independently of them.

The HSV genes are then expressed in three temporally regulated phases: immediate-early (IE, α), early (E, β) and late (L; γ_1 and γ_2) phases, based on the requirements for their expression (Hones and Roizman, 1974). Immediate-early genes are transcribed in the absence of *de novo* viral protein synthesis. The expression of E genes depends on functional IE proteins, but not on viral DNA replication (Roizman, Knipe, and Whitley, 2007). Late genes are subdivided into two classes: early-late (γ_1) and true-late (γ_2) genes. True-late gene expression is absolutely dependent on viral DNA synthesis, whereas expression of early-late genes is not (Godowski and Knipe, 1986).

HSV genomes encode seven proteins essential for DNA replication. In addition to the essential viral proteins, cellular proteins and enzymes, and non-essential viral proteins, also contribute to viral DNA synthesis. For example, enzymes, such as TK, that contribute substrates for DNA synthesis are required (Roizman, Knipe, and Whitley, 2007). HSV DNA replication produces “head-to-tail” concatemeric molecules (Roizman, Knipe, and Whitley, 2007). Genome-sized pieces are then cleaved and packaged during virion assembly.

1.4.2.4 Egress

Following nucleocapsid assembly in the nucleus, the progeny virions are enveloped and egress. Egressing nucleocapsids acquire a primary lipid envelope by budding through the inner nuclear membrane into the perinuclear space

(Darlington and Moss, 1968). Two mechanisms of egress from the perinuclear space have been proposed. In both models, progeny virions interact with the Golgi apparatus and are released from the cell by fusion of secretory vesicles with plasma membranes (Mettenleiter, Klupp, and Granzow, 2009). The precise details of the interaction between HSV and Golgi are still subject to debate.

The single envelopment (or *luminal*) model of egress proposes that after primary envelopment of nucleocapsids at the inner nuclear membrane, virions are transported along the exocytic or secretory pathway in vesicles acquired by budding from the outer nuclear membrane, or possibly through enlarged nuclear pores (although no viral mutants that influence pore size have been yet been identified) (Wild et al., 2005). The single envelopment pathway implies that the tegument, immature glycoproteins and lipids are all acquired in the nucleus or perinuclear space (Campadelli-Fiume and Roizman, 2006).

The second proposed mechanism of egress is termed “the envelopment-deenvelopment-reenvelopment” model (Skepper et al., 2001). According to this model, capsids budded from the inner nuclear membrane lose their envelope by fusing with the outer nuclear membrane, and are then released in the cytoplasm as naked nucleocapsids (Vlazny, Kwong, and Frenkel, 1982). These nucleocapsids would then undergo a second envelopment by budding into vesicles within the TGN. This model suggests that virions acquire the tegument in the cytoplasm and their envelope at the *trans*-Golgi. Both their tegument and envelope may therefore differ in composition from the primary envelopment at the inner nuclear membrane.

The precise mechanisms and pathways whereby assembling progeny virions egress from the perinuclear to the extracellular space are among the major outstanding aspects of HSV replication (Lee and Chen, 2010).

1.5 Rationale and hypothesis

Current antivirals target viral proteins or their interactions with cellular ones. As such, they have several important limitations, such as the prompt selection for drug-resistant variants and a narrow spectrum of activity against only one or a few closely related viruses. Most must also be intracellularly metabolized into their active form, and as such are often metabolized into unwanted by-products that can also be toxic. Entry inhibitors aimed at early steps in the viral replication cycle do not have to be intracellularly metabolized into an active form. Drugs targeting entry have the potential for both therapeutic and prophylactic uses too. However, current strategies targeting viral or cellular entry proteins still suffer the same limitations as drugs targeting other steps in replication. Despite these limitations, viral entry remains an attractive target (Teissier, Penin, and Pecheur, 2011).

Targeting envelope lipids to inhibit viral fusion presents an attractive alternative. Virion lipids are not encoded within mutable viral genomes, and fusion occurs extracellularly. Such properties are highly desirable characteristics for agents pursued as microbicides to prevent transmission of STIs, such as HIV (Buckheit et al., 2010; Cutler and Justman, 2008). Moreover, the mechanisms of viral fusion are well conserved among otherwise unrelated enveloped viruses, many of which cause disease in humans.

Virion envelopes are metabolically inert extracellular lipid bilayers of positive curvature. The envelope must make a local, highly negative, curvature to form the hemifusion stalk. These energetically costly transitions occur using only the limited energy released by binding and rearrangements of virion glycoproteins. In contrast to cellular vesicle fusion, virions cannot use ATP as energy donor or remodel and rearrange their envelope lipids across leaflets. Therefore, viral fusion is likely to be more sensitive to increases in the energy barrier to fusion than cellular fusion events. Viral fusion thus presents a unique biological process that could be selectively targeted by novel antivirals, without affecting cellular fusion processes.

The formation of the negative curvature required for viral fusion is inhibited by natural lipids of inverted-cone shape. Such naturally occurring phospholipids are not pharmaceutically useful, however. They are too rapidly metabolized and are toxic. I hypothesize that small molecules of appropriate molecular shape (with hydrophilic regions of larger cross-section than their hydrophobic regions) could be designed to inhibit the formation of negative envelope curvature required for the hemifusion stalk. Compounds that disfavor the formation of negative envelope curvature may be able to increase the energy barrier for fusion beyond that which is provided by virion glycoproteins. If this increase was limited, then cellular lipid remodeling and translocations, and ATP consumption might compensate to allow physiological cellular fusions.

Such a novel antiviral approach may help to overcome the limitations of current antiviral strategies. Fusion occurs extracellularly and is among the first

steps in replication. Therefore, such drugs require no intracellular delivery or metabolism. Compounds inhibiting the biophysical properties of virion envelopes in fusion could thus be useful as antivirals or microbicides. Moreover, the target is not encoded by any viral gene, and the genetic barrier for resistance is thus likely to be higher than current drugs targeting viral proteins. Finally, the mechanisms of viral envelope fusion are well conserved among all enveloped viruses. Such small molecules could therefore have the potential to be developed as broad-spectrum antiviral compounds.

Rigid amphipathic molecules of appropriate molecular shape (containing a highly hydrophobic and rigid planar moiety capable of insertion into the hydrophobic core of the lipid envelope, attached to a hydrophilic moiety of adequate shape to interact with charged phospholipid headgroups in the envelope), could be developed (**Figure 1.4**). Indeed, the chemical synthesis of a family of nucleoside derivatives with an appropriate rigid, amphipathic molecular shapes was already described (for examples, see Korshun et al., 1997; Korshun et al., 1998). Under the proposed model, such compounds could selectively target envelope bilayers to prevent the lipid reorganizations required for any viral fusion. Insertion of such compounds into the external leaflet of virion bilayers would disfavor the formation of negative curvature, thus increasing the energy barrier for the formation of the hemifusion stalk beyond that released by binding and rearrangements of the viral fusion glycoproteins.

1.6 References

- Abel, S., Back, D. J., and Vourvahis, M. (2009). Maraviroc: pharmacokinetics and drug interactions. *Antivir Ther* **14**(5), 607-18.
- Akhtar, J., and Shukla, D. (2009). Viral entry mechanisms: cellular and viral mediators of herpes simplex virus entry. *Febs Journal* **276**(24), 7228-7236.
- Aloia, R. C., Tian, H. R., and Jensen, F. C. (1993). Lipid-Composition and Fluidity of the Human-Immunodeficiency-Virus Envelope and Host-Cell Plasma-Membranes. *Proceedings of the National Academy of Sciences of the United States of America* **90**(11), 5181-5185.
- Anastassopoulou, C. G., Ketas, T. J., Klasse, P. J., and Moore, J. P. (2009). Resistance to CCR5 inhibitors caused by sequence changes in the fusion peptide of HIV-1 gp41. *Proceedings of the National Academy of Sciences of the United States of America* **106**(13), 5318-5323.
- Armstrong, R. T., Kushnir, A. S., and White, J. M. (2000). The transmembrane domain of influenza hemagglutinin exhibits a stringent length requirement to support the hemifusion to fusion transition. *Journal of Cell Biology* **151**(2), 425-437.
- Atanasiu, D., Whitbeck, J. C., Cairns, T. M., Reilly, B., Cohen, G. H., and Eisenberg, R. J. (2007). Bimolecular complementation reveals that glycoproteins gB and gH/gL of herpes simplex virus interact with each other during cell fusion. *Proceedings of the National Academy of Sciences of the United States of America* **104**(47), 18718-18723.
- Avitabile, E., Forghieri, C., and Campadelli-Fiume, G. (2007). Complexes between herpes simplex virus glycoproteins gD, gB, and gH detected in cells by complementation of split enhanced green fluorescent protein. *Journal of Virology* **81**(20), 11532-11537.
- Azad, R. F., Driver, V. B., Tanaka, K., Crooke, R. M., and Anderson, K. P. (1993). Antiviral Activity of a Phosphorothioate Oligonucleotide Complementary to Rna of the Human Cytomegalovirus Major Immediate-Early Region. *Antimicrobial Agents and Chemotherapy* **37**(9), 1945-1954.
- Backovic, M., and Jardetzky, T. S. (2009). Class III viral membrane fusion proteins. *Current Opinion in Structural Biology* **19**(2), 189-196.
- Backovic, M., Longnecker, R., and Jardetzky, T. S. (2009). Structure of a trimeric variant of the Epstein-Barr virus glycoprotein B. *Proceedings of the National Academy of Sciences of the United States of America* **106**(8), 2880-2885.
- Balzarini, J. (2004). Current status of the non-nucleoside reverse transcriptase inhibitors of human immunodeficiency virus type 1. *Current Topics in Medicinal Chemistry* **4**(9), 921-944.
- Barman, S., and Nayak, D. P. (2007). Lipid raft disruption by cholesterol depletion enhances influenza A virus budding from MDCK cells. *J Virol* **81**(22), 12169-78.
- Barre-Sinoussi, F., Chermann, J. C., Rey, F., Nugeyre, M. T., Chamaret, S., Gruest, J., Dauguet, C., Axlerblin, C., Vezinetbrun, F., Rouzioux, C.,

- Rozenbaum, W., and Montagnier, L. (1983). Isolation of a T-Lymphotropic Retrovirus from a Patient at Risk for Acquired Immune-Deficiency Syndrome (AIDS). *Science* **220**(4599), 868-871.
- Basanez, G., Goni, F. M., and Alonso, A. (1998). Effect of single chain lipids on phospholipase C-promoted vesicle fusion. A test for the stalk hypothesis of membrane fusion. *Biochemistry* **37**(11), 3901-3908.
- Bean, A. J., Seifert, R., Chen, Y. A., Sacks, R., and Scheller, R. H. (1997). Hrs-2 is an ATPase implicated in calcium-regulated secretion. *Nature* **385**(6619), 826-829.
- Beer, B. E., Doncel, G. F., Krebs, F. C., Shattock, R. J., Fletcher, P. S., Buckheit, R. W., Watson, K., Dezzutti, C. S., Cummins, J. E., Bromley, E., Richardson-Harman, N., Pallansch, L. A., Lackman-Smith, C., Osterling, C., Mankowski, M., Miller, S. R., Catalone, B. J., Welsh, P. A., Howett, M. K., Wigdahl, B., Turpin, J. A., and Reichelderfer, P. (2006). In vitro preclinical testing of nonoxynol-9 as potential anti-human immunodeficiency virus microbicide: a retrospective analysis of results from five laboratories. *Antimicrobial Agents and Chemotherapy* **50**(2), 713-723.
- Bentz, J., Alford, D., Cohen, J., and Duzgunes, N. (1988). La³⁺-Induced Fusion of Phosphatidylserine Liposomes - Close Approach, Intermembrane Intermediates, and the Electrostatic Surface-Potential. *Biophysical Journal* **53**(4), 593-607.
- Bergelson, J. M., Cunningham, J. A., Droguett, G., KurtJones, E. A., Krithivas, A., Hong, J. S., Horwitz, M. S., Crowell, R. L., and Finberg, R. W. (1997). Isolation of a common receptor for coxsackie B viruses and adenoviruses 2 and 5. *Science* **275**(5304), 1320-1323.
- Bloom, J. D., Gong, L. I., and Baltimore, D. (2010). Permissive Secondary Mutations Enable the Evolution of Influenza Oseltamivir Resistance. *Science* **328**(5983), 1272-1275.
- Blumenthal, R., Sarkar, D. P., Durell, S., Howard, D. E., and Morris, S. J. (1996). Dilation of the influenza hemagglutinin fusion pore revealed by the kinetics of individual cell-cell fusion events. *Journal of Cell Biology* **135**(1), 63-71.
- Bonifacino, J. S., and Glick, B. S. (2004). The mechanisms of vesicle budding and fusion. *Cell* **116**(2), 153-166.
- Bourdais, J., Biondi, R., Sarfati, S., Guerreiro, C., Lascu, I., Janin, J., and Veron, M. (1996). Cellular phosphorylation of Anti-HIV nucleosides - Role of nucleoside diphosphate kinase. *Journal of Biological Chemistry* **271**(14), 7887-7890.
- Brandenburg, B., Lee, L. Y., Lakadamyali, M., Rust, M. J., Zhuang, X., and Hogle, J. M. (2007). Imaging poliovirus entry in live cells. *PLoS Biol* **5**(7), e183.
- Brandimarti, R., Huang, T. M., Roizman, B., and Campadellifume, G. (1994). Mapping of Herpes-Simplex Virus-1 Genes with Mutations Which Overcome Host Restrictions to Infection. *Proceedings of the National Academy of Sciences of the United States of America* **91**(12), 5406-5410.

- Brasseur, R., Cornet, B., Burny, A., Vandenbranden, M., and Ruyschaert, J. M. (1988). Mode of Insertion into a Lipid-Membrane of the N-Terminal HIV gp41 Peptide Segment. *Aids Research and Human Retroviruses* **4**(2), 83-90.
- Bremer, C. M., Bung, C., Kott, N., Hardt, M., and Glebe, D. (2009). Hepatitis B virus infection is dependent on cholesterol in the viral envelope. *Cellular Microbiology* **11**(2), 249-260.
- Brown, D. A., and London, E. (1998). Structure and origin of ordered lipid domains in biological membranes. *Journal of Membrane Biology* **164**(2), 103-114.
- Brown, D. A., and Rose, J. K. (1992). Sorting of Gpi-Anchored Proteins to Glycolipid-Enriched Membrane Subdomains during Transport to the Apical Cell-Surface. *Cell* **68**(3), 533-544.
- Brown, W. J., Chambers, K., and Doody, A. (2003). Phospholipase A2 (PLA2) enzymes in membrane trafficking: Mediators of membrane shape and function. *Traffic* **4**(4), 214-221.
- Brugger, B., Glass, B., Haberkant, P., Leibrecht, I., Wieland, F. T., and Krausslich, H. G. (2006). The HIV lipidome: A raft with an unusual composition. *Proceedings of the National Academy of Sciences of the United States of America* **103**(8), 2641-2646.
- Brugger, B., Krautkramer, E., Tibroni, N., Munte, C. E., Rauch, S., Leibrecht, I., Glass, B., Breuer, S., Geyer, M., Krausslich, H. G., Kalbitzer, H. R., Wieland, F. T., and Fackler, O. T. (2007a). Human immunodeficiency virus type 1 Nef protein modulates the lipid composition of virions and host cell membrane microdomains. *Retrovirology* **4**, 70.
- Brugger, B., Krautkramer, E., Tibroni, N., Munte, C. E., Rauch, S., Leibrecht, I., Glass, B., Breuer, S., Geyer, M., Krausslich, H. G., Kalbitzer, H. R., Wieland, F. T., and Fackler, O. T. (2007b). Human immunodeficiency virus type 1 nef protein modulates the lipid composition of virions and host cell membrane microdomains. *Retrovirology* **4**, -.
- Brugh, M. (1977). Butylated Hydroxytoluene Protects Chickens Exposed to Newcastle-Disease Virus. *Science* **197**(4310), 1291-1292.
- Buckheit, R. W., Watson, K. M., Morrow, K. M., and Ham, A. S. (2010). Development of topical microbicides to prevent the sexual transmission of HIV. *Antiviral Research* **85**(1), 142-158.
- Bullough, P. A., Hughson, F. M., Skehel, J. J., and Wiley, D. C. (1994). Structure of Influenza Hemagglutinin at the pH of Membrane-Fusion. *Nature* **371**(6492), 37-43.
- Burger, K. N. J. (2000). Greasing membrane fusion and fission machineries. *Traffic* **1**(8), 605-613.
- Cai, W. H., Gu, B. H., and Person, S. (1988). Role of Glycoprotein-B of Herpes-Simplex Virus Type-1 in Viral Entry and Cell-Fusion. *Journal of Virology* **62**(8), 2596-2604.
- Cairns, T. M., Shaner, M. S., Zuo, Y., Ponce-de-Leon, M., Baribaud, I., Eisenberg, R. J., Cohen, G. H., and Whitbeck, J. C. (2006). Epitope mapping of herpes simplex virus type 2 gH/gL defines distinct antigenic

- sites, including some associated with biological function. *Journal of Virology* **80**(6), 2596-2608.
- Campadelli-Fiume, G., Amasio, M., Avitabile, E., Cerretani, A., Forghieri, C., Gianni, T., and Menotti, L. (2007). The multipartite system that mediates entry of herpes simplex virus into the cell. *Reviews in Medical Virology* **17**(5), 313-326.
- Campadelli-Fiume, G., Arsenakis, M., Farabegoli, F., and Roizman, B. (1988). Entry of Herpes-Simplex Virus-1 in BJ Cells That Constitutively Express Viral Glycoprotein D Is by Endocytosis and Results in Degradation of the Virus. *Journal of Virology* **62**(1), 159-167.
- Campadelli-Fiume, G., and Roizman, B. (2006). The egress of herpesviruses from cells: the unanswered questions. *Journal of Virology* **80**(13), 6716-6717.
- Campadelli-Fiume, G., Stirpe, D., Boscaro, A., Avitabile, E., Foatomasi, L., Barker, D., and Roizman, B. (1990). Glycoprotein C-Dependent Attachment of Herpes-Simplex Virus to Susceptible Cells Leading to Productive Infection. *Virology* **178**(1), 213-222.
- Carfi, A., Willis, S. H., Whitbeck, J. C., Krummenacher, C., Cohen, G. H., Eisenberg, R. J., and Wiley, D. C. (2001). Herpes simplex virus glycoprotein D bound to the human receptor HveA. *Molecular Cell* **8**(1), 169-179.
- Carneiro, F. A., Lapido-Loureiro, P. A., Cordo, S. M., Stauffer, F., Weissmuller, G., Bianconi, M. L., Juliano, M. A., Juliano, L., Bisch, P. M., and Poian, A. T. D. (2006). Probing the interaction between vesicular stomatitis virus and phosphatidylserine. *European Biophysics Journal with Biophysics Letters* **35**(2), 145-154.
- Chan, R., Uchil, P. D., Jin, J., Shui, G. H., Ott, D. E., Mothes, W., and Wenk, M. R. (2008). Retroviruses Human Immunodeficiency Virus and Murine Leukemia Virus Are Enriched in Phosphoinositides. *Journal of Virology* **82**(22), 11228-11238.
- Chen, A., Leikina, E., Melikov, K., Podbilewicz, B., Kozlov, M. M., and Chernomordik, L. V. (2008). Fusion-pore expansion during syncytium formation is restricted by an actin network. *Journal of Cell Science* **121**(21), 3619-3628.
- Chen, J., Lee, K. H., Steinhauer, D. A., Stevens, D. J., Skehel, J. J., and Wiley, D. C. (1998). Structure of the hemagglutinin precursor cleavage site, a determinant of influenza pathogenicity and the origin of the labile conformation. *Cell* **95**(3), 409-417.
- Chernomordik, L. (1996). Non-bilayer lipids and biological fusion intermediates. *Chemistry and Physics of Lipids* **81**(2), 203-213.
- Chernomordik, L., Kozlov, M. M., and Zimmerberg, J. (1995). Lipids in biological membrane fusion. *J Membr Biol* **146**(1), 1-14.
- Chernomordik, L. V., and Kozlov, M. M. (2003). Protein-lipid interplay in fusion and fission of biological membranes. *Annual Review of Biochemistry* **72**, 175-207.
- Chernomordik, L. V., and Kozlov, M. M. (2005). Membrane hemifusion: Crossing a chasm in two leaps. *Cell* **123**(3), 375-382.

- Chernomordik, L. V., and Kozlov, M. M. (2008). Mechanics of membrane fusion. *Nature Structural & Molecular Biology* **15**(7), 675-683.
- Chernomordik, L. V., Kozlov, M. M., Melikyan, G. B., Abidor, I. G., Markin, V. S., and Chizmadzhev, Y. A. (1985). The Shape of Lipid Molecules and Monolayer Membrane-Fusion. *Biochimica et Biophysica Acta* **812**(3), 643-655.
- Chernomordik, L. V., Leikina, E., Kozlov, M. M., Frolov, V. A., and Zimmerberg, J. (1999). Structural intermediates in influenza haemagglutinin-mediated fusion. *Molecular Membrane Biology* **16**(1), 33-42.
- Chernomordik, L. V., Melikyan, G. B., and Chizmadzhev, Y. A. (1987). Biomembrane Fusion - a New Concept Derived from Model Studies Using 2 Interacting Planar Lipid Bilayers. *Biochimica Et Biophysica Acta* **906**(3), 309-352.
- Chowdary, T. K., Cairns, T. M., Atanasiu, D., Cohen, G. H., Eisenberg, R. J., and Heldwein, E. E. (2010). Crystal structure of the conserved herpesvirus fusion regulator complex gH-gL. *Nat Struct Mol Biol* **17**(7), 882-8.
- Chowdary, T. K., and Heldwein, E. E. (2010). Syncytial Phenotype of C-Terminally Truncated Herpes Simplex Virus Type 1 gB Is Associated with Diminished Membrane Interactions. *Journal of Virology* **84**(10), 4923-4935.
- Chung, R. T., Gale, M., Jr., Polyak, S. J., Lemon, S. M., Liang, T. J., and Hoofnagle, J. H. (2008). Mechanisms of action of interferon and ribavirin in chronic hepatitis C: Summary of a workshop. *Hepatology* **47**(1), 306-20.
- Churchward, M. A., Rogasevskaia, T., Hofgen, J., Bau, J., and Coorsen, J. R. (2005). Cholesterol facilitates the native mechanism of Ca²⁺-triggered membrane fusion. *Journal of Cell Science* **118**(20), 4833-4848.
- Cihlar, T., and Ray, A. S. (2010). Nucleoside and nucleotide HIV reverse transcriptase inhibitors: 25 years after zidovudine. *Antiviral Research* **85**(1), 39-58.
- Cocchi, F., Fusco, D., Menotti, L., Gianni, T., Eisenberg, R. J., Cohen, G. H., and Campadelli-Fiume, G. (2004). The soluble ectodomain of herpes simplex virus gD contains a membrane-proximal pro-fusion domain and suffices to mediate virus entry. *Proceedings of the National Academy of Sciences of the United States of America* **101**(19), 7445-7450.
- Cocchi, F., Menotti, L., Mirandola, P., Lopez, M., and Campadelli-Fiume, G. (1998). The ectodomain of a novel member of the immunoglobulin subfamily related to the poliovirus receptor has the attributes of a bona fide receptor for herpes simplex virus types 1 and 2 in human cells. *Journal of Virology* **72**(12), 9992-10002.
- Coelmont, L., Gallay, P., Bobardt, M., Kaptein, S., Paeshuyse, J., Vliegen, I., Vuagniaux, G., and Neyts, J. (2009a). In vitro Anti-hepatitis C Virus (HCV) Activities and Resistance Profile of Debio 025, A Non-immunosuppressive Cyclophilin Binding Molecule. *Antiviral Research* **82**(2), A20-A20.

- Coelmont, L., Hanouille, X., Chatterji, U., Berger, C., Snoeck, J., Bobardt, M., Lim, P., Vliegen, I., Paeshuyse, J., Vuagniaux, G., Vandamme, A. M., Bartenschlager, R., Gallay, P., Lippens, G., and Neyts, J. (2010). DEB025 (Alisporivir) inhibits hepatitis C virus replication by preventing a cyclophilin A induced cis-trans isomerisation in domain II of NS5A. *PLoS One* **5**(10), e13687.
- Coelmont, L., Kaptein, S., Paeshuyse, J., Vliegen, I., Dumont, J. M., Vuagniaux, G., and Neyts, J. (2009b). Debio 025, a Cyclophilin Binding Molecule, Is Highly Efficient in Clearing Hepatitis C Virus (HCV) Replicon-Containing Cells When Used Alone or in Combination with Specifically Targeted Antiviral Therapy for HCV (STAT-C) Inhibitors. *Antimicrobial Agents and Chemotherapy* **53**(3), 967-976.
- Coen, D. M., and Schaffer, P. A. (1980). 2 Distinct Loci Confer Resistance to Acycloguanosine in Herpes-Simplex Virus Type-1. *Proceedings of the National Academy of Sciences of the United States of America-Biological Sciences* **77**(4), 2265-2269.
- Cohen, F. S., and Melikyan, G. B. (2004). The energetics of membrane fusion from binding, through hemifusion, pore formation, and pore enlargement. *Journal of Membrane Biology* **199**(1), 1-14.
- Coil, D. A., and Miller, A. D. (2005). Enhancement of enveloped virus entry by phosphatidylserine. *Journal of Virology* **79**(17), 11496-11500.
- Collins, P. J., Haire, L. F., Lin, Y. P., Liu, J. F., Russell, R. J., Walker, P. A., Skehel, J. J., Martin, S. R., Hay, A. J., and Gamblin, S. J. (2008). Crystal structures of oseltamivir-resistant influenza virus neuraminidase mutants. *Nature* **453**(7199), 1258-U61.
- Condit, R. C., Moussatche, N., and Traktman, P. (2006). In a nutshell: structure and assembly of the vaccinia virion. *Adv Virus Res* **66**, 31-124.
- Conner, S. D., and Schmid, S. L. (2003). Regulated portals of entry into the cell. *Nature* **422**(6927), 37-44.
- Connor, E. M., Sperling, R. S., Gelber, R., Kiselev, P., Scott, G., Osullivan, M. J., Vandyke, R., Bey, M., Shearer, W., Jacobson, R. L., Jimenez, E., Oneill, E., Bazin, B., Delfraissy, J. F., Culnane, M., Coombs, R., Elkins, M., Moye, J., Stratton, P., and Balsley, J. (1994). Reduction of Maternal-Infant Transmission of Human-Immunodeficiency-Virus Type-1 with Zidovudine Treatment. *New England Journal of Medicine* **331**(18), 1173-1180.
- Cooke, I. R., and Deserno, M. (2006). Coupling between lipid shape and membrane curvature. *Biophysical Journal* **91**(2), 487-495.
- Cutler, B., and Justman, J. (2008). Vaginal microbicides and the prevention of HIV transmission. *Lancet Infectious Diseases* **8**(11), 685-697.
- Danieli, T., Pelletier, S. L., Henis, Y. I., and White, J. M. (1996). Membrane fusion mediated by the influenza virus hemagglutinin requires the concerted action of at least three hemagglutinin trimers. *Journal of Cell Biology* **133**(3), 559-569.
- Darlington, R. W., and Moss, L. H. (1968). Herpesvirus Envelopment. *Journal of Virology* **2**(1), 48-55.

- Davies, W. L., Hoffmann, C. E., Paulshock, M., Wood, T. R., Haff, R. F., Grunert, R. R., Watts, J. C., Hermann, E. C., Neumayer, E. M., and McGahen, J. W. (1964). Antiviral Activity of 1-Adamantanamine (Amantadine). *Science* **144**(362), 862-&.
- Davison, A. J., Eberle, R., Ehlers, B., Hayward, G. S., McGeoch, D. J., Minson, A. C., Pellett, P. E., Roizman, B., Studdert, M. J., and Thiry, E. (2009). The order Herpesvirales. *Arch Virol* **154**(1), 171-7.
- Davletov, B., and Montecucco, C. (2010). Lipid function at synapses. *Curr Opin Neurobiol* **20**(5), 543-9.
- De Beeck, A. O., Voisset, C., Bartosch, B., Ciczora, Y., Cocquerel, L., Keck, Z., Fong, S., Cosset, F. L., and Dubuisson, J. (2004). Characterization of functional hepatitis C virus envelope glycoproteins. *Journal of Virology* **78**(6), 2994-3002.
- de Bethune, M. P. (2010). Non-nucleoside reverse transcriptase inhibitors (NNRTIs), their discovery, development, and use in the treatment of HIV-1 infection: A review of the last 20 years (1989-2009). *Antiviral Research* **85**(1), 75-90.
- De Clercq, E. (2001). Antiviral drugs: current state of the art. *Journal of Clinical Virology* **22**(1), 73-89.
- De Clercq, E. (2004). Antiviral drugs in current clinical use. *Journal of Clinical Virology* **30**(2), 115-133.
- De Clercq, E. (2007a). The acyclic nucleoside phosphonates from inception to clinical use: Historical perspective. *Antiviral Research* **75**(1), 1-13.
- De Clercq, E. (2007b). Three decades of antiviral drugs. *Nat Rev Drug Discov* **6**(12), 941-941.
- De Clercq, E. (2008a). Antivirals: current state of the art. *Future Virology* **3**(4), 393-405.
- De Clercq, E. (2008b). Emerging antiviral drugs. *Expert Opinion on Emerging Drugs* **13**(3), 393-416.
- De Clercq, E., and Holy, A. (2005). Acyclic nucleoside phosphonates: a key class of antiviral drugs. *Nat Rev Drug Discov* **4**(11), 928-40.
- Dean, H. J., Terhune, S. S., Shieh, M. T., Susmarski, N., and Spear, P. G. (1994). Single Amino-Acid Substitutions in Gd of Herpes-Simplex Virus-1 Confer Resistance to Gd-Mediated Interference and Cause Cell-Type-Dependent Alterations in Infectivity. *Virology* **199**(1), 67-80.
- Desplanques, A. S., Nauwynck, H. J., Vercauteren, D., Geens, T., and Favoreel, H. W. (2008). Plasma membrane cholesterol is required for efficient pseudorabies virus entry. *Virology* **376**(2), 339-345.
- Deval, J. (2009). Antimicrobial Strategies Inhibition of Viral Polymerases by 3 '-Hydroxyl Nucleosides. *Drugs* **69**(2), 151-166.
- Devaux, P. F., Herrmann, A., Ohlwein, N., and Kozirov, M. M. (2008). How lipid flippases can modulate membrane structure. *Biochimica Et Biophysica Acta-Biomembranes* **1778**(7-8), 1591-1600.
- Devaux, P. F., and Morris, R. (2004). Transmembrane asymmetry and lateral domains in biological membranes. *Traffic* **5**(4), 241-246.

- Deville-Bonne, D., El Amri, C., Meyer, P., Chen, Y. X., Agrofoglio, L. A., and Janin, J. (2010). Human and viral nucleoside/nucleotide kinases involved in antiviral drug activation: Structural and catalytic properties. *Antiviral Research* **86**(1), 101-120.
- Dolnik, O., Kolesnikova, L., and Becker, S. (2008). Filoviruses: Interactions with the host cell. *Cellular and Molecular Life Sciences* **65**(5), 756-776.
- Doms, R. W., Blumenthal, R., and Moss, B. (1990). Fusion of Intracellular and Extracellular Forms of Vaccinia Virus with the Cell-Membrane. *Journal of Virology* **64**(10), 4884-4892.
- Dorr, P., Westby, M., Dobbs, S., Griffin, P., Irvine, B., Macartney, M., Mori, J., Rickett, G., Smith-Burchnell, C., Napier, C., Webster, R., Armour, D., Price, D., Stammen, B., Wood, A., and Perros, M. (2005). Maraviroc (UK-427,857), a potent, orally bioavailable, and selective small-molecule inhibitor of chemokine receptor CCR5 with broad-spectrum anti-human immunodeficiency virus type 1 activity. *Antimicrob Agents Chemother* **49**(11), 4721-32.
- Edelmann, L., Hanson, P. I., Chapman, E. R., and Jahn, R. (1995). Synaptobrevin binding to synaptophysin: a potential mechanism for controlling the exocytic fusion machine. *The EMBO Journal* **14**(2), 224-231.
- Effferth, T., Romero, M. R., Wolf, D. G., Stamminger, T., Marin, J. J. G., and Marschall, M. (2008). The antiviral activities of artemisinin and artesunate. *Clinical Infectious Diseases* **47**(6), 804-811.
- Elion, G. B., Furman, P. A., Fyfe, J. A., Demiranda, P., Beauchamp, L., and Schaeffer, H. J. (1977). Selectivity of Action of an Anti-Herpetic Agent, 9-(2-Hydroxyethoxymethyl)Guanine. *Proceedings of the National Academy of Sciences of the United States of America* **74**(12), 5716-5720.
- Epand, R. M. (2003). Fusion peptides and the mechanism of viral fusion. *Biochimica Et Biophysica Acta-Biomembranes* **1614**(1), 116-121.
- Evans, M. J., von Hahn, T., Tscherne, D. M., Syder, A. J., Panis, M., Wolk, B., Hatzioannou, T., McKeating, J. A., Bieniasz, P. D., and Rice, C. M. (2007). Claudin-1 is a hepatitis C virus co-receptor required for a late step in entry. *Nature* **446**(7137), 801-805.
- Fantini, J., Garmy, N., Mahfoud, R., and Yahi, N. (2002). Lipid rafts: structure, function and role in HIV, Alzheimer's and prion diseases. *Expert Reviews in Molecular Medicine* **4**, 1-22.
- Farge, E., Ojcius, D. M., Subtil, A., and Dautry-Varsat, A. (1999). Enhancement of endocytosis due to aminophospholipid transport across the plasma membrane of living cells. *American Journal of Physiology-Cell Physiology* **276**(3), C725-C733.
- Fasshauer, D., Sutton, R. B., Brunger, A. T., and Jahn, R. (1998). Conserved structural features of the synaptic fusion complex: SNARE proteins reclassified as Q- and R-SNAREs. *Proceedings of the National Academy of Sciences of the United States of America* **95**(26), 15781-15786.
- Feld, J. J., and Hoofnagle, J. H. (2005). Mechanism of action of interferon and ribavirin in treatment of hepatitis C. *Nature* **436**(7053), 967-972.

- Feng, Y., Broder, C. C., Kennedy, P. E., and Berger, E. A. (1996). HIV-1 entry cofactor: Functional cDNA cloning of a seven-transmembrane, G protein-coupled receptor. *Science* **272**(5263), 872-877.
- Fischer, K. P., and Tyrrell, D. L. (1996). Generation of duck hepatitis B virus polymerase mutants through site-directed mutagenesis which demonstrate resistance to lamivudine [(--)-beta-L-2', 3'-dideoxy-3'-thiacytidine] in vitro. *Antimicrob Agents Chemother* **40**(8), 1957-60.
- Fitzsimmons, M. E., and Collins, J. M. (1997). Selective biotransformation of the human immunodeficiency virus protease inhibitor saquinavir by human small-intestinal cytochrome P4503A4: potential contribution to high first-pass metabolism. *Drug Metab Dispos* **25**(2), 256-66.
- Fong, B. S., and Brown, J. C. (1978). Asymmetric Distribution of Phosphatidylethanolamine Fatty Acyl Chains in Membrane of Vesicular Stomatitis-Virus. *Biochimica Et Biophysica Acta* **510**(2), 230-241.
- Fong, B. S., Hunt, R. C., and Brown, J. C. (1976). Asymmetric Distribution of Phosphatidylethanolamine in Membrane of Vesicular Stomatitis-Virus. *Journal of Virology* **20**(3), 658-663.
- Forrester, A., Farrell, H., Wilkinson, G., Kaye, J., Davispoynter, N., and Minson, T. (1992). Construction and Properties of a Mutant of Herpes-Simplex Virus Type-1 with Glycoprotein-H Coding Sequences Deleted. *Journal of Virology* **66**(1), 341-348.
- Fujita, H., Tamai, K., Kawachi, M., Saga, K., Shimbo, T., Yamazaki, T., and Kaneda, Y. (2011). Methyl-beta cyclodextrin alters the production and infectivity of Sendai virus. *Archives of Virology* **156**(6), 995-1005.
- Fusco, D., Forghieri, C., and Campadelli-Fiume, G. (2005). The pro-fusion domain of herpes simplex virus glycoprotein D (gD) interacts with the gD N terminus and is displaced by soluble forms of viral receptors. *Proceedings of the National Academy of Sciences of the United States of America* **102**(26), 9323-9328.
- Galdiero, S., Vitiello, M., D'Isanto, M., Falanga, A., Cantisan, M., Browne, H., Pedone, C., and Galdiero, M. (2008). The identification and characterization of fusogenic domains in herpes virus glycoprotein B molecules. *Chembiochem* **9**(5), 758-767.
- Gallo, R. C., Salahuddin, S. Z., Popovic, M., Shearer, G. M., Kaplan, M., Haynes, B. F., Palker, T. J., Redfield, R., Oleske, J., Safai, B., White, G., Foster, P., and Markham, P. D. (1984). Frequent Detection and Isolation of Cytopathic Retroviruses (Htlv-Iii) from Patients with Aids and at Risk for Aids. *Science* **224**(4648), 500-503.
- Gao, L. H., Lipowsky, R., and Shillcock, J. (2008). Tension-induced vesicle fusion: pathways and pore dynamics. *Soft Matter* **4**(6), 1208-1214.
- Garry, R. F., and Dash, S. (2003). Proteomics computational analyses suggest that hepatitis C virus E1 and pestivirus E2 envelope glycoproteins are truncated class II fusion proteins. *Virology* **307**(2), 255-265.
- Gaudin, Y. (2000). Rabies virus-induced membrane fusion pathway. *Journal of Cell Biology* **150**(3), 601-611.

- Gaudin, Y., Tuffereau, C., Segretain, D., Knossow, M., and Flamand, A. (1991). Reversible Conformational-Changes and Fusion Activity of Rabies Virus Glycoprotein. *Journal of Virology* **65**(9), 4853-4859.
- Geraghty, R. J., Krummenacher, C., Cohen, G. H., Eisenberg, R. J., and Spear, P. G. (1998). Entry of alphaherpesviruses mediated by poliovirus receptor-related protein 1 and poliovirus receptor. *Science* **280**(5369), 1618-1620.
- Gianni, T., Fato, R., Bergamini, C., Lenaz, G., and Campadelli-Fiume, G. (2006). Hydrophobic alpha-helices 1 and 2 of herpes simplex virus gH interact with lipids, and their mimetic peptides enhance virus infection and fusion. *Journal of Virology* **80**(16), 8190-8198.
- Gibbons, D. L., Vaney, M. C., Roussel, A., Vigouroux, A., Reilly, B., Lepault, J., Kielian, M., and Rey, F. A. (2004). Conformational change and protein-protein interactions of the fusion protein of Semliki Forest virus. *Nature* **427**(6972), 320-325.
- Glomb-Reinmund, S., and Kielian, M. (1998). The role of low pH and disulfide shuffling in the entry and fusion of Semliki Forest virus and Sindbis virus. *Virology* **248**(2), 372-81.
- Godowski, P. J., and Knipe, D. M. (1986). Transcriptional Control of Herpesvirus Gene-Expression - Gene Functions Required for Positive and Negative Regulation. *Proceedings of the National Academy of Sciences of the United States of America* **83**(2), 256-260.
- Gonzalez-Candelas, F., and Lopez-Labrador, X. F. (2010). Clinical relevance of genetic heterogeneity in HCV. *Future Virology* **5**(1), 33-49.
- Graham, D. R. M., Chertova, E., Hilburn, J. M., Arthur, L. O., and Hildreth, J. E. K. (2003). Cholesterol depletion of human immunodeficiency virus type 1 and simian immunodeficiency virus with beta-cyclodextrin inactivates and permeabilizes the virions: Evidence for virion-associated lipid rafts. *Journal of Virology* **77**(15), 8237-8248.
- Gruner, S. M. (1985). Intrinsic Curvature Hypothesis for Biomembrane Lipid-Composition - a Role for Nonbilayer Lipids. *Proceedings of the National Academy of Sciences of the United States of America* **82**(11), 3665-3669.
- Gunther-Ausborn, S., Praetor, A., and Stegmann, T. (1995). Inhibition of Influenza-Induced Membrane-Fusion by Lysophosphatidylcholine. *Journal of Biological Chemistry* **270**(49), 29279-29285.
- Guo, Y. P., Kotova, E., Chen, Z. S., Lee, K., Hopper-Borge, E., Belinsky, M. G., and Kruh, G. D. (2003). MRP8, ATP-binding cassette C11 (ABCC11), is a cyclic nucleotide efflux pump and a resistance factor for fluoropyrimidines 2',3'-dideoxycytidine and 9'-(2'-phosphonylmethoxyethyl) adenine. *Journal of Biological Chemistry* **278**(32), 29509-29514.
- Guzman, R. E., Schwarz, Y. N., Rettig, J., and Bruns, D. (2010). SNARE Force Synchronizes Synaptic Vesicle Fusion and Controls the Kinetics of Quantal Synaptic Transmission. *Journal of Neuroscience* **30**(31), 10272-10281.
- Haase, A. T. (2010). Targeting early infection to prevent HIV-1 mucosal transmission. *Nature* **464**(7286), 217-223.

- Hamm, M., and Kozlov, M. M. (2000). Elastic energy of tilt and bending of fluid membranes. *European Physical Journal E* **3**, 323-335.
- Hannah, B. P., Cairns, T. M., Bender, F. C., Whitbeck, J. C., Lou, H., Eisenberg, R. J., and Cohen, G. H. (2009). Herpes Simplex Virus Glycoprotein B Associates with Target Membranes via Its Fusion Loops. *Journal of Virology* **83**(13), 6825-6836.
- Hannah, B. P., Heldwein, E. E., Bender, F. C., Cohen, G. H., and Eisenberg, R. J. (2007). Mutational evidence of internal fusion loops in herpes simplex virus glycoprotein B. *Journal of Virology* **81**(9), 4858-4865.
- Harada, S. (2005). The broad anti-viral agent glycyrrhizin directly modulates the fluidity of plasma membrane and HIV-1 envelope. *Biochemical Journal* **392**, 191-199.
- Hazuda, D., Ogert, R., Howe, J., Barnard, R., Striszki, J., Brass, C., Burroughs, M., Boparai, N., Albrecht, J., and Howe, A. (2011). *6th IAS Conference on HIV pathogenesis, Treatment and Prevention, Rome, Italy*.
- Heldwein, E. E., Lou, H., Bender, F. C., Cohen, G. H., Eisenberg, R. J., and Harrison, S. C. (2006). Crystal structure of glycoprotein B from herpes simplex virus 1. *Science* **313**(5784), 217-220.
- Herlocher, M. L., Truscon, R., Elias, S., Yen, H. L., Roberts, N. A., Ohmit, S. E., and Monto, A. S. (2004). Influenza viruses resistant to the antiviral drug oseltamivir: Transmission studies in ferrets. *Journal of Infectious Diseases* **190**(9), 1627-1630.
- Herold, B. C., Visalli, R. J., Susmarski, N., Brandt, C. R., and Spear, P. G. (1994). Glycoprotein-C-Independent Binding of Herpes-Simplex Virus to Cells Requires Cell-Surface Heparan-Sulfate and Glycoprotein-B. *Journal of General Virology* **75**, 1211-1222.
- Herold, B. C., Wudunn, D., Soltys, N., and Spear, P. G. (1991). Glycoprotein-C of Herpes-Simplex Virus Type-1 Plays a Principal Role in the Adsorption of Virus to Cells and in Infectivity. *Journal of Virology* **65**(3), 1090-1098.
- Hicks, D. R., Martin, L. S., Getchell, J. P., Heath, J. L., Francis, D. P., McDougal, J. S., Curran, J. W., and Voeller, B. (1985). Inactivation of Htlv-Iii Lav-Infected Cultures of Normal Human-Lymphocytes by Nonoxynol-9 In vitro. *Lancet* **2**(8469), 1422-1423.
- Hillier, S. (2008). Safety and acceptability of daily and coitally dependent use of 1% tenofovir over six months of use. Abstract #655. In "Microbicides", New Delhi, India.
- Hiraga, N., Imamura, M., Abe, H., Hayes, C. N., Kono, T., Onishi, M., Tsuge, M., Takahashi, S., Ochi, H., Iwao, E., Kamiya, N., Yamada, I., Tateno, C., Yoshizato, K., Matsui, H., Kanai, A., Inaba, T., Tanaka, S., and Chayama, K. (2011). Rapid Emergence of Telaprevir Resistant Hepatitis C Virus Strain from Wildtype Clone In Vivo. *Hepatology* **54**(3), 781-788.
- Ho, H. T., and Hitchcock, M. J. M. (1989). Cellular Pharmacology of 2',3'-Dideoxy-2',3'-Didehydrothymidine, a Nucleoside Analog Active against Human Immunodeficiency Virus. *Antimicrobial Agents and Chemotherapy* **33**(6), 844-849.

- Hodge, V. A. (2011). Scientific report: highlights of 24th ICAR, 8-11 May 2011, Sofia, Bulgaria. *Antivir Chem Chemother* **22**(2), 75-85.
- Hoffmann, C. (2007). The epidemiology of HIV coreceptor tropism. *European Journal of Medical Research* **12**(9), 385-390.
- Hogle, J. M. (2002). Poliovirus cell entry: Common structural themes in viral cell entry pathways. *Annual Review of Microbiology* **56**, 677-702.
- Honess, R. W. (1984). Herpes simplex and 'the herpes complex': diverse observations and a unifying hypothesis. The eighth Fleming lecture. *J Gen Virol* **65 (Pt 12)**, 2077-107.
- Honess, R. W., and Roizman, B. (1974). Regulation of Herpesvirus Macromolecular-Synthesis .1. Cascade Regulation of Synthesis of 3 Groups of Viral Proteins. *Journal of Virology* **14**(1), 8-19.
- Hostetler, K. Y. (2009). Alkoxyalkyl prodrugs of acyclic nucleoside phosphonates enhance oral antiviral activity and reduce toxicity: Current state of the art. *Antiviral Research* **82**(2), A84-A98.
- Hu, K. A., Carroll, J., Rickman, C., and Davletov, B. (2002). Action of complexin on SNARE complex. *Journal of Biological Chemistry* **277**(44), 41652-41656.
- Huang, H. L., Li, Y. M., Sadaoka, T., Tang, H. M., Yamamoto, T., Yamanishi, K., and Mori, Y. (2006). Human herpesvirus 6 envelope cholesterol is required for virus entry. *Journal of General Virology* **87**, 277-285.
- Huang, T. M., and Campadelli-Fiume, G. (1996). Anti-idiotypic antibodies mimicking glycoprotein D of herpes simplex virus identify a cellular protein required for virus spread from cell to cell and virus-induced polykaryocytosis. *Proceedings of the National Academy of Sciences of the United States of America* **93**(5), 1836-1840.
- Hui, S. W., Stewart, T. P., Boni, L. T., and Yeagle, P. L. (1981). Membrane-Fusion through Point-Defects in Bilayers. *Science* **212**(4497), 921-923.
- Hunsucker, S. A., Mitchell, B. S., and Spychala, J. (2005). The 5'-nucleotidases as regulators of nucleotide and drug metabolism. *Pharmacology & Therapeutics* **107**(1), 1-30.
- Hutchinson, L., Browne, H., Wargent, V., Davispoynter, N., Primorac, S., Goldsmith, K., Minson, A. C., and Johnson, D. C. (1992). A Novel Herpes-Simplex Virus Glycoprotein, gL, Forms a Complex with Glycoprotein H (gH) and Affects Normal Folding and Surface Expression of gH. *Journal of Virology* **66**(4), 2240-2250.
- Imai, M., Mizuno, T., and Kawasaki, K. (2006). Membrane fusion by single influenza hemagglutinin trimers - Kinetic evidence from image analysis of hemagglutinin-reconstituted vesicles. *Journal of Biological Chemistry* **281**(18), 12729-12735.
- Innaimo, S. F., Seifer, M., Bisacchi, G. S., Strandring, D. N., Zahler, R., and Colonno, R. J. (1997). Identification of EMS-200475 as a potent and selective inhibitor of hepatitis B virus. *Antimicrobial Agents and Chemotherapy* **41**(7), 1444-1448.
- Izzedine, H., Launay-Vacher, V., and Deray, G. (2005a). Antiviral drug-induced nephrotoxicity. *Am J Kidney Dis* **45**(5), 804-17.

- Izzedine, H., Launay-Vacher, V., and Deray, G. (2005b). Renal tubular transporters and antiviral drugs: an update. *Aids* **19**(5), 455-62.
- Jackson, M. B. (2009). Minimum Membrane Bending Energies of Fusion Pores. *Journal of Membrane Biology* **231**(2-3), 101-115.
- Jelesarov, I., and Lu, M. (2001). Thermodynamics of trimer-of-hairpins formation by the SIV gp41 envelope protein. *J Mol Biol* **307**(2), 637-56.
- Johannsdottir, H. K., Mancini, R., Kartenbeck, J., Amato, L., and Helenius, A. (2009). Host cell factors and functions involved in vesicular stomatitis virus entry. *J Virol* **83**(1), 440-53.
- Johnson, D. C., Burke, R. L., and Gregory, T. (1990). Soluble Forms of Herpes-Simplex Virus Glycoprotein-D Bind to a Limited Number of Cell-Surface Receptors and Inhibit Virus Entry into Cells. *Journal of Virology* **64**(6), 2569-2576.
- Johnson, R. M., and Spear, P. G. (1989). Herpes-Simplex Virus Glycoprotein-D Mediates Interference with Herpes-Simplex Virus-Infection. *Journal of Virology* **63**(2), 819-827.
- Johnson, V. A., Brun-Vezinet, F., Clotet, B., Gunthard, H. F., Kuritzkes, D. R., Pillay, D., Schapiro, J., and Richman, D. D. (2009). Update of the drug resistance mutations in HIV-1. *Topics in HIV Medicine* **17**(5), 138-145.
- Kalvodova, L., Sampaio, J. L., Cordo, S., Ejsing, C. S., Shevchenko, A., and Simons, K. (2009). The Lipidomes of Vesicular Stomatitis Virus, Semliki Forest Virus, and the Host Plasma Membrane Analyzed by Quantitative Shotgun Mass Spectrometry. *Journal of Virology* **83**(16), 7996-8003.
- Karim, Q. A., Karim, S. S., Frohlich, J. A., Grobler, A. C., Baxter, C., Mansoor, L. E., Kharsany, A. B., Sibeko, S., Mlisana, K. P., Omar, Z., Gengiah, T. N., Maarschalk, S., Arulappan, N., Mlotshwa, M., Morris, L., and Taylor, D. (2010). Effectiveness and Safety of Tenofovir Gel, an Antiretroviral Microbicide, for the Prevention of HIV Infection in Women. *Science* **329**, 1168-1174.
- Katsov, K., Muller, M., and Schick, M. (2004). Field theoretic study of bilayer membrane fusion. I. Hemifusion mechanism. *Biophysical Journal* **87**(5), 3277-3290.
- Keller, M. J., Mesquita, P. M., Torres, N. M., Cho, S., Shust, G., Madan, R. P., Cohen, H. W., Petrie, J., Ford, T., Soto-Torres, L., Profy, A. T., and Herold, B. C. (2010). Postcoital bioavailability and antiviral activity of 0.5% PRO 2000 gel: implications for future microbicide clinical trials. *PLoS One* **5**(1), e8781.
- Keller, M. J., Zerhouni-Layachi, B., Cheshenko, N., John, M., Hogarty, K., Kasowitz, A., Goldberg, C. L., Wallenstein, S., Profy, A. T., Klotman, M. E., and Herold, B. C. (2006). PRO 2000 gel inhibits HIV and herpes simplex virus infection following vaginal application: A double-blind placebo-controlled trial. *Journal of Infectious Diseases* **193**(1), 27-35.
- Kielian, M., and Rey, F. A. (2006). Virus membrane-fusion proteins: more than one way to make a hairpin. *Nature Reviews Microbiology* **4**(1), 67-76.

- Kim, K. S., Moon, H. M., Sapienza, V., Carp, R. I., and Pullarkat, R. (1978). Inactivation of Cytomegalovirus and Semliki Forest Virus by Butylated Hydroxytoluene. *Journal of Infectious Diseases* **138**(1), 91-94.
- Klyachkin, Y. M., Stoops, K. D., and Geraghty, R. J. (2006). Herpes simplex virus type 1 glycoprotein L mutants that fail to promote trafficking of glycoprotein H and fail to function in fusion can induce binding of glycoprotein L-dependent anti-glycoprotein H antibodies. *J Gen Virol* **87**(Pt 4), 759-67.
- Koch, P., Lampe, M., Godinez, W. J., Muller, B., Rohr, K., Krausslich, H. G., and Lehmann, M. J. (2009). Visualizing fusion of pseudotyped HIV-1 particles in real time by live cell microscopy. *Retrovirology* **6**, -.
- Kooijman, E. E., Chupin, V., de Kruijff, B., and Burger, K. N. J. (2003). Modulation of membrane curvature by phosphatidic acid and lysophosphatidic acid. *Traffic* **4**(3), 162-174.
- Korshun, V. A., Manasova, E. V., Balakin, K. V., Malakhov, A. D., Perepelov, A. V., Sokolova, T. A., and Berlin, Y. A. (1998). New fluorescent nucleoside derivatives - 5-alkynylated 2'-deoxyuridines. *Nucleosides & Nucleotides* **17**(9-11), 1809-1812.
- Korshun, V. A., Prokhorenko, I. A., Gontarev, S. V., Skorobogaty, M. V., Balakin, K. V., Manasova, E. V., Malakhov, A. D., and Berlin, Y. A. (1997). New pyrene derivatives for fluorescent labeling of oligonucleotides. *Nucleosides & Nucleotides* **16**(7-9), 1461-1464.
- Koudriakova, T., Iatsimirskaia, E., Utkin, I., Gangl, E., Vouros, P., Storozhuk, E., Orza, D., Marinina, J., and Gerber, N. (1998). Metabolism of the human immunodeficiency virus protease inhibitors indinavir and ritonavir by human intestinal microsomes and expressed cytochrome P4503A4/3A5: Mechanism-based inactivation of cytochrome P4503A by ritonavir. *Drug Metabolism and Disposition* **26**(6), 552-561.
- Kozlov, M. M., Leikin, S. L., Chernomordik, L. V., Markin, V. S., and Chizmadzhev, Y. A. (1989). Stalk Mechanism of Vesicle Fusion - Intermixing of Aqueous Contents. *European Biophysics Journal with Biophysics Letters* **17**(3), 121-129.
- Kozlov, M. M., McMahon, H. T., and Chernomordik, L. V. (2010). Protein-driven membrane stresses in fusion and fission. *Trends Biochem Sci* **35**(12), 699-706.
- Kozlovsky, Y., Efrat, A., Siegel, D. A., and Kozlov, M. M. (2004). Stalk phase formation: Effects of dehydration and saddle splay modulus. *Biophysical Journal* **87**(4), 2508-2521.
- Kozlovsky, Y., and Kozlov, M. M. (2002). Stalk model of membrane fusion: Solution of energy crisis. *Biophysical Journal* **82**(2), 882-895.
- Krummenacher, C., Nicola, A. V., Whitbeck, J. C., Lou, H., Hou, W., Lambris, J. D., Geraghty, R. J., Spear, P. G., Cohen, G. H., and Eisenberg, R. J. (1998). Herpes simplex virus glycoprotein D can bind to poliovirus receptor-related protein 1 or herpesvirus entry mediator, two structurally unrelated mediators of virus entry. *J Virol* **72**(9), 7064-74.

- Krummenacher, C., Supekar, V. M., Whitbeck, J. C., Lazear, E., Connolly, S. A., Eisenberg, R. J., Cohen, G. H., Wiley, D. C., and Carfi, A. (2005). Structure of unliganded HSV gD reveals a mechanism for receptor-mediated activation of virus entry. *Embo Journal* **24**(23), 4144-4153.
- Kuzmin, P. I., Akimov, S. A., Chizmadzhev, Y. A., Zimmerberg, J., and Cohen, F. S. (2005). Line tension and interaction energies of membrane rafts calculated from lipid splay and tilt. *Biophysical Journal* **88**(2), 1120-1133.
- Kuzmin, P. I., Zimmerberg, J., Chizmadzhev, Y. A., and Cohen, F. S. (2001). A quantitative model for membrane fusion based on low-energy intermediates. *Proceedings of the National Academy of Sciences of the United States of America* **98**(13), 7235-7240.
- Kwo, P. Y., Lawitz, E. J., McCone, J., Schiff, E. R., Vierling, J. M., Pound, D., Davis, M. N., Galati, J. S., Gordon, S. C., Ravendhran, N., Rossaro, L., Anderson, F. H., Jacobson, I. M., Rubin, R., Koury, K., Pedicone, L. D., Brass, C. A., Chaudhri, E., and Albrecht, J. K. (2010). Efficacy of boceprevir, an NS3 protease inhibitor, in combination with peginterferon alfa-2b and ribavirin in treatment-naïve patients with genotype 1 hepatitis C infection (SPRINT-1): an open-label, randomised, multicentre phase 2 trial. *Lancet* **376**(9742), 705-16.
- Kwong, P. D., Wyatt, R., Robinson, J., Sweet, R. W., Sodroski, J., and Hendrickson, W. A. (1998). Structure of an HIV gp120 envelope glycoprotein in complex with the CD4 receptor and a neutralizing human antibody. *Nature* **393**(6686), 648-659.
- Lande, M. B., Donovan, J. M., and Zeidel, M. L. (1995). The relationship between membrane fluidity and permeabilities to water, solutes, ammonia, and protons. *J Gen Physiol* **106**(1), 67-84.
- Langeland, N., Moore, L. J., Holmsen, H., and Haarr, L. (1988). Interaction of polylysine with the cellular receptor for herpes simplex virus type 1. *J Gen Virol* **69 (Pt 6)**, 1137-45.
- Lanier, R., Lampert, B., Robertson, A., Almond, M., and Painter, G. (2009). Hexadecyloxypropyl tenofovir associates directly with HIV and subsequently inhibits viral replication in untreated cells. In "16th Conference on Retroviruses and Opportunistic Infections", Montreal, Canada.
- Larder, B. A., Cheng, Y. C., and Darby, G. (1983). Characterization of Abnormal Thymidine Kinases Induced by Drug-Resistant Strains of Herpes-Simplex Virus Type-1. *Journal of General Virology* **64**(MAR), 523-532.
- Lauring, A. S., and Andino, R. (2010). Quasispecies theory and the behavior of RNA viruses. *PLoS Pathog* **6**(7), e1001005.
- Lee, C. P., and Chen, M. R. (2010). Escape of herpesviruses from the nucleus. *Rev Med Virol* **20**(4), 214-30.
- Leikin, S., Parsegian, V. A., Rau, D. C., and Rand, R. P. (1993). Hydration Forces. *Annual Review of Physical Chemistry* **44**, 369-395.
- Leikina, E., Ramos, C., Markovic, I., Zimmerberg, J., and Chernomordik, L. V. (2002). Reversible stages of the low-pH-triggered conformational change in influenza virus hemagglutinin. *Embo J* **21**(21), 5701-10.

- Lentz, B. R. (2007). PEG as a tool to gain insight into membrane fusion. *European Biophysics Journal with Biophysics Letters* **36**(4-5), 315-326.
- Ligas, M. W., and Johnson, D. C. (1988). A Herpes-Simplex Virus Mutant in Which Glycoprotein-D Sequences Are Replaced by Beta-Galactosidase Sequences Binds to but Is Unable to Penetrate into Cells. *Journal of Virology* **62**(5), 1486-1494.
- Lin, R. C., and Scheller, R. H. (2000). Mechanisms of synaptic vesicle exocytosis. *Annual Reviews of Cell and Developmental Biology* **16**, 19-49.
- Liu, C. G., Eichelberger, M. C., Compans, R. W., and Air, G. M. (1995). Influenza Type-a Virus Neuraminidase Does Not Play a Role in Viral Entry, Replication, Assembly, or Budding. *Journal of Virology* **69**(2), 1099-1106.
- Liu, S. T. H., Sharon-Friling, R., Ivanova, P., Milne, S. B., Myers, D. S., Rabinowitz, J. D., Brown, H. A., and Shenk, T. (2011). Synaptic vesicle-like lipidome of human cytomegalovirus virions reveals a role for SNARE machinery in virion egress. *Proceedings of the National Academy of Sciences of the United States of America* **108**(31), 12869-12874.
- Lopez, M., Cocchi, F., Menotti, L., Avitabile, E., Dubreuil, P., and Campadelli-Fiume, G. (2000). Nectin2 alpha (PRR2 alpha or HveB) and nectin2 delta are low-efficiency mediators for entry of herpes simplex virus mutants carrying the Leu25Pro substitution in glycoprotein D. *Journal of Virology* **74**(3), 1267-1274.
- Lorizate, M., and Krausslich, H. G. (2011). Role of lipids in virus replication. *Cold Spring Harb Perspect Biol* **3**(10).
- Lu, J., Deeks, S. G., Hoh, R., Beatty, G., Kuritzkes, B. A., Martin, J. N., and Kuritzkes, D. R. (2006). Rapid emergence of enfuvirtide resistance in HIV-1-infected patients: Results of a clonal analysis. *J AIDS-Journal of Acquired Immune Deficiency Syndromes* **43**(1), 60-64.
- Lycke, E., Johansson, M., Svennerholm, B., and Lindahl, U. (1991). Binding of Herpes-Simplex Virus to Cellular Heparan-Sulfate, an Initial Step in the Adsorption Process. *Journal of General Virology* **72**, 1131-1137.
- Mammano, F., Petit, C., and Clavel, F. (1998). Resistance-associated loss of viral fitness in human immunodeficiency virus type 1: Phenotypic analysis of protease and gag coevolution in protease inhibitor-treated patients. *Journal of Virology* **72**(9), 7632-7637.
- Mao, J. C. H., and Robishaw, E. E. (1975). Mode of Inhibition of Herpes-Simplex Virus DNA-Polymerase by Phosphonoacetate. *Biochemistry* **14**(25), 5475-5479.
- Markin, V. S., and Albanesi, J. P. (2002). Membrane fusion: Stalk model revisited. *Biophysical Journal* **82**(2), 693-712.
- Markin, V. S., Kozlov, M. M., and Borovjagin, V. L. (1984). On the Theory of Membrane-Fusion - the Stalk Mechanism. *General Physiology and Biophysics* **3**(5), 361-377.
- Markosyan, R. M., Leung, M. Y., and Cohen, F. S. (2009). The six-helix bundle of human immunodeficiency virus Env controls pore formation and

- enlargement and is initiated at residues proximal to the hairpin turn. *J Virol* **83**(19), 10048-57.
- Marrink, S. J., and Mark, A. E. (2004). Molecular view of hexagonal phase formation in phospholipid membranes. *Biophysical Journal* **87**(6), 3894-3900.
- Martens, S., and McMahon, H. T. (2008). Mechanisms of membrane fusion: disparate players and common principles. *Nature Reviews Molecular Cell Biology* **9**(7), 543-556.
- Maurer, U. E., Sodeik, B., and Grunewald, K. (2008). Native 3D intermediates of membrane fusion in herpes simplex virus 1 entry. *Proceedings of the National Academy of Sciences of the United States of America* **105**(30), 10559-10564.
- May, S. (2002). Structure and Energy of Fusion Stalks: The Role of Membrane Edges. *Biophysical Journal* **83**, 2969-2980.
- McColl, D. J., Chappey, C., Parkin, N. T., and Miller, M. D. (2008). Prevalence, genotypic associations and phenotypic characterization of K65R, L74V and other HIV-1 RT resistance mutations in a commercial database. *Antiviral Therapy* **13**(2), 189-197.
- McColl, D. J., and Chen, X. W. (2010). Strand transfer inhibitors of HIV-1 integrase: Bringing IN new era of antiretroviral therapy. *Antiviral Research* **85**(1), 101-118.
- McMahon, H. T., and Gallop, J. L. (2005). Membrane curvature and mechanisms of dynamic cell membrane remodelling. *Nature* **438**(7068), 590-596.
- McMahon, M. A., Jilek, B. L., Brennan, T. P., Shen, L., Zhou, Y., Wind-Rotolo, M., Xing, S. F., Bhat, S., Hale, B., Hegarty, R., Chong, C. R., Liu, J. O., Siliciano, R. F., and Thio, C. L. (2007). Brief report - The HBV drug entecavir - Effects on HIV-1 replication and resistance. *New England Journal of Medicine* **356**(25), 2614-2621.
- Meertens, L., Bertaux, C., and Dragic, T. (2006). Hepatitis C virus entry requires a critical postinternalization step and delivery to early endosomes via clathrin-coated vesicles. *Journal of Virology* **80**(23), 11571-11578.
- Melby, T. (2007). HIV coreceptor use in heavily treatment-experienced patients: Does it take two to tangle? *Clinical Infectious Diseases* **44**(4), 596-598.
- Melikyan, G. B., Brener, S. A., Ok, D. C., and Cohen, F. S. (1997). Inner but not outer membrane leaflets control the transition from glycosylphosphatidylinositol-anchored influenza hemagglutinin-induced hemifusion to full fusion. *Journal of Cell Biology* **136**(5), 995-1005.
- Mendelsohn, C. L., Wimmer, E., and Racaniello, V. R. (1989). Cellular Receptor for Poliovirus - Molecular-Cloning, Nucleotide-Sequence, and Expression of a New Member of the Immunoglobulin Superfamily. *Cell* **56**(5), 855-865.
- Menendez-Arias, L. (2010). Molecular basis of human immunodeficiency virus drug resistance: An update. *Antiviral Research* **85**(1), 210-231.
- Menon, A. K. (1995). Flippases. *Trends Cell Biol* **5**(9), 355-60.
- Merz, A., Long, G., Hiet, M. S., Brugger, B., Chlanda, P., Andre, P., Wieland, F., Krijnse-Locker, J., and Bartenschlager, R. (2011). Biochemical and

- morphological properties of hepatitis C virus particles and determination of their lipidome. *J Biol Chem* **286**(4), 3018-32.
- Mettenleiter, T. C., Klupp, B. G., and Granzow, H. (2006). Herpesvirus assembly: a tale of two membranes. *Current Opinion in Microbiology* **9**(4), 423-429.
- Mettenleiter, T. C., Klupp, B. G., and Granzow, H. (2009). Herpesvirus assembly: an update. *Virus Res* **143**(2), 222-34.
- Milne, R. S. B., Nicola, A. V., Whitbeck, J. C., Eisenberg, R. J., and Cohen, G. H. (2005). Glycoprotein D receptor-dependent, low-pH-Independent Endocytic entry of herpes simplex virus type 1. *Journal of Virology* **79**(11), 6655-6663.
- Mitsuya, H., Weinhold, K. J., Furman, P. A., Stclair, M. H., Lehrman, S. N., Gallo, R. C., Bolognesi, D., Barry, D. W., and Broder, S. (1985). 3'-Azido-3'-Deoxythymidine (Bw A509u) - an Antiviral Agent That Inhibits the Infectivity and Cytopathic Effect of Human Lymphotropic-T Virus Type-Iii Lymphadenopathy-Associated Virus In vitro. *Proceedings of the National Academy of Sciences of the United States of America* **82**(20), 7096-7100.
- Mittal, A., Leikina, E., Chernomordik, L. V., and Bentz, J. (2003). Kinetically differentiating influenza hemagglutinin fusion and hemifusion machines. *Biophysical Journal* **85**(3), 1713-1724.
- Montgomery, R. I., Warner, M. S., Lum, B. J., and Spear, P. G. (1996). Herpes simplex virus-1 entry into cells mediated by a novel member of the TNF/NGF receptor family. *Cell* **87**(3), 427-436.
- Moody, C. A., and Laimins, L. A. (2010). Human papillomavirus oncoproteins: pathways to transformation. *Nature Reviews Cancer* **10**(8), 550-560.
- Moore, N. F., Patzer, E. J., Shaw, J. M., Thompson, T. E., and Wagner, R. R. (1978). Interaction of Vesicular Stomatitis-Virus with Lipid Vesicles - Depletion of Cholesterol and Effect on Virion Membrane Fluidity and Infectivity. *Journal of Virology* **27**(2), 320-329.
- Moradpour, D., Penin, F., and Rice, C. M. (2007). Replication of hepatitis C virus. *Nat Rev Microbiol* **5**(6), 453-63.
- Morgan, Rose, H. M., and Mednis, B. (1968). Electron Microscopy of Herpes Simplex Virus .I. Entry. *Journal of Virology* **2**(5), 507-&.
- Moscona, A. (2005). Drug therapy - Neuraminidase inhibitors for influenza. *New England Journal of Medicine* **353**(13), 1363-1373.
- Moscona, A. (2009). Global Transmission of Oseltamivir-Resistant Influenza. *New England Journal of Medicine* **360**(10), 953-956.
- Moss, B. (2006). Poxvirus entry and membrane fusion. *Virology* **344**(1), 48-54.
- Moyle, G. J., Wildfire, A., Mandalia, S., Mayer, H., Goodrich, J., Whitcomb, J., and Gazzard, B. G. (2005). Epidemiology and predictive factors for chemokine receptor use in HIV-1 infection. *Journal of Infectious Diseases* **191**(6), 866-872.
- Muggeridge, M. I. (2000). Characterization of cell-cell fusion mediated by herpes simplex virus 2 glycoproteins gB, gD, gH and gL in transfected cells. *Journal of General Virology* **81**, 2017-2027.

- Munoz-Barroso, I., Cobaleda, C., Zhadan, G., Shnyrov, V., and Villar, E. (1997). Dynamic properties of Newcastle Disease Virus envelope and their relations with viral hemagglutinin-neuraminidase membrane glycoprotein. *Biochimica Et Biophysica Acta-Biomembranes* **1327**(1), 17-31.
- Nemerow, G. R., Pache, L., Reddy, V., and Stewart, P. L. (2009). Insights into adenovirus host cell interactions from structural studies. *Virology* **384**(2), 380-388.
- Nicola, A. V., Hou, J., Major, E. O., and Straus, S. E. (2005). Herpes simplex virus type 1 enters human epidermal keratinocytes, but not neurons, via a pH-dependent endocytic pathway. *Journal of Virology* **79**(12), 7609-7616.
- Nijhuis, M., Schuurman, R., de Jong, D., Erickson, J., Gustchina, E., Albert, J., Schipper, P., Gulnik, S., and Boucher, C. A. B. (1999). Increased fitness of drug resistant HIV-1 protease as a result of acquisition of compensatory mutations during suboptimal therapy. *Aids* **13**(17), 2349-2359.
- Ogert, R. A., Wojcik, L., Buontempo, C., Ba, L., Buontempo, P., Ralston, R., Strizki, J., and Howe, J. A. (2008). Mapping resistance to the CCR5 co-receptor antagonist vicriviroc using heterologous chimeric HIV-1 envelope genes reveals key determinants in the C2-V5 domain of gp120. *Virology* **373**(2), 387-399.
- Ohyama, A., Hosaka, K., Komiyama, Y., Akagawa, K., Yamauchi, E., Taniguchi, H., Sasagawa, N., Kumakura, K., Mochida, S., Yamauchi, T., and Igarashi, M. (2002). Regulation of exocytosis through Ca²⁺/ATP-dependent binding of autophosphorylated Ca²⁺/calmodulin-activated protein kinase II to syntaxin 1A. *Journal of Neuroscience* **22**(9), 3342-3351.
- Ojala, P. M., Sodeik, B., Ebersold, M. W., Kutay, U., and Helenius, A. (2000). Herpes simplex virus type 1 entry into host cells: Reconstitution of capsid binding and uncoating at the nuclear pore complex in vitro. *Molecular and Cellular Biology* **20**(13), 4922-4931.
- Ono, A., and Freed, E. O. (2001). Plasma membrane rafts play a critical role in HIV-1 assembly and release. *Proceedings of the National Academy of Sciences of the United States of America* **98**(24), 13925-13930.
- Pabst, S., Margittai, M., Vainius, D., Langen, R., Jahn, R., and Fasshauer, D. (2002). Rapid and selective binding to the synaptic SNARE complex suggests a modulatory role of complexins in neuroexocytosis. *Journal of Biological Chemistry* **277**(10), 7838-7848.
- Pal, R., Barenholz, Y., and Wagner, R. R. (1981). Depletion and Exchange of Cholesterol from the Membrane of Vesicular Stomatitis-Virus by Interaction with Serum-Lipoproteins or Poly(Vinylpyrrolidone) Complexed with Bovine Serum-Albumin. *Biochemistry* **20**(3), 530-539.
- Pal, R., Petri, W. A., and Wagner, R. R. (1980). Alteration of the Membrane Lipid-Composition and Infectivity of Vesicular Stomatitis-Virus by Growth in a Chinese-Hamster Ovary Cell Sterol Mutant and in Lipid-Supplemented Baby Hamster-Kidney Clone 21 Cells. *Journal of Biological Chemistry* **255**(16), 7688-7693.

- Parsegian, V. A., Fuller, N., and Rand, R. P. (1979). Measured Work of Deformation and Repulsion of Lecithin Bilayers. *Proceedings of the National Academy of Sciences of the United States of America* **76**(6), 2750-2754.
- Pastor-Anglada, M., Cano-Soldado, P., Molina-Arcas, M., Lostao, M. P., Larrayoz, I., Martinez-Picado, J., and Casado, F. J. (2005). Cell entry and export of nucleoside analogues. *Virus Res* **107**(2), 151-64.
- Patzer, E. J., Moore, N. F., Barenholz, Y., Shaw, J. M., and Wagner, R. R. (1978). Lipid Organization of the Membrane of Vesicular Stomatitis-Virus. *Journal of Biological Chemistry* **253**(13), 4544-4550.
- Pawlotsky, J. M. (2000). Hepatitis C virus resistance to antiviral therapy. *Hepatology* **32**(5), 889-896.
- Pearse, B. M. F. (1975). Coated Vesicles from Pig Brain - Purification and Biochemical Characterization. *Journal of Molecular Biology* **97**(1), 93-&.
- Pellet, P. E., and Roizman, B. (2007). The Family Herpesviridae: A Brief Introduction. In "Fields' Virology, 5th ed." (D. M. Knipe, P. M. Howley, D. E. Griffin, R. A. Lamb, M. A. Martin, B. Roizman, and S. E. Straus, Eds.), pp. 2479-2499. Lippincott-Williams & Wilkins, Philadelphia, PA.
- Peng, T., de Leon, M. P., Novotny, M. J., Jiang, H. B., Lambris, J. D., Dubin, G., Spear, P. G., Cohen, G. H., and Eisenberg, R. J. (1998). Structural and antigenic analysis of a truncated form of the herpes simplex virus glycoprotein gH-gL complex. *Journal of Virology* **72**(7), 6092-6103.
- Phillips, A. N., Leen, C., Wilson, A., Anderson, J., Dunn, D., Schwenk, A., Orkin, C., Hill, T., Fisher, M., Walsh, J., Pillay, D., Bansi, L., Gazzard, B., Easterbrook, P., Gilson, R., Johnson, M., and Sabin, C. A. (2007). Risk of extensive virological failure to the three original antiretroviral drug classes over long-term follow-up from the start of therapy in patients with HIV infection: an observational cohort study. *Lancet* **370**(9603), 1923-8.
- Pileri, P., Uematsu, Y., Campagnoli, S., Galli, G., Falugi, F., Petracca, R., Weiner, A. J., Houghton, M., Rosa, D., Grandi, G., and Abrignani, S. (1998). Binding of hepatitis C virus to CD81. *Science* **282**(5390), 938-941.
- Pillay, D. (2007). The priorities for antiviral drug resistance surveillance and research. *Journal of Antimicrobial Chemotherapy* **60**, 157-158.
- Ploss, A., Evans, M. J., Gaysinskaya, V. A., Panis, M., You, H. N., de Jong, Y. P., and Rice, C. M. (2009). Human occludin is a hepatitis C virus entry factor required for infection of mouse cells. *Nature* **457**(7231), 882-886.
- Popovic, M., Sarin, P. S., Robertguroff, M., Kalyanaraman, V. S., Mann, D., Minowada, J., and Gallo, R. C. (1983). Isolation and Transmission of Human Retrovirus (Human T-Cell Leukemia-Virus). *Science* **219**(4586), 856-859.
- Popovic, M., Sarngadharan, M. G., Read, E., and Gallo, R. C. (1984). Detection, Isolation, and Continuous Production of Cytopathic Retroviruses (Htlv-Iii) from Patients with Aids and Pre-Aids. *Science* **224**(4648), 497-500.
- Quetglas, S., Iborra, C., Sasakawa, N., De Haro, L., Kumakura, K., Sato, K., Leveque, C., and Seagar, M. (2002). Calmodulin and lipid binding to

- synaptobrevin regulates calcium-dependent exocytosis. *Embo Journal* **21**(15), 3970-3979.
- Ramstedt, B., and Slotte, J. P. (2002). Membrane properties of sphingomyelins. *Febs Letters* **531**(1), 33-37.
- Rawat, S. S., Viard, M., Gallo, S. A., Rein, A., Blumenthal, R., and Puri, A. (2003). Modulation of entry of enveloped viruses by cholesterol and sphingolipids (Review). *Mol Membr Biol* **20**(3), 243-54.
- Ray, A. S., Cihlar, T., Robinson, K. L., Tong, L., Vela, J. E., Fuller, M. D., Wieman, L. M., Eisenberg, E. J., and Rhodes, G. R. (2006). Mechanism of active renal tubular efflux of tenofovir. *Antimicrobial Agents and Chemotherapy* **50**(10), 3297-3304.
- Ray, N., Blackburn, L. A., and Doms, R. W. (2009). HR-2 Mutations in Human Immunodeficiency Virus Type 1 gp41 Restore Fusion Kinetics Delayed by HR-1 Mutations That Cause Clinical Resistance to Enfuvirtide. *Journal of Virology* **83**(7), 2989-2995.
- Resetar, A., and Spector, T. (1989). Glucuronidation of 3'-Azido-3'-Deoxythymidine - Human and Rat Enzyme Specificity. *Biochemical Pharmacology* **38**(9), 1389-1393.
- Rey, F. A., Heinz, F. X., Mandl, C., Kunz, C., and Harrison, S. C. (1995). The Envelope Glycoprotein from Tick-Borne Encephalitis-Virus at 2 Angstrom Resolution. *Nature* **375**(6529), 291-298.
- Roberts, K. L., and Smith, G. L. (2008). Vaccinia virus morphogenesis and dissemination. *Trends Microbiol* **16**(10), 472-9.
- Robinson, M. S. (2004). Adaptable adaptors for coated vesicles. *Trends Cell Biol* **14**(4), 167-74.
- Roche, S. (2006). Crystal structure of the low-pH form of the vesicular stomatitis virus glycoprotein G (vol 313, pg 187, 2006). *Science* **313**(5792), 1389-1389.
- Roche, S., Rey, F. A., Gaudin, Y., and Bressanelli, S. (2007). Structure of the prefusion form of the vesicular stomatitis virus glycoprotein G. *Science* **315**(5813), 843-848.
- Roddy, R. E., Zekeng, L., Ryan, K. A., Tamoufe, U., Weir, S. S., and Wong, E. L. (1998). A controlled trial of nonoxynol 9 film to reduce male-to-female transmission of sexually transmitted diseases. *New England Journal of Medicine* **339**(8), 504-510.
- Roizman, B., Knipe, D. M., and Whitley, R. (2007). The replication of Herpes simplex virus. In "Fields' virology, 5th ed." (D. M. Knipe, P. M. Howley, D. E. Griffin, R. A. Lamb, M. A. Martin, B. Roizman, and S. E. Straus, Eds.), pp. 2501-2601. Lippincott-Williams & Wilkins, Philadelphia, PA.
- Roop, C., Hutchinson, L., and Johnson, D. C. (1993). A Mutant Herpes Simplex Virus Type-1 Unable to Express Glycoprotein L Cannot Enter Cells, and Its Particles Lack Glycoprotein H *Journal of Virology* **67**(4), 2285-2297.
- Ross, L., Lim, M. L., Liao, Q. M., Wine, B., Rodriguez, A. E., Weinberg, W., and Shaefer, M. (2007). Prevalence of antiretroviral drug resistance and resistance-associated mutations in antiretroviral therapy-naive HIV-

- infected individuals from 40 United States cities. *Hiv Clinical Trials* **8**(1), 1-8.
- Russell, R. J., Haire, L. F., Stevens, D. J., Collins, P. J., Lin, Y. P., Blackburn, G. M., Hay, A. J., Gamblin, S. J., and Skehel, J. J. (2006). The structure of H5N1 avian influenza neuraminidase suggests new opportunities for drug design. *Nature* **443**(7107), 45-49.
- Sarafianos, S. G., Das, K., Clark, A. D., Ding, J. P., Boyer, P. L., Hughes, S. H., and Arnold, E. (1999). Lamivudine (3TC) resistance in HIV-1 reverse transcriptase involves steric hindrance with beta-branched amino acids. *Proceedings of the National Academy of Sciences of the United States of America* **96**(18), 10027-10032.
- Scarlatti, G., Tresoldi, E., Bjorndal, A., Fredriksson, R., Colognesi, C., Deng, H. K., Malnati, M. S., Plebani, A., Siccardi, A. G., Littman, D. R., Fenyo, E. M., and Lusso, P. (1997). In vivo evolution of HIV-1 co-receptor usage and sensitivity to chemokine-mediated suppression. *Nature Medicine* **3**(11), 1259-1265.
- Scarselli, E., Ansuini, H., Cerino, R., Roccasecca, R. M., Acali, S., Filocamo, G., Traboni, C., Nicosia, A., Cortese, R., and Vitelli, A. (2002). The human scavenger receptor class B type I is a novel candidate receptor for the hepatitis C virus. *Embo Journal* **21**(19), 5017-5025.
- Schaeffer, H. J., Beauchamp, L., Miranda, P. D., Elion, G. B., Bauer, D. J., and Collins, P. (1978). 9-(2-Hydroxyethoxymethyl)Guanine Activity against Viruses of Herpes Group. *Nature* **272**(5654), 583-585.
- Schaffner, C. P., Plescia, O. J., Pontani, D., Sun, D., Thornton, A., Pandey, R. C., and Sarin, P. S. (1986). Antiviral Activity of Amphotericin-B Methyl-Ester - Inhibition of Htlv-Iii Replication in Cell-Culture. *Biochemical Pharmacology* **35**(22), 4110-4113.
- Schang, L. M., St. Vincent, MR, Lacasse, JJ (2006). Five years of progress on cyclin-dependent kinases and other cellular proteins as potential targets for antiviral drugs. *Antiviral Chemistry & Chemotherapy* **17**, 293-320.
- Schief, W. R. (2009). Challenges for structure-based HIV vaccine design. *Current Opinion in HIV & AIDS* **4**(5), 431-440.
- Schinazi, R. F., Bassit, L., and Gavegnano, C. (2010). HCV drug discovery aimed at viral eradication. *Journal of Viral Hepatitis* **17**(2), 77-90.
- Schols, D., Pauwels, R., Desmyter, J., and Declercq, E. (1990). Dextran Sulfate and Other Polyanionic Anti-Hiv Compounds Specifically Interact with the Viral Gp120 Glycoprotein Expressed by T-Cells Persistently Infected with Hiv-1. *Virology* **175**(2), 556-561.
- Schrag, J. D., Prasad, B. V. V., Rixon, F. J., and Chiu, W. (1989). 3-Dimensional Structure of the Hsv1 Nucleocapsid. *Cell* **56**(4), 651-660.
- Schuetz, J. D., Connelly, M. C., Sun, D. X., Paibir, S. G., Flynn, P. M., Srinivas, R. V., Kumar, A., and Fridland, A. (1999). MRP4: A previously unidentified factor in resistance to nucleoside-based antiviral drugs. *Nature Medicine* **5**(9), 1048-1051.
- Scordi-Bello, I. A., Mosoian, A., He, C. J., Chen, Y. B., Cheng, Y., Jarvis, G. A., Keller, M. J., Hogarty, K., Waller, D. P., Profy, A. T., Herold, B. C., and

- Klotman, M. E. (2005). Candidate sulfonated and sulfated topical microbicides: Comparison of anti-human immunodeficiency virus activities and mechanisms of action. *Antimicrobial Agents and Chemotherapy* **49**(9), 3607-3615.
- Sharma, M., Yi, M., Dong, H., Qin, H., Peterson, E., Busath, D. D., Zhou, H. X., and Cross, T. A. (2010). Insight into the mechanism of the influenza A proton channel from a structure in a lipid bilayer. *Science* **330**(6003), 509-12.
- Sharma, N. R., Mateu, G., Dreux, M., Grakoui, A., Cosset, F. L., and Melikyan, G. B. (2011). Hepatitis C Virus Is Primed by CD81 Protein for Low pH-Dependent Fusion. *J Biol Chem* **286**(35), 30361-76.
- Shaw, J. M., Moore, N. F., Patzer, E. J., Correiafreire, M. C., Wagner, R. R., and Thompson, T. E. (1979). Compositional Asymmetry and Transmembrane Movement of Phosphatidylcholine in Vesicular Stomatitis-Virus Membranes. *Biochemistry* **18**(3), 538-543.
- Shieh, M. T., Wudunn, D., Montgomery, R. I., Esko, J. D., and Spear, P. G. (1992). Cell-Surface Receptors for Herpes-Simplex Virus Are Heparan-Sulfate Proteoglycans. *Journal of Cell Biology* **116**(5), 1273-1281.
- Shukla, D., Liu, J., Blaiklock, P., Shworak, N. W., Bai, X. M., Esko, J. D., Cohen, G. H., Eisenberg, R. J., Rosenberg, R. D., and Spear, P. G. (1999). A novel role for 3-O-sulfated heparan sulfate in herpes simplex virus 1 entry. *Cell* **99**(1), 13-22.
- Siegel, D. P. (1993). Energetics of Intermediates in Membrane-Fusion - Comparison of Stalk and Inverted Micellar Intermediate Mechanisms. *Biophysical Journal* **65**(5), 2124-2140.
- Siegel, D. P. (1999). The modified stalk mechanism of lamellar/inverted phase transitions and its implications for membrane fusion. *Biophysical Journal* **76**(1), 291-313.
- Simons, K., and Garoff, H. (1980). The budding mechanisms of enveloped animal viruses. *Journal of General Virology* **50**, 1-21.
- Sista, P. R., Melby, T., Davison, D., Jin, L., Mosier, S., Mink, M., Nelson, E. L., DeMasi, R., Cammack, N., Salgo, M. P., Matthews, T. J., and Greenberg, M. L. (2004). Characterization of determinants of genotypic and phenotypic resistance to enfuvirtide in baseline and on-treatment HIV-1 isolates. *Aids* **18**(13), 1787-94.
- Skehel, J. J., Bayley, P. M., Brown, E. B., Martin, S. R., Waterfield, M. D., White, J. M., Wilson, I. A., and Wiley, D. C. (1982). Changes in the Conformation of Influenza-Virus Hemagglutinin at the pH Optimum of Virus-Mediated Membrane-Fusion. *Proceedings of the National Academy of Sciences of the United States of America-Biological Sciences* **79**(4), 968-972.
- Skepper, J. N., Whiteley, A., Browne, H., and Minson, A. (2001). Herpes simplex virus nucleocapsids mature to progeny virions by an envelopment -> deenvelopment -> reenvelopment pathway. *Journal of Virology* **75**(12), 5697-5702.

- Sluis-Cremer, N., Temiz, N. A., and Bahar, I. (2004). Conformational changes in HIV-1 reverse transcriptase induced by nonnucleoside reverse transcriptase inhibitor binding. *Current Hiv Research* **2**(4), 323-332.
- Sodeik, B., Ebersold, M. W., and Helenius, A. (1997). Microtubule-mediated transport of incoming herpes simplex virus 1 capsids to the nucleus. *Journal of Cell Biology* **136**(5), 1007-1021.
- Sollner, T., Whitehart, S. W., Brunner, M., Erdjumentbromage, H., Geromanos, S., Tempst, P., and Rothman, J. E. (1993). Snap Receptors Implicated in Vesicle Targeting and Fusion. *Nature* **362**(6418), 318-324.
- Soriano, V., Vispo, E., Labarga, P., Medrano, J., and Barreiro, P. (2010). Viral hepatitis and HIV co-infection. *Antiviral Research* **85**(1), 303-315.
- Stampfer, S. D., Lou, H., Cohen, G. H., Eisenberg, R. J., and Heldwein, E. E. (2010). Structural basis of local, pH-dependent conformational changes in glycoprotein B from herpes simplex virus type 1. *J Virol* **84**(24), 12924-33.
- Starcich, B. R., Hahn, B. H., Shaw, G. M., Mcneely, P. D., Modrow, S., Wolf, H., Parks, E. S., Parks, W. P., Josephs, S. F., Gallo, R. C., and Wongstaa, F. (1986). Identification and Characterization of Conserved and Variable Regions in the Envelope Gene of Htlv-Iii Lav, the Retrovirus of Aids. *Cell* **45**(5), 637-648.
- Stiasny, K., Fritz, R., Pangerl, K., and Heinz, F. X. (2009). Molecular mechanisms of flavivirus membrane fusion. *Amino Acids*.
- Stiasny, K., and Heinz, F. X. (2004). Effect of membrane curvature-modifying lipids on membrane fusion by tick-borne encephalitis virus. *Journal of Virology* **78**(16), 8536-8542.
- Stouffer, A. L., Acharya, R., Salom, D., Levine, A. S., Di Costanzo, L., Soto, C. S., Tereshko, V., Nanda, V., Stayrook, S., and DeGrado, W. F. (2008). Structural basis for the function and inhibition of an influenza virus proton channel. *Nature* **451**(7178), 596-U13.
- Subramanian, R. P., and Geraghty, R. J. (2007). Herpes simplex virus type 1 mediates fusion through a hemifusion intermediate by sequential activity of glycoproteins D, H, L, and B. *Proceedings of the National Academy of Sciences of the United States of America* **104**(8), 2903-2908.
- Sudhof, T. C., and Rothman, J. E. (2009). Membrane fusion: grappling with SNARE and SM proteins. *Science* **323**(5913), 474-7.
- Suetsugu, S. (2010). The proposed functions of membrane curvatures mediated by the BAR domain superfamily proteins. *J Biochem* **148**(1), 1-12.
- Sun, X., Belouzard, S., and Whittaker, G. R. (2008). Molecular architecture of the bipartite fusion loops of vesicular stomatitis virus glycoprotein G, a class III viral fusion protein. *Journal of Biological Chemistry* **283**(10), 6418-6427.
- Sun, X. J., and Whittaker, G. R. (2003). Role for influenza virus envelope cholesterol in virus entry and infection. *Journal of Virology* **77**(23), 12543-12551.

- Sun, X. J., Yau, V. K., Briggs, B. J., and Whittaker, G. R. (2005). Role of clathrin-mediated endocytosis during vesicular stomatitis virus entry into host cells. *Virology* **338**(1), 53-60.
- Suzuki, T., Ishii, K., Aizaki, H., and Wakita, T. (2007). Hepatitis C viral life cycle. *Advanced Drug Delivery Reviews* **59**, 1200-1212.
- Suzuki, T., Takahashi, T., Guo, C. T., Hidari, K. I. P. J., Miyamoto, D., Goto, H., Kawaoka, Y., and Suzuki, Y. (2005). Sialidase activity of influenza A virus in an endocytic pathway enhances viral replication. *Journal of Virology* **79**(18), 11705-11715.
- Szczeczek, L. A. (2008). Renal dysfunction and tenofovir toxicity in HIV-infected patients. *Top HIV Med* **16**(4), 122-6.
- Takahashi, K., Nakanishi, H., Miyahara, M., Mandai, K., Satoh, K., Satoh, A., Nishioka, H., Aoki, J., Nomoto, A., Mizoguchi, A., and Takai, Y. (1999). Nectin/PRR: An immunoglobulin-like cell adhesion molecule recruited to cadherin-based adherens junctions through interaction with afadin, a PDZ domain-containing protein. *Journal of Cell Biology* **145**(3), 539-549.
- Takai, Y., and Nakanishi, H. (2003). Nectin and afadin: novel organizers of intercellular junctions. *Journal of Cell Science* **116**(1), 17-27.
- Tam, R. C., Lau, J. Y. N., and Hong, Z. (2001). Mechanisms of action of ribavirin in antiviral therapies. *Antiviral Chemistry & Chemotherapy* **12**(5), 261-272.
- Tambuyzer, L., Azijn, H., Rimsky, L. T., Vingerhoets, J., Lecocq, P., Kraus, G., Picchio, G., and de Bethune, M. P. (2009). Compilation and prevalence of mutations associated with resistance to non-nucleoside reverse transcriptase inhibitors. *Antiviral Therapy* **14**(1), 103-109.
- Tan, K. M., Liu, J. H., Wang, J. H., Shen, S., and Lu, M. (1997). Atomic structure of a thermostable subdomain of HIV-1 gp41. *Proceedings of the National Academy of Sciences of the United States of America* **94**(23), 12303-12308.
- Teissier, E., and Pecheur, E. I. (2007). Lipids as modulators of membrane fusion mediated by viral fusion proteins. *European Biophysics Journal with Biophysics Letters* **36**(8), 887-899.
- Teissier, E., Penin, F., and Pecheur, E. I. (2011). Targeting Cell Entry of Enveloped Viruses as an Antiviral Strategy. *Molecules* **16**(1), 221-250.
- Tilton, J. C., and Doms, R. W. (2010). Entry inhibitors in the treatment of HIV-1 infection. *Antiviral Research* **85**(1), 91-100.
- Tsai, B. (2007). Penetration of nonenveloped viruses into the cytoplasm. *Annual Review of Cell and Developmental Biology* **23**, 23-43.
- Tsai, C. C., Follis, K. E., Sabo, A., Beck, T. W., Grant, R. F., Bischofberger, N., Benveniste, R. E., and Black, R. (1995). Prevention of Siv Infection in Macaques by (R)-9-(2-Phosphonylmethoxypropyl)Adenine. *Science* **270**(5239), 1197-1199.
- Tsai, K. H., and Lenard, J. (1975). Asymmetry of Influenza-Virus Membrane Bilayer Demonstrated with Phospholipase-C. *Nature* **253**(5492), 554-555.
- Tscherne, D. M., Jones, C. T., Evans, M. J., Lindenbach, B. D., McKeating, J. A., and Rice, C. M. (2006). Time- and temperature-dependent activation of

- hepatitis C virus for low-pH-triggered entry. *Journal of Virology* **80**(4), 1734-1741.
- Turner, A., Bruun, B., Minson, T., and Browne, H. (1998a). Glycoproteins gB, gD, and gHgL of herpes simplex virus type 1 are necessary and sufficient to mediate membrane fusion in a Cos cell transfection system. *Journal of Virology* **72**(1), 873-875.
- Turner, D. C., and Gruner, S. M. (1992). X-Ray-Diffraction Reconstruction of the Inverted Hexagonal (Hii) Phase in Lipid Water-Systems. *Biochemistry* **31**(5), 1340-1355.
- Turner, S. R., Strohbach, J. W., Tommasi, R. A., Aristoff, P. A., Johnson, P. D., Skulnick, H. I., Dolak, L. A., Seest, E. P., Tomich, P. K., Bohanan, M. J., Horng, M. M., Lynn, J. C., Chong, K. T., Hinshaw, R. R., Watenpaugh, K. D., Janakiraman, M. N., and Thaisrivongs, S. (1998b). Tipranavir (PNU-140690): A potent, orally bioavailable nonpeptidic HIV protease inhibitor of the 5,6-dihydro-4-hydroxy-2-pyrone sulfonamide class. *Journal of Medicinal Chemistry* **41**(18), 3467-3476.
- Van Damme, L., Govinden, R., Mirembe, F. M., Guedou, F., Solomon, S., Becker, M. L., Pradeep, B. S., Krishnan, A. K., Alary, M., Pande, B., Ramjee, G., Deese, J., Crucitti, T., and Taylor, D. (2008). Lack of effectiveness of cellulose sulfate gel for the prevention of vaginal HIV transmission. *New England Journal of Medicine* **359**(5), 463-472.
- Van Damme, L., Ramjee, G., Alary, M., Vuylsteke, B., Chandeying, V., Rees, H., Sirivongrangson, P., Mukenge-Tshibaka, L., Ettiegne-Traore, V., Uaheowitchai, C., Karim, S. S. A., Masse, B., Perriens, J., Laga, M., and Grp, C.-S. (2002). Effectiveness of COL-1492, a nonoxynol-9 vaginal gel, on HIV-1 transmission in female sex workers: a randomised controlled trial. *Lancet* **360**(9338), 971-977.
- van Genderen, I. L., Brandimarti, R., Torrisoni, M. R., Campadelli, G., and Vanmeer, G. (1994). The Phospholipid Composition of Extracellular Herpes-Simplex Virions Differs from That of Host-Cell Nuclei. *Virology* **200**(2), 831-836.
- van Meer, G., Voelker, D. R., and Feigenson, G. W. (2008). Membrane lipids: where they are and how they behave. *Nature Reviews Molecular Cell Biology* **9**(2), 112-124.
- Van Rompay, A. R., Johansson, M., and Karlsson, A. (2000). Phosphorylation of nucleosides and nucleoside analogs by mammalian nucleoside monophosphate kinases. *Pharmacology & Therapeutics* **87**(2-3), 189-198.
- Veal, G. J., Barry, M. G., Khoo, S. H., and Back, D. J. (1997). In vitro screening of nucleoside analog combinations for potential use in anti-HIV therapy. *Aids Research and Human Retroviruses* **13**(6), 481-484.
- Virgin, H. W., and Walker, B. D. (2010). Immunology and the elusive AIDS vaccine. *Nature* **464**(7286), 224-231.
- Vlazny, D. A., Kwong, A., and Frenkel, N. (1982). Site-Specific Cleavage Packaging of Herpes-Simplex Virus-DNA and the Selective Maturation of Nucleocapsids Containing Full-Length Viral-DNA. *Proceedings of the*

- National Academy of Sciences of the United States of America-Biological Sciences* **79**(5), 1423-1427.
- Vogel, S. S., Leikina, E. A., and Chernomordik, L. V. (1993). Lysophosphatidylcholine Reversibly Arrests Exocytosis and Viral Fusion at a Stage between Triggering and Membrane Merger. *Journal of Biological Chemistry* **268**(34), 25764-25768.
- von Hahn, T., and McKeating, J. A. (2007). In vitro veritas? The challenges of studying hepatitis C virus infectivity in a test tube. *Journal of Hepatology* **46**(3), 355-358.
- von Hahn, T., and Rice, C. M. (2008). Hepatitis C virus entry. *Journal of Biological Chemistry* **283**(7), 3689-3693.
- Waheed, A. A., Ablan, S. D., Roser, J. D., Sowder, R. C., Schaffner, C. P., Chertova, E., and Freed, E. O. (2007). HIV-1 escape from the entry-inhibiting effects of a cholesterol-binding compound via cleavage of gp41 by the viral protease. *Proceedings of the National Academy of Sciences of the United States of America* **104**(20), 8467-8471.
- Waheed, A. A., Ablan, S. D., Soheilian, F., Nagashima, K., Ono, A., Schaffner, C. P., and Freed, E. O. (2008). Inhibition of human immunodeficiency virus type 1 assembly and release by the cholesterol-binding compound amphotericin B methyl ester: Evidence for Vpu dependence. *Journal of Virology* **82**(19), 9776-9781.
- Waheed, A. A., and Freed, E. O. (2010). The Role of Lipids in Retrovirus Replication. *Viruses* **2**(5), 1146-1180.
- Wang, K. S., Kuhn, R. J., Strauss, E. G., Ou, S., and Strauss, J. H. (1992). High-Affinity Laminin Receptor Is a Receptor for Sindbis Virus in Mammalian Cells. *Journal of Virology* **66**(8), 4992-5001.
- Warner, M. S., Geraghty, R. J., Martinez, W. M., Montgomery, R. I., Whitbeck, J. C., Xu, R. L., Eisenberg, R. J., Cohen, G. H., and Spear, P. G. (1998). A cell surface protein with herpesvirus entry activity (HveB) confers susceptibility to infection by mutants of herpes simplex virus type 1, herpes simplex virus type 2, and pseudorabies virus. *Virology* **246**(1), 179-189.
- Weber, T., Zemelman, B. V., McNew, J. A., Westermann, B., Gmachl, M., Parlati, F., Sollner, T. H., and Rothman, J. E. (1998). SNAREpins: Minimal machinery for membrane fusion. *Cell* **92**(6), 759-772.
- Wei, X. P., Decker, J. M., Liu, H. M., Zhang, Z., Arani, R. B., Kilby, J. M., Saag, M. S., Wu, X. Y., Shaw, G. M., and Kappes, J. C. (2002). Emergence of resistant human immunodeficiency virus type 1 in patients receiving fusion inhibitor (T-20) monotherapy. *Antimicrobial Agents and Chemotherapy* **46**(6), 1896-1905.
- Weissenhorn, W., Hinz, A., and Gaudin, Y. (2007). Virus membrane fusion. *Febs Letters* **581**(11), 2150-2155.
- Welsch, C., Domingues, F. S., Susser, S., Antes, I., Hartmann, C., Mayr, G., Schlicker, A., Sarrazin, C., Albrecht, M., Zeuzem, S., and Lengauer, T. (2008). Molecular basis of telaprevir resistance due to V36 and T54

- mutations in the NS3-4A protease of the hepatitis C virus. *Genome Biol* **9**(1), R16.
- Wensing, A. M. J., van Maarseveen, N. M., and Nijhuis, M. (2010). Fifteen years of HIV Protease Inhibitors: raising the barrier to resistance. *Antiviral Research* **85**(1), 59-74.
- Westby, M., Smith-Burchnell, C., Mori, J., Lewis, M., Mosley, M., Stockdale, M., Dorr, P., Ciaramella, G., and Perros, M. (2007). Reduced maximal inhibition in phenotypic susceptibility assays indicates that viral strains resistant to the CCR5 antagonist maraviroc utilize inhibitor-bound receptor for entry. *Journal of Virology* **81**(5), 2359-2371.
- Whitbeck, C. J., Foo, C. H., de Leon, M. P., Eisenberg, R. J., and Cohen, G. H. (2009). Vaccinia virus exhibits cell-type-dependent entry characteristics. *Virology* **385**(2), 383-391.
- White, J. M., Delos, S. E., Brecher, M., and Schornberg, K. (2008). Structures and mechanisms of viral membrane fusion proteins: Multiple variations on a common theme. *Critical Reviews in Biochemistry and Molecular Biology* **43**(3), 189-219.
- Wickham, T. J., Mathias, P., Cheresch, D. A., and Nemerow, G. R. (1993). Integrin-Alpha-V-Beta-3 and Integrin-Alpha-V-Beta-5 Promote Adenovirus Internalization but Not Virus Attachment. *Cell* **73**(2), 309-319.
- Wiethoff, C. M., Wodrich, H., Gerace, L., and Nemerow, G. R. (2005). Adenovirus protein VI mediates membrane disruption following capsid disassembly. *Journal of Virology* **79**(4), 1992-2000.
- Wild, C. T., Shugars, D. C., Greenwell, T. K., Mcdanal, C. B., and Matthews, T. J. (1994). Peptides Corresponding to a Predictive Alpha-Helical Domain of Human-Immunodeficiency-Virus Type-1 GP41 Are Potent Inhibitors of Virus-Infection. *Proceedings of the National Academy of Sciences of the United States of America* **91**(21), 9770-9774.
- Wild, P., Engels, M., Senn, C., Tobler, K., Ziegler, U., Schraner, E. M., Loepfe, E., Ackermann, M., Mueller, M., and Walther, P. (2005). Impairment of nuclear pores in bovine herpesvirus 1-infected MDBK cells. *Journal of Virology* **79**(2), 1071-1083.
- Wilson, I. A., Skehel, J. J., and Wiley, D. C. (1981). Structure of the Hemagglutinin Membrane Glycoprotein of Influenza-Virus at 3-A Resolution. *Nature* **289**(5796), 366-373.
- Wittels, M., and Spear, P. G. (1991). Penetration of Cells by Herpes-Simplex Virus Does Not Require a Low pH-Dependent Endocytic Pathway. *Virus Research* **18**(2-3), 271-290.
- Wu, L., Gerard, N. P., Wyatt, R., Choe, H., Parolin, C., Ruffing, N., Borsetti, A., Cardoso, A. A., Desjardin, E., Newman, W., Gerard, C., and Sodroski, J. (1996). CD4-induced interaction of primary HIV-1 gp120 glycoproteins with the chemokine receptor CCR-5. *Nature* **384**(6605), 179-83.
- Wudunn, D., and Spear, P. G. (1989). Initial Interaction of Herpes-Simplex Virus with Cells Is Binding to Heparan-Sulfate. *Journal of Virology* **63**(1), 52-58.

- Wyatt, R., Kwong, P. D., Desjardins, E., Sweet, R. W., Robinson, J., Hendrickson, W. A., and Sodroski, J. G. (1998). The antigenic structure of the HIV gp120 envelope glycoprotein. *Nature* **393**(6686), 705-711.
- Yagnik, A. T., Lahm, A., Meola, A., Roccasceca, R. M., Ercole, B. B., Nicosia, A., and Tramontano, A. (2000). A model for the hepatitis C virus envelope glycoprotein E2. *Proteins-Structure Function and Genetics* **40**(3), 355-366.
- Yang, F., Robotham, J. M., Nelson, H. B., Irsigler, A., Kenworthy, R., and Tang, H. (2008). Cyclophilin A is an essential cofactor for hepatitis C virus infection and the principal mediator of cyclosporine resistance in vitro. *J Virol* **82**(11), 5269-78.
- Yang, L., Ding, L., and Huang, H. W. (2003). New phases of phospholipids and implications to the membrane fusion problem. *Biochemistry* **42**(22), 6631-6635.
- Yang, L., and Huang, H. W. (2002). Observation of a membrane fusion intermediate structure. *Science* **297**(5588), 1877-1879.
- Yang, X. Z., Kurteva, S., Ren, X. P., Lee, S., and Sodroski, J. (2005). Stoichiometry of envelope glycoprotein trimers in the entry of human immunodeficiency virus type 1. *Journal of Virology* **79**(19), 12132-12147.
- Yeagle, P. L., Smith, F. T., Young, J. E., and Flanagan, T. D. (1994). Inhibition of Membrane-Fusion by Lysophosphatidylcholine. *Biochemistry* **33**(7), 1820-1827.
- Yu, C. I., and Chiang, B. L. (2010). A New Insight into Hepatitis C Vaccine Development. *Journal of Biomedicine and Biotechnology*, -.
- Zavorotinskaya, T., Qian, Z. H., Franks, J., and Albritton, L. M. (2004). A point mutation in the binding subunit of a retroviral envelope protein arrests virus entry at hemifusion. *Journal of Virology* **78**(1), 473-481.
- Zeldin, R. K., and Petruschke, R. A. (2004). Pharmacological and therapeutic properties of ritonavir-boosted protease inhibitor therapy in HIV-infected patients. *Journal of Antimicrobial Chemotherapy* **53**(1), 4-9.
- Zhang, X. D., Kim-Miller, M. J., Fukuda, M., Kowalchuk, J. A., and Martin, T. F. J. (2002). Ca²⁺-dependent synaptotagmin binding to SNAP-25 is essential for Ca²⁺-triggered exocytosis. *Neuron* **34**(4), 599-611.
- Zhang, Z., and Jackson, M. B. (2010). Membrane Bending Energy and Fusion Pore Kinetics in Ca²⁺-Triggered Exocytosis. *Biophysical Journal* **98**(11), 2524-2534.
- Zimmerberg, J., and Kozlov, M. M. (2006). How proteins produce cellular membrane curvature. *Nature Reviews Molecular Cell Biology* **7**(1), 9-19.

Drug	Target	Virus
Nucleoside & Nucleotide Analogues		
Acyclic Nucleoside Analogues		
Acyclovir	viral DNA polymerase	HSV-1, HSV-2, VZV
Valaciclovir	viral DNA polymerase	HSV-1, HSV-2, VZV, EBV, HCMV
Penciclovir	viral DNA polymerase	HSV-1, HSV-2
Famciclovir	viral DNA polymerase	HSV-1, HSV-2, VZV
Ganciclovir	viral DNA polymerase	HCMV
Valganciclovir	viral DNA polymerase	HCMV (in AIDS patients)
Cyclic Nucleoside Analogues		
Brivudin	viral DNA polymerase	HSV-1, VZV
Entecavir	viral DNA polymerase (RT)	HBV
Idoxuridine	viral DNA polymerase	HSV-1, HSV-2
Trifluridine	viral DNA polymerase	HSV-1, HSV-2
Ribavirin (+ pegIFN)	viral DNA polymerase (RT)	RSV, HCV
Telbivudine	viral DNA polymerase (RT)	HBV
2',3'-Dideoxynucleosides		
Zidovudine	viral DNA polymerase (RT)	HIV-1
Didanosine	viral DNA polymerase (RT)	HIV-1
Zalcitabine*	viral DNA polymerase (RT)	HIV-1
Stavudine	viral DNA polymerase (RT)	HIV-1
Lamivudine	viral DNA polymerase (RT)	HIV-1, HBV
Abacavir	viral DNA polymerase (RT)	HIV-1
Emtricitabine	viral DNA polymerase (RT)	HIV-1, HBV
Nucleoside phosphonates		
Tenofovir disoproxil fumarate	viral DNA polymerase (RT)	HIV-1, HBV
Adefovir dipivoxil	viral DNA polymerase (RT)	HBV
Cidofovir	viral DNA polymerase	HCMV (in AIDS patients)
Oligonucleotide		
Fomivirsen	viral IE mRNA	HCMV (in AIDS patients)
Peptidomimetics		
Saquinavir mesylate	viral protease	HIV-1
Ritonavir	viral protease	HIV-1
Indinavir	viral protease	HIV-1
Nelfinavir mesylate	viral protease	HIV-1
Amprenavir	viral protease	HIV-1
Lopinavir	viral protease	HIV-1
Atazanavir	viral protease	HIV-1
Fosamprenavir	viral protease	HIV-1
Darunavir	viral protease	HIV-1
Enfuvirtide	viral fusion glycoprotein	HIV-1
Boceprevir‡	viral protease	HCV
Telaprevir‡	viral protease	HCV
Sialic Acid Analogues		
Oseltamivir	viral neuraminidase	Influenza A and B
Zanamivir	viral neuraminidase	Influenza A and B
Cyclic Amines		
Amantadine	viral matrix protein	Influenza A
Rimantadine	viral matrix protein	Influenza A

Drug	Target	Virus
Others		
Foscarnet	viral DNA polymerase	HCMV, HSV-1, HSV-2
Nevirapine	viral DNA polymerase (RT)	HIV-1
Delavirdine	viral DNA polymerase (RT)	HIV-1
Efavirenz	viral DNA polymerase (RT)	HIV-1
Etravirine	viral DNA polymerase (RT)	HIV-1
Rilpivirine	viral DNA polymerase (RT)	HIV-1
Tripanavir	viral protease	HIV-1, HIV-2
Raltegravir	viral integrase	HIV-1
Maraviroc	CCR5	HIV-1

Table 1.1 Clinically approved antiviral drugs. HSV-1, herpes simplex virus type-1; VZV, varicella zoster virus; HBV, hepatitis B virus; HSV-2, herpes simplex virus type-2; RSV, human respiratory syncytial virus; HCV, hepatitis C virus; HCMV, human cytomegalovirus; HIV-1, human immunodeficiency virus type-1; HIV-2, human immunodeficiency virus type-2; AIDS, acquired immunodeficiency syndrome; RT, reverse transcriptase; CCR5, cellular chemokine receptor 5. *Zalcitabine is no longer marketed since 2006. ‡Boceprevir and Telaprevir are approved as a combination with Ribavirin and pegylated interferon (pegIFN).

Compound	Target	Virus	Drug Class	Generation	Status
Small-molecules					
CMX157	viral DNA polymerase (RT)	HIV-1	ANP	2 nd	phase 1
Elvitegravir	viral IN	HIV-1	IN inhibitor	2 nd	phase 3
2-(quinolin-3-yl)acetic acid derivatives	IN-LEDGF/p75 interactions	HIV-1	IN inhibitor	1 st	investigational
ST-246	viral p37 phospholipase	Variola	phospholipase	1 st	phase 2
BMS-790052	viral NS5A	HCV	assembly	1 st	phase 2
RN-18	Vif-A3G interactions	HIV-1	immune booster	1 st	investigational
Ivermectin	helicase*	YFV, TBEV, Dengue, JEV	replication	1 st	investigational
Alisporivir	CypA-replication complex interactions*	HCV	replication	1 st	phase 3
Antibody					
PRO-140	gp120-CCR5 interactions	HIV-1	entry	2 nd	phase 2

Table 1.2 Select antivirals under development. Table summarizing select drugs currently under development, the antiviral target, drug class and generation, and current clinical status. HIV-1, human immunodeficiency virus type-1; HCV, hepatitis C virus; HSV-1, herpes simplex virus type-1; YFV, yellow fever virus; JEV, Japanese encephalitis virus; TBEV, tick-borne encephalitis; RT, reverse transcriptase; ANP, acyclic nucleoside phosphonate; IN, integrase; A3G, apolipoprotein B mRNA-editing enzyme-catalytic polypeptide-like 3G; LEDGF, lens epithelium-derived growth factor; CypA, cyclophilin A. * antiviral target and mechanism not yet fully elucidated.

Vaccine Type	Species	Genus	Family
<i>Inactivated</i>			
polio	poliovirus	<i>Enterovirus</i>	<i>Picornaviridae</i>
hepatitis A	hepatitis A virus	<i>Hepatovirus</i>	<i>Picornaviridae</i>
rabies	rabies virus	<i>Lyssavirus</i>	<i>Rhabdoviridae</i>
Tick-borne encephalitis	Tick-borne encephalitis virus	<i>Flavivirus</i>	<i>Flaviviridae</i>
<i>Attenuated</i>			
smallpox	variola virus	<i>Orthopoxvirus</i>	<i>Poxviridae</i>
yellow fever	yellow fever virus	<i>Flavivirus</i>	<i>Flaviviridae</i>
viral encephalitis	Japanese encephalitis virus	<i>Flavivirus</i>	<i>Flaviviridae</i>
measles	morbilli virus	<i>Morbillivirus</i>	<i>Paramyxoviridae</i>
mumps	mumps virus	<i>Rubulavirus</i>	<i>Paramyxoviridae</i>
rubella	rubella virus	<i>Rubivirus</i>	<i>Togaviridae</i>
chicken pox	varicella zoster virus	<i>Varicellovirus</i>	<i>Herpesviridae</i>
rotavirus flu	rotavirus	<i>Rotavirus</i>	<i>Reoviridae</i>
<i>Subunit</i>			
Influenza	influenza A and B virus	<i>Influenzavirus A and B</i>	<i>Orthomyxoviridae</i>
hepatitis B	hepatitis B virus	<i>Orthohepadnavirus</i>	<i>Hepadnaviridae</i>
human papillomavirus	HPV-6, -11, -16, -18	<i>Alphapapillomavirus</i>	<i>Papillomaviridae</i>

Table 1.3 Clinical human vaccines. Table summarizing approved vaccines against viral pathogens. HPV, human papillomavirus.

Class	Family	Proteins needed	Fusion pH	Fusion peptide location
I	<i>Orthomyxoviridae</i>	HA	Low	N-terminal
I	<i>Retroviridae</i>	Env	Neutral	N-terminal
I	<i>Paramyxoviridae</i>	F	Neutral	N-terminal
I	<i>Coronaviridae</i>	S	Neutral	Internal
I	<i>Filoviridae</i>	GP	Low	Internal
I	<i>Arenaviridae</i>	GPC	Low	nd
II	<i>Flaviviridae</i>	E(TBEV), E1/E2 (HCV)	Low	Internal
II	<i>Togaviridae</i>	E1/E2	Low	Internal
II	<i>Bunyaviridae</i>	G _N /G _C	Low	Internal
III	<i>Rhabdoviridae</i>	G	Low	Internal bipartite
III	<i>Herpesviridae</i>	gB, gD, gH/gL	Neutral	Internal bipartite
nc	<i>Poxviridae</i>	8 proteins	nd	nd

Table 1.4 Viral fusion protein classification. Table summarizing fusion protein and pH requirements for viral fusion. HA, hemagglutinin; Env, envelope; TBEV, Tick-borne encephalitis virus; HCV, hepatitis C virus, nd, not determined; nc, not classified

Host membrane	Virus
Nuclear membrane	Herpesvirus
Endoplasmic reticulum	Hepadnavirus, Rotavirus
Intermediate compartment	Poxvirus
Golgi complex	Alphavirus, Bunyavirus, Rubivirus, Herpesvirus
Plasma membrane	
Apical	Alphavirus (Sindbis), Orthomyxovirus, Paramyxovirus, Rubivirus
Basolateral	Alphavirus (Semliki Forest virus), Arenavirus, Filovirus, Retrovirus, Rhabdovirus

Table 1.5 Budding sites of enveloped viruses. Table summarizing the cell membranes into which enveloped viruses bud.

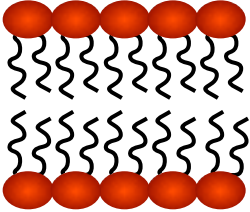
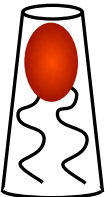
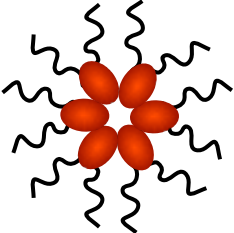
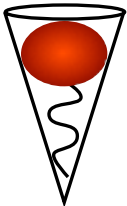
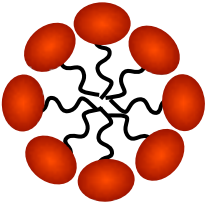
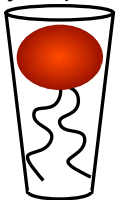
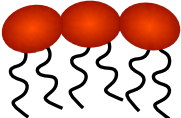
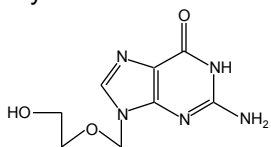
Molecular Shape	Phase	Lipids
Cylindrical 	Lamellar 	phosphatidylcholine sphingomyelin phosphatidylserine phosphatidylinositol
Cone 	Inverted-hexagonal 	phosphatidylethanolamine <i>cis</i> -unsaturated fatty acids (e.g. oleic acid)
Inverted-cone 	Micellar 	lysophospholipids
Hydrophilic region of larger cross-section than hydrophobic tail 		glycolipids

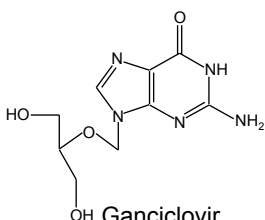
Table 1.6 Molecular shapes and polymorphic phases exhibited by natural lipids. Table summarizing the influence of molecular shape on polymorphic phase. Cylindrical shaped lipids (e.g. phosphatidylcholine) adopt bilayer phases with no net curvature. Cone shaped lipids (e.g. oleic acid) adopt reverse-micellar (inverted-hexagonal) phases of negative curvature. Inverted-cone shaped lipids (e.g. lysophosphatidylcholine) adopt micellar phases of positive curvature. Glycolipids also promote positive curvature.

A. Inhibitors of genome replication

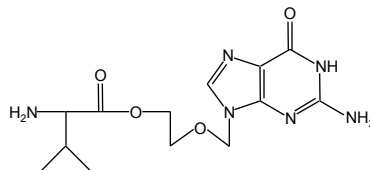
I Acyclic nucleoside analogues



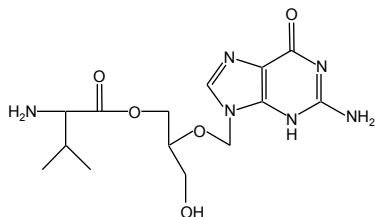
Acyclovir



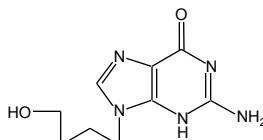
Ganciclovir



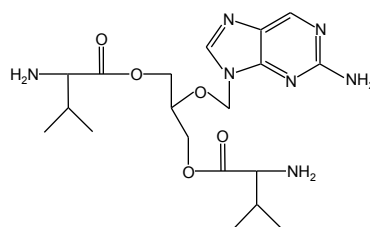
Valaciclovir



Valganciclovir

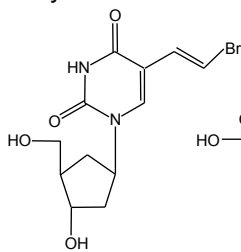


Penciclovir

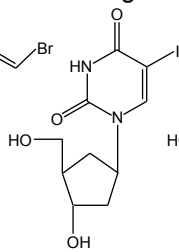


Famciclovir

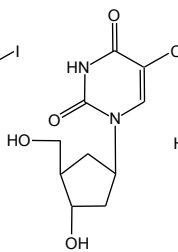
II Cyclic nucleoside analogues



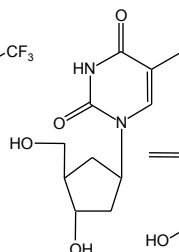
Brivudine



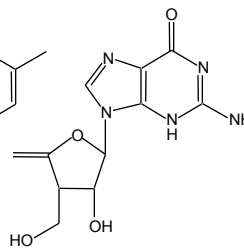
Idoxuridine



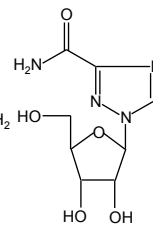
Trifluridine



Telbivudine

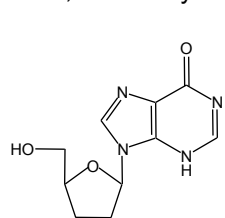


Entecavir

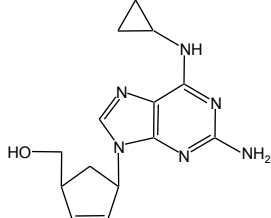


Ribavirin

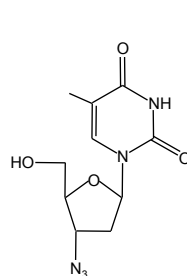
III. 2',3'-dideoxynucleosides



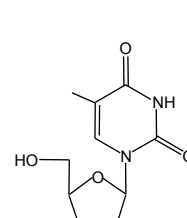
Didanosine



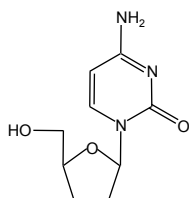
Abacavir



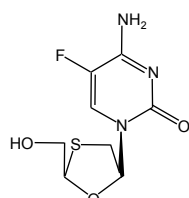
Zidovudine



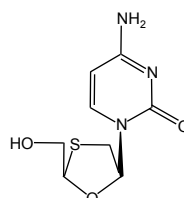
Stavudine



Zalcitabine

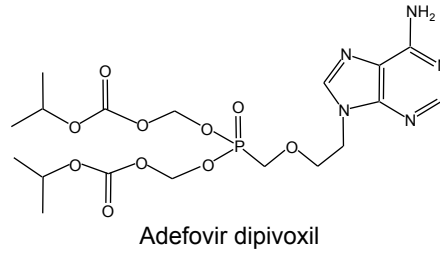
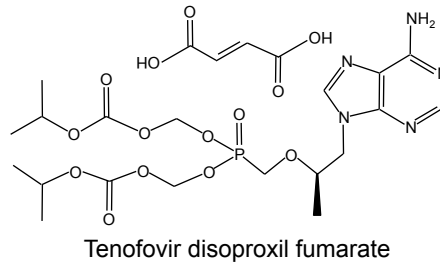
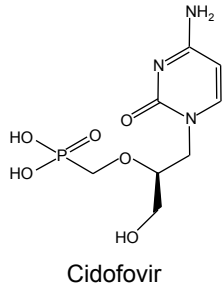


Emtricitabine

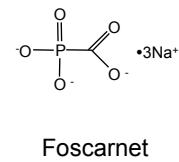
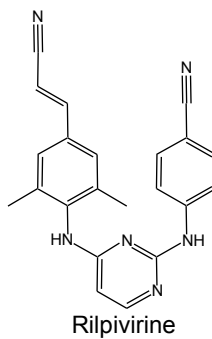
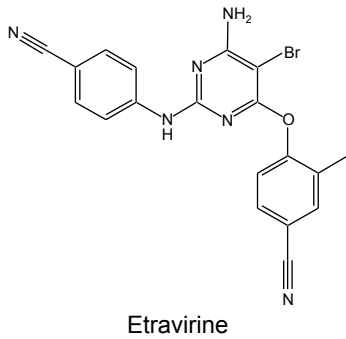
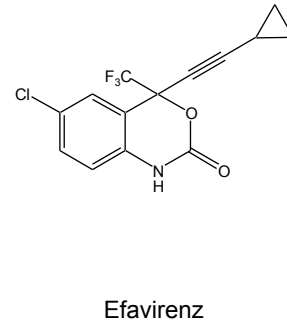
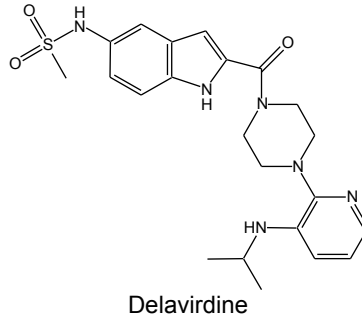
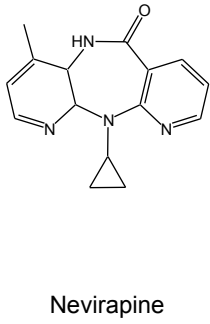


Lamivudine

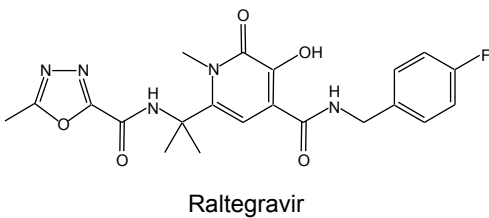
IV Acyclic nucleotide phosphonates



V Non-nucleosides



B. Inhibitor of integration



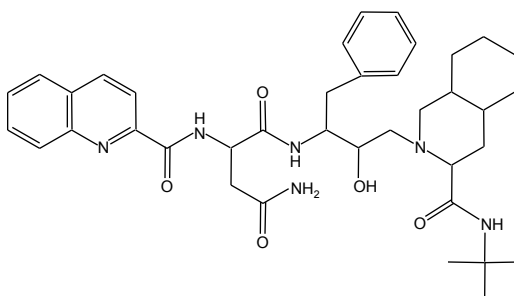
C. Inhibitor of gene expression



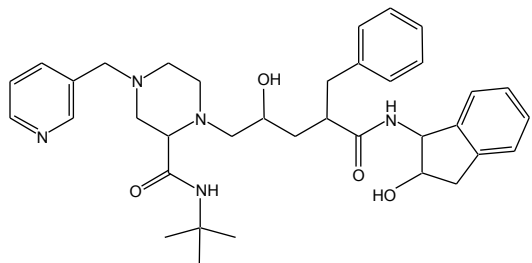
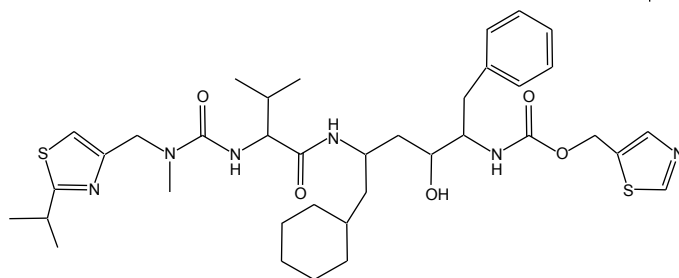
Fomivirsen

D. Inhibitors of protease

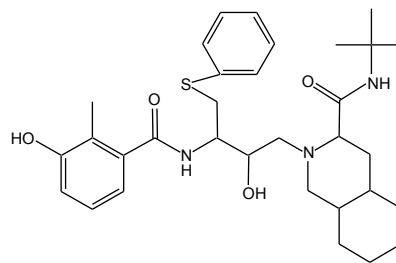
Saquinavir mesylate



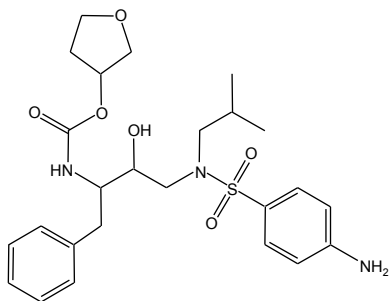
Ritonavir



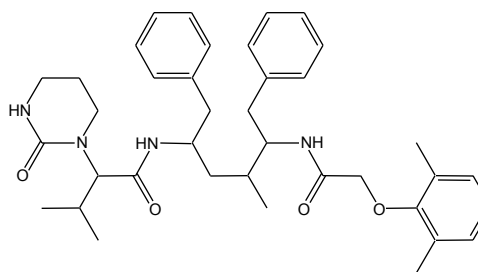
Indinavir



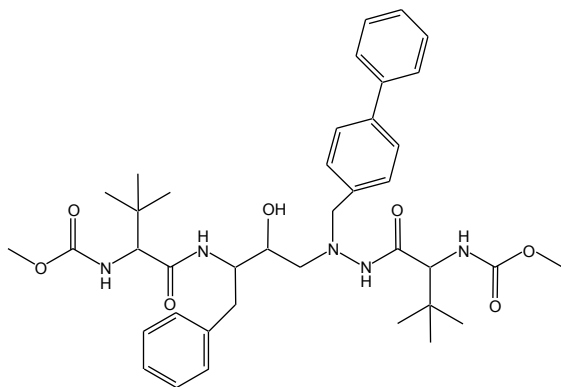
Nelfinavir mesylate



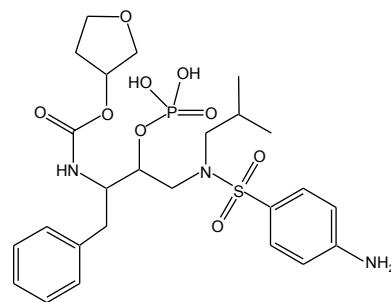
Amprenavir



Lopinavir



Atazanavir



Fosamprenavir

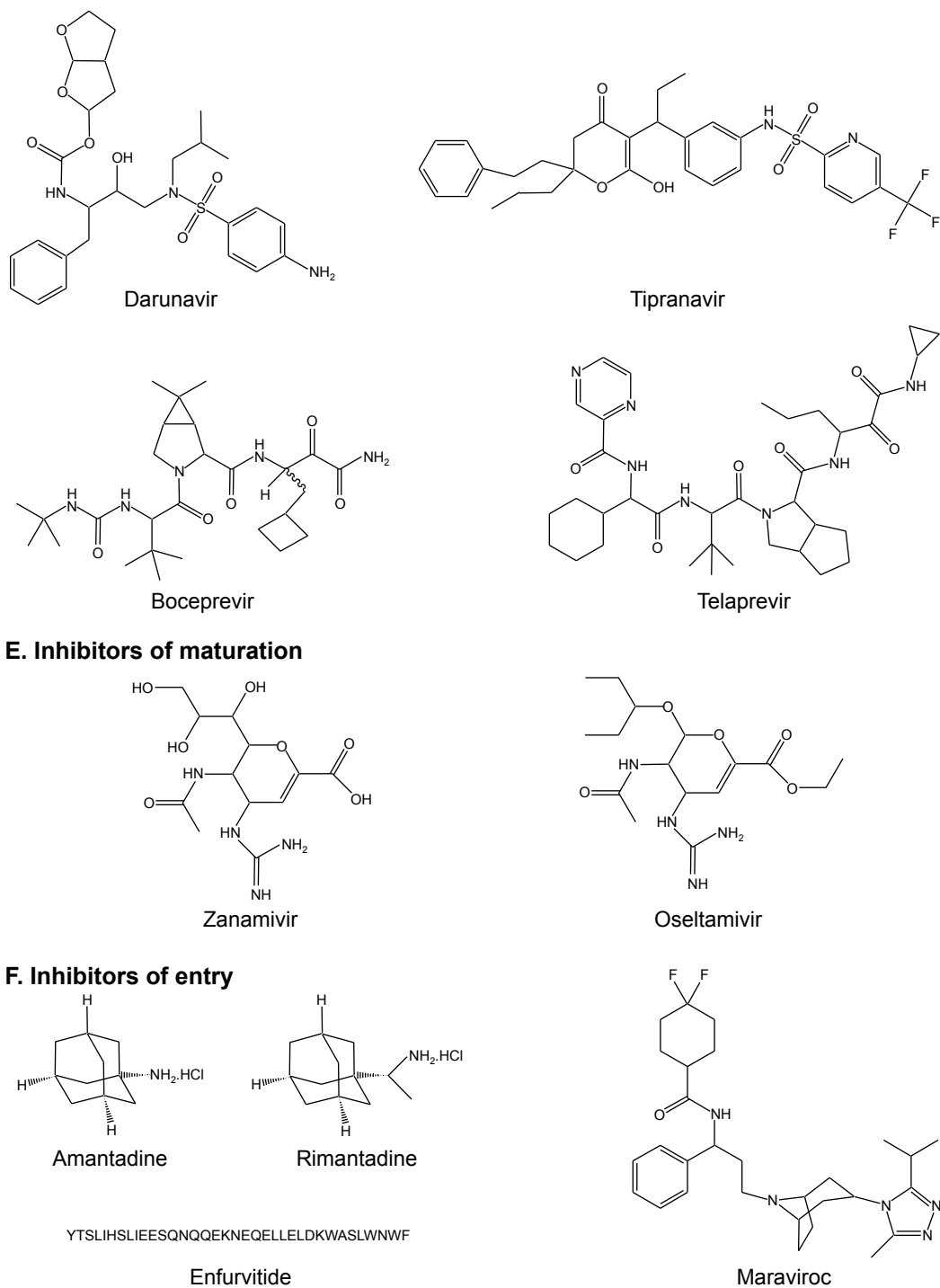


Figure 1.1 Clinically approved antiviral drugs. Chemical structure of clinical antiviral drugs targeting viral genome replication (**A,B,C**); assembly, maturation or release (**C,D,E**); or entry (**F**). Drugs targeting polymerases are further categorized as acyclic (I), cyclic (II), 2',3'-dideoxy (III), acyclic nucleotide phosphonates (IV), or non-nucleosidic (V).

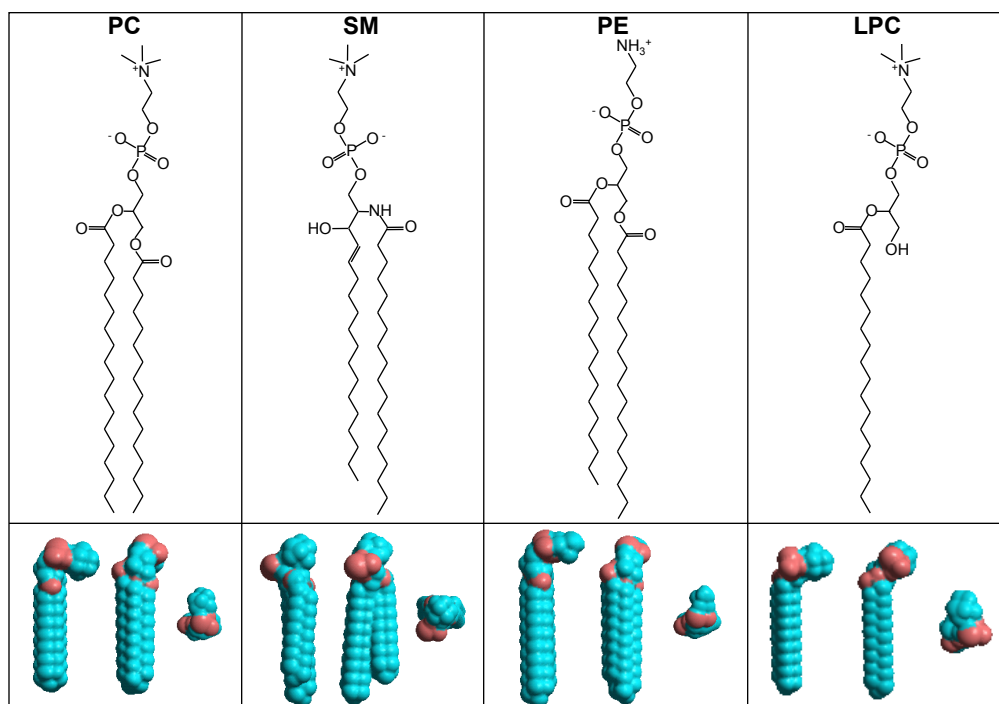


Figure 1.2 Natural membrane phospholipids. Chemical structures and three-dimensional space-filling models of naturally occurring phospholipids phosphatidylcholine (PC), sphingomyelin (SM), phosphatidylethanolamine (PE), and lysophosphatidylcholine (LPC), displayed in 3 orthogonal planes. Grey, carbon; teal, hydrogen; pink, oxygen; blue, nitrogen; red, phosphate.

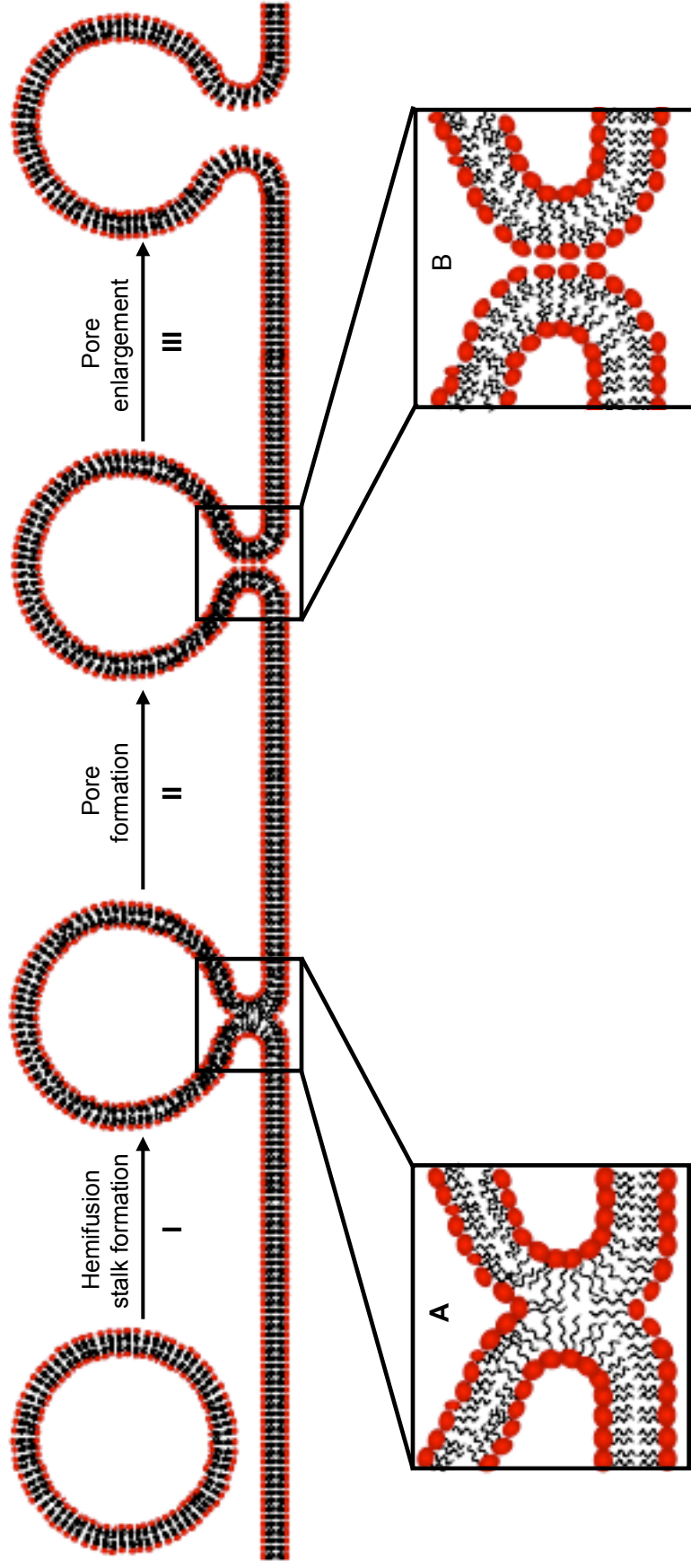


Figure 1.3 Lipid reorganizations during fusion. Cartoon representation depicting the intermediate lipid structures formed during fusion, according to the hemifusion stalk model: **I**, outer leaflet fusion to form the hemifusion stalk (**A**, inset); **II**, inner leaflet fusion to form the pore (**B**, inset); and **III**, pore enlargement. Inset, hemifusion stalk (**A**) or pore (**B**) showing the outer leaflets with negative curvature (lipid headgroups bent towards each other) and the inner leaflets with positive curvature (lipid headgroups bent away from each other).

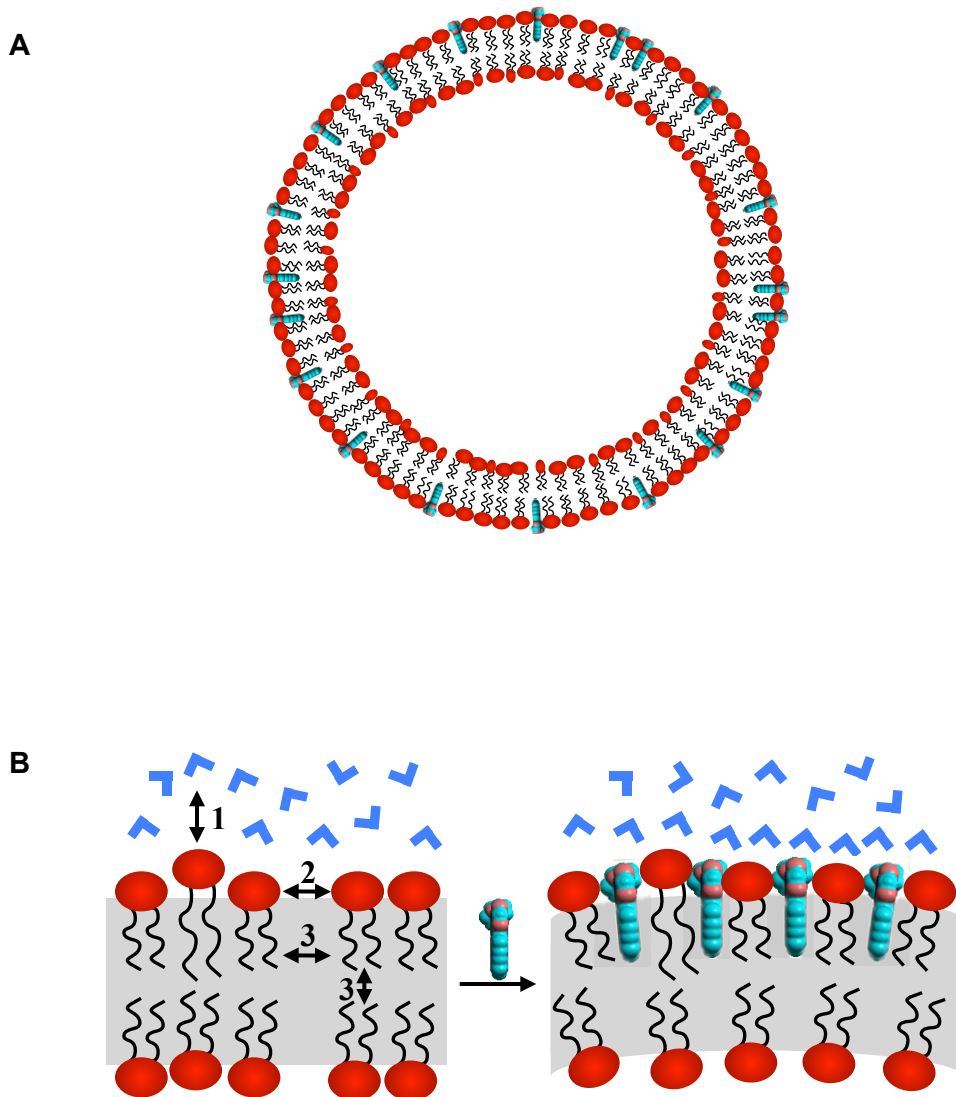


Figure 1.4 Extracellular exposure of vesicles to synthetic rigid amphiphiles. Cartoon representation of the insertion of rigid amphipathic fusion inhibitor molecules into the external leaflet of a virion envelope (**A**) and potential interactions with surrounding molecules (**B**). Interactions depicted are 1, hydrophilic headgroup-aqueous; 2, hydrophilic headgroup-headgroup ; and 3, hydrophobic acylchain-acylchain.

CHAPTER 2: MATERIALS AND METHODS

2.1 Introduction

This chapter describes the materials and methods used to identify and characterize the novel antiviral activities of the rigid amphipathic fusion inhibitors (RAFIs) I discovered during my PhD studies.

2.2 Cells and virus

The immortalized African green monkey kidney epithelial cell line (Vero) and human foreskin fibroblasts (HFF) were kind gifts from Dr. Priscilla A. Schaffer (University of Pennsylvania, Philadelphia, PA, USA). Human embryonic kidney cells (HEK293) and HeLa cervical cancer cells (HeLa) were obtained from Drs. Frank L. Graham (McGill University, Montréal, Qc, CANADA) and Luc G. Berthiaume (University of Alberta, Edmonton, AB, CANADA), respectively. Human osteosarcoma (U2OS) epithelial cells were obtained from American Type Culture Collection (catalogue HTB-96; ATCC, Manassas, VA, USA). Vero, HFF, HEK293, HeLa and U2OS cells were maintained in Dulbecco's modified Minimum Eagle's Medium (DMEM) (catalogue 11885-084; Invitrogen, Burlington, ON, CANADA) supplemented with 5% fetal bovine serum (FBS; catalogue A15-071; PAA Laboratories Inc., Etobicoke, ON, CANADA). Vero clone 57 cells were previously constructed in our laboratory (Diwan, Lacasse, and Schang, 2004) and express a red fluorescent reporter protein (RFP) under the control of the HSV-1 ICP0 promoter. Vero clone 57 cells were maintained as

described above. Huh7.5 cells were obtained from Dr. Charles M. Rice (Rockefeller University, New York, NY, USA) and maintained in DMEM-10% FBS. All cells types were detached by trypsin digestion, unless otherwise indicated. Trypsin-ethylenediaminetetraacetic acid (EDTA; catalogue 15400-054; Invitrogen) was prepared as a 0.05% trypsin, 0.053 mM EDTA solution in phosphate-buffered saline (PBS; pH 7.4, 150 mM NaCl, 3 mM Na₂HPO₄, 1 mM KH₂PO₄).

Low-passage (passage 10, p10) wild-type herpes simplex virus type-1 (HSV-1) strain KOS, phosphonoacetic acid resistant HSV-1 (PAA^{r5}), and herpes simplex virus type-2 (HSV-2) strains 333 and 186 were kind gifts from Dr. Priscilla A. Schaffer (University of Pennsylvania). Thymidine kinase null (TK-) HSV-1 was a kind gift from Dr. Donald M. Cohen (University of Pennsylvania). All HSV strains were propagated in Vero cells maintained with DMEM-5% FBS. Sindbis virus (SIN), vesicular stomatitis virus (VSV) and vaccinia virus (VV) were kind gifts from Drs. Tom C. Hobman, Paul Melançon and Michele M. Barry (University of Alberta, Edmonton, AB, CANADA), respectively. They were propagated in Vero cells maintained in DMEM-5% FBS. Green fluorescent protein (GFP)-expressing adenovirus (AdV) was obtained from Dr. René L. Jacobs (Dr. Dennis E. Vance, University of Alberta) and was titrated in HEK293 cells maintained with DMEM-5% FBS. Poliovirus (PV) Mahoney strain complementary DNA (cDNA) was obtained from Dr. Jiang Yin (Dr. Michael N. James, University of Alberta) and used to produce PV seed (as described in **section 2.5.1.2**). Poliovirus was propagated in Vero cells maintained in DMEM-

10% FBS. Hepatitis C virus (HCV) genotype 2a (JFH-1 strain) was obtained from Dr. Lorne J. Tyrrell at the University of Alberta (originally from Dr. Takaji Wakita, Tokyo Metropolitan Institute for Neuroscience, Tokyo, JAPAN). Viral stocks were propagated and titrated on monolayers of Vero cells as described in **sections 2.5.1** and **2.6**, respectively, unless otherwise indicated.

2.3 Drugs

Rigid amphipathic fusion inhibitors (RAFIs) were synthesized at the Shemyakin-Ovchinnikov Institute of Bioorganic Chemistry (Russian Academy of Sciences, Moscow, RUSSIA). Markiewicz's protective group was used to facilitate purification of intermediate products, and their synthesis is described elsewhere (Andronova et al., 2003; Skorobogatyj et al., 2006; St Vincent et al., 2010). Test compounds were dissolved in dimethylsulfoxide (DMSO) as 100 mM stocks before further diluting in DMSO to 10 mM stocks, except for dUY5 and aUY1, which were dissolved as 10 mM stocks. All compounds were stored at -20°C as 10 mM stocks and were diluted to indicated concentrations in DMEM supplemented with or without 5% FBS just prior to use. The highest tested concentration for each experiment was prepared using 10 mM stock RAFI, unless otherwise indicated. Subsequent concentrations were prepared as 2X concentrations. For infectivity assays, except HCV, cell protection and progeny infectivity (**sections 2.7.2**, **2.7.4** and **2.10**, respectively), RAFIs were prepared as 2X concentrations. For all assays, a DMSO concentration equivalent to that required for the highest test drug concentration was added to the controls.

Stocks of phosphonoacetic acid (PAA) and acyclovir (ACV) (Sigma-Aldrich, Oakville, ON, CANADA) were dissolved in serum-free DMEM media (SFM) at a concentration of 100 mg/mL and 10 mg/mL, respectively. PAA was neutralized with sodium hydroxide. PAA and ACV stocks were filter-sterilized before storing at -20°C. PAA and ACV were diluted to the desired concentrations in DMEM-5% FBS just before use. Stocks of heparin (Sigma-Aldrich) were dissolved in SFM at a concentration of 100 mg/mL and stored at -20°C. Stock heparin was diluted in SFM to the desired concentrations (from 30 to 1,000 µg/mL) just prior to use.

IgePal CA-630 (catalogue I8896-50; Sigma-Aldrich) was prepared as a 10% stock in distilled deionized water and stored at room temperature. IgePal CA-630 was diluted to 1.5% in SFM just prior to use, unless otherwise indicated.

2.4 Cytotoxicity assays

Vero cell monolayers (2×10^5 cells per 35 mm diameter tissue culture dish) were mock infected with 200 µl of SFM at 37°C in 5% CO₂ for 1 hour, rocking and rotating the dishes every 10 min. After removal of mock inocula, cells were washed twice with ice-cold PBS and overlaid with DMEM supplemented with 5% FBS and 0, 7, 20, 70, or 150 µM dUY11 (1X test concentration). Media were replaced with fresh complete media supplemented with 0, 7, 20, 70, or 150 µM dUY11 at 24 and 48 hours. Cells were harvested at 0, 24, 48 and 72 hours after mock-infection. Cell number and viability were analyzed by trypan blue exclusion. At the indicated times, cells were washed once with 1 mL per well of

PBS at room temperature. Two hundred microliters of trypsin was added and cells were incubated at 37°C until they detached (approximately 5 min). Trypsin was inactivated by addition of 800 µl of DMEM-5% FBS at room temperature, and the cells were transferred into 14-mL snap-cap conical tubes. Cells were pelleted by centrifugation at 2,000 revolutions per minute (rpm) in swinging bucket rotor A-4-62 in an Eppendorf 5810R centrifuge (Eppendorf Canada, Mississauga, ON, CANADA) for 5 min at room temperature. The supernatant was removed and the cell pellet was resuspended in 200 µl of SFM at room temperature. One hundred microliters of the cell suspension was then added to 100 µl of 0.4% trypan blue (catalogue T8154; Sigma-Aldrich) pre-warmed to 37°C, and incubated for 5 min at room temperature. Stained cells were loaded into a hemocytometer and white (viable) and blue (non-viable) cells were counted. Cytotoxic effects were defined as more than 5% non-viable cells.

2.5 Virus infections

2.5.1 Virus stocks

2.5.1.1 Herpes simplex virus types 1 and 2 stock preparation

HSV-1 and HSV-2 virus stocks were produced by infection of Vero cell monolayers at a low multiplicity of infection (MOI; 0.05 plaque-forming units per cell – PFU/cell). Vero cell monolayers (1.2×10^6 cells per 100 mm diameter tissue culture dish) were infected with HSV-1 strains KOS, PAA^{T5} or TK-, or HSV-2 strains 333 or 186 in 1.5 mL of SFM at 37°C in a 5% CO₂ incubator for 1 hour, rocking and rotating the dishes every 10 min. Unbound virions were then

removed by vacuuming the inocula. Cells were washed twice with 5 mL of ice-cold SFM per wash and overlaid with 6 mL of DMEM-5% FBS. Infected cells were then returned to 37°C in 5% CO₂ until cytopathic effect (CPE) was generalized (4+), as determined by microscopic observation of infected cell rounding, but with minimal detachment (approximately 50 hours).

Cells were harvested by scraping using sterile disposable cell lifters. The cells and supernatants were then transferred into 50 mL screw-cap conical tubes (4 dishes per conical tube). Medium was clarified by centrifugation at 4,000 rpm in swinging bucket rotor A-4-62 in an Eppendorf 5810R centrifuge (Eppendorf Canada) for 30 min at 4°C. Supernatants were collected and pooled into a 250 mL Beckman centrifuge bottle (Beckman Coulter Inc, Mississauga, ON, CANADA). Virions were pelleted by ultracentrifugation at 10,000 x g in the JA-14 rotor of a Beckman Coulter J-series ultracentrifuge (Beckman Coulter Inc) at 4°C for 2 hours. Meanwhile, cell pellets were resuspended in SFM (1 mL SFM per three 50 mL screw-cap conical tubes, or per 12 dishes), pooled into a 14 mL snap-cap conical tube, and lysed by 3 freeze-thaw cycles, alternating between freezing in an ethanol-dry ice bath and thawing in a 37°C water bath. Cell lysates were then placed in an ice-water bath and subjected to 3 cycles of macroprobe sonication using an Ultrasonic Processor XL 2020 (Mandel Scientific Company Ltd., Guelph, ON, CANADA) at a power setting of 3 for 30 sec, separated by 15 sec rest periods. Cellular debris was pelleted by centrifugation at 4,000 rpm in swinging bucket rotor A-4-62 of an Eppendorf 5810R centrifuge (Eppendorf Canada) at 4°C for 30 min.

After ultracentrifugation of released virions, medium was removed using disposable 15-mL plastic pipettes, with careful attention not to disturb the virion pellet. Supernatant from the cellular fraction was collected using a P1000 micropipette and used to resuspend the virion pellet. The resulting stock preparations were separated into 100 μ l aliquots in glass screw-cap vials and stored at -80°C . An aliquot of the frozen stock was then titrated, as described in **section 2.6**. Yields were approximately 10^9 virions/ 10^6 cells for HSV-1 strain KOS, strain PAA¹⁵, and strain TK-, or approximately 5×10^7 virions/ 10^6 cells for HSV-2 strains 333 and 186. Yields were consistent between stock preparations.

2.5.1.2 Poliovirus stock preparation

PV Mahoney strain cDNA was linearized by DraI (1 unit per μ g of cDNA; Invitrogen) restriction enzyme digestion and reverse transcribed *in vitro* following the methods of Cello et al. (2002). Briefly, 0.5 μ g of linearized template PV cDNA was transcribed in a 40 μ l reaction mixture containing 40 mM Tris-HCl [pH 8.0], 8 mM MgCl_2 , 25 mM NaCl, 4 mM dithiothreitol (DTT), 2 mM spermidine, 1 mM each nucleoside triphosphate (NTP), 80 units of RNase inhibitor, and 200 units of T7 RNA polymerase. The reaction mixture was incubated at 37°C for 2 hours. Transcribed RNA was then precipitated with lithium chloride in isopropanol at -80°C for 2 hours. The RNA was pelleted by centrifugation and washed with 70% ethanol prepared in diethylpyrocarbonate (DEPC)-treated water. The purified viral RNA was resuspended in DEPC-treated water. Purified RNA was then transfected into HeLa cells using

diethylaminoethyl (DEAE) dextran (Amersham Pharmacia Biotech Inc., Piscataway, NJ, USA). RNA transcripts were incubated with 1 mg/mL DEAE dextran in Hanks Balanced Salt Solution (HBSS; 137 mM NaCl, 5.4 mM KCl, 0.25 mM Na₂HPO₄, 0.44 mM KH₂PO₄, 1.3 mM CaCl₂, 1 mM MgSO₄, 4.2 mM NaHCO₃) on ice for 30 min. HeLa cells (3.5 x 10⁵ cells per well in 6-well plates) were washed twice with 1 mL SFM per wash and incubated with the RNA-DEAE dextran mixture at room temperature for 30 min, rocking and rotating every 10 min. Transfected cells were washed twice with SFM at room temperature and overlaid with 2 mL per well of DMEM-5% FBS. HeLa cells were passaged 1:5 24 hours later. Supernatants containing seed PV were collected (into 15-mL screw-cap conical tubes) 120 hours after infection.

Seed PV was then used to prepare PV stocks. Stocks were produced by infection of Vero cell monolayers (1 x 10⁶ cells per 100 mm diameter tissue culture dish) at a MOI of 0.05 PFU per cell at 37°C in 5% CO₂ for 1 hour. Following adsorption, cells were washed twice with 1 mL ice-cold SFM per wash and overlaid with 6 mL of DMEM-10% FBS. Infected cells were incubated at 37°C in 5% CO₂ until 4+ CPE was observed microscopically (approximately 70 hours).

Cells were scraped with sterile disposable cell lifters, and cells and supernatants were collected into 50-mL screw-cap conical tubes, as described for HSV-1 and HSV-2 (**section 2.5.1.1**). The medium was clarified by centrifugation at 4,000 rpm in swinging bucket rotor A-4-62 in an Eppendorf 5810R centrifuge (Eppendorf Canada) at 4°C for 30 min. Supernatants were collected with a sterile

10-mL disposable plastic pipette, pooled and used as virus stock. Stock preparations produced were separated into 500 µl aliquots in glass screw-cap vials and stored at -80°C. An aliquot of the frozen stock was then titrated, as described in **section 2.6**, with yields of approximately 2.5×10^7 virions/ 10^6 cells.

2.5.2 Herpes simplex virus type-1 infection

Vero cell monolayers, in 6- or 12-well plates, were infected at a MOI of 3 PFU per cell of wild-type strain KOS, PAA^{T5} or TK- HSV-1 in 200 µl or 100 µl of SFM, respectively, unless otherwise indicated. Alternatively, Vero cell monolayers were mock or HSV-1 infected (7.5×10^5 cells per 100 mm diameter tissue culture dish) with 5 PFU per cell in 1.5 mL SFM. Plates were rocked and rotated every 10 min during the 1-hour adsorption at 37°C in 5% CO₂. Unbound virions were then removed by vacuuming the inocula. Infected-cell monolayers were washed twice with 2, 1 or 5 mL (6-/12-well plates or 100 mm tissue culture dishes, respectively) of ice-cold SFM per wash and then incubated with DMEM supplemented with 5% FBS alone, or with the concentration of dUY11, PAA or ACV indicated for each experiment.

Mock- or HSV-1-infected cells and their supernatants were harvested separately at 1, 5, 18 or 24 hours post infection (hpi) following the protocol described in **section 2.5.4**. Infectious virions were titrated by standard plaque assay as described in **section 2.6**, or viral DNA levels were measured as described in **section 2.13**. HSV replicated with the efficiency expected in the absence of any

drug. Yields were approximately 1×10^8 PFU/ 10^6 cells for HSV-1 strains KOS and PAA^{r5}, or 1×10^6 virions/ 10^6 cells for HSV-1 strain TK-.

2.5.3 Sindbis virus infection

Vero cell monolayers (1×10^5 cells per well in 12-well plates) were infected at a MOI of 0.2 PFU per cell in 150 μ l of SFM, unless otherwise indicated. After a 1 hour adsorption at 37°C in 5% CO₂, inocula containing unbound virions were removed, cells were washed twice with 1 mL of ice-cold SFM per wash and then incubated in DMEM supplemented with 5% FBS alone or with the indicated dUY11 concentrations.

Cells and virus-containing supernatants were harvested at the times indicated for each experiment, as described in **section 2.5.4**. Virus-containing supernatants were then titrated by standard plaque assay as described in **section 2.6**, with yields of 2.5×10^6 PFU/ 10^6 cells in 24 hours (depending on the experiment) in the absence of drug. Yields were consistent between experiments.

2.5.4 Virus harvest

Cells and media were harvested at 24 hpi unless otherwise indicated. To harvest cells and virus-containing supernatants together, infected-cell monolayers were first scraped using sterile disposable cell lifters. Cells and supernatants were then transferred together into 14-mL snap-cap conical tubes using a P1000 micropipette. To harvest extracellular released virus separately from intracellular cell-associated virus, supernatants were collected first into 14-mL snap-cap

conical tubes using a P1000 micropipette. Then, 500 μ l of SFM (unless otherwise indicated) were added to infected-cell monolayers, and the cells were scraped using sterile disposable cell lifters. Harvested cells and supernatants, collected into the 14-mL conical snap-cap conical tubes, were subjected to 3 freeze-thaw cycles by alternating between an ethanol-dry ice bath and a 37°C water bath, to disrupt cell membranes. To homogenize virus preparations, collected samples were placed in an ice-water bath and subjected to 3 cycles of macroprobe sonication using an Ultrasonic Processor XL 2020 (Mandel Scientific Company Ltd.) at a power setting of 3 for 30 sec, separated by 15 sec rest periods. Cell debris were then centrifuged at 4,000 rpm in swinging bucket rotor A-4-62 in an Eppendorf 5810R centrifuge (Eppendorf Canada) at 4°C for 30 min. Supernatants were collected using a P200 micropipette, with careful attention not to disturb the pelleted debris, and transferred into 14-mL snap-cap conical tubes. Samples were stored at -80°C.

2.6 Virus titrations

Frozen aliquots were thawed in a 37°C water bath and immediately placed on ice. To prepare serial dilutions, 2.5 μ l of each test sample were added to 247.5 μ l of ice-cold SFM (-2 dilution). The first dilution was then gently mixed using a standard mini vortexer at 4000 rpm on continuous mode for approximately 3 sec. To prepare the subsequent dilution (-3), 25 μ l of the -2 dilution were added to 225 μ l of ice-cold SFM. The above-procedure was repeated for the preparation of subsequent dilutions (-4 to -8). Volumes were doubled when titrations were

performed in duplicate. The serial 1:10 dilutions were then used to infect Vero cell monolayers.

Near-confluent Vero cell monolayers in 6- or 12-well plates (approximately 3 or 1.5×10^5 cells per well, respectively) were infected with 200 or 100 μ l, respectively, of the relevant 1:10 serial dilutions. Inocula were removed after a 1-hour adsorption and cells were washed twice with 2 or 1 mL, respectively, of ice-cold SFM per wash. Cells were then overlaid with 3 or 2 mL, respectively, of DMEM supplemented with 5% FBS and 2% (w/v) methyl cellulose (MC). Infected cells were incubated at 37°C in 5% CO₂ until well-defined plaques were clearly visible (typically 2 to 3 days). The cells were fixed and stained with crystal violet (CV) in methanol (1% w/v crystal violet, 17% v/v methanol in H₂O) for 24 to 48 hours. Excess MC and CV were removed by washing the plates in a 4L plastic beaker containing lukewarm water, and dried overnight on a bench. The plates were then scanned using a HP Scanjet 5370C. Plaques were counted and recorded.

2.7 Viral infectivity assays

2.7.1 Virion infectivity assay

One hundred microliters of SFM containing 200 infectious virions (HSV-1, HSV-2, VSV, SIN or PV) were pre-warmed to 37°C for approximately 5 min and added to 100 μ l of pre-warmed SFM supplemented with 2X concentration of test compound pre-warmed to 37°C for a minimum of 10 min. Virus and RAFI

preparations were mixed by gentle pipetting up and down 3 times, and then further incubated at 37°C for 5 min, unless otherwise indicated.

Vero cell monolayers (approximately 2×10^5 cells per well in 6-well plates) were infected with the so-pretreated virions at 37°C in 5% CO₂ for 1 hour, rocking and rotating the plates every 10 min. Following 1-hour adsorption, the cells were washed twice with 2 mL of ice-cold SFM per wash and overlaid with 3 mL of drug-free DMEM supplemented with 5% FBS and 2% MC. Infected cells were incubated in 5% CO₂ at 37°C. Once well-defined plaques had developed (2 to 3 days post-infection; dpi), the cells were fixed and stained with CV in methanol (1% w/v crystal violet, 17% v/v methanol in H₂O) for 24-48 hours. Excess MC and CV were removed by washing the plates in a 4L plastic beaker containing lukewarm water, and dried overnight on a bench. Plaques were then counted and recorded.

2.7.2 Hepatitis C virus infectivity assay

The HCV genotype 2a strain JFH-1 stock, kindly provided by Dr. Lorne J. Tyrrell (University of Alberta), was divided into 500 µl aliquots in 14-mL snap-cap conical tubes and pre-warmed to 37°C for 10 min. Each aliquot consisted of DMEM supplemented with 10% FBS and contained 1.5×10^6 HCV genome copy equivalents. Sufficient 1 mM stock dUY11 was added to prepare 1X test concentrations of 7 and 2 µM dUY11, 0.1 mM stock dUY11 to obtain test concentrations of 0.7 and 0.2 µM, or 0.01 mM stock dUY11 to prepare test concentrations of 0.07 and 0.02 µM dUY11. Virus and compound were then

further incubated at 37°C in a water bath for 5 min. Meanwhile, Huh7.5 cell monolayers (5 x 10⁵ cells per well in 6-well plates) were washed twice at room temperature with 2 mL per wash of DMEM supplemented with 10% FBS. Washed cells were infected with the so-pretreated virions at 37°C in 5% CO₂ for 4 hours, rocking and rotating the plates every 30 min. Following adsorption, cells were washed thrice at room temperature with 1 mL per wash of DMEM-10% FBS. Infected cell monolayers were overlaid with 2 mL of DMEM-10% FBS, passaged at 2 dpi, and harvested at 4 dpi.

To passage HCV-infected cells, media was removed and the cells were washed once at room temperature with 1 mL of PBS. Washed cells were then detached at 37°C with 500 µl of trypsin, and resuspended with DMEM-10% FBS in a final volume of 1.5 mL. Seven hundred and fifty microliters from each recovered cell monolayer were then seeded into a separate well (1:2) to which 1.25 mL of DMEM-10% FBS were added.

To harvest HCV-infected cells, cell monolayers were washed once with PBS and lysed using radioimmunoprecipitation assay buffer (10 mM Tris-HCL [pH 8.0], 140 mM NaCl, 0.02% sodium azide, 1% Triton X-100, 0.1% sodium dodecyl sulphate (SDS), 1% deoxycholic acid) supplemented with protease inhibitors (Roche, Indianapolis, IN, USA). Infected-cell lysates were collected and pooled into 2 mL microcentrifuge tubes and vortexed using a mini-vortexer on continuous mode at 5,000 rpm for approximately 1 min, or until cell aggregates were disrupted into a more homogenous suspension. The samples were then placed in an ice-water bath, sonicated as described in **section 2.5.4**, and

incubated on ice for 30 min. Supernatants containing infected-cell proteins were recovered into new microcentrifuge tubes and stored at -80°C. Protein concentration was determined using BioRad D_C Protein Assay (Bio-Rad Laboratories, Mississauga, ON, CANADA). Twenty five micrograms of protein were separated on a 10% SDS-polyacrylamide gel electrophoresis (SDS-PAGE), transferred onto polyvinylidene fluoride (PVDF) membrane using a semi-dry transfer apparatus, and analyzed by Western blot for NS3 helicase (a non-structural protein), as described in **section 2.12**.

2.7.3 Infectivity of green fluorescent protein-expressing viruses

Fifty microliter aliquots of SFM each containing 100,000 virions of recombinant HSV-1 or AdV expressing GFP reporter genes (GFP HSV-1 or GFP AdV, respectively) were placed in 14-mL snap-cap conical tubes and pre-warmed to 37°C for approximately 10 min. Fifty microliters of pre-warmed 2X test concentrations of dUY11 in SFM (final test concentrations; 0,0.05, 0.2, 0.65, 2 or 20 µM dUY11) were added to each virus aliquot, mixed by gently pipetting up and down three times and then further incubated in a water bath at 37°C for 5 min. Following dUY11-exposure, 900 µl of ice-cold SFM were added to each tested aliquot and the samples were placed on ice. Working quickly and on ice, 10-fold serial dilutions of each tested concentration were prepared. One hundred microliters of the each undiluted test sample were added to 900 µl of ice-cold SFM to produce the -1 dilution. The -1 dilution was mixed by gentle pipetting up and down using a P1000 micropipette, and 100 µl were then transferred into a 14-

mL snap-cap conical tube containing 900 μ l of ice-cold SFM to prepare the -2 dilution. The above-described procedure was repeated to prepare the -3 to -5 dilutions.

HEK293 cell monolayers (2.5×10^5 cells per well in 12-well plates) were then infected with 200 μ l of the 10-fold serial (0 to -5) dilutions at 37°C in 5% CO₂ for 1 hour, rocking and rotating the plates every 10 min. Following adsorption, cells were washed twice at room temperature with 1 mL of ice-cold SFM per wash and overlaid with 1 mL of DMEM-5% FBS. GFP expression was visualized using a fluorescence microscope with an ultraviolet (UV) light source (Leica DM IRB, Itzlar, GERMANY) and documented using a digital camera (QIMAGING RETIGA 1300, Burnaby, BC, CANADA). Pictures were taken at 100x magnifications (excitation/emission = 480/520 nm) at 18 hpi for GFP HSV-1 or 36 hpi for GFP AdV, to reach equivalent CPE.

2.7.4 Cell protection assay

Vero cell monolayers (3×10^5 cells per well in 6-well plates) were overlaid with 2 mL of DMEM supplemented with 5% FBS and 0, 2, 7, 20 or 70 μ M dUY11 (1X test concentration) and incubated at 37°C in 5% CO₂ for 15 to 60 min. Cells were subsequently washed twice at room temperature with 2 mL of DMEM-5% FBS per wash, and then infected with 200 μ l of SFM containing 200 infectious HSV-1 virions. Following adsorption, cells were washed twice with 2 mL of ice-cold SFM per wash and overlaid with 3 mL of DMEM supplemented with 5% FBS and 2% MC. Infected cells were incubated at 37°C in 5% CO₂ until well-defined

plaques were clearly visible (2 to 3 dpi). Cells were then fixed and stained with CV in methanol (1% w/v CV, 17% v/v methanol in H₂O), typically for 24 to 48 hours. Plates were washed in a 4L plastic beaker containing lukewarm water, and dried overnight on a bench. Plaques were then counted and recorded.

2.8 Temperature dependence assay

HSV-1 KOS inocula (approximately 1×10^7 PFU per mL in SFM) were divided into two aliquots in 14-mL snap-cap conical tubes. One aliquot was pre-warmed to 37°C in a water bath, whereas the other was pre-cooled to 4°C on ice, for approximately 20 min. Four micromolar dUY11 prepared from a 1 mM dUY11 stock was likewise divided into two aliquots. One aliquot was pre-warmed to 37°C in a water bath, whereas the other was pre-cooled to 4°C on ice, for approximately 20 min. Twenty microliter aliquots of 4 µM dUY11 or DMSO control pre-warmed to 37°C or pre-cooled to 4°C were added to 20 µl virus aliquots containing 100,000 infectious HSV-1 virions in 14-mL snap-cap conical tubes (pre-warmed to 37°C or pre-cooled to 4°C, respectively). The mixtures were gently pipetted up and down three times and then further incubated in a 37°C water bath for 0 or 5 min, or at 4°C on ice for 0 or 60 min. Exposures were terminated by adding 360 µl of ice-cold SFM to each test condition and the samples were placed on ice. Working quickly and on ice, dUY11-exposed virions were then serially diluted 10-fold in ice-cold SFM. Forty microliters of each test sample were added to 360 µl of ice-cold SFM to produce the -1 dilution. The -1

dilution was mixed by gently pipetting up and down using a P1000 micropipette. The above-described procedures were repeated to prepare the -2 to -5 dilutions.

Vero cell monolayers (2.5×10^5 cells per well in 6-well plates) were then infected with 200 μ l of each of the 10-fold serial (0 to -5) dilutions containing 50,000; 5,000, 500, 50, 5, or 0.5 dUY11-exposed virions. The virions were absorbed onto cell monolayers on ice for 1 hour, rocking and rotating every 10 min. Following adsorption, cells were washed twice with 2 mL of ice-cold SFM per wash and then overlaid with 3 mL of DMEM supplemented with 5% FBS and 2% w/v MC. Infected cells were then transferred to 37°C in 5% CO₂ and incubated until well-defined plaques were evident (typically 2 to 3 days). Cells were then fixed and stained with CV in methanol (1% w/v CV, 17% v/v methanol in H₂O) for 24 to 48 hours. Plates were washed in a 4L plastic beaker containing lukewarm water and dried overnight on a bench. The plates were scanned using a HP Scanjet 5370C, and plaques were counted and recorded.

2.9 Cellular localization

Vero cells (4×10^5 cells per well in 6-well plates) were seeded onto sterile 12 mm (thickness 0.13-0.17 mm; number 1) cover slips (catalog 12-545-82; Fisher Scientific, Pittsburgh, PA, USA) at 37°C in 5% CO₂. Media was removed and monolayers were overlaid with 500 μ l of DMEM supplemented with 5% FBS and 200 nM dUY11 at 37°C in 5% CO₂ for 30 min. Following treatment, cells were washed twice with 1 mL per wash of SFM pre-warmed to 37°C. Cell monolayers were then overlaid with 250 μ l of 250 nM PKH26-GL membrane dye (Sigma-

Aldrich) and further incubated at 37°C in 5% CO₂ for 5 min. Following membrane labeling, cells were washed twice with 1 mL of DMEM-5% FBS per wash. Cover slips were then mounted face down onto microscope slides with 1 drop (approximately 10 µl) of PBS and sealed with clear nail enamel. Live cells were visualized by fluorescence microscopy (Leica DM IRB) and documented at 1,000x magnifications using a digital camera (QIMAGING RETIGA 1300; Openlab software).

2.10 Analysis of progeny virions

2.10.1 Herpes simplex virus type-1 DNA replication and progeny infectivity

To analyze the levels of progeny infectivity, Vero cells monolayers (1 x 10⁵ cells per well in 12-well plates) were infected with 3 PFU per cell of HSV-1 strain KOS in 150 µl of SFM at 37°C in 5% CO₂ for 1 hour, rocking and rotating the plates every 10 min. Following adsorption, cells were washed twice with 2 mL of ice-cold SFM per wash. Cells were then treated for 23 hours with 1 mL of complete media supplemented with 0, 0.002, 0.007, 0.02, 0.07, 0.2, 0.7, 2, 7, 20 or 70 µM dUY11 (1X test concentration). Alternatively, infected cells were treated for only one hour, from 1 to 2 h after infection. For the latter procedure, the dUY11-containing medium was removed following the 1-hour treatment, cells were washed twice with 2 mL of ice-cold SFM per wash and then overlaid with drug-free complete media for 22 more hours at 37°C in 5% CO₂. Cell-free progeny virions from supernatants and cell-associated progeny virions were harvested separately at 24 hpi as described in **section 2.5.4**. Equal volumes (that

contained 200 infectious units in controls) were titrated by standard plaque assay, as described in **section 2.6**.

To analyze HSV-1 DNA replication or the release of progeny HSV-1 virions, ten 100 mm diameter tissue culture dishes of Vero cell monolayers (1.75×10^6 cells per dish) were infected at a MOI of 10 or 5 PFU per cell, respectively, in 1.5 mL of SFM at 37°C in 5% CO₂ for 1 hour, rocking and rotating the plates every 10 min. Following 1-hour adsorption, the infected cells were washed twice with 5 mL per wash of ice-cold PBS. Infected cells were then overlaid with 8 mL of DMEM supplemented with 5% FBS and dUY11. To analyze DNA replication, DMEM-5% FBS was also supplemented with 0 or 2 µM dUY11, or with 0 or 7 µM dUY11 for progeny release (5 dishes per treatment). The dishes containing infected and treated cells were then returned to 5% CO₂ at 37°C for 23 hours. At 24 hpi, one dish each of infected cell monolayers treated with 0, 2 or 7 µM dUY11 was harvested as described in **section 2.5.4** and titrated as described in **section 2.6**.

The levels of intracellular and released extracellular progeny virions were also measured at 24 hpi. Supernatants from the remaining 4 dishes of infected and treated cells were collected first and pooled into a 50-mL screw-cap conical tube. Cell debris was removed by centrifugation at 4,000 rpm in swinging bucket rotor A-4-62 in an Eppendorf 5810R centrifuge (Eppendorf Canada) at 4°C for 10 min. Supernatants were recovered using a sterile 10-mL disposable plastic pipette and transferred into a 50-mL screw-cap conical tube. Released progeny virions were then pelleted by centrifugation at 10,000 x g in the JA-14 rotor of a Beckman

Coulter J-series ultracentrifuge (Beckman Coulter Inc.) at 4°C for 2 hours. Supernatant was removed using a sterile 25-mL disposable plastic pipette. Virion pellets were resuspended in 200 µl of SFM per pellet, layered onto 12 mL of a 20% sucrose cushion and ultracentrifuged at 100,000 x g in swinging bucket rotor SW40 Ti in a Beckman Ultracentrifuge XL-90 (Beckman Canada) at 4°C for 1 hour. Sucrose was carefully decanted and virion pellets were resuspended in 120 µl of sodium chloride-Tris-EDTA buffer (STE; 0.1 M NaCl, 10 mM Tris-HCl, 1 mM EDTA) per pellet. Fifteen microliters were recovered to determine infectivity by standard titration (**section 2.6**) and the remaining sample was analyzed by Southern blot (**section 2.13**).

The infected-cell monolayers were meanwhile washed once with 5 mL of PBS at room temperature before adding 1.5 mL of trypsin-EDTA. Cell monolayers were placed at 37°C in 5% CO₂ until all cells were detached (approximately 5 min). Trypsin was inactivated by adding 4.5 mL of DMEM-5% FBS per dish. Cell suspensions were pooled into 50-mL screw-cap conical tubes and pelleted by centrifugation at 4,000 rpm in swinging bucket rotor A-4-62 in an Eppendorf 5810R centrifuge (Eppendorf Canada) for 10 min at 4°C. Supernatant was removed and cell pellets were resuspended in 7 mL of PBS each at room temperature. The resuspended cells were again pelleted by centrifugation at 4,000 rpm in swinging bucket rotor A-4-62 in an Eppendorf 5810R centrifuge (Eppendorf Canada) at 4°C for 10 min. Cell pellets were resuspended in 1X STE at a concentration of 2×10^7 cells per mL (450 µl) and split in halves in 2 mL

microcentrifuge tubes. Cells were lysed by adding 20% SDS to obtain a final concentration of 0.5% SDS and analyzed by Southern blot (**section 2.13**).

2.10.2 Progeny Sindbis virus infectivity

Vero cells monolayers (1×10^5 cells per well in 12-well plates) were infected with 3 PFU per cell of SIN in 150 μ l of SFM, as described in **section 2.5.3**. Following a 1-hour adsorption, cells were washed twice with 1 mL of ice-cold SFM per wash. Cells were then treated for 23 hours with 1 mL of complete media supplemented with 0, 0.002, 0.007, 0.02, 0.07, 0.2, 0.7, 2, 7, 20 or 70 μ M dUY11 (1X test concentration). Alternatively, infected cells were treated for only 1 hour, from 1 to 2 hours after infection. For the latter procedure, the drug-containing medium was removed following the 1-hour treatment of infected cells. The cells were washed twice with 1 mL of ice-cold SFM per wash and then overlaid with drug-free complete medium for 22 more hours. Progeny virions from the supernatants were then harvested at 24 hpi, as described in **section 2.5.4**. Equal volumes (that contained 200 infectious units in DMSO controls) were titrated by standard plaque assay, as described in **section 2.6**.

2.11 Virion integrity analysis

Aliquots of infectious HSV-1 virions (2×10^8 virions in 125 μ l of SFM) were pre-warmed to 37°C in a water bath for approximately 15 min. The pre-warmed inocula was then mixed with 125 μ l of 0 or 14 μ M dUY11 (2X final test concentration; 0 or 7 μ M dUY11, respectively) prepared from 1 mM dUY11

stock in pre-warmed SFM. Virus and dUY11 were then incubated together in a 37°C water bath for 10 min. Alternatively, 125 µl of SFM containing 2×10^8 infectious virions were pre-cooled on ice for 10 min and were then incubated with 10% IgePal CA-630 (final concentration, 1.5%; Sigma-Aldrich) for 30 min on ice to strip virion envelopes (Gupta and Rapp, 1977). Twenty microliter aliquots (each containing 1.6×10^7 drug-exposed virions) from each treatment (DMSO, dUY11 or IgePal CA-630) were then collected for analysis of virion infectivity by standard plaque assay (**section 2.6**).

The remaining HSV-1 virions (230 µl containing 1.84×10^8 treated virions) were layered onto 12 mL of a 20% sucrose cushion in Beckman 14-mL conical tubes and ultracentrifuged at 200,000 x g in swinging bucket rotor SW40 Ti in a Beckman Ultracentrifuge XL-90 (Beckman Canada) at 4°C for 3 hours. The cushion was then carefully decanted. Viral pellets were resuspended in 20 µl STE buffer (1 mM Tris-Cl [pH 8.0], 100 mM NaCl, 1 mM EDTA) and lysed by adding 0.5 µl of 20% SDS (final concentration, 0.5% SDS). Samples were then divided in two halves, to be analyzed by Western (**section 2.12**) or Southern (**section 2.13**) blots.

2.12 Western blot analyses

2.12.1 Virion and cell lysate preparations

HCV-infected cell lysates were prepared as described in **section 2.7.2**. HSV-1 virion protein lysates were prepared as described in **section 2.11**.

2.12.2 Protein separation

Twenty five micrograms of protein from HCV-infected cells, or one quarter of lysates from HSV-1 infected cells, were separated on a 10% SDS- PAGE. Briefly, the 10% separating gel (375 mM TRIS [pH 8.8], 10% Acrylamide/Bis (29:1), 0.1% ammonium persulfate (APS), 0.1% SDS) was prepared by catalysis polymerization with N,N,N,N-tetramethylethylenediamine (TEMED). The mixture was poured into a BioRad SDS-PAGE casting apparatus and left to polymerize at room temperature for 30 min. The stacking gel (125 mM TRIS [pH 6.8], 8% Acrylamide/Bis (29:1), 0.1% SDS, 0.1% APS) was mixed next. Polymerization was catalyzed with TEMED. The mix was then poured onto the stacking gel, and left to polymerize at room temperature for 25 min, with 15- or 10-well combs (1 mm thick; Bio-Rad Laboratories). The gel was then securely placed in the holding box and 1 L of SDS-PAGE running buffer (250 mM TRIS, 1.92 M glycine, 1% SDS) was added. Meanwhile, samples were resuspended in 4X SDS gel-loading buffer (200 mM Tris [pH 6.8], 8% SDS, 0.4% bromophenol blue, 40% glycerol, 400 mM DTT) and denatured in boiling water for 5 min. The samples were centrifuged at 5,000 rpm at room temperature for 5 sec and loaded into the wells of the SDS-PAGE gel. Ten microliters of Precision Plus Protein Standard (catalogue 161-0373; Bio-Rad Laboratories) were used as the protein mass marker. Gel electrophoresis was performed for 30 min at 40V, or until samples had run through the stacking gel, followed by 2 hours at 60V, or until the dye front reached the bottom edge of the gel. Gels were then removed from the glass plates and the resolving gel was cut off.

2.12.3 Protein transfer

Proteins were transferred from the SDS-PAGE gel to PVDF immuno-blot membranes (catalogue 162-0177; Bio-Rad Laboratories) using a semi-dry transfer apparatus (Bio-Rad Laboratories). Before blotting, membranes were activated by soaking for 1 min in approximately 100 mL of 100% methanol. The activated membranes were washed twice on a rocker at room temperature with approximately 100 mL of distilled-deionized water per wash, and equilibrated for 30 min in approximately 100 mL of anode buffer (1X Tris-CAPS, 15% methanol). The resolving gel containing the separated proteins (**section 2.12.2**) was meanwhile equilibrated for 30 min in approximately 100 mL of cathode buffer (1X Tris-CAPS, 0.1% SDS). Two thick chromatography papers (catalogue 05-714-4; Fisher Scientific) cut to the size of the SDS-PAGE gel were equilibrated at room temperature for 10 min in approximately 100 mL of anode or cathode buffer. The transfer sandwich was then assembled by stacking 2 anode-equilibrated filters, the membrane, the gel and two cathode-equilibrated filters. Transfer was performed at 55 mA for 2 hours.

2.12.4 Western blot

The membranes were incubated at room temperature with 10 mL of 1:1 PBS:Odyssey blocking buffer (LI-COR Biosciences, Lincoln, NE, USA) on a rotator. Blocked membranes were then further incubated for 2 hours at room temperature with 4 mL mouse monoclonal anti-hepatitis C virus NS3 helicase domain antibody (catalogue MAB8691; Chemicon (Millipore) International,

Temecula, CA, USA) diluted 1:2,000; rabbit monoclonal anti-gD or anti-gH (kind gifts from Dr. Gary H. Cohen, University of Pennsylvania) diluted 1:1,000; or rabbit polyclonal anti-HSV-1 (catalogue B0114; DakoCytomation Canada Inc., Mississauga, ON, CANADA) diluted 1:2,000 in 1:1 Odyssey blocking buffer-PBS. Membranes were then washed thrice at room temperature in 75 mL of PBS-Tween 0.1% per wash on a rocker for 5 min, followed by one wash in 75 mL of PBS. Rolled membranes were next transferred into 50-mL screw-cap conical tubes (with the protein side facing outward) and incubated at room temperature with 10 mL of goat anti-mouse or anti-rabbit secondary antibody labeled with IRDye 800 (Rockland Immunochemicals, Gilbertsville, PA, USA), diluted 1:20,000 in 1:1 Odyssey blocking buffer-PBS mixture. Membranes were then washed in the dark four times as described above, scanned and quantitated using an Odyssey Infrared Imaging System (LI-COR Biosciences, NE, USA). To detect actin, membranes were incubated with mouse monoclonal anti-actin (catalogue MAB1501R; Chemicon (Millipore) International) diluted 1:10,000, followed by goat anti-mouse secondary antibody labeled with IRDye 800, as described above.

2.13 Southern blot analyses

2.13.1 DNA purification

Viral DNA from drug-exposed virions, supernatants, nuclei of infected cells or sucrose-purified virions, was digested in STE buffer containing 5% SDS and 200 µg/mL proteinase K for 5 hours at 55°C. DNA was then extracted by the addition of an equal volume of phenol:chloroform:isoamyl alcohol (25:24:1). The phases

were separated at 14,000 rpm in a tabletop centrifuge at room temperature for 10 min. The upper phase was transferred to a new eppendorf and an equal volume of room temperature chloroform:isoamyl alcohol (24:1) was added. The phases were separated at 14,000 rpm in a tabletop centrifuge at room temperature for 10 min. The upper phases were transferred to new eppendorfs. DNA was precipitated overnight with 2.5 volumes of 100% ethanol at -20°C, and pelleted at 14,000 rpm in a fixed angled rotor FA45-30-11 in an Eppendorf 5810R centrifuge (Eppendorf Canada) for 20 min at 4°C. Supernatants were carefully decanted, without disturbing the DNA pellets. Pellets were rinsed with 1 mL of 70% ethanol per eppendorf, and centrifuged at 10,000 rpm in a tabletop centrifuge at room temperature for approximately 10 sec. Ethanol was carefully decanted, and the residual ethanol was evaporated by inverting the eppendorfs at room temperature for approximately 10 min. Viral pellets were resuspended in tris-ethylenediaminetetracetic acid (TE; 10 mM Tris-Cl [pH 7.5], 1 mM EDTA). Purified DNA was digested with 1 unit/μg of HindIII restriction enzyme (Invitrogen) in a volume of 50 μl or less of appropriate buffer.

2.13.2 DNA separation

DNA was resolved by electrophoresis in 0.7% agarose. To cast the gel, 0.7 g of UltraPure agarose (catalogue 15510-027; Invitrogen) were dissolved in 100 mL of Tris-acetate and EDTA (TAE) buffer (40 mM Tris-acetate, 1 mM EDTA) by heating in a microwave for 60 sec, interrupted every 20 sec to stir. After cooling to approximately 40°C, ethidium bromide (final concentration, 0.5 μg/mL) was

added and the melted solution was immediately poured into a casting tray containing an appropriate sized comb. After gelling for approximately 50 min, the comb was carefully removed and the gel was covered with TAE buffer. DNA was resuspended in 6X gel loading buffer (0.25% bromophenol blue, 15% Ficoll in water, 0.25% xylene cyanol) and centrifuged at 5,000 rpm in a tabletop centrifuge for 5 sec. Samples and marker (1 µg of Fermentas GeneRuler 1kb DNA ladder, catalogue SM0134; Fermentas Life Sciences, Burlington, ON, CANADA) were then loaded into the wells. Electrophoresis was performed at 100V for approximately 2 hours, or until the dye front had migrated to the front edge of the gel. The gel was photographed using Quantity One software (Bio-Rad Laboratories).

2.13.3 DNA transfer

Agarose gels were incubated at room temperature on a rocker with approximately 200 mL of acidic buffer (0.25M HCl) for 10 min, or until the dye front had turned yellow. Gels were rinsed with distilled deionized water and washed twice with approximately 200 mL of alkaline buffer (0.4N NaOH, 1M NaCl) for 15 min per wash on a rocker at room temperature. Gels were rinsed again with distilled deionized water, followed by washes with approximately 200 mL each of neutralization buffer (2M Tris-Cl [pH 7.4], 3M NaCl) per wash on a rocker at room temperature for 15 min. Gels were then washed in alkaline buffer for 30 min. Meanwhile, a BiodyneB Nylon membrane (catalogue 60207; Pall Corporation, Pensacola, FL, USA) was wet with distilled deionized water and

soaked in 10X saline sodium citrate (SSC; 150mM CH₃COONa.3H₂O [pH 5.2], 1.5M NaCl) for 15 min. Three thick chromatography papers (catalogue 05-714-4; Fisher Scientific) were cut to the size of the gel. A larger piece of chromatography paper was prepared as the wick, which was placed on an overturned gel box in a pyrex dish. One chromatography paper, the gel (with the open-well side face down), the membrane, and the other two chromatography papers were then placed on top of the wick. Air bubbles were rolled out using a disposable 10-mL plastic pipette. A stack of identical-sized paper towels was placed on top of the chromatography papers, onto which a weight was balanced. The pyrex dish was filled with 10X SSC, and plastic wrap was placed from the gel to the edge of the pyrex dish to prevent evaporation. The transfer proceeded overnight (usually 18 hours). The transfer stack was then dismantled and the membrane was immersed in 0.4N NaOH at room temperature for 1 minute, with the DNA-containing side of the membrane facing down. Membranes were washed with 500 mL of 0.2N Tris (30mM CH₃COONa.3H₂O [pH 5.2], 300mM NaCl, 200 mM Tris [pH 7.4]) for 5 min at room temperature. Membranes were either dried at room temperature overnight or in an air current for 2 hours.

2.13.4. Hybridization analyses

2.13.4.1 Random-primed DNA labeling

The HSV-1 probe used was the HSV-1 EcoRI JK fragment (Lacasse and Schang, 2010). DNA was radiolabeled with [α -³²P] deoxycytidine triphosphate (dCTP) according to the manufacturer's instructions (Amersham Biosciences). Briefly, 50

ng of probe was denatured at 100°C for 10 min and immediately transferred to ice for 5 min. The denatured DNA and 5 µl (50 µCi) of [α -³²P] dCTP were added to the random-prime reaction tube, thoroughly mixed, and incubated at 37°C in a water bath for 1 hour. Meanwhile, 20 µg of blocker DNA was prepared. Vero cell DNA isolated from uninfected Vero cells by proteinase K digestion and phenol-chloroform extraction (**section 2.13.1**) was denatured at 100°C for 10 min and immediately transferred to ice for 5 min. The labeling reaction was then denatured at 100°C for 10 min and immediately cooled on ice for 5 min before adding to Rapid Hybrid Buffer pre-warmed to 80°C and containing the blocker DNA.

2.13.4.2 Hybridization

Dried membranes were pre-hybridized with 12 mL of rapid hybrid buffer (Amersham Sciences) at 80°C for a minimum of 1 hour, and then hybridized with the ³²P-dCTP labeled JK HSV-1 fragment at 80°C for 3 hours. Membranes were washed twice at room temperature in approximately 200 mL of hybridization wash buffer (30mM CH₃COONa.3H₂O [pH 5.2], 300mM NaCl, 0.1 % SDS) for 15 min per wash. Washed membranes were exposed to Kodak PhosphorImager screens for 24 hours, scanned and quantitated using BioRad Molecular Imager FX (BIO-RAD, Mississauga, ON, CANADA).

2.14 Binding assays

2.14.1 Production of radiolabeled herpes simplex virus type-1 virions

Vero cell monolayers (2×10^6 cells per 100 mm diameter tissue culture dish) were mock- or HSV-1 infected with 5 PFU per cell in 1.5 mL of SFM in 5% CO₂ at 37°C for 1 hour, rocking and rotating the dishes every 10 min. Following adsorption, cells were washed twice with 5 mL of ice-cold SFM per wash, overlaid with 5 mL of DMEM-5% FBS and returned to 37°C in 5% CO₂. Three hours later, infected cells were methionine-starved for 2 hours by replacing the complete media with methionine-free DMEM (catalogue 21013-024; Gibco) supplemented with 5% FBS. At 5 hpi, the cells were washed twice with 6 mL of warmed PBS per wash and overlaid with 4 mL of methionine-free DMEM supplemented with 10% FBS and 42µCi/mL of ³⁵S-methionine (Amersham Sciences). The dishes were incubated at 37°C until 4+ CPE was determined (approximately 45 hours).

The supernatants containing infectious progeny ³⁵S-radiolabeled HSV-1 virions were then collected and pooled into 50-mL screw-cap conical tubes. The medium was clarified by centrifugation at 4,000 rpm in a swinging bucket rotor A-4-62 in an Eppendorf 5810R centrifuge (Eppendorf Canada) at 4°C for 30 min. Supernatant was recovered and virions were concentrated by centrifugation at 10,000 x g in a JA-14 rotor in a Beckman Coulter J-series ultracentrifuge (Beckman Coulter Inc.) at 4°C for 2 hours. The virion pellets were resuspended in 100 µl of SFM and stored at -80°C. Viral titers were assessed by standard plaque assays (**section 2.6**) using 1 µl of the stock (-3 to -8 dilutions). Radiolabeling

efficiency was determined by fixing 1 μl of the stock ^{35}S -radiolabeled HSV-1 virions or mock preparation in 100 μl of 100% ethanol. The 1:100 dilutions were then transferred into scintillation vials containing 5 mL of aqueous counting scintillant (NACS 104; Amersham Biosciences). Radioactivity was evaluated in a Beckman Coulter LS 500 Multi-Purpose Scintillation Counter (Beckman Coulter). Radiolabeled HSV-1 preparations yielded titers of approximately 2×10^7 PFU/mL and an average of 0.5 counts-per-minute (cpm) per μL (approximately 1.2 cpm per PFU).

2.14.2 Total binding assay

Twenty microliters containing 3×10^5 metabolically labeled HSV-1 virions (approximately 1.2 cpm per PFU; **section 2.14.1**) were pre-warmed to 37°C in a water bath, before adding to 14-mL snap-cap conical tubes pre-warmed to 37°C and containing no drug, 7 μM dUY11 or 100 $\mu\text{g}/\text{mL}$ heparin (final test concentrations) in a final volume of 200 μl . Virions and drug were mixed by gentle pipetting up and down 3 times using a P200 micropipette, then further incubated in a 37°C water bath for 5 min. Inocula were then immediately transferred to ice at 4°C and diluted 1:100 (1.5 μl sample and 148.5 μl of ice-cold SFM supplemented with no drug, 7 μM dUY11, or 100 $\mu\text{g}/\text{mL}$ heparin). Vero cell monolayers (5×10^4 cells per well in 24-well plates) were pre-cooled by replacing the complete media with 500 μl of ice-cold SFM and then setting both on ice for 15 min.

One hundred and fifty microliters of undiluted (1:1) or 1:100 diluted aliquots of the pretreated and ³⁵S-Met radiolabeled HSV-1 virions (approximately 2.5 x 10⁵ or 2.5 x 10³ cpm for 1:1 or 1:100 dilutions, respectively) were then adsorbed onto Vero cell monolayers (MOI, 5 or 0.05 PFU per cell for 1:1 or 1:100 inocula) on ice for 1 hour, rocking and rotating every 10 min. Supernatants from mock- or HSV-1 infected cells were then collected and transferred into scintillation vials containing 200 µl lysis buffer (10mM Tris [pH 7.6], 150mM NaCl, 1% SDS). Cells were washed three times with 200 µl per wash of ice-cold serum-free DMEM supplemented with no drug, 7 µM dUY11, or 100 µg/mL heparin. Cells were recovered in 200 µL of lysis buffer by scraping with sterile disposable cell lifters and then transferring to liquid scintillation vials. Five milliliters of liquid scintillant fluid were added to each vial, and radioactivity was evaluated by Beta-scintillation counting. Total virion binding was calculated using the following formula:

$$\% \text{ binding} = \frac{(\text{cpm bound})}{(\text{total recovered cpm})} \times 100\%$$

Total recovered counts include the radioactivity recovered from unbound inocula, all washes, and lysed cells. The percent binding was adjusted by background apparent binding of inocula from mock-infected cells.

To evaluate the infectivity of treated virions, non-radiolabeled HSV-1 virions were subjected in parallel to similar procedures as the radiolabeled HSV-1. Briefly, 50 µl aliquots of SFM containing 3.25 x 10⁵ PFU of infectious non-radiolabeled HSV-1 virions were pre-warmed to 37°C in a water bath. The

aliquots were then mixed in a final volume of 200 μ l with pre-warmed SFM containing no drug, 7 μ M dUY11 or 100 μ g/mL heparin (final test concentrations). The virions were then further incubated in a 37°C water bath for 5 min. The samples were then cooled on ice and diluted 1:20 (10 μ l sample and 190 μ l of ice-cold SFM supplemented with no drug, 7 μ M dUY11, or 100 μ g/mL heparin) or 1:100 (2 μ l sample and 198 μ l of ice-cold SFM supplemented with no drug, 7 μ M dUY11, or 100 μ g/mL heparin). Vero cell monolayers (2 x 10⁵ cells per well in 12-well plates) were pre-cooled by replacing complete media with 1 mL of ice-cold SFM and then setting both on ice for 15 min.

Two hundred microliters of undiluted, 1:20, or 1:100 diluted aliquots of the non-radiolabeled pretreated virions were then adsorbed onto the Vero cell monolayers on ice for 1 hour, rocking and rotating the plates every 10 min. Cells were then washed twice with 1 mL of ice-cold PBS per wash and overlaid with 2 mL of drug-free DMEM supplemented with 5% FBS and 2% MC. Infected cells were incubated at 37°C in 5% CO₂ until well-defined plaques were clearly visible (2 to 3 dpi). Cells were then fixed and stained with CV in methanol (1% w/v CV, 17% v/v methanol in H₂O) for 24 to 48 hours. Excess MC and CV were removed by washing the plates in a 4L plastic beaker containing lukewarm water, and dried overnight on a bench. Plates were then scanned using a HP Scanjet 5370C.

2.14.3 High-affinity binding assay

To assess high-affinity binding, 8 μ l aliquots containing 3.3 x 10⁵ ³⁵S-Met radiolabeled HSV-1 virions (approximately 1.2 cpm per PFU; **section 2.14.1**)

were pre-warmed to 37°C in a water bath before adding to 15-mL snap-cap conical tubes pre-warmed to 37°C and containing 0 or 7 µM dUY11 (final test concentration) to a final volume of 125 µl. Virions and drug were mixed by gentle pipetting up and down three times using a P200 micropipette and then further incubated in a 37°C water bath for 5 min. Inocula were cooled on ice and diluted 1:10 (15 µl sample and 135 µl of ice-cold SFM supplemented with 7 µM dUY11 or DMSO). Vero cell monolayers (0.5×10^4 cells per well in 24-well plates) were pre-cooled by replacing complete media with 500 µl of ice-cold SFM and then setting both on ice for 15 min. Pre-cooled Vero cell monolayers were then mock infected or infected with 150 µl of the so- pretreated ³⁵S-Met radiolabeled virions (1:10) on ice at 4°C. After 15 min, one set of infected cells was washed twice with 200 µl of SFM per wash and lysed to assess total binding, as described in **section 2.14.2**. All other infected cells were washed twice with 200 µl of ice-cold SFM per wash. Inocula and washes were recovered in scintillation vials containing 200 µl of lysis buffer (10mM Tris [pH 7.6], 150mM NaCl, 1% SDS). Afterward, cells were washed with SFM supplemented with 0, 30, 100, 300 or 1,000 µg/mL heparin for 1 hour, rocking and rotating the plates every 10 min. Cells were washed twice with 200 µl per wash of ice-cold SFM supplemented with 0, 30, 100, 300 or 1,000 µg/mL heparin. Each wash was collected and transferred into scintillation vials containing 200 µl of lysis buffer. The cells were then recovered in 200 µL of lysis buffer by scraping with sterile disposable cell lifters and transferred to liquid scintillation vials. Five milliliters of liquid scintillant fluid were added to each vial, and radioactivity was evaluated by Beta-scintillation

counting. 100% binding was defined as cell-bound cpm following all washes after the 15 min adsorption. The percentage of high-affinity virion binding was calculated using the following formula:

$$\% \text{ high-affinity binding} = \frac{\text{(cell-bound cpm following heparin washes)}}{\text{(total recoverable cpm following adsorption)}} \times 100\%$$

To evaluate the infectivity of treated virions, non-radiolabeled HSV-1 virions were subjected in parallel to the similar procedures as radiolabeled HSV-1. Briefly, 50 μl aliquots of SFM containing 3.25×10^5 PFU of infectious non-radiolabeled HSV-1 virions were pre-warmed to 37°C in a water bath. The aliquots were then mixed in a final volume of 250 μl with pre-warmed SFM containing no drug, 7 μM dUY11 or 100 $\mu\text{g}/\text{mL}$ heparin (final test concentrations). The samples were then further incubated at 37°C in a water bath for 5 min, and then cooled on ice. Cooled samples were then diluted 1:10 (20 μl of sample and 180 μl of ice-cold SFM supplemented with 0 or 7 μM dUY11 in DMSO) or 1:100 (2 μl sample and 198 μl of ice-cold SFM supplemented with 7 μM dUY11 or DMSO). Vero cell monolayers (2×10^5 cells per well in 12-well plates) were pre-cooled by replacing complete media with 1 mL of ice-cold SFM and then setting both on ice for 15 min.

Two hundred microliters of undiluted, 1:10, or 1:100 diluted aliquots of non-radiolabeled pretreated HSV-1 virions were then adsorbed onto the pre-cooled Vero cell monolayers at 4°C for 15 min. Cells were washed twice with 1 mL of ice-cold SFM per wash. One set of infected cells was then overlaid with 2 mL of drug-free DMEM supplemented with 5% FBS and 2% MC. All other

infected cells were washed with 1 mL of SFM supplemented with 0, 30, 100, 300 or 1,000 µg/mL heparin for 1 hour, rocking and rotating the plates every 10 min. Cells were then washed twice with 1 mL per wash of ice-cold SFM supplemented with 0, 30, 100, 300 or 1,000 µg/mL heparin and overlaid with DMEM supplemented with 5% FBS and 2% (w/v) MC. Infected cells were incubated at 37°C in 5% CO₂ until well-defined plaques were clearly visible (2 to 3 days). The cells were then fixed and stained with CV in methanol (1% w/v CV, 17% v/v methanol in H₂O) for 24 to 48 hours. Excess MC and CV were removed by washing the plates in a 4L plastic beaker containing lukewarm water, and dried overnight on a bench. The plates were then scanned using a HP Scanjet 5370C. Plaques were counted and recorded.

2.15 Herpes simplex virus type-1 entry assay

2.15.1 UV inactivation of herpes simplex virus type-1

Two milliliters of stock HSV-1 strain KOS in SFM were pelleted by centrifugation at 10,000 x g in a JA-14 rotor in a Beckman Coulter J-series ultracentrifuge (Beckman Coulter Inc) at 4°C for 2 hours. The supernatant was then removed using a sterile 5-mL disposable plastic pipette, and the virion pellet was resuspended in 2 mL of PBS. Virus was dispensed in 100 µl aliquots in 10 mm diameter tissue culture dishes and subjected to UV light (3,000 mJ; UV Stratalinker 2400; Stratagene) from 0 to 5 min at 30 sec intervals. Original and UV-inactivated virus suspensions were titrated by standard plaque assays (**section 2.6**). Only viral stocks inactivated by 4 orders of magnitude but which still fully

induced RFP expression in Vero clone 57 cells were used (Diwan, Lacasse, and Schang, 2004).

2.15.2 VP16 entry assay

Ten microliter aliquots of UV-inactivated HSV-1 KOS (each containing 1.5×10^6 PFU) were pre-warmed to 37°C in a water bath for 10 min. Each aliquot was then mixed with 10 μl of pre-warmed SFM supplemented with 2X final test concentration of dUY11 (final test concentrations; 0, 0.05, 0.20, 0.65, 2 μM dUY11), and further incubated at 37°C for 5 min. Treatment was terminated by addition of 980 μl ice-cold SFM and immediately placing the samples on ice. One hundred and fifty microliters of each sample were used to infect Vero clone 57 cell monolayers (3.5×10^5 clone 57 cells per well; MOI, 0.6 PFU per cell) in 6-well plates at 37°C in 5% CO_2 for 1 hour, rocking and rotating the plates every 10 min. Inocula were then removed, cells were washed twice with 2 mL of ice-cold SFM per wash, overlaid with complete medium and returned to 5% CO_2 at 37°C . RFP expression was evaluated 24 hours after infection using a fluorescence microscope with an UV light source (Leica DM IRB) and documented using a digital camera (QIMAGING RETIGA 1300). Pictures were taken at a magnification of 200x (excitation/emission = 620/700 nm) with a 3 second exposure time for fluorescent images, or 10 second exposure time for visible images.

2.16 Differential scanning calorimetry

Differential scanning calorimetry was performed by Drs. Richard and Rachel Epand (McMaster University, Hamilton, ON, CANADA). Solutions of RAFIs were made in chloroform:methanol (2:1) and concentrations were determined by absorbance at 467 nm in methanol:water (1:1). A stock solution of dielaidoylphosphatidylethanolamine (DEPE; Avanti Polar Lipids, Alabaster, AL, USA) was prepared in chloroform:methanol (2:1). Aliquots containing 5 mg DEPE were mixed in glass tubes with appropriate amounts of test compound solutions to prepare the mole fractions (0, 0.0021, 0.0048, 0.0086, 0.0129, 0.0172, or 0.0216 mole fraction dUY11; 0, 0.0092, 0.0271, 0.0445, 0.0851 or 0.1500 mole fraction dUY2; or 0, 0.0037, 0.0092, 0.0271, 0.0444, 0.0867 or 0.1500 mole fractions dUY4). The samples were then dried under nitrogen to make thin films on the walls of the glass tubes and then placed in a vacuum desiccator for 3 hours. Dried films were hydrated with 0.8 mL of 20mM PIPES, 0.14M NaCl, 1mM EDTA [pH 7.4] by extensive vortexing, degassed and then placed in the calorimeter cell. Samples were loaded into a high-sensitivity scanning calorimeter and excess heat capacity measured at a scan rate of 1° per minute, with buffer in the reference cells. Buffer vs. buffer scans were subtracted from all sample scans. The results were plotted with the program ORIGIN 7.0 and analyzed with the curve fitting program DA-2 supplied by Microcal Inc. (Northampton, MA, USA).

2.17 Drug-selective pressure

Selection for dUY11 resistance was conducted by Vanessa del Fabbro under my direct supervision.

2.17.1 Plaque purification

U2OS cells, which are highly susceptible to syncytia formation by HSV-1 infection, were used to plaque purify low-passage (p10) wild-type HSV-1 KOS strain. U2OS cell monolayers (1.75×10^6 cells per 100 mm diameter tissue culture dish) were infected with HSV-1 (MOI, 0.004 PFU per cell) at 37°C in 5% CO₂ for 1 hour, rocking and rotating the dishes every 10 min. Following 1-hour adsorption, inocula were removed and the cells were washed twice with 5 mL of ice-cold PBS per wash. Each dish of infected cells was overlaid with 10 mL DMEM supplemented with 5% FBS and 1% MC. Four clear plaques were identified and picked.

Isolated plaques were picked with a P20 micropipette, using the tip to scrape the cells in and around the plaque. Virus from each plaque was resuspended in 1.5 mL of SFM and used as inocula for a second round of plaque purification in U2OS cells, performed as described above.

Following the second plaque-purification round, six non-syncytia forming plaques were picked and resuspended in 200 µl of SFM each. Each was then used as inocula to infect Vero cell monolayers (1.5×10^5 cells per well in a 6-well plate) at 37°C in 5% CO₂ for 1 hour, rocking and rotating the plate every 10 min. Following a 1-hour adsorption, the cells were washed twice with 2 mL of ice-cold

PBS per wash, overlaid with 3 mL of DMEM-5% FBS and returned to 37°C in 5% CO₂.

Infected cells were harvested at 4+ CPE by scraping with sterile disposable cell lifters. The cells and supernatants were transferred into 14-mL snap-cap conical tubes (1 well per tube). Medium was clarified by centrifugation at 4,000 rpm in swinging bucket rotor A-4-62 in an Eppendorf 5810R centrifuge (Eppendorf Canada) at 4°C for 30 min. Supernatants were collected and stored at -80°C. Supernatants were titrated as described in **section 2.6**, and used as seed to grow stocks of plaque-purified HSV-1 as described in **section 2.5.1.1**.

2.17.2 Standard serial passage selection

2.17.2.1 Infections and harvest

Plaque-purified (p12) HSV-1 KOS was passaged in medium containing no drug or increasing concentrations of dUY11 or PAA. Vero cell monolayers (2×10^6 cells) were infected with HSV-1 strain KOS at a MOI of 0.1 PFU per cell, unless otherwise indicated, for 1 hour, rocking and rotating the dishes every 10 min. Inocula were then removed and cells were washed twice with 5 mL of ice-cold SFM per wash. Infected cells were overlaid with DMEM supplemented with 5% FBS with no drug or with increasing concentrations of PAA or dUY11, as indicated for each passage. Infected cells were harvested when generalized (4+) CPE was detected.

Cells and supernatants were harvested by scraping monolayers with sterile disposable plastic lifters. Cells and supernatants were collected into 50-mL screw-

cap conical tubes. Medium was clarified by centrifugation at 4,000 rpm in swinging bucket rotor A-4-62 in an Eppendorf 5810R centrifuge (Eppendorf Canada) at 4°C for 30 min. Virus was harvested as described in **section 2.5.4**. Virus from each passage was used as the inocula for the subsequent passage.

2.17.2.2 Percent resistance analyses

To determine the percent PAA-resistance for each passage, Vero cell monolayers (1×10^5 cells per well in 6-well plates) were infected with 200 HSV-1 virions from each passage at 37°C in 5% CO₂ for 1 hour, rocking and rotating the plates every 10 min. Following 1-hour adsorption, the infected cells were washed twice with 2 mL of ice-cold SFM per wash and overlaid with MC supplemented with 5% FBS and 0 or 100 µg/mL PAA. Forty-eight hours post-infection, cells were fixed and stained overnight with CV in methanol (1% w/v CV, 17% v/v methanol in H₂O). Plates were washed in a 4L plastic beaker containing lukewarm water and dried overnight on a bench. Plaques were then counted and recorded.

Percentage of resistant virus was calculated using the following formula:

$$\% \text{ resistance to PAA} = \frac{(\text{plaques in the presence of PAA})}{(\text{plaques in the absence of drug})} \times 100$$

To determine the percent resistance under dUY11-selective pressure, 200 virions (in a volume of 100 µl) from passages 1, 2, 3 or 11 were pre-warmed to 37°C in a water bath and mixed with 100 µl of SFM with no drug or with 4 µM dUY11 (final test concentration, 2 µM) in a water bath at 37°C for 5 min. Vero cell monolayers (2×10^5 cells per well in 6-well plates) were infected with the so-

exposed virions at 37°C in 5% CO₂ for 1 hour, rocking and rotating the plates every 10 min. Following 1-hour adsorption, the cells were washed twice with 2 mL of ice-cold SFM per wash and overlaid with DMEM supplemented with 5% FBS and 1% MC. Forty eight hours post infection, cells were fixed and stained overnight with CV in methanol (1% w/v CV, 17% v/v methanol in H₂O). Plates were washed in a 4L plastic beaker containing lukewarm water and dried overnight on a bench. Plaques were then counted and recorded. Percentage of dUY11-resistant virus was calculated using the following formula:

$$\% \text{ dUY11-resistance} = \frac{(\# \text{ plaques after dUY11 exposure})}{(\# \text{ plaques after DMSO-exposure})} \times 100$$

2.18 *In vivo* studies

All animal experiments were approved by the Health Sciences Animal Care and Use Committee (Office of Research Certifications and Approvals, University of Alberta, Edmonton, AB, CANADA). Animal handling certification was obtained by the University Animal Policy and Welfare Committee (The Care and Use of Animals in Research, Teaching and Testing; certified March 29, 2006).

2.18.1 Oestrus synchronization

Female BALB/C mice (17-20 g) were synchronized 6 days before HSV-2 infection by sub-cutaneous injection of 3 mg/kg of sterile medroxyprogesterone acetate (“Depo-Provera”). Animals were returned to their cages and housed in containment level 2. All animals were monitored daily to assess health and to check feed and water consumption.

2.18.2 Animal infections

2.18.2.1 Anesthesia

Six days following synchronization, four groups of 5 mice each were randomized. Restrained mice were then anesthetized by intraperitoneal injection of 150 mg/kg Ketamine and 10 mg/kg of Xylazine. Anesthetic plane was determined by monitoring respiration and pedal reflex (toe pinch). Anesthetized animals were then transferred to Biohazard tissue culture hoods.

2.18.2.2 Herpes simplex virus type-2 infection

Animal studies were performed using either 1- or 3- lethal doses to 50% of animals (LD_{50} ; 1,000 or 3,000 PFU per animal, respectively). One hundred and fifty microliter aliquots containing 1×10^4 infectious HSV-2 virions (strain 186), or 125 μ l aliquots containing 2.5×10^4 infectious HSV-2 virions (strain 186) ($1LD_{50}$ or $3LD_{50}$, respectively) were pre-warmed in a water bath to 37°C for 15 min. Inocula were then added to 14-mL snap-cap conical tubes containing either 150 μ l ($1LD_{50}$) or 125 μ l ($3LD_{50}$) of 140 μ M dUY11 (final test concentration, 70 μ M dUY11) or DMSO. Virus and compound were mixed by gentle pipetting up and down, and then further incubated at 37°C in a water bath for 5 min. One group of 5 anesthetized animals (**section 2.18.2.1**) was infected intravaginally with 30 μ l of dUY11-exposed HSV-2, using a sterile P200 micropipette tip. The other group of 5 anesthetized animals was infected intravaginally with 30 μ l of DMSO-exposed HSV-2, using a sterile P200 micropipette tip. Remaining inocula was (back-)titrated, as described in **section 2.6**, following animal infection.

2.18.2.3 Animal monitoring

Animals were photographed and monitored for weight, shedding of infectious virus (by standard titration of vaginal lavages) and clinical signs on days 1 through 5, 6.5, 8, 9 and 11 in studies using 1LD₅₀, or on days 2 through 4, 5.5, 7, 8, 10 and 14 in studies using 3LD₅₀. Food and water consumption was monitored daily for both studies.

2.18.2.3.1 Clinical monitoring of infection

Clinical signs were scored using a five-point scale (**Table 2.1**) modified from that established by Gillgrass et al. (2003); 0, no sign of infection; 0+, mild redness and swelling of external vagina; 1, mild redness and swelling of external vagina with localized hair loss; 2, moderate redness and swelling of external genitalia; 2+, moderate redness and swelling of external genitalia, with hair loss; 3, severe redness and inflammation of external vagina, and hair loss in genital area; 4, localized genital ulceration, with severe inflammation, redness and hair loss in genital area and surrounding tissue; 5, severe genital ulceration extending to surrounding tissue, or neurological symptoms, such as hind-limb paralysis. Mice were euthanized by CO₂ when they developed clinical signs of terminal illness (disseminated infection, ulcerated secondary infection, hind-limb paralysis, or more than 10% of body weight loss).

2.18.2.3.2 Virus shedding

To collect vaginal lavages, 50 µl of PBS was gently introduced into the vagina using a P200 micropipette. The PBS was recovered without removal of the tip from the vagina. Each lavage was vortexed to disrupt the mucus plugs and then serially diluted 1:10 in SFM. Six microliters of the lavage was transferred to a 2 mL microcentrifuge tube containing 54 µl of ice-cold SFM (-1 dilution). The -1 dilution was mixed by vortexing, and 6 µl was then transferred to an eppendorf containing 54 µl of ice-cold SFM (-2 dilution). The above-described procedure was followed to prepare -3, -4, -5 and -6 dilutions.

Vero cell monolayers (0.6×10^5 cells per well in 24-well plates) were then infected with 50 µl of each lavage dilution at 37°C in 5% CO₂ for 1 hour, rocking and rotating the plates every 10 min. Following 1-hour adsorption, cells monolayers were overlaid with 1 mL of DMEM supplemented with 5% FBS, 1% MC (w/v) and 10 units of penicillin G sodium, 100 µg of streptomycin sulfate and 0.25 µg of amphotericin B per mL (Fungizone, catalogue 15240; Gibco). Infected cells were returned to 37°C in 5% CO₂. Cells were fixed and stained for 24 to 48 hours with CV in methanol (1% w/v CV, 17% v/v methanol in H₂O) when well-defined plaques were clearly visible (typically, 1 to 2 days after infection). Plates were washed in a 4L plastic beaker containing lukewarm water and dried overnight on a bench. Plaques were then counted and recorded.

2.19 Statistical analyses

Dose response curves were graphed using GraphPad Prism software (version 5.0b for Macintosh). The graph curves are the mean \pm the standard deviation, unless otherwise indicated. Prism software was used to perform all the curve fits (unconstrained three parameter nonlinear regression, unless otherwise indicated), and to calculate the concentrations that inhibit infectivity by 50% (IC₅₀), by 95% (IC₉₅), or by 99% (IC₉₉), the 95% confidence intervals and the P values (determined by performing an unpaired t test or one-way ANOVA).

2.20 References

- Andronova, V. L., Skorobogaty, M. V., Manasova, E. V., Berlin Iu, A., Korshun, V. A., and Galegov, G. A. (2003). [Antiviral activity of some 5-arylethynyl 2'-deoxyuridine derivatives]. *Bioorg Khim* **29**(3), 290-5.
- Cello, J., Paul, A. V., and Wimmer, E. (2002). Chemical synthesis of poliovirus cDNA: generation of infectious virus in the absence of natural template. *Science* **297**(5583), 1016-8.
- Diwan, P., Lacasse, J. J., and Schang, L. M. (2004). Roscovitine inhibits activation of promoters in herpes simplex virus type 1 genomes independently of promoter-specific factors. *J Virol* **78**(17), 9352-65.
- Gillgrass, A. E., Ashkar, A. A., Rosenthal, K. L., and Kaushic, C. (2003). Prolonged exposure to progesterone prevents induction of protective mucosal responses following intravaginal immunization with attenuated herpes simplex virus type 2. *Journal of Virology* **77**(18), 9845-9851.
- Gupta, P., and Rapp, F. (1977). Identification of Virion Polypeptides in Hamster Cells Transformed by Herpes-Simplex Virus Type-1. *Proceedings of the National Academy of Sciences of the United States of America* **74**(1), 372-374.
- Lacasse, J. J., and Schang, L. M. (2010). During lytic infections, herpes simplex virus type 1 DNA is in complexes with the properties of unstable nucleosomes. *J Virol* **84**(4), 1920-33.
- Skorobogaty, M. V., Ustinov, A. V., Stepanova, I. A., Pchelintseva, A. A., Petrunina, A. L., Andronova, V. L., Galegov, G. A., Malakhov, A. D., and Korshun, V. A. (2006). 5-Arylethynyl-2'-deoxyuridines, compounds active against HSV-1. *Org Biomol Chem* **4**(6), 1091-6.
- St Vincent, M. R., Colpitts, C. C., Ustinov, A. V., Muqadas, M., Joyce, M. A., Barsby, N. L., Epand, R. F., Epand, R. M., Khramyshev, S. A., Valueva, O. A., Korshun, V. A., Tyrrell, D. L. J., and Schang, L. M. (2010). Rigid amphipathic fusion inhibitors, small molecule antiviral compounds against enveloped viruses. *Proceedings of the National Academy of Sciences of the United States of America* **107**(40), 17339-17344.

Score	Clinical signs
0	no sign of infection
0+	mild redness and swelling of the external vagina
1	mild redness and swelling of the external vagina; localized hair loss
2	moderate redness and swelling of the external genitalia
2+	moderate redness and swelling of the external genitalia; localized hair loss
3	severe redness and inflammation of the external genitalia; hair loss in the genital area
4	severe redness, inflammation and hair loss in the genital area and surrounding tissue; localized genital ulcerations
5	severe genital ulcerations extending to surrounding tissue, ulcerated secondary infection; neurological symptoms

Table 2.1 Clinical scoring of vaginal HSV-2 infection. Table summarizing 5-point scoring scale of clinical signs in mice infected intravaginally with HSV-2 strain 186. This 5-point scale was adapted from that established by Gillgrass et al. (2003).

CHAPTER 3: THE CHARACTERIZATION OF THE ANTIVIRAL ACTIVITIES OF RIGID AMPHIPATHIC FUSION INHIBITORS

A version of this chapter has been published. (St.Vincent, MR et al., Proceedings of the National Academy of Sciences of the USA 107:17339-17344)

3.1 Introduction

Although virion entry is dependent on (glyco)proteins and lipids, all five current entry inhibitors target proteins exclusively (**Table 1.1**). Targeting entry proteins suffers important limitations. Among the major ones, this strategy results in the prompt selection for resistance, has a very limited number of drugable targets and each drug is specific for only one virus or even a virus variant. One such example is the HIV entry inhibitor maraviroc. Maraviroc binds the CCR5 co-receptor allosterically, inducing conformational changes that prevent HIV gp120 binding to CCR5 (Dorr et al., 2005). Maraviroc is thus specific for only HIV variants that engage CCR5 as co-receptor, being inactive against CXCR4 using variants (Westby et al., 2007). Despite targeting interactions with a cellular protein, moreover, several pathways for selection of resistance to maraviroc have been characterized, such as the selection for variants that can utilize maraviroc bound CCR5 for entry (Westby et al., 2007), or for CXCR4 tropic HIV (Hoffmann, 2007; Scarlatti et al., 1997). Alternate antiviral strategies to overcome these limitations are needed.

The lipids involved in viral fusion may present a novel antiviral strategy for entry inhibitors (Teissier, Penin, and Pecheur, 2011). Virions must form several energetically demanding lipid intermediates to fuse to cell membranes (Basanez, 2002; Burger, 2000). The outer leaflet of virion envelopes must form a negative curvature first, to form the hemifusion stalk. The formation of such negative curvature requires major reorganizations of envelope lipids and can use only the limited energy provided by glycoprotein attachment and rearrangements (Basanez, 2002).

Membrane curvature, including that of virion envelopes, is in part modulated by the lipids in the fusing membranes (Teissier and Pecheur, 2007). The lipid composition of envelopes thus has important consequences for fusion. For example, lipids with hydrophilic heads of smaller cross-section than their hydrophobic tails promote negative curvature, and consequently, the formation of the hemifusion stalk (Stiasny and Heinz, 2004). In contrast, amphipathic lysophospholipids with hydrophilic heads of larger cross-section than their hydrophobic tails (inverted-cone shape), promote positive curvature and thus disfavor the formation of the hemifusion stalk (Yeagle et al., 1994). Consequently, such lipids with an inverted-cone shape inhibit fusion. Naturally occurring lysophospholipids, however, are not pharmacologically useful. They are too rapidly metabolized, and are cytotoxic detergents.

Synthetic compounds that mimic natural lipids could be designed to target bilayers. Small molecules of appropriate molecular shape and amphipathicity may interfere with envelope fusion by increasing the energy barrier beyond that which

can be provided by glycoprotein attachment, binding and rearrangements. Such compounds could potentially have broad antiviral activities, as the basic principles of envelope fusion are conserved among otherwise unrelated enveloped viruses.

Nucleoside derivatives are well-characterized as antiviral scaffolds. They are hydrophilic, and can be readily derivatized to hydrophobic moieties to produce amphipathic molecules. The synthesis of a particularly suitable family of compounds was already described (Korshun et al., 1998; Korshun et al., 1997; Malakhov et al., 2000; Skorobogaty et al., 2006a). A family of deoxynucleosides was derivatized with polyaryl substituents to develop fluorescent probes to label DNA. Some of these compounds were then described to have anti-herpetic activities through unknown mechanisms (Andronova et al., 2003; Skorobogaty et al., 2006b).

In this chapter, I report the discovery and characterization of the viral fusion inhibitory activities of these rigid amphipathic nucleoside derivatives. They target the virion envelope to inhibit the infectivity of herpes simplex virus type-1 (HSV-1). They are not cytotoxic, and do not destabilize the association between virion proteins and envelopes. Moreover, they inhibit phase transitions in model bilayer systems that require the formation of negative curvatures.

3.2 Results

3.2.1 Structure activity relationship studies

My hypothesis is that small molecules of appropriate molecular shape can be designed to inhibit the formation of the negative curvature required for the hemifusion stalk. I identified a family of deoxyuridine analogues that served as a particularly fitting scaffold, as they could be derivatized with hydrophobic substituents to produce amphipathic molecules with a hydrophilic moiety of larger cross-section than their hydrophobic region. In collaboration with a group of chemists under the direction of Dr. Alexey Ustinov at the Shemyakin-Ovchinnikov Institute of Bioorganic Chemistry (Moscow, Russia), we first performed structure activity relationship (SAR) studies to identify the characteristics of such derivatives that are important for their antiviral activities.

All compounds were synthesized at the Shemyakin-Ovchinnikov Institute of Bioorganic Chemistry under the supervision of Dr. Ustinov. I then tested their activities on the infectivity of HSV-1, a most useful model for antiviral drug discovery (Schang, 2006). Under the proposed model, the nucleoside derivative would interact with the lipids of the envelope bilayer. Their hydrophobic moieties would interact with acyl chains in the core of the bilayer, and their hydrophilic moieties would interact with polar headgroups of the phospholipids. I thus tested the effects of amphipathicity, rigidity, planarity and the relative cross-section sizes between the hydrophobic and hydrophilic regions of the compounds.

The hydrophilic regions of the tested compounds were 2'-deoxyuridine, arabinouridine, didexoxyuridine, 5'-*O*-pivaloyl-2',3'-dideoxyuridine or 3',5'-*O*-

(tetraisopropylidisiloxane-1,3-diyl)-2'-deoxyuridine (**Figure 3.1I**). The hydrophobic regions were aryl moieties joined to position 5 of the bases by either a non-polar rigid ethynyl or a polar flexible propargyloxymethyl linker (**Figure 3.1II-VI**).

3.2.1.1 Effects of different hydrophilic heads

I first applied SAR studies to test the activities of chemically distinct compounds of similar molecular shapes (**Figure 3.1II**). Each tested compound had the same perylene hydrophobic group, but the hydrophilic moieties were differentially derivatized. An ethynylpyrelyne was joined to position 5 of 2'-deoxyuridine (R , **Figure 3.1I**) to produce compound **dUY11**, of arabinouridine (R_a , **Figure 3.1I**) to produce **aUY11**, or of 2',3'-dideoxyuridine (R_b , **Figure 3.1I**) to produce **ddUY11**. Ethynylpyrelyne was joined to position 5 of 5'-*O*-pivaloyl-2',3'-dideoxyuridine (R_c , **Figure 3.1I**) to produce **Pv-ddY11**. Lastly, ethynylpyrelyne was linked to position 5 of 3',5'-*O*-(tetraisopropylidisiloxane-1,3-diyl)-2'-deoxyuridine (R_d , **Figure 3.1I**) to produce **Mk-dY11**. **dUY11**, **aUY11** and **ddUY11** have near-identical molecular shape (**Figure 3.1II**). **Pv-ddY11** and **Mk-dY11** have bulkier functional groups at position 5, and consequently have larger hydrophilic regions (**Figure 3.1II**). Moreover, **Mk-dY11** has a hydrophilic moiety rotated by 90° relative to the hydrophobic moiety, when compared to **dUY11**, **aUY11**, **ddUY11** and **Pv-ddY11**. All five compounds contained a hydrophilic moiety of larger cross-section than their hydrophobic one.

Infectious HSV-1 virions (200 plaque-forming units- PFU) were pre-exposed to media containing increasing concentration of test compound for 5 minutes at 37°C. The so-exposed virions were then adsorbed onto Vero cells for 1 hour. Following adsorption, the cells were washed and overlaid with semi-solid medium to monitor plaquing efficiency to assess viral infectivity. The concentration that inhibited infectivity by fifty percent (IC₅₀), the standard deviation, the 95% confidence interval (95% CI) and the P-values (determined by performing unpaired t tests or one-way ANOVA) were calculated using Prism software (version 5.0 for Macintosh).

Compounds dUY11, ddUY11, aUY11 and Pv-dUY11 all inhibited HSV-1 infectivity, with similar IC₅₀ (**Figure 3.2I**). Their IC₅₀ against HSV-1 infectivity were within a 4.5-fold range (IC₅₀ (95% CI, μ M); 0.038 (0.036 to 0.042), 0.062 (0.053 to 0.073), 0.129 (0.115 to 0.144) or 0.168 μ M (0.144 to 0.197) for dUY11, ddUY11, aUY11 and Pv-dUY11, respectively; **Table 3.1**). Of these, only ddUY11 was cytotoxic, as determined visibly by microscopic observation of changes in cell morphology. dUY11 was the most potent; its IC₅₀ was 38 nM (95% CI, 36 to 42 nM; **Table 3.1, Figures 3.2I and 3.3**). In contrast, the IC₅₀ of Mk-dY11 was more than 4,900-fold higher than dUY11 (IC₅₀ of 188 μ M (95% CI, 143 to 245 μ M) compared to 0.038 μ M (95% CI, 0.036 to 0.042 μ M; **Table 3.1, Figure 3.2I**; P<0.001). The shape and relative orientation of the hydrophilic region is therefore important for antiviral activities.

3.2.1.2 Effects of polarity of the hydrophobic moiety

I next evaluated the effects of polarity of the hydrophobic moiety. The first series of compounds contained a polar estrone group derivatized to 2'-deoxyuridine (R, **Figure 3.1I**) by a rigid non-polar ethynyl (**dUY1**) or by a flexible polar propargyloxymethyl (**dUY9**) linker, or to arabinouridine (R_a, **Figure 3.1I**) by a rigid non-polar ethynyl linker (**aUY1**) (**Figure 3.1III**). A polar 4-hydroxybezophenone was joined to 2'-deoxyuridine by a flexible polar propargyloxymethyl linker (**dUY7**), or the ethynyl linker in **dUY11** was replaced by a flexible polar propargyloxymethyl linker (**aY12**) (**Figure 3.1IV**).

Insertion of polar groups in the linker or core hydrophobic moiety, which decrease amphipathicity, should therefore prevent proper positioning of the compounds into membranes. The introduction of polar groups in the linker, which also disrupts the rigidity of the linker, should also interfere with the compounds ability to inhibit lipid reorganizations. Consistently, an increase in polarity of the hydrophobic moiety disrupted antiviral activities (IC_{50} , >200 μ M for **dUY1** and **dUY9**, **Figure 3.2II**; **dUY7**, **Figure 3.2III**; **Table 3.1**). Introduction of a polar and flexible group into **dUY11** (**aY12**) increased IC_{50} by more than 300-fold, to 12 μ M (95% CI, 11 to 14 μ M; **Table 3.1** and **Figure 3.2III**, compared to 0.038 μ M for **dUY11**; **Table 3.1** and **Figure 3.2I**; $P < 0.001$).

Reducing the hydrophobicity of the 5-derivative could, however, be partially rescued by increasing the polarity of the hydrophilic region (IC_{50} (95% CI, μ M) 55 μ M (42 to 73) for **aUY1**, compared to >200 μ M for **dUY9** or **dUY1**;

Figure 3.2II, Table 3.1; P<0.01). Therefore, amphipathicity and rigidity are important for antiviral activities.

3.2.1.3 Effects of aryl size of the hydrophobic moiety

I next tested the effect of the size of the hydrophobic moiety on antiviral activities. The three compounds in this series contained planar and rigid hydrophobic derivatives, but of different sizes. Compounds **dUY2** and **dUY3** had a hydrophobic ethynylpyrene (**Figure 3.1V**), smaller than the ethynylperylene group in **dUY11** (**Figure 3.1II**). Decreasing the size of the rigid and planar hydrophobic moiety also decreased antiviral activities (**dUY2** or **dUY3**, **Figure 3.2IV**; compared to **dUY11**, **Figure 3.2I**). Compounds **dUY2** and **dUY3** were 974-fold and 868-fold less potent, respectively, than **dUY11** (IC_{50} (95% CI, μM), 37 (26 to 53) or 33 μM (27 to 40), respectively, compared to 0.038 μM (0.036 to 0.042); **Table 3.1; P<0.001**). The IC_{50} of **dUY2** and **dUY3** against HSV-1 infectivity are nearly identical (within a 1.1-fold range; $P>0.05$), indicating that these slight differences in pyrene attachment (at carbon 8 in **dUY2**, or carbon 9 in **dUY3**) did not affect potency. Therefore, a large aryl group size is important for antiviral activities.

3.2.1.4 Effects of planarity and flexibility of the hydrophobic moiety

I next evaluated the activities of amphipathic compounds that differed by the flexibility and planarity of their hydrophobic moieties. The series consisted of 2'-deoxyuridines (R, **Figure 3.1I**) joined at position 5 by 10-ethynyl-9-

phenylethynylanthracene (**dUY4**), by 4-tritylphenyl (**dUY6**), or by 4-tritylphenol (**dUY8**) (**Figure 3.1VI**). All of these compounds had some rotational flexibility. Compound **dUY4** had rotational flexibility within its hydrophobic moiety at the linker joining the anthracene to the phenyl group. Compounds **dUY6** and **dUY8** had rotational flexibility at the tritylphenyl or tritylphenol groups, respectively. All three compounds contained similarly sized hydrophobic regions. A 4-(adamantan-1-yl)phenylethynyl was joined to 2'-deoxyuridine (**dUY5**, **Figure 3.1VII**). **dUY5** also had rotational flexibility within its hydrophobic region, which is also smaller than that of **dUY4**, **dUY6** or **dUY8**.

The antiviral activities of compounds with similarly sized hydrophobic regions were reduced by rotational flexibility or non-planarity of the hydrophobic region (**dUY4**, **dUY6** or **dUY8**; **Figure 3.2VI**; compared to **dUY11**, **Figure 3.2I**). Compounds **dUY4**, **dUY6** and **dUY8** had 210-fold, 842-fold and 158-fold lower potency, respectively (IC_{50} (95% CI, μM); 8 (7 to 9), 32 (24 to 44) or 6 μM (4 to 7), respectively; **Table 3.1**), than **dUY11** (IC_{50} of 0.038 μM (95% CI, 0.036 to 0.042 μM); **Table 3.1**; $P < 0.001$). The adamantane derivative **dUY5** had an apparent IC_{50} of 27 μM (95% CI, 22 to 32 μM ; **Table 3.1**, **Figure 3.2III**), but this compound was cytotoxic, as determined visibly by microscopic observation of changes in cell morphology. The compounds in this series are all non-planar. They also all had higher IC_{50} than the planar compounds evaluated in the first series (**Table 3.1**, **Figures 3.1III** and **3.2I**). Therefore, planarity and rigidity of the hydrophobic derivative is important for antiviral activity.

Taken together, the SAR studies revealed that amphipathicity, together with rigidity, planarity and molecular shape, are all important for antiviral activities. We thus named the compounds rigid amphipathic fusion inhibitors, or RAFIs. dUY11 was the most potent RAFI identified (IC_{50} , 0.038 μ M (95% CI, 0.036 to 0.042 μ M); IC_{99} , 2.16 μ M (95% CI, 2.01 to 2.31 μ M); **Figure 3.3**) and was selected to characterize the antiviral activities of RAFIs in detail.

3.2.2 dUY11 localizes to Vero cell membranes

I next evaluated the cellular localization of dUY11. Under the model proposed, RAFIs interact with lipids. Consistently, SAR studies indicated that molecular shape and amphipathicity were critical for the antiviral properties of RAFIs. If this model was correct, RAFIs should interact with cellular bilayers too.

dUY11 is fluorescent (Korshun et al., 1998; Korshun et al., 1997). I therefore analyzed the cellular distribution of dUY11 by fluorescence, using the general membrane lipid dye PKH26 as the counter-stain.

Mock-infected Vero cells were treated with 200 nM dUY11 (5-fold above IC_{50} , **Figure 3.3**) for 30 minutes. Treated cells were then washed extensively and incubated with 250 nM PKH26. Cells were washed again and evaluated by fluorescence microscopy.

Compound dUY11 distributed to the plasma and intracellular membranes (left panels, fluorescent; **Figure 3.4**), in agreement with the model proposing that RAFIs interact with lipid bilayers. dUY11 was however absent from filipodia (right panels, fluorescent; **Figure 3.4**), regions undergoing constant changes in

membrane curvature. The exclusion of dUY11 from regions of high curvature such as filopodia suggests that cells can regulate the distribution of dUY11, or could result from mechanical constraints imposed by its molecular shape.

3.2.3 dUY11 is not cytotoxic and is only mildly cytostatic

dUY11 does localize to cellular membranes (**Figure 3.4**). The inhibition of HSV-1 infectivity by dUY11 (**Figure 3.3**) could therefore have resulted from cytotoxicity, if virions exposed to dUY11 then delivered it to the cells. I therefore performed cytotoxicity analyses by trypan blue exclusion. Trypan blue is excluded from metabolically viable cells, but stains nonviable cells with damaged membranes (Altman, Randers, and Rao, 1993). Cells with leaky or damaged membranes are thus stained blue and identified as nonviable.

Vero cells were mock-infected for 1 hour, washed, and overlaid with increasing concentration of dUY11. Total cell membrane area doubles with every cell doubling. Therefore, fresh dUY11-containing media was replenished every 24 hours (approximately the doubling time for the Vero cells used), for a total of 72 hours. Viable and non-viable cells were counted by trypan blue exclusion at 24-hour intervals for 3 days.

dUY11 was only mildly cytostatic (**Figure 3.5A, Table 3.2**), even after 3 days of exposure at concentrations 3,947-fold above IC_{50} . Non-viable cells accounted for less than 4% of total cells at any time for any tested concentration (**Figure 3.5B, Table 3.3**). The inhibition of viral infectivity is thus not a result of cytotoxic or cytostatic effects. The selectivity index (SI) was larger than 1,800,

but could not actually be determined because 50% cytotoxicity was not reached at any concentration at which dUY11 was stable in DMEM (up to 70,000 nM).

3.2.4 Rigid amphipathic fusion inhibitors inhibit infectivity

3.2.4.1 Virion exposure to dUY11 before adsorption inhibits infectivity

Compound dUY11 inhibited the infectivity of HSV-1 when virions were directly exposed before adsorption (**Figure 3.3**), but it was not cytotoxic to cells (**Figure 3.5**). dUY11 could inhibit a post-adsorption step. I therefore next evaluated the effects of dUY11 on plaquing when virions were exposed before adsorption or after, when infected cells were exposed to it in methylcellulose media.

Infectious HSV-1 virions pre-warmed to 37°C were exposed to 0 or 2 µM dUY11 at 37°C for 0 or 5 minutes. Virion exposure was terminated by addition of ice-cold media. The samples were then serially diluted 10-fold and used to infect Vero cell monolayers at 4°C, as indicated in the cartoon representation (**Figure 3.6A**). Following adsorption, infected cells were washed and overlaid with methylcellulose containing no drug. Alternatively, cells infected with virions exposed to no drug were overlaid with methylcellulose containing 0 or 2 µM dUY11.

Virion infectivity was inhibited when virions were exposed to dUY11 for 5 minutes prior to infection (left half, center panel; **Figure 3.6B**), as expected, and consistently with **Figure 3.3**. Minimal exposure (so-called 0 minute) reduced infectivity by approximately one order of magnitude (left half, left panel; **Figure 3.6B**), and is most likely a result of the time the virions were exposed to dUY11

before cooling down. Treatment with 2 μ M dUY11 in methylcellulose media after infection of non-treated cells with unexposed virions had no effect on plaquing efficiency (post-adsorption; **Figure 3.6B**). Therefore, dUY11 did not inhibit plaquing when already-infected cells were exposed to it in methylcellulose media, indicating that virion exposure before adsorption was necessary for its antiviral activities.

3.2.4.2 dUY11 does not lyse virions

I next focused on identifying the specific HSV-1 infectivity functions inhibited by dUY11. RAFIs have a hydrophilic moiety of larger cross-section than their hydrophobic region. Micellar forming lipids, which have inverted-cone shapes, are surfactants or detergents (Tilcock, 1986). The apparent inhibition of HSV-1 infectivity could thus have resulted from virion lysis. I therefore evaluated the integrity of dUY11-exposed virions.

HSV-1 virions were exposed to 0 or 7 μ M dUY11. This high concentration of dUY11 fully inhibits plaquing (>99%, **Figure 3.3**). It was selected to increase the sensitivity for detection of even mild lytic effects. As a control, I exposed HSV-1 virions to 1.5% Igepal CA-630, which lyses HSV-1 envelopes (Spear and Roizman, 1972). Aliquots of the so-exposed virions were then serially diluted 10-fold and their infectivity was analyzed by plaquing.

As expected (**Figure 3.3**), dUY11 inhibited the infectivity of the pre-exposed virions (bottom panel; **Figure 3.7A**). Also as expected, exposure to 1.5% Igepal CA-630, which lyses virions, also inhibited infectivity (middle panel;

Figure 3.7A). Igepal CA-630 was cytotoxic at 0.015% (first dilution of the middle panel; **Figure 3.7A**), also as expected for a detergent.

The remaining virions were fractionated through a 20% sucrose cushion, such that virions and naked capsids pellet through the cushion, whereas proteins or DNA released by lysis remain in the supernatant. Pelleted virions and capsids were then analyzed for DNA and protein by Southern and Western blots, respectively.

I first analyzed the proteins in the virion pellets. As expected from envelope destabilization, Igepal CA-630 treatment resulted in the loss of the envelope glycoproteins H (gH) and D (gD) from the virion pellets (center lane of top and middle panels, respectively; **Figure 3.7B**). In contrast, exposure of virions to 7 μ M dUY11 before fractionation did not reduce the levels of gH or gD in the virion pellet (right lane of top and middle panels, respectively; **Figure 3.7B**). The membranes were then re-probed with a polyspecific anti-HSV-1 antibody that recognizes multiple envelope, tegument and capsid proteins. Equivalent amounts of capsid (e.g. VP5) and tegument (e.g. VP16) proteins were present in the pellets of virions pre-exposed to no drug, 7 μ M dUY11, or 1.5% Igepal CA-630 (bottom panel, **Figure 3.7B**), confirming equal loading. Southern blot analysis also revealed that equal HSV-1 DNA levels were recovered in the pellet of purified virions exposed to 0 or 7 μ M dUY11, or 1.5% Igepal CA-630 (**Figure 3.7C**), indicating equal infection under all three exposure conditions. These results indicate that exposure of virions to dUY11 did not lyse their envelope.

3.2.4.3 dUY11 does not inhibit primary herpes simplex virus type-1 attachment

dUY11 interacts with exposed virions to inhibit their infectivity (**Figure 3.3**), without lysing them (**Figure 3.7**). Compound dUY11 could inhibit infectivity by preventing virion binding to cells. Four HSV-1 glycoproteins mediate fusion of the virion envelope with plasma membranes (reviewed in Akhtar and Shukla, 2009). HSV-1 virions first attach to heparan sulphate (HS) glycosaminoglycans (GAG) on the cell surface proteoglycans by low-affinity interactions primarily mediated by virion glycoprotein C (gC) (Herold et al., 1994; Wudunn and Spear, 1989). This low-affinity interaction is followed by high-affinity secondary binding between gD with one of its receptors, herpes virus entry A (HveA) (Montgomery et al., 1996), nectins 1 and 2 (Cocchi et al., 1998; Geraghty et al., 1998), or specific 3-*O*-sulphated HS (Shukla et al., 1999).

Heparin inhibits HSV-1 infectivity by binding to gC, thereby inhibiting the binding of gC to GAG and, consequently, virion attachment (Wudunn and Spear, 1989). The inhibition of HSV-1 infectivity by dUY11 could likewise result from an inhibition of virion binding.

HSV-1 virions radiolabeled with ³⁵S-methionine (³⁵S-met) were exposed to 0 or 7 μM dUY11. I selected this high concentration of dUY11 (which inhibited plaquing by >99%; **Figure 3.3**) for these assays, to maximize the sensitivity to detect even mild inhibition of binding. dUY11-exposed ³⁵S-Met virions were adsorbed onto Vero cells at 4°C to allow both primary attachment and high-affinity secondary binding, but not fusion (Herold et al., 1996). After a

1-hour adsorption, cells were washed to remove unbound virions, and then lysed to assess total binding by beta-scintillation counting. Unlabeled virions were exposed under identical conditions in parallel and then used to infect cells. These infected cells were overlaid with semi-solid media to assess infectivity by plaquing.

Approximately 7% of unexposed or dUY11-exposed HSV-1 virions bound to the cells (no drug (ND) or dUY11, respectively; **Figure 3.8A**; $P>0.05$). Such binding levels are expected for untreated virions (Wudunn and Spear, 1989). Heparin reduced HSV-1 binding by $>90\%$ (Hep, **Figure 3.8A**; $P<0.01$), also as expected (Wudunn and Spear, 1989). Consequently, heparin also inhibited HSV-1 infectivity by $>90\%$ (Hep, **Figure 3.8B**). Exposure of HSV-1 virions to $7\ \mu\text{M}$ dUY11 also inhibited their infectivity, as expected (dUY11, **Figure 3.8B**; consistently with **Figure 3.3**). However, dUY11 did not inhibit their binding (dUY11, **Figure 3.8A**). These results indicate that the inhibition of HSV-1 infectivity by dUY11 did not result from an inhibition of virion attachment.

3.2.4.4 dUY11 does not inhibit high-affinity herpes simplex virus type-1 virion binding

dUY11 had no effect on primary virion attachment to cells (**Figure 3.8**). It could, however, still inhibit the high-affinity secondary binding of gD to its cell surface receptors. The previous studies did not discriminate between primary gC attachment or secondary gD binding. It is therefore possible that virions pre-exposed to dUY11 were bound to cells exclusively by their low-affinity primary

attachment. To test for this possibility, I next evaluated the effects of dUY11 on secondary gD binding.

Virions were pre-exposed to 0 or 7 μM dUY11 and then absorbed onto Vero cells for 15 minutes at 4°C, to allow both primary, low-affinity, attachment and secondary, high-affinity, binding, but not fusion. Virions were therefore allowed to attach by low-affinity gC-GAG interactions, and then to undergo secondary gD binding to its receptors. Unbound inocula were removed and cells were then washed with ice-cold heparin to remove virions attached only by primary, low-affinity, interactions. Heparin only competes with low-affinity gC-GAG interactions, but not with high-affinity gD-protein receptor ones.

Similar percentage of HSV-1 virions exposed to 0 or 7 μM dUY11 bound to cells during the 15-minute adsorption (**Figure 3.9A**), consistently with the results presented in **Figure 3.8A**. Specifically, 3% of HSV-1 virions pre-exposed to no drug, or nearly 4% of HSV-1 virions pre-exposed to 7 μM dUY11 bound to cells in 15 minutes (**Figure 3.9A**; $P>0.05$). Approximately 85% or 90% of untreated or dUY11 pre-exposed virions, respectively, remained bound after washing with (30 to 1,000 $\mu\text{g}/\text{mL}$) heparin (**Figure 3.9B**; $P<0.05$). These results indicate that dUY11 exposure does not prevent secondary, high-affinity, virion binding. Therefore, dUY11 inhibits virion infectivity at a step following secondary binding.

3.2.4.5 dUY11 inhibits herpes simplex virus type-1 entry

dUY11 inhibited plaquing efficiency (**Figure 3.3**) without lysing HSV-1 virions (**Figure 3.7**) or inhibiting binding (**Figures 3.8** and **3.9**). Under the antiviral mechanism proposed, RAFIs target virion envelopes to inhibit their fusion with cell membranes. Therefore, I next tested the effects of dUY11 on HSV-1 entry.

HSV-1 entry can be assessed by several means, including monitoring the entry of virion tegument proteins into infected cells. Virion protein 16 (VP16) is located in the proteinaceous tegument layer of HSV-1 virions. After fusion of the virion envelope to the cell membrane, tegument proteins and capsids enter the cell cytoplasm. VP16 is then transported into the nucleus by host cell factors to activate transcription of VP16-responsive genes (La Boissiere, Hughes, and O'Hare, 1999).

Entry was tested using reporter Vero (clone 57) cells containing a red fluorescence protein (RFP) gene under the control of a HSV-1 promoter activated by VP16 (Diwan, Lacasse, and Schang, 2004). When clone 57 cells are infected with ultraviolet (UV)-inactivated HSV-1 virions, no HSV-1 genes are expressed, but tegument proteins enter the cells. VP16 then activates expression of the RFP reporter gene. Expression of RFP therefore indicates that VP16 has reached the nucleus and, indirectly, that the HSV-1 envelope had fused with cell membranes.

HSV-1 virions were first inactivated by exposure to UV light. Limited UV inactivation crosslinks viral DNA without compromising virion proteins. Inactivation by UV light ensured I could evaluate the effects of dUY11 exclusively on HSV-1 entry because no viral proteins that would otherwise

activate viral promoters (such as the transcription activators ICP0 or ICP4) are expressed (Roizman, Knipe, and Whitley, 2007). Ultraviolet-inactivated HSV-1 virions were pre-exposed to 0, 0.02, 0.05, 0.65 or 2 μ M dUY11 for 5 minutes at 37°C. Vero clone 57 cells were infected with the so-exposed virions at a multiplicity of infection (MOI) of 0.6 PFU per cell. RFP expression was evaluated 24 hours later.

Twenty five percent of cells infected with UV-inactivated and unexposed HSV-1 virions expressed RFP (0, top left panel; **Figure 3.10A**). In contrast, less than 1% of the cells infected with virions pre-exposed to 2 μ M dUY11 expressed RFP (2, top right panel; **Figure 3.10A**). The percent of cells expressing RFP was, as expected, dependent on the concentration of dUY11 to which virions were exposed (0.05, 0.20, 0.65 and 2, **Figures 3.10A** and **3.10B**). Virions pre-exposed to dUY11 therefore did not enter the cells.

3.2.4.6 Rigid amphipathic fusion inhibitors inhibit lamellar to inverted-hexagonal phase transitions

Compound dUY11 inhibited entry (**Figure 3.10**) but did not inhibit high-affinity secondary binding (**Figures 3.9**) or lyse virions (**Figure 3.7**). The major step between high-affinity HSV-1 virion binding and entry of its capsid and tegument into the cell is fusion between the envelope and plasma membrane. For fusion to occur, the external leaflets of virion envelopes must form the negatively curved stalk intermediates (Basanez, 2002). My hypothesis is that RAFIs have molecular shapes (hydrophilic region of larger cross-section than their hydrophobic ones)

that disfavor the formation of the negative curvature required for the hemifusion stalk. I tested next the effects of RAFIs on negative membrane curvature.

Lipid membrane curvature transitions can be studied in experimental systems by evaluating phase transitions of model bilayers. Pure phospholipids are useful models for studying membrane behavior. Hydrated phospholipids spontaneously aggregate into ordered structures in the presence of water (Leikin et al., 1993). Many phospholipids form lamellar phases in such experimental systems, depending on both internal and external factors such as molecular shape, fatty acyl chain length, ionic strength and temperature (Popova and Hinch, 2011). Such lamella are formed when the bilayers are stacked on top of each other and separated by a layer of water. These phospholipids undergo a cooperative phase transition from the lamellar gel state (L_{β}) to the bilayer liquid crystal state (L_{α}) at a given temperature (first peak, **Figure 3.11A**). At higher temperatures, the L_{α} phase of some phospholipids converts to a non-bilayer inverted-hexagonal, or H_{II} , phase (second peak, **Figure 3.11A**). The lower-temperature event involves the melting of the lipid hydrocarbon chains (lamellar gel-to-fluid transition), whereas the higher-temperature event involves the transition from (flat) lamellar to (negatively curved) inverted-hexagonal phase (Erand and Erand, 1988). Lipids that adopt the non-bilayer H_{II} phase favor the negative membrane curvature required for hemifusion stalk. The effects of different molecules on the $L_{\alpha} \rightarrow H_{II}$ phase transition can be measured using differential scanning calorimetry (DSC).

In collaboration with Drs. Richard and Raquel Erand (McMaster University, Hamilton, ON, CA), we tested the effects of RAFIs on the formation

of lipid structures with negative curvature. Dielaidoylphosphatidylethanolamine (DEPE) exhibits sharp and well-characterized lamellar gel-to-fluid ($L_{\beta} \rightarrow L_{\alpha}$) and lamellar to inverted-hexagonal ($L_{\alpha} \rightarrow H_{II}$) phase transitions (Epanand, 1985). DEPE lamellas undergo the lamellar gel L_{β} to fluid L_{α} , and L_{α} to H_{II} phase transitions at approximately 37 or 63°C, respectively (Marsh, 1990). The thermograms thereby exhibit two endothermic transition temperatures, as depicted in the cartoon (**Figure 3.11A**).

DEPE lipid films containing increasing mole ratios of test RAFI were prepared and DSC was performed to evaluate the $L_{\alpha} \rightarrow H_{II}$ phase transitions.

3.2.4.6.1 dUY11 inhibits lamellar to inverted-hexagonal phase transitions

We first tested dUY11. DEPE lamellas were prepared with 0, 0.0021, 0.0048, 0.0086, 0.0129, 0.0172 or 0.0216 mole fraction dUY11. The transition temperatures from lamellar gel-to-fluid ($L_{\beta} \rightarrow L_{\alpha}$) and from lamellar to inverted-hexagonal ($L_{\alpha} \rightarrow H_{II}$) phases were measured by DSC.

DEPE exhibited lamellar gel-to-fluid, and lamellar-to-inverted-hexagonal, transitions at approximately 37 and 65°C, respectively (bottom thermogram, 0; **Figure 3.11B**), as expected (Epanand and Epanand, 1988). dUY11 broadened and increased the lamellar to inverted-hexagonal phase transition temperature (thermograms from 0.021 to 0.0216 mole fraction dUY11; **Figure 3.11B**). Just 0.0216 % dUY11 in DEPE increased the (flat) lamellar to (negatively curved) inverted-hexagonal phase transition temperature by 2.5°C (**Figure 3.11C**; regression of 121.3 ± 13.33 degrees/mol fraction, $r^2 = 0.943$). Such a high positive

slope indicated that dUY11 disfavors the formation of membranes with negative curvature. dUY11 would therefore be expected to inhibit fusion.

3.2.4.6.2 Other rigid amphipathic fusion inhibitors inhibit lamellar to inverted-hexagonal phase transitions

dUY11 increased the lamellar to inverted-hexagonal phase transition temperature (**Figure 3.11**). If RAFIs inhibit viral infectivity by preventing fusion, other active RAFIs should too inhibit lamellar to inverted-hexagonal phase transitions. We next tested whether the latter activity was conserved among other RAFIs. We tested two moderately active RAFIs, dUY2 and dUY4 (IC_{50} (95% CI, μM), 37 (26 to 53) and 8 μM (7 to 9), respectively; **Table 3.1**).

DEPE lamellas were prepared with increasing mole fraction of test RAFI from 0.0037 to 0.1500. The transition of DEPE from the (flat) lamellar to (negatively curved) non-bilayer inverted hexagonal phase was evaluated by DSC.

Like dUY11, both dUY2 and dUY4 increased the temperature of transition from $L_{\alpha} \rightarrow H_{II}$ (**Figure 3.12A** and **B**, respectively). These effects on the formation of an H_{II} phase with negative curvature are characterized by a regression of 60 ± 14 or 40 ± 4 (values kindly provided by Drs R. and R. Epan) for dUY2 and dUY4, respectively. These findings indicated that, like dUY11, at least two other active RAFIs also disfavor the formation of negative curvature.

dUY11 had the most potent effect against HSV-1 infectivity (IC_{50} , 0.038 μM ; **Table 3.1**) and also had the strongest effect on the formation of negative curvature ($121.3 \pm 13.33^{\circ}\text{C}$) (**Figure 3.11**).

3.2.5 Rigid amphipathic fusion inhibitors target virion envelope bilayers

Under the proposed mechanism of action, RAFIs target envelope bilayers to inhibit fusion. Consistently with the proposed model, dUY11 localized to membranes (**Figure 3.4**) and inhibited HSV-1 entry (**Figure 3.10**) without inhibiting binding (**Figures 3.8** and **3.9**) or lysing virions (**Figure 3.7**). Further supporting my hypothesis, dUY11 disfavors the formation of membranes with negative curvature (**Figure 3.11**) required for viral fusion. These results are all most consistent with RAFIs inhibiting viral fusion. Viral fusion is dependent on the merger of two membranes, the virion envelope and the cell membrane. I therefore next identified which of these two membranes is targeted by RAFIs.

3.2.5.1 The antiviral activities of dUY11 are cell-type independent

The general lipid composition of virions is well-conserved, despite differences in the lipid composition of the cells used to propagate them (**Appendix 1**). The basic principles of virion bilayer fusion are also well-conserved. Several cell types are permissive to infection by HSV-1, for example, and the lipid reorganizations required to form the hemifusion stalk are conserved and required for fusion to any of them. I next tested the effects of dUY11-exposure on HSV-1 infectivity in different cell types. To this end, I evaluated the plaquing efficiency of dUY11-exposed virions to several unrelated cell types, human foreskin fibroblasts (HFF), human embryonic kidney (HEK293), cervical cancer (HeLa) or African green monkey kidney epithelial (Vero) cells.

Infectious HSV-1 virions (200 PFU) were pre-exposed to increasing concentration of dUY11 for 5 minutes at 37°C. The so-exposed virions were then used to infect HFF, HEK293, HeLa or Vero cells, and their infectivity was assessed by plaquing.

dUY11 inhibited the infectivity of HSV-1 in all cell types tested (**Figure 3.13**) with the same IC₅₀ (IC₅₀ (95% CI, μM); 0.038 (0.036 to 0.042), 0.036 (0.027 to 0.048), 0.030 (0.024 to 0.037) and 0.040 μM (0.034 to 0.047) for Vero, HFF, HEK293 and HeLa cells, respectively; **Table 3.4**; P>0.05). Therefore, the antiviral activities of RAFIs are independent of the cell type to which exposed envelopes fuse.

3.2.5.2 dUY11 primarily targets virion envelopes

dUY11 inhibited HSV-1 infectivity when virions were exposed to it before infection (**Figure 3.3**). However, dUY11 also localized to cell membranes (**Figure 3.4**). Cellular membranes may also be a target, if dUY11-exposed virions delivered the drug to the membrane targets. Pretreating cells should then inhibit plaquing more efficiently than exposing virions.

Vero cells or HSV-1 virions were exposed to increasing concentration of dUY11 prior to infection. Pre-exposed virions were used to infect untreated cells, or unexposed virions were used to infect pretreated cells. Virion infectivity was evaluated by monitoring plaquing efficiency.

Infectivity was inhibited by 100% only when the virions were exposed prior to infection (IC₅₀ (95% CI), 0.038 μM (0.036 to 0.042 μM), **Figure 3.14** and

Table 3.5; consistently with **Figure 3.3** and **Table 3.1**). In contrast, pretreatment of cells reduced HSV-1 infectivity by only up to 75%, and at 129-fold higher concentrations (IC_{50} (95% CI), 4.9 μ M (3.9 to 6.0 μ M); **Table 3.5**; $P < 0.001$). Thus, the membrane primarily targeted is the virion envelope.

3.2.5.3 dUY11 inhibits herpes simplex virus type-1 infectivity as a result of its interactions with fluid envelopes

dUY11 primarily targets virion envelopes (**Figure 3.14**). I next asked whether dUY11 targeted envelope lipids or proteins. These interactions could be distinguished by evaluating the effects of exposure temperature. Most eukaryotic lipid bilayers, including virion envelopes, are rigid at 4°C (Polozov et al., 2008). Such rigidity would prevent the insertion of hydrophobic compounds into envelopes, but not their potential interactions with exposed glycoproteins.

Infectious HSV-1 virions were either pre-cooled to 4°C or pre-warmed to 37°C. Pre-cooled virions were exposed for 5 minutes to 0 or 2 μ M dUY11 at 4°C, whereas pre-warmed virions were exposed for 5 minutes to 0 or 2 μ M dUY11 at 37°C. I tested this high concentration of dUY11 (IC_{99} , **Figure 3.3**) to increase the sensitivity to detect even mild effects. Virion exposure to dUY11 was terminated by addition of ice-cold media. The samples were then serially diluted 10-fold and used to infect Vero cell monolayers at 4°C, with 50,000; 5,000; 500; 50; 5; or 0.5 of the so-exposed virions, as indicated in the cartoon representation (**Figure 3.15A**). Infected cells were washed 1 hour later and overlaid with semi-solid media with no drug.

Virions exposed to 2 μM dUY11 at 37°C were non-infectious (top right panel, **Figure 3.15B**), as expected (**Figure 3.3**). In contrast, virions exposed to 2 μM dUY11 at 4°C retained most of their infectivity (top left panel, **Figure 3.15B**). Unexposed virions were of course infectious independently of the pseudo-exposure temperature (bottom panels, **Figure 3.15B**), as expected. Therefore, the inhibitory interactions of dUY11 with virions did not occur when virions with rigid envelopes were exposed to the compound. These results are consistent with the proposed model, whereby RAFIs interact with lipid envelope bilayers to inhibit virion infectivity.

3.3 Discussion

I have discovered a novel mechanism of antiviral action for a unique family of nucleoside analogues. These compounds target the formation of negative curvature required for viral fusion. SAR studies revealed that molecular shape, amphipathicity and rigidity were all essential properties for their antiviral activities (**Figure 3.2**, **Table 3.1**). We therefore named the compounds rigid amphipathic fusion inhibitors (RAFIs).

I used the most potent RAFI, dUY11, and HSV-1 to characterize the novel mechanism of antiviral action. Under the proposed mechanism of action, RAFIs target lipid bilayers to inhibit viral fusion. Consistently with the proposed target, dUY11 distributed to plasma and intracellular membranes (**Figure 3.4**), but fully inhibited HSV-1 infectivity only when virions were exposed to it (**Figure 3.14**, **Table 3.5**). The antiviral activities of dUY11 were independent of the infected

cell type (**Figure 3.13**), but were dependent on interactions with fluid HSV-1 virion envelopes (**Figures 3.15**). These results are all most consistent with RAFIs targeting envelope bilayers. Consistently with the proposed mechanism of action, dUY11 specifically inhibited HSV-1 entry (**Figure 3.10**), but did not lyse virions (**Figure 3.7**) nor did it prevent virion binding (**Figures 3.8** and **3.9**). The only step between high-affinity binding and entry is fusion between the virion and cellular membranes. Compound dUY11 and two other tested RAFIs inhibited lamellar to inverted-hexagonal phase transitions that model the formation of negative curvature required for fusion (**Figures 3.11** and **3.12**). These results are all most consistent with RAFIs inhibiting viral infectivity by preventing the formation of the negatively curved lipid intermediates.

RAFIs have a hydrophilic region of larger cross-section than their hydrophobic moiety. Some naturally occurring lipids have hydrophilic heads of larger cross-section than their hydrophobic tails, and adopt spontaneous positive curvature (Chernomordik, Kozlov, and Zimmerberg, 1995b). In liposome fusion studies, the exogenous addition of lipids such as lysophosphatidylcholine (LPC) and lysophosphatidic acid (LPA), which favor positive curvature, inhibit vesicle fusion (Chernomordik, Kozlov, and Zimmerberg, 1995a; Vogel, Leikina, and Chernomordik, 1993; Yeagle et al., 1994). Such lipids also inhibit the fusion of enveloped viruses (Chernomordik et al., 1999; Gaudin, 2000; Gunther-Ausborn, Praetor, and Stegmann, 1995; Melikyan et al., 1997; Stiasny and Heinz, 2004). The further addition of natural lipids which favor the opposite membrane curvature (i.e. negative) restored viral fusion (Gaudin, 2000; Stiasny and Heinz,

2004). Therefore, the inhibitory properties of LPC on viral membrane fusion resulted from the modulation of envelope curvature. Similarly to these naturally occurring lipids with hydrophilic heads of larger cross-section than their hydrophobic tails, the inhibitory properties of RAFIs appear to result from disfavoring the negative curvature required for the formation of the hemifusion stalk (**Figures 3.11** and **3.12**). Then, the further addition of natural lipids that promote negative curvature, for example oleic acid, should restore fusion of RAFI-exposed virions. Such effects on the modulation of membrane curvature could be evaluated by monitoring the fusion of so-exposed virions in fluorescence dequenching assays.

Two members of this family of compounds (dUY4 and dUY11), originally synthesized as fluorescent DNA probes, were later reported to have selective anti-herpetic activities (Andronova et al., 2003; Pchelintseva et al., 2005). The IC_{50} for dUY11 in multiple HSV-1 replication cycles was previously reported as 7.8 $\mu\text{g}/\text{mL}$, or 15.5 μM , and expressed as the inhibitory dose which reduces viral CPE by 50% (ID_{50}) 48 hours after infection at a MOI of 0.1 PFU per cell (Andronova et al., 2003). The concentration which caused the death of no more than 50% of cells (CD_{50}) was reported to be 250 $\mu\text{g}/\text{mL}$, or 497 μM , measured by trypan blue exclusion 72 hours after compound addition (Andronova et al., 2003). It is unclear how the high concentration of dUY11 (497 μM) solution reported by Andronova et al. was obtained (Andronova et al., 2003). Nonetheless, dUY11 was therefore characterized as having a SI of 32, expressed as the CD_{50}/ID_{50} ratio (Andronova et al., 2003). When I exposed HSV-1 virions directly to dUY11 before infection, the

IC₅₀ against infectivity (IC₅₀ 0.038 μM, **Figure 3.3**) was 408-fold lower than the ID₅₀ calculated by Andronova et al. at 48 hpi (ID₅₀ 15.5 μM) (Andronova et al., 2003). I also used trypan blue viability to assess cytotoxicity and non-viable cells accounted for less than 4% of total cells, even after 3 days of exposure at concentrations 3,947-fold above IC₅₀ (**Figure 3.5B**, **Table 3.3**). The SI calculated from my experiments was therefore larger than 1,800, but could not actually be determined because 50% cytotoxicity was not reached at any dUY11 concentration at which dUY11 was stable in DMEM (up to 70,000 nM).

The differences in the IC₅₀ reported against HSV-1 result from the different methods used to evaluate the antiviral effects of RAFIs. Andronova et al. reported the IC₅₀ of these fusion inhibitors by calculating viral yields in RAFI-treated cells 48 hours post-infection (hpi) (2003). I reported the IC₅₀ that was determined by directly measuring the effects of RAFIs on HSV-1 infectivity, a more relevant parameter given that these compounds are fusion inhibitors.

The activities of RAFIs also appear to be specific to virions, an important characteristic for any antiviral compound. In exposed cells, dUY11 distributed to cellular membranes (**Figure 3.4**). Yet, dUY11 did not inhibit Vero cell doubling (**Table 3.2**) nor block membrane trafficking required for the formation of filopodia (**Figure 3.4**). These are two examples of cellular processes in which membranes undergo constant remodeling. Such dynamic remodeling of membranes requires extensive changes in curvature for fusion and fission (McMahon and Gallop, 2005), and yet these are not inhibited in dUY11-treated cells. The exclusion of dUY11 from regions of high curvature such as filopodia suggests that cells can

regulate the distribution of dUY11, or its exclusion from these membrane regions could result from mechanical constraints imposed by its molecular shape.

The selectivity of RAFIs may be explained by the sensitivity of viral fusion to increases in energy barriers to fusion, in contrast to the apparent insensitivity of cellular fusion events. Cell membranes and virion envelopes have several important differences that may contribute to their differential sensitivity to fusion energy barriers. Virion envelopes are extracellular vesicles of positive curvature. Consequently, envelope lipids must undergo major reorganizations during viral fusion to form the (negatively curved) stalk, using only the energy provided by glycoprotein binding and rearrangements. The chemical composition of the leaflets of virion envelopes is static; there is no exchange of lipids across leaflets, and no changes in lipid composition to accommodate the formation of membrane curvature (Rothman et al., 1976). The diffusion and tilting of envelope lipids, and stretching and splaying of their acyl chains, are the only lipid reorganizations possible to overcome the energy barrier to form the hemifusion stalk (Siegel, 1999).

In contrast, several mechanisms contribute to membrane deformation in cells, such as changes in lipid composition and cytoskeletal polymerization, the assembly of protein scaffolds at bilayer interfaces and the binding of proteins that bend membranes (McMahon and Gallop, 2005). The chemical properties of different lipid acyl chains or headgroups favor different membrane curvatures, for example (Holthuis and Levine, 2005). Enzymes such as lysophosphatidic acid acyl transferase and phospholipase A₂, which interconvert LPA and phosphatidic

acid, favor opposite curvatures (Brown, Chambers, and Doody, 2003). Flippases that transfer lipids from one leaflet to the other modulate the composition of each leaflet, thus affecting membrane stress and, consequently, curvature (Farge et al., 1999). Lipid exchange is thus highly dynamic in cell membranes, and membrane remodeling is facilitated by lipid-binding or modifying enzymes and by membrane bending proteins (Farsad and De Camilli, 2003; Janmey and Kinnunen, 2006). All of these cellular processes for membrane remodeling are energy-dependent. Cellular fusion events thus have access to several mechanisms to overcome the energy barriers for fusion. These could all contribute to modulating membrane curvature to enable cellular fusion events to proceed, even if the energy barriers for fusion were increased. Consequently, viral fusion is likely to be more sensitive to increases in energy barriers for fusion, whereas cellular processes that require membrane bending are less likely to be sensitive. An increase in the energy barrier for fusion would inhibit viral fusion, while allowing cellular fusion to proceed.

Previous attempts at targeting virion lipids used agents that non-specifically destabilize envelopes or modulate the fluidity by targeting cholesterol, which is also required for cell membrane integrity and function (Goluszko and Nowicki, 2005). Such approaches therefore resulted in agents that often resulted in cytotoxicity, mucosal injuries, or inflammation, which all actually enhance infection (Morris and Lacey, 2010).

Many naturally occurring inverted-cone shaped lipids are detergents (Hilmarsson, Kristmundsdottir, and Thormar, 2005). RAFIs, however, do not lyse

virions (**Figure 3.7**). In contrast to these natural lipids, RAFIs selectively target the formation of the negative envelope curvature, which is conserved and required for the fusion of all enveloped viruses. Consequently, RAFIs should be active against all enveloped viruses, including variants resistant to classical antivirals that inhibit DNA replication. Moreover, the sensitivity of viral fusion to increases in the energy barrier is an antiviral approach specific to virions. RAFIs are thus less likely to be toxic than previous strategies that aimed at envelope characteristics that are also required for cell membrane integrity. This novel antiviral strategy has yet to be evaluated *in vivo*, but may help to overcome the limitations of strategies targeting membrane fluidity and stability, or viral and cellular proteins.

This work serves as a proof-of-concept that small molecule fusion inhibitors targeting envelope lipid bilayers can inhibit viral infectivity in cultured cells. The RAFIs described here are the first nucleoside derivatives that inhibit viral fusion, and the first reported small molecule inhibitors of viral infectivity that target envelope bilayer curvature transitions to inhibit fusion.

3.4 References

- Akhtar, J., and Shukla, D. (2009). Viral entry mechanisms: cellular and viral mediators of herpes simplex virus entry. *Febs Journal* **276**(24), 7228-7236.
- Altman, S. A., Randers, L., and Rao, G. (1993). Comparison of trypan blue dye exclusion and fluorometric assays for mammalian cell viability determinations. *Biotechnol Prog* **9**(6), 671-4.
- Andronova, V. L., Skorobogaty, M. V., Manasova, E. V., Berlin Iu, A., Korshun, V. A., and Galegov, G. A. (2003). [Antiviral activity of some 5-arylethynyl 2'-deoxyuridine derivatives]. *Bioorg Khim* **29**(3), 290-5.
- Basanez, G. (2002). Membrane fusion: the process and its energy suppliers. *Cellular and Molecular Life Sciences* **59**(9), 1478-1490.
- Brown, W. J., Chambers, K., and Doody, A. (2003). Phospholipase A2 (PLA2) enzymes in membrane trafficking: Mediators of membrane shape and function. *Traffic* **4**(4), 214-221.
- Burger, K. N. J. (2000). Greasing membrane fusion and fission machineries. *Traffic* **1**(8), 605-613.
- Chernomordik, L., Kozlov, M. M., and Zimmerberg, J. (1995a). Lipids in biological membrane fusion. *J Membr Biol* **146**(1), 1-14.
- Chernomordik, L., Kozlov, M. M., and Zimmerberg, J. (1995b). Lipids in Biological Membrane-Fusion. *Journal of Membrane Biology* **146**(1), 1-14.
- Chernomordik, L. V., Leikina, E., Kozlov, M. M., Frolov, V. A., and Zimmerberg, J. (1999). Structural intermediates in influenza haemagglutinin-mediated fusion. *Mol Membr Biol* **16**(1), 33-42.
- Cocchi, F., Menotti, L., Mirandola, P., Lopez, M., and Campadelli-Fiume, G. (1998). The ectodomain of a novel member of the immunoglobulin subfamily related to the poliovirus receptor has the attributes of a bona fide receptor for herpes simplex virus types 1 and 2 in human cells. *Journal of Virology* **72**(12), 9992-10002.
- Diwan, P., Lacasse, J. J., and Schang, L. M. (2004). Roscovitine inhibits activation of promoters in herpes simplex virus type 1 genomes independently of promoter-specific factors. *J Virol* **78**(17), 9352-65.
- Dorr, P., Westby, M., Dobbs, S., Griffin, P., Irvine, B., Macartney, M., Mori, J., Rickett, G., Smith-Burchnell, C., Napier, C., Webster, R., Armour, D., Price, D., Stammen, B., Wood, A., and Perros, M. (2005). Maraviroc (UK-427,857), a potent, orally bioavailable, and selective small-molecule inhibitor of chemokine receptor CCR5 with broad-spectrum anti-human immunodeficiency virus type 1 activity. *Antimicrob Agents Chemother* **49**(11), 4721-32.
- Epanand, R. M. (1985). High-Sensitivity Differential Scanning Calorimetry of the Bilayer to Hexagonal Phase-Transitions of Diacylphosphatidylethanolamines. *Chemistry and Physics of Lipids* **36**(4), 387-393.

- Epand, R. M., and Epand, R. F. (1988). Kinetic Effects in the Differential Scanning Calorimetry Cooling Scans of Phosphatidylethanolamines. *Chemistry and Physics of Lipids* **49**(1-2), 101-104.
- Farge, E., Ojcius, D. M., Subtil, A., and Dautry-Varsat, A. (1999). Enhancement of endocytosis due to aminophospholipid transport across the plasma membrane of living cells. *American Journal of Physiology-Cell Physiology* **276**(3), C725-C733.
- Farsad, K., and De Camilli, P. (2003). Mechanisms of membrane deformation. *Current Opinion in Cell Biology* **15**(4), 372-381.
- Gaudin, Y. (2000). Rabies virus-induced membrane fusion pathway. *Journal of Cell Biology* **150**(3), 601-611.
- Geraghty, R. J., Krummenacher, C., Cohen, G. H., Eisenberg, R. J., and Spear, P. G. (1998). Entry of alphaherpesviruses mediated by poliovirus receptor-related protein 1 and poliovirus receptor. *Science* **280**(5369), 1618-1620.
- Goluszko, P., and Nowicki, B. (2005). Membrane cholesterol: a crucial molecule affecting interactions of microbial pathogens with mammalian cells. *Infect Immun* **73**(12), 7791-6.
- Gunther-Ausborn, S., Praetor, A., and Stegmann, T. (1995). Inhibition of influenza-induced membrane fusion by lysophosphatidylcholine. *J Biol Chem* **270**(49), 29279-85.
- Herold, B. C., Gerber, S. I., Belval, B. J., Siston, A. M., and Shulman, N. (1996). Differences in the susceptibility of herpes simplex virus types 1 and 2 to modified heparin compounds suggest serotype differences in viral entry. *Journal of Virology* **70**(6), 3461-3469.
- Herold, B. C., Visalli, R. J., Susmarski, N., Brandt, C. R., and Spear, P. G. (1994). Glycoprotein-C-Independent Binding of Herpes-Simplex Virus to Cells Requires Cell-Surface Heparan-Sulfate and Glycoprotein-B. *Journal of General Virology* **75**, 1211-1222.
- Hilmarsson, H., Kristmundsdottir, T., and Thormar, H. (2005). Virucidal activities of medium- and long-chain fatty alcohols, fatty acids and monoglycerides against herpes simplex virus types 1 and 2: comparison at different pH levels. *Acta Pathologica, Microbiologica et Immunologica Scandinavica* **113**(1), 58-65.
- Hoffmann, C. (2007). The epidemiology of HIV coreceptor tropism. *European Journal of Medical Research* **12**(9), 385-390.
- Holthuis, J. C., and Levine, T. P. (2005). Lipid traffic: floppy drives and a superhighway. *Nat Rev Mol Cell Biol* **6**(3), 209-20.
- Janmey, P. A., and Kinnunen, P. K. (2006). Biophysical properties of lipids and dynamic membranes. *Trends Cell Biol* **16**(10), 538-46.
- Korshun, V. A., Manasova, E. V., Balakin, K. V., Malakhov, A. D., Perepelov, A. V., Sokolova, T. A., and Berlin, Y. A. (1998). New fluorescent nucleoside derivatives - 5-alkynylated 2'-deoxyuridines. *Nucleosides & Nucleotides* **17**(9-11), 1809-1812.
- Korshun, V. A., Prokhorenko, I. A., Gontarev, S. V., Skorobogaty, M. V., Balakin, K. V., Manasova, E. V., Malakhov, A. D., and Berlin, Y. A.

- (1997). New pyrene derivatives for fluorescent labeling of oligonucleotides. *Nucleosides & Nucleotides* **16**(7-9), 1461-1464.
- La Boissiere, S., Hughes, T., and O'Hare, P. (1999). HCF-dependent nuclear import of VP16. *Embo Journal* **18**(2), 480-489.
- Leikin, S., Parsegian, V. A., Rau, D. C., and Rand, R. P. (1993). Hydration Forces. *Annual Review of Physical Chemistry* **44**, 369-395.
- Malakhov, A. D., Malakhova, E. V., Kuznitsova, S. V., Grechishnikova, I. V., Skorobogatyj, M. V., Korshun, V. A., and Berlin, Y. A. (2000). Synthesis and Fluorescent Properties of 5-(1-pyrenylethynyl)-2'-deoxyuridine-containing oligodeoxynucleotides. *Russian journal of Bioorganic Chemistry* **26**(1), 39-50.
- Marsh, D. (1990). "CRC Handbook of Lipid Bilayers." (D. Marsh, Ed.) CRC Press, Boca Raton.
- McMahon, H. T., and Gallop, J. L. (2005). Membrane curvature and mechanisms of dynamic cell membrane remodelling. *Nature* **438**(7068), 590-596.
- Melikyan, G. B., Brener, S. A., Ok, D. C., and Cohen, F. S. (1997). Inner but not outer membrane leaflets control the transition from glycosylphosphatidylinositol-anchored influenza hemagglutinin-induced hemifusion to full fusion. *J Cell Biol* **136**(5), 995-1005.
- Montgomery, R. I., Warner, M. S., Lum, B. J., and Spear, P. G. (1996). Herpes simplex virus-1 entry into cells mediated by a novel member of the TNF/NGF receptor family. *Cell* **87**(3), 427-436.
- Morris, G. C., and Lacey, C. J. (2010). Microbicides and HIV prevention: lessons from the past, looking to the future. *Curr Opin Infect Dis* **23**(1), 57-63.
- Pchelintseva, A. A., Skorobogatyj, M. V., Petrunina, A. L., Andronova, V. L., Galegov, G. A., Astakhova, I. V., Ustinov, A. V., Malakhov, A. D., and Korshun, V. A. (2005). Synthesis and evaluation of anti-HSV activity of new 5-alkynyl-2'-deoxyuridines. *Nucleosides Nucleotides & Nucleic Acids* **24**(5-7), 923-926.
- Polozov, I. V., Bezrukov, L., Gawrisch, K., and Zimmerberg, J. (2008). Progressive ordering with decreasing temperature of the phospholipids of influenza virus. *Nature Chemical Biology* **4**(4), 248-255.
- Popova, A. V., and Hinch, D. K. (2011). Thermotropic phase behavior and headgroup interactions of the nonbilayer lipids phosphatidylethanolamine and monogalactosyldiacylglycerol in the dry state. *BMC Biophys* **4**, 11.
- Roizman, B., Knipe, D. M., and Whitley, R. (2007). The replication of Herpes simplex virus. In "Fields' virology, 5th ed." (D. M. Knipe, P. M. Howley, D. E. Griffin, R. A. Lamb, M. A. Martin, B. Roizman, and S. E. Straus, Eds.), pp. 2501-2601. Lippincott-Williams & Wilkins, Philadelphia, PA.
- Rothman, J. E., Tsai, D. K., Dawidowicz, E. A., and Lenard, J. (1976). Transbilayer Phospholipid Asymmetry and Its Maintenance in Membrane of Influenza-Virus. *Biochemistry* **15**(11), 2361-2370.
- Scarlati, G., Tresoldi, E., Bjorndal, A., Fredriksson, R., Colognesi, C., Deng, H. K., Malnati, M. S., Plebani, A., Siccardi, A. G., Littman, D. R., Fenyo, E. M., and Lusso, P. (1997). In vivo evolution of HIV-1 co-receptor usage

- and sensitivity to chemokine-mediated suppression. *Nature Medicine* **3**(11), 1259-1265.
- Schang, L. M. (2006). Herpes simplex viruses in antiviral drug discovery. *Current Pharmaceutical Design* **12**(11), 1357-1370.
- Shukla, D., Liu, J., Blaiklock, P., Shworak, N. W., Bai, X. M., Esko, J. D., Cohen, G. H., Eisenberg, R. J., Rosenberg, R. D., and Spear, P. G. (1999). A novel role for 3-O-sulfated heparan sulfate in herpes simplex virus 1 entry. *Cell* **99**(1), 13-22.
- Siegel, D. P. (1999). The modified stalk mechanism of lamellar/inverted phase transitions and its implications for membrane fusion. *Biophysical Journal* **76**(1), 291-313.
- Skorobogaty, M. V., Malakhov, A. D., Pchelintseva, A. A., Turban, A. A., Bondarev, S. L., and Korshun, V. A. (2006a). Fluorescent 5-alkynyl-2'-deoxyuridines: High emission efficiency of a conjugated perylene nucleoside in a DNA duplex. *Chembiochem* **7**(5), 810-816.
- Skorobogaty, M. V., Ustinov, A. V., Stepanova, I. A., Pchelintseva, A. A., Petrunina, A. L., Andronova, V. L., Galegov, G. A., Malakhov, A. D., and Korshun, V. A. (2006b). 5-Arylethynyl-2'-deoxyuridines, compounds active against HSV-1. *Organic & Biomolecular Chemistry* **4**(6), 1091-1096.
- Spear, P. G., and Roizman, B. (1972). Proteins Specified by Herpes-Simplex Virus .5. Purification and Structural Proteins of Herpesvirion. *Journal of Virology* **9**(1), 143-&.
- Stiasny, K., and Heinz, F. X. (2004). Effect of membrane curvature-modifying lipids on membrane fusion by tick-borne encephalitis virus. *Journal of Virology* **78**(16), 8536-8542.
- Teissier, E., and Pecheur, E. I. (2007). Lipids as modulators of membrane fusion mediated by viral fusion proteins. *European Biophysics Journal with Biophysics Letters* **36**(8), 887-899.
- Teissier, E., Penin, F., and Pecheur, E. I. (2011). Targeting Cell Entry of Enveloped Viruses as an Antiviral Strategy. *Molecules* **16**(1), 221-250.
- Tilcock, C. P. (1986). Lipid polymorphism. *Chem Phys Lipids* **40**(2-4), 109-25.
- Vogel, S. S., Leikina, E. A., and Chernomordik, L. V. (1993). Lysophosphatidylcholine reversibly arrests exocytosis and viral fusion at a stage between triggering and membrane merger. *J Biol Chem* **268**(34), 25764-8.
- Westby, M., Smith-Burchnell, C., Mori, J., Lewis, M., Mosley, M., Stockdale, M., Dorr, P., Ciaramella, G., and Perros, M. (2007). Reduced maximal inhibition in phenotypic susceptibility assays indicates that viral strains resistant to the CCR5 antagonist maraviroc utilize inhibitor-bound receptor for entry. *Journal of Virology* **81**(5), 2359-2371.
- Wudunn, D., and Spear, P. G. (1989). Initial Interaction of Herpes-Simplex Virus with Cells Is Binding to Heparan-Sulfate. *Journal of Virology* **63**(1), 52-58.

Yeagle, P. L., Smith, F. T., Young, J. E., and Flanagan, T. D. (1994). Inhibition of Membrane-Fusion by Lysophosphatidylcholine. *Biochemistry* **33**(7), 1820-1827.

Compound	IC₅₀, μM (95% CI)
dUY11	0.038 (0.036 to 0.042)
ddUY11†	0.062 (0.053 to 0.073)
aUY11‡	0.129 (0.115 to 0.144)
Pv-ddY11	0.168 (0.144 to 0.197)
Mk-dY11‡	188 (143 to 245)
aY12	12 (11 to 14)
dUY1*	>200
aUY1	55 (42 to 73)
dUY2	37 (26 to 53)
dUY3	33 (27 to 40)
dUY4	8 (7 to 9)
dUY5†	27 (22 to 32)
dUY6	32 (24 to 44)
dUY7*	>200
dUY8	6 (4 to 7)
dUY9*	>200

Table 3.1 IC₅₀ of RAFIs against HSV-1 infectivity. Table summarizing 50% inhibitory concentration (IC₅₀) and 95% confidence interval (CI) for each compound against HSV-1 infectivity. IC₅₀ and 95% CI for all compounds were calculated from four or more experiments using Prism software (nonlinear regression curve fit). ‡Mk-dY11 and aUY11 form aggregates in DMSO. †dUY5 and ddUY11 were cytotoxic at 20 μM, as determined by cell shrinkage observed under microscopic evaluation. *No concentration up to 200 μM of dUY1, dUY7 or dUY9 inhibited HSV-1 infectivity by 50%.

dUY11, μM	Time, days	Relative cell number ± range
0	0	1.00±0.16
	1	2.79±0.02
	2	6.05±0.28
	3	11.8±0.5
7	0	1.00±0.16
	1	3.06±0.66
	2	4.59±0.76
	3	11.8±4.1
20	0	1.00±0.16
	1	2.67±0.15
	2	6.39±1.08
	3	9.94±3.05
70	0	1.00±0.16
	1	3.15±0.24
	2	4.72±0.47
	3	8.99±1.31
150	0	1.00±0.16
	1	2.26±0.06
	2	2.88±0.32
	3	7.38±0.37

Table 3.2 Effects of dUY11 on cell doubling. Table summarizing viable cell numbers following exposure to 7, 20, 70 or 150 μM dUY11 after 1, 2 or 3 days, relative to viable cell numbers at time zero. Ranges represent the count of viable cells from duplicate samples from one experiment.

dUY11, μM	Time, days	Non-viable cells ± range, %
0	0	0.430±0.213
	1	1.44±0.94
	2	0.784±0.429
	3	0.821±0.333
7	0	0.430±0.213
	1	0.886±0.053
	2	3.03±1.08
	3	1.55±1.17
20	0	0.430±0.213
	1	0.919±0.322
	2	0.491±0.357
	3	3.68±1.98
70	0	0.430±0.213
	1	0.469±0.297
	2	0.683±0.375
	3	1.18±0.12
150	0	0.430±0.213
	1	0.791±0.576
	2	0.381±0.088
	3	1.08±0.05

Table 3.3 Effects of dUY11 on cell viability. Table summarizing the percent of non-viable cells following exposure to 0, 7, 20, 70 or 150 μM dUY11 for up to 3 days. Ranges represent the percent of non-viable cells from duplicate samples from one experiment.

Cell type	IC₅₀, μM (95% CI)
Vero	0.038 (0.036 to 0.042)
HFF	0.036 (0.027 to 0.048)
HEK293	0.030 (0.024 to 0.037)
HeLa	0.040 (0.034 to 0.047)

Table 3.4 IC₅₀ of dUY11 against HSV-1 infectivity to different cell lines.

Table summarizing 50% inhibitory concentration (IC₅₀) and 95% confidence interval (CI) of dUY11 against HSV-1 infectivity to monkey kidney epithelial cells (Vero), human foreskin fibroblasts (HFF), human embryonic kidney cells (HEK293) or cervical cancer cells (HeLa). The IC₅₀, 95% CI and P-values for all cell types were calculated from three or more experiments using Prism software (nonlinear regression curve fit). The means are not significantly different (P>0.05).

Treatment	IC₅₀, μM (95% CI)
Exposed HSV-1 virions	0.038 (0.036 to 0.042)
Cell protection	4.9 (3.9 to 6.0)

Table 3.5 IC₅₀ of dUY11 against HSV-1 infectivity by direct virion exposure or by cell pretreatment. Table summarizing the 50% inhibitory concentration (IC₅₀) and 95% confidence interval (CI) against HSV-1 infectivity when virions were exposed to dUY11 before adsorption, or when cells were pretreated with dUY11 before infection with unexposed virions. The IC₅₀, 95% CI and P-values were calculated from four or more experiments using Prism software (nonlinear regression curve fit). P<0.001. HSV-1, herpes simplex virus type-1.

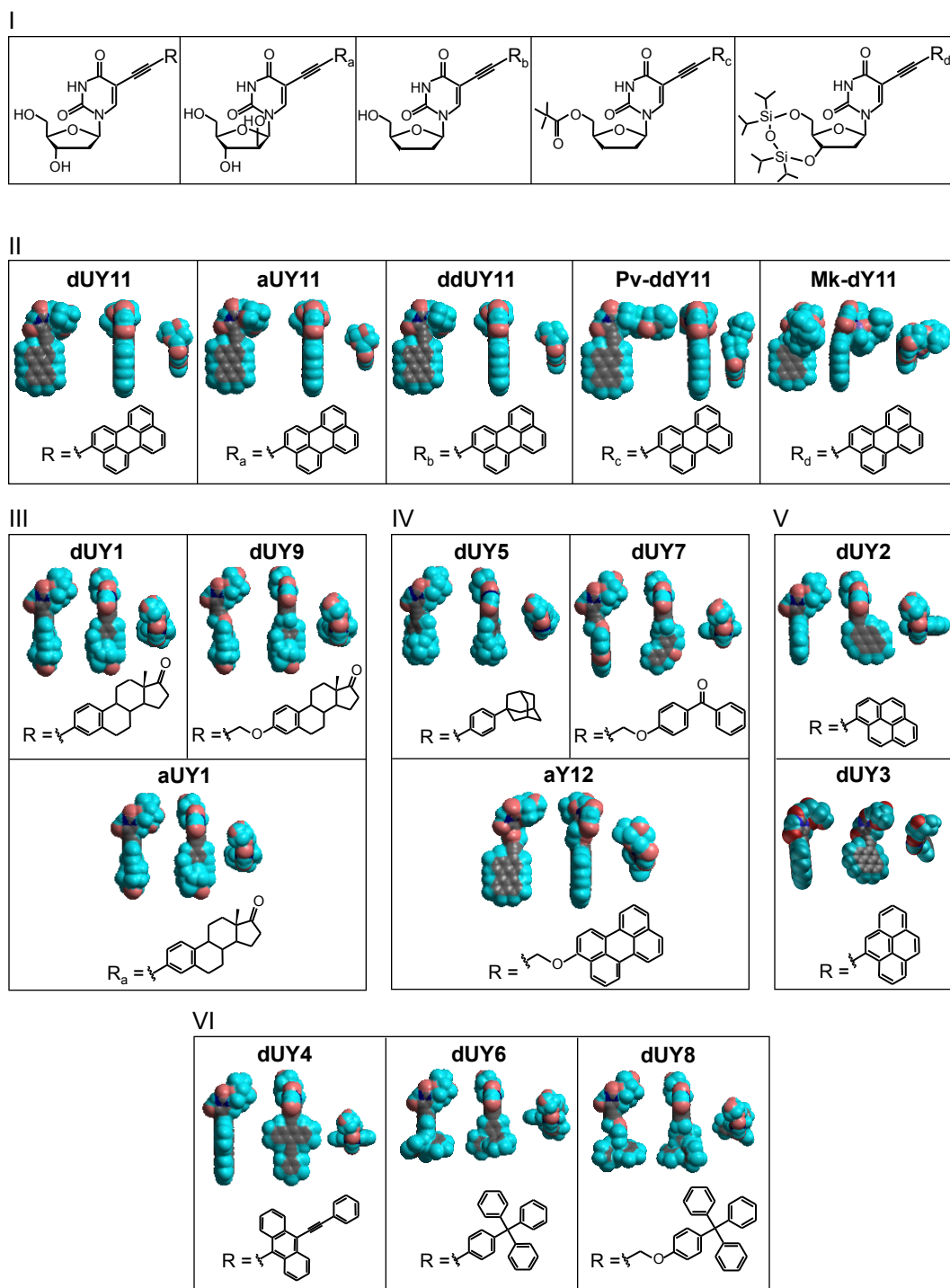


Figure 3.1 Structures of rigid amphipathic fusion inhibitors. Chemical structures and three-dimensional space-filling models displayed in 3 orthogonal planes of 5-alkynyl nucleoside derivatives. Grey, carbon; teal, hydrogen; pink, oxygen; blue, nitrogen.

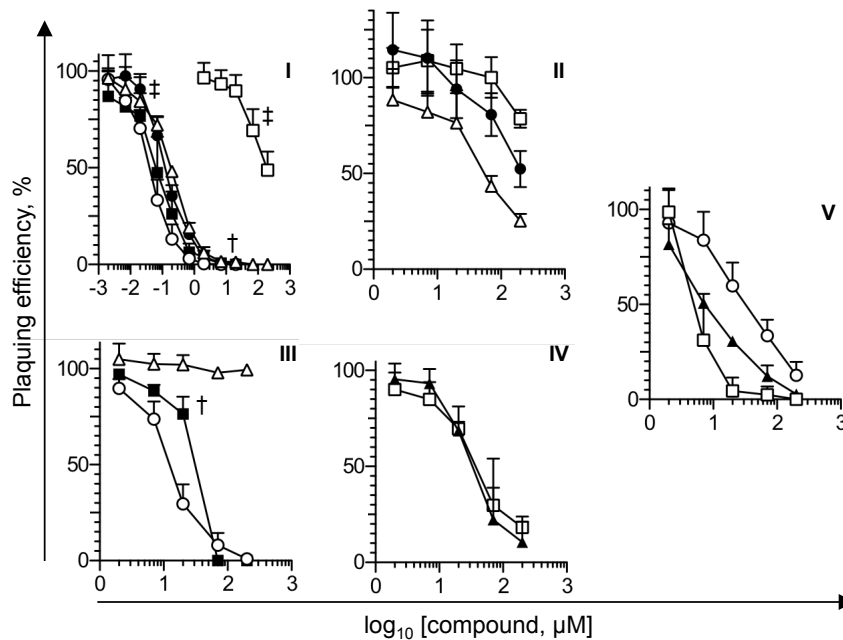
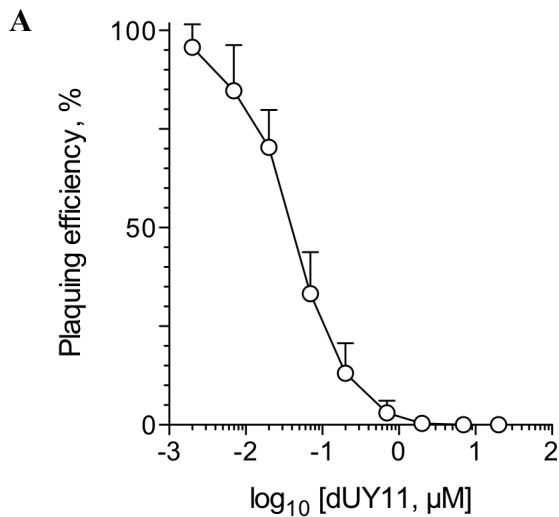


Figure 3.2 RAFIs inhibit HSV-1 infectivity. Semi-logarithmic line graphs showing HSV-1 plaquing efficiency plotted against the logarithm of compound concentration. HSV-1 KOS (200 plaque-forming units) was pre-exposed to 0, 0.002, 0.007, 0.02, 0.07, 0.2, 0.7, 2, 7, 20, 70 or 200 μM dUY11 (\circ), aUY11 (\bullet), ddUY11 (\blacksquare), Pv-ddY11 (\triangle), or Mk-dY11 (\square) (I); dUY1 (\bullet), dUY9 (\square), or aUY1 (\triangle) (II); dUY5 (\blacksquare), dUY7 (\triangle), or aY12 (\circ) (III); dUY2 (\square), or dUY3 (\blacktriangle) (IV); or dUY4 (\blacktriangle), dUY6 (\circ), or dUY8 (\square) (V) for 5 minutes at 37°C . Vero cells were then infected with the so-exposed virions, and plaques counted. Error bars, standard deviation of four or more experiments. \ddagger Mk-dY11 and aUY11 form aggregates in DMSO. \dagger dUY5 and ddUY11 were cytotoxic at 20 μM , as determined by cell shrinkage observed under microscopic evaluation.



B

Percent inhibitory concentration	IC, μM (95% CI)
IC ₅₀	0.038 (0.036 to 0.042)
IC ₉₉	2.16 (2.01 to 2.31)

Figure 3.3 dUY11 inhibits HSV-1 infectivity with an IC₅₀ of 38 nM and an IC₉₉ of 2.16 μM. Semi-logarithmic line graph showing HSV-1 plaquing efficiency plotted against the logarithm of dUY11 concentration (**A**) and table summarizing inhibitory concentration (IC) of dUY11 against HSV-1 infectivity (**B**). HSV-1 KOS (200 plaque-forming units) were incubated with 0, 0.002, 0.007, 0.02, 0.07, 0.2, 0.7, 2, 7 or 20 μM dUY11 for 5 minutes at 37°C. Vero cells were then infected with the so-exposed virions for 1 hour, washed and overlaid with medium supplemented with 5% FBS and 2 % methyl cellulose (**A**). The concentration of dUY11 which inhibited 50 or 99% (IC₅₀ and IC₉₉, respectively) of HSV-1 infectivity were calculated using Prism software (nonlinear regression curve fit) (**B**). Error bars, standard deviation of twenty-two experiments (**A**).

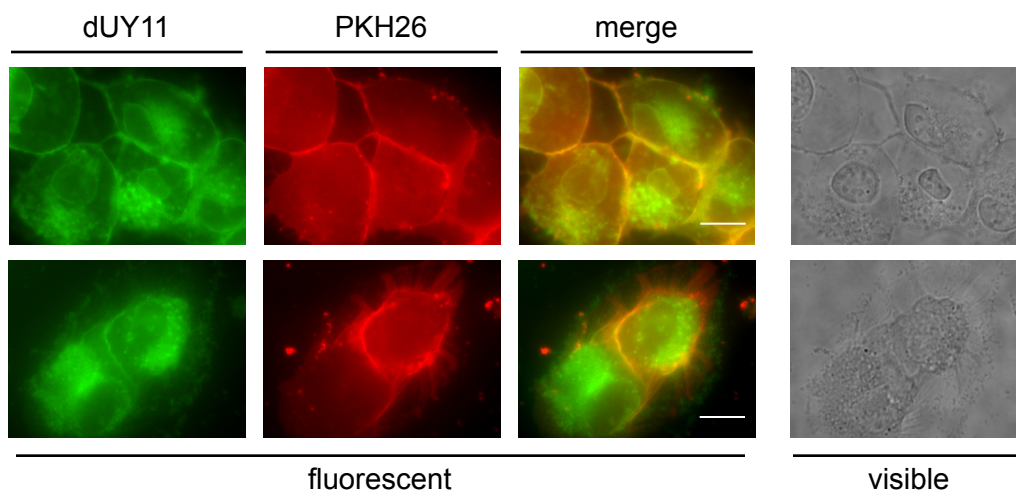


Figure 3.4 dUY11 localizes to cell membranes. Photographic images showing dUY11 cellular localization. Vero cells were treated at 37°C with 200 nM dUY11 for 30 minutes followed by a 5 minute incubation with 250 nM PKH26 membrane dye. Following lipid labeling, cells were washed and evaluated by fluorescence microscopy (**fluorescent**, left panels) or visible light (**visible**, right panels). Images were taken at 1,000 magnifications. Approximate scale bar, 5 μ m.

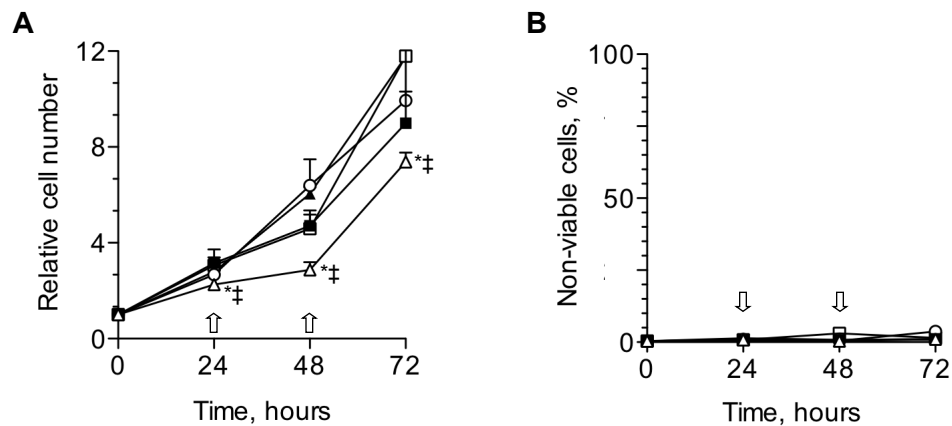


Figure 3.5 dUY11 has no cytotoxic effects and is only mildly cytostatic. Line graphs showing relative cell numbers (**A**) and percent non-viable cells (**B**) plotted against time of dUY11 exposure. Mock-infected Vero cells were treated with 0 (▲), 7 (□), 20 (○), 70 (■) or 150 (△) μM dUY11. Media was replaced with fresh media supplemented with 0, 7, 20, 70 or 150 μM of dUY11 every 24 hours (block arrows). Viable (**A**) and non-viable (**B**) cells were counted by trypan blue exclusion at 0, 24, 48 and 72 hours. Non-viable cells accounted for less than 4% of total cells for all samples at all times (**B**). Error bars represent ranges of duplicate samples from one experiment, except for (*), where they represent ranges of duplicate counts of one sample. ‡150 μM dUY11 forms aggregates.

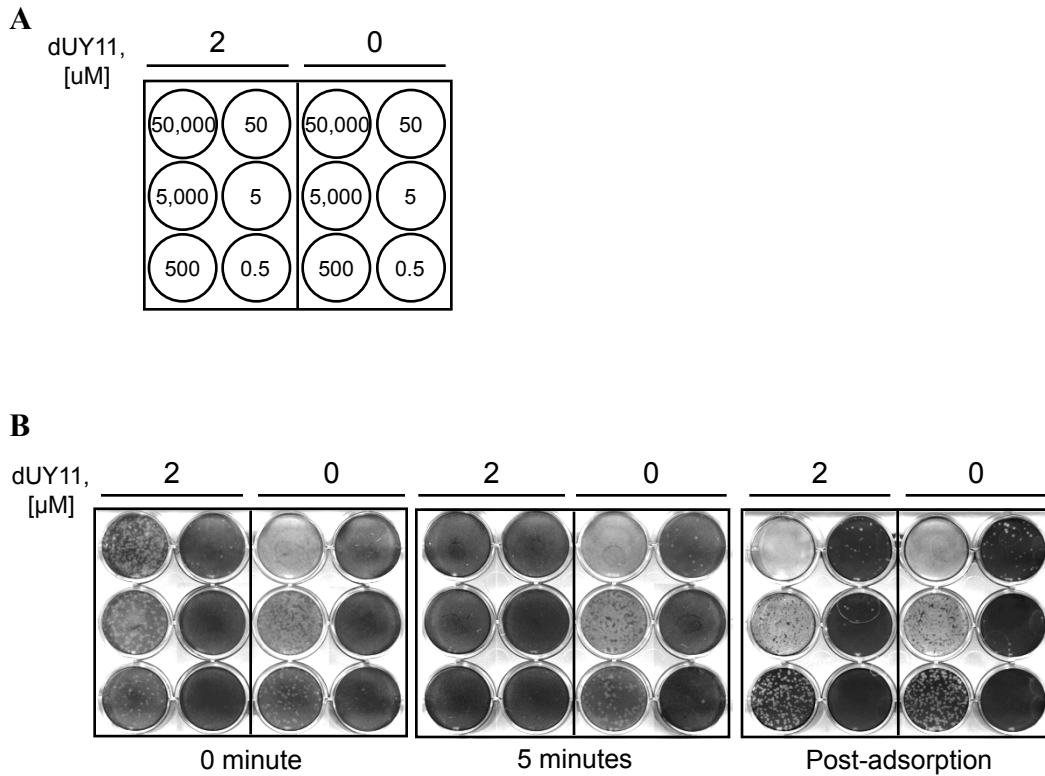


Figure 3.6 dUY11 exposure in semi-solid media after adsorption of HSV-1 virions does not inhibit plaquing. Vero cells were infected with 50,000; 5,000; 500; 50; 5; or 0.5 plaque-forming units of HSV-1 virions, as indicated in the cartoon **(A)**. HSV-1 KOS inocula were pre-exposed at 37°C for 0 or 5 minutes with 2 μ M dUY11 (**2**, left half of leftmost and middle panels) or DMSO vehicle (**0**, right half of leftmost and middle panels). Infected cells were washed and overlaid with semi-solid medium **(B)**. Alternatively, Vero cells were infected with untreated virions and overlaid with semi-solid medium supplemented with 2 μ M dUY11 (**2**, left half of rightmost panel) or DMSO vehicle (**0**, right half of rightmost panel; Post-adsorption) **(B)**.

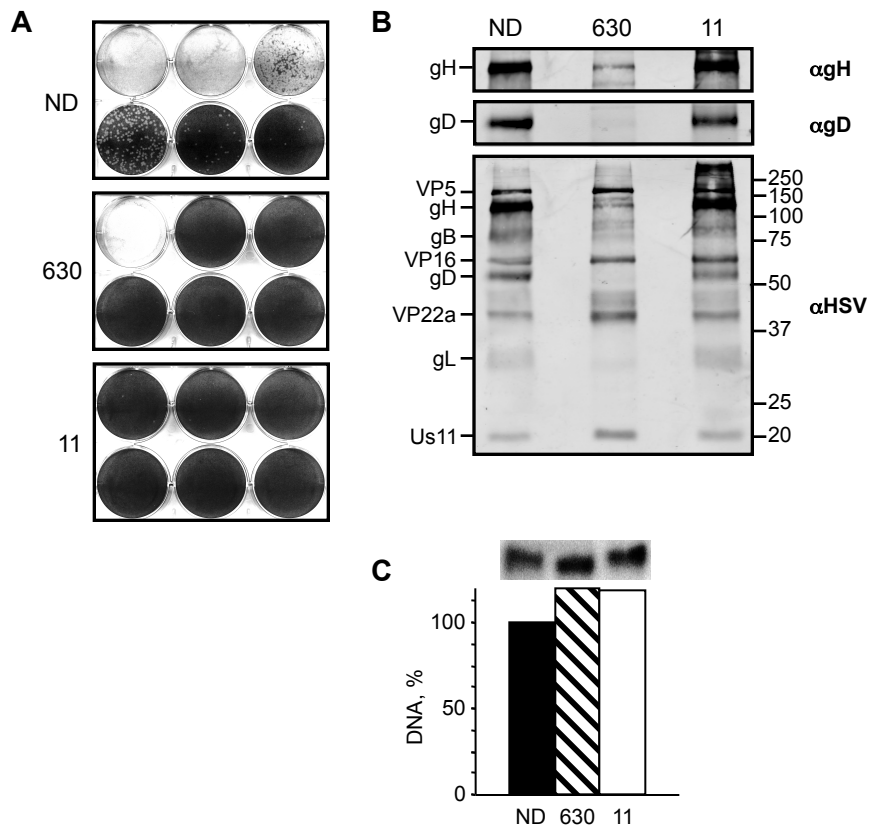


Figure 3.7 dUY11 does not lyse HSV-1 virions. Photographic images and bar graphs showing virion infectivity (**A**) and protein (**B**) or DNA (**C**) levels. HSV-1 virions were pre-exposed at 37°C for 5 min to no drug (**ND**; top panel, **A**; left lane, **B**; black bar, **C**), 1.5% IgePal CA-630 (**630**; middle panel, **A**; center lane, **B**; striped bar, **C**), or 7 μ M dUY11 (**11**; bottom panel, **A**; right lane, **B**; open bar, **C**). The so-exposed virions were analyzed for infectivity by standard plaque assays (**A**). Alternatively, the so-exposed virions were sucrose-purified, lysed and virion protein (**B**) or DNA (**C**) levels were analyzed by Western (**B**) or Southern (**C**) blot, respectively. Proteins were detected by monoclonal antibodies against gH (α gH, top panel), gD (α gD, middle panel) or by molecular weight following detection using a polyclonal anti-HSV-1 antibody (α HSV, bottom panel) (**B**).

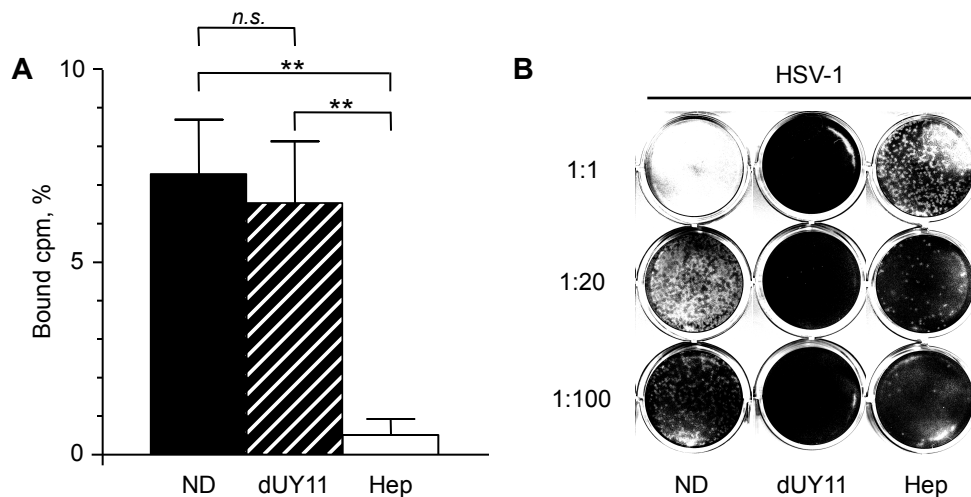


Figure 3.8 dUY11 does not inhibit total HSV-1 binding. Bar graph and photographic image showing total HSV-1 binding **(A)** or infectivity **(B)**. ³⁵S-methionine radiolabeled **(A)** or not **(B)** HSV-1 KOS was pretreated with no drug **(ND)**, 7 μ M dUY11 **(dUY11)** or 100 μ g/mL heparin **(Hep)**. Cooled samples were diluted 1:10, 1:20, or 1:100 in ice-cold serum-free media supplemented with 0 or 7 μ M dUY11, or 100 μ g/mL heparin, and adsorbed onto Vero cells at 4°C for 60 minutes. Cells were then washed with ice-cold serum-free medium supplemented with 0 or 7 μ M dUY11, or with 100 μ g/mL heparin, and lysed **(A)**. Alternatively, cells were overlaid with semi-solid medium with no drug, then fixed and stained when plaques were clearly visible **(B)**. Percent of virions bound to cells **(A)** were quantitated by liquid scintillation. Error bars, standard deviation of three experiments **(A)**. *n.s.*, not significant ($P>0.05$); **, $P<0.01$. 216

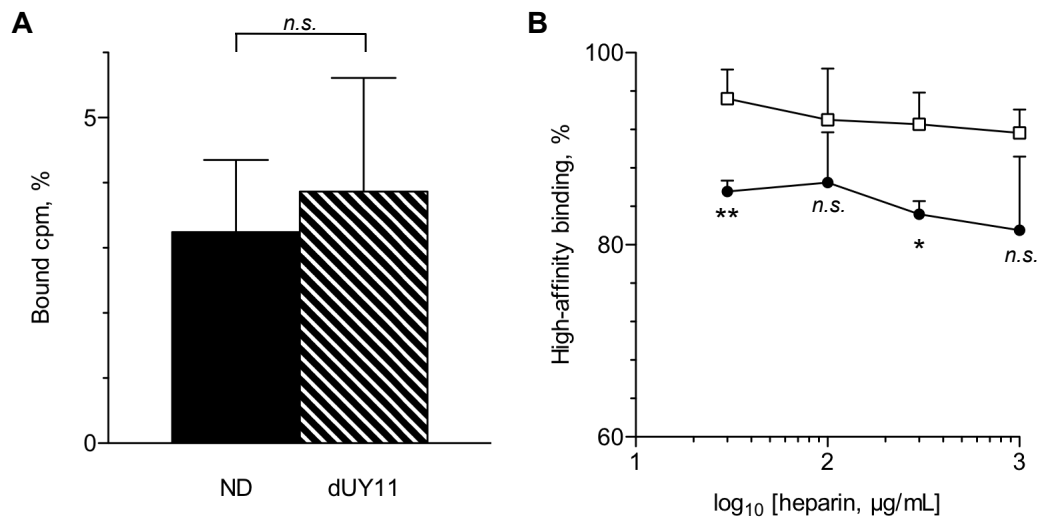


Figure 3.9 dUY11 does not inhibit high-affinity HSV-1 binding. Bar and semi-logarithmic line graph showing total (**A**) or high-affinity (**B**) HSV-1 binding. [³⁵S]-methionine radiolabeled HSV-1 KOS were pretreated with no drug (ND, black bar, **A**; ●, **B**) or with 7 µM dUY11 (dUY11, striped bar, **A**; □, **B**) for 5 minutes at 37°C. Cooled samples were diluted 1:10, 1:20, or 1:100 in ice-cold serum-free media supplemented with 0 or 7 µM dUY11 and absorbed onto Vero cells at 4°C for 15 minutes. Cells were then washed with ice-cold serum-free medium supplemented with 0 or 7 µM dUY11 and lysed (**A**) or washed for 1 more hour with ice-cold serum-free media supplemented with 0, 30, 100, 300 or 1,000 µg/mL of heparin (**B**). Percent of virions bound to cells (**A**) or removed by heparin (**B**) were quantitated by liquid scintillation. Error bars represent the range of two experiments (**A**) or the standard deviation of six experiments (**B**). *n.s.*, not significant ($P > 0.05$); *, $P < 0.05$; **, $P < 0.01$.

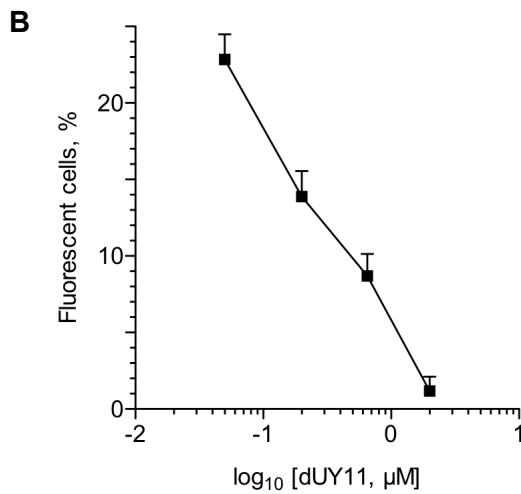
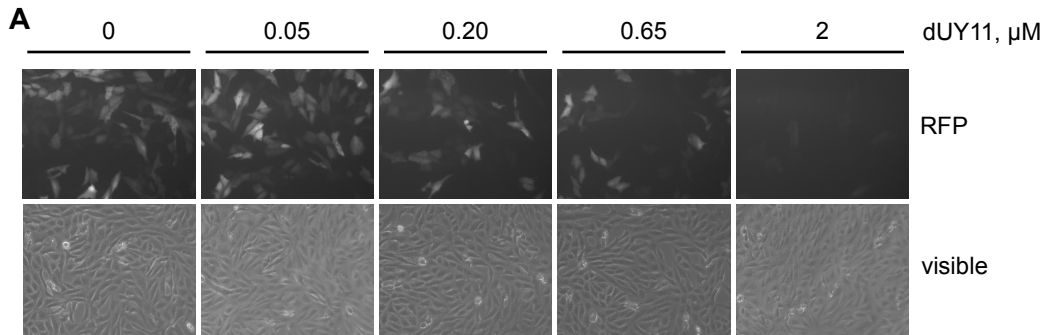


Figure 3.10 dUY11 inhibits HSV-1 entry. Representative pictures (**A**) and quantitation (**B**) of red fluorescent protein (RFP) expression in Vero cells containing a RFP reporter gene recombined into their cellular genomes under the control of an HSV-1 ICP0 promoter. Cells were infected with UV-inactivated HSV-1 KOS virions pretreated with 0, 0.05, 0.2, 0.65 or 2 μM dUY11 and visualized 24 hours later by fluorescence microscopy (**RFP**, top panels) and visible light (**visible**, bottom panels) (**A**) at 200 magnifications. Total number of fluorescent and visible cells were quantitated from images recorded 24 hours post-infection and are expressed as percent fluorescence against the logarithm of dUY11 concentration (**B**). Error bars, standard deviation of counts from four microscopic fields with similar cell densities.

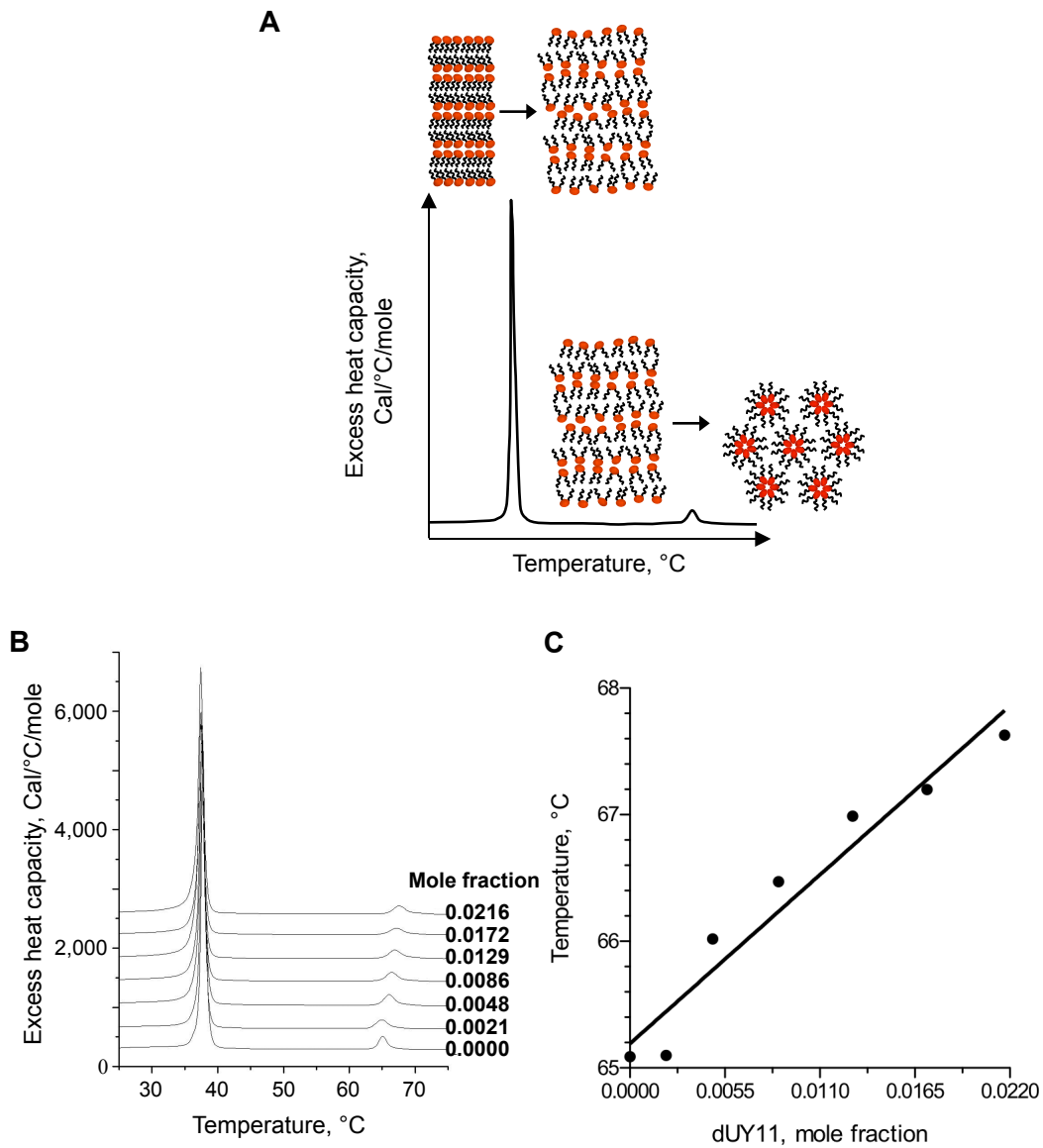


Figure 3.11 dUY11 inhibits lamellar to inverted-hexagonal phase transitions. Cartoon representation (**A**) of phase transition thermograms measured by differential scanning calorimetry (**B**) and corresponding line graph (**C**) showing the effects of dUY11 on phase transitions of dielaidoylphosphatidylethanolamine (DEPE). The first and second peaks represent transitions from gel-to-fluid or lamellar to inverted-hexagonal phases, respectively (**A,B**). DEPE lipid films containing dUY11 at increasing mole fraction were prepared. Samples were loaded into a scanning calorimeter and excess heat capacity measured to monitor the effect of dUY11 on lamellar to inverted-hexagonal phase transition (**B**). Maximal energy in (**B**) were used to produce (**C**). The thermograms are representative of three experiments (**B**). 219

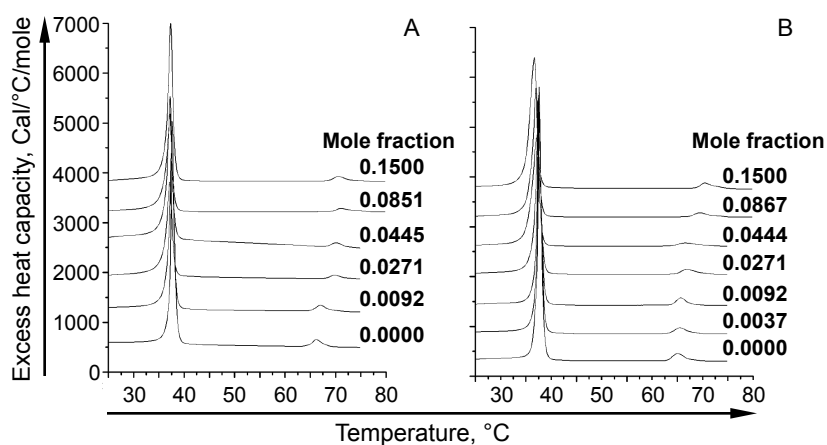


Figure 3.12 dUY2 and dUY4 inhibit lamellar to inverted-hexagonal phase transitions. Differential scanning calorimetry thermograms of dUY2 (**A**) and dUY4 (**B**) in dielaidoylphosphatidylethanolamine (DEPE). DEPE lipid films containing the indicated mole fraction of RAFI (from 0 to 0.15) were prepared. Samples were loaded into a scanning calorimeter and excess heat capacity measured to monitor the effect of RAFIs on lamellar to inverted-hexagonal phase transition.

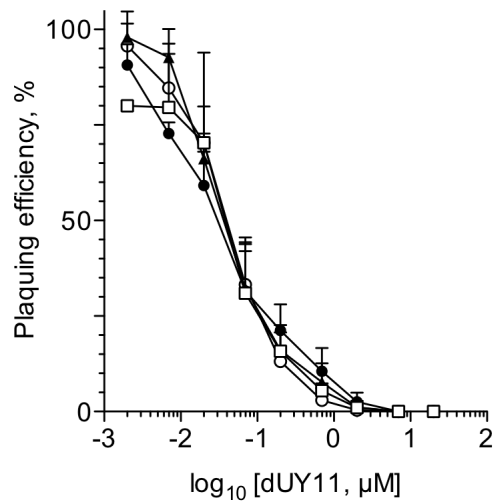


Figure 3.13 dUY11-mediated inhibition of HSV-1 infectivity is independent of cell type. Semi-logarithmic line graph showing HSV-1 plaquing efficiency against the logarithm of dUY11 concentration for different cell types. HSV-1 KOS (200 plaque-forming units) was pre-incubated for 5 min at 37°C with 0, 0.002, 0.007, 0.02, 0.07, 0.2, 0.7, 2, 7 or 20 μM dUY11. HEK293 (●), HFF (□), HeLa (▲), or Vero cells (○) were then infected with the so-exposed virions, and plaques counted. Error bars, standard deviation of three or more experiments. $P > 0.05$.

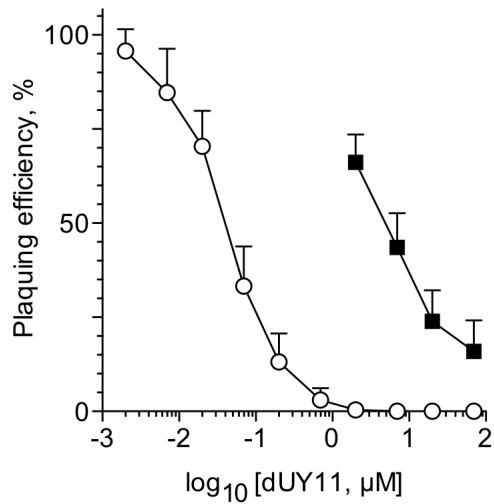


Figure 3.14 dUY11 primarily targets virion envelopes. Semi-logarithmic line graph showing HSV-1 plaquing efficiency plotted against the logarithm of dUY11 concentration. HSV-1 KOS (200 plaque-forming units) were incubated with 0, 0.002, 0.007, 0.02, 0.07, 0.2, 0.7, 2, 7, 20 or 70 μM dUY11 for 5 minutes at 37°C. Vero cells were then infected with the so-exposed virions for 1 hour, washed and overlaid with semi-solid medium with no drug (\circ). Alternatively, untreated inocula were used to infect Vero cells pretreated at 37°C for 15 to 60 min with 0, 2, 7, 20 or 70 μM dUY11 (\blacksquare). Maximum inhibition is 100% for virion pretreatment, or 75 % for cell pretreatment. Error bars, standard deviation of four or more experiments. $P < 0.001$.

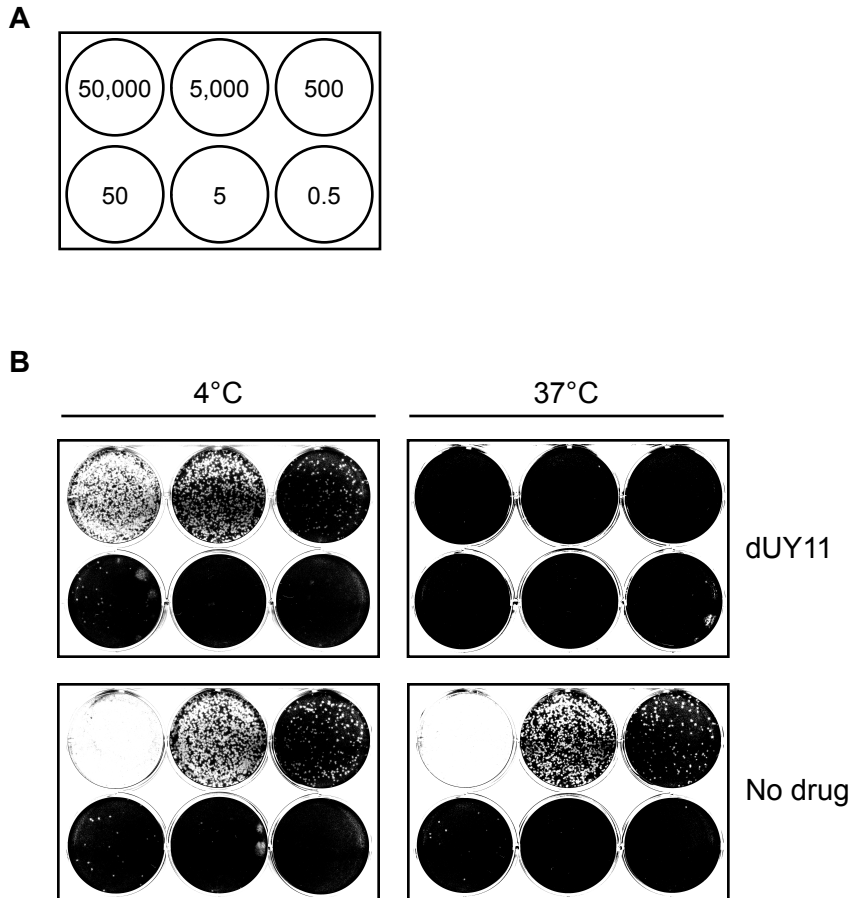


Figure 3.15 dUY11 inhibits HSV-1 infectivity only when virions with fluid envelopes are exposed to it. Cartoon representation (A) and photographic images (B) showing HSV-1 plaquing. HSV-1 KOS inocula were pre-exposed on ice (4°C, left panels) or in a 37°C water bath (37°C, right panels) for 5 minutes with 2 μM dUY11 (dUY11, top panels) or DMSO vehicle (No drug, bottom panels) (B). Vero cells were infected with 50,000; 5,000; 500; 50; 5; or 0.5 plaque-forming units of the so-exposed HSV-1 virions, as indicated in the cartoon (A), washed and overlaid with semi-solid medium.

CHAPTER 4: THE CHARACTERIZATION OF THE SPECIFICITY OF RIGID AMPHIPATHIC FUSION INHIBITORS

This chapter contains unpublished results and published work. (St.Vincent, MR et al. Proceedings of the National Academy of Sciences of the USA 107:17339-17344)

4.1 Introduction

The specificity for only one virus, or even a subgroup of one virus, is among the major limitations of current antivirals targeting proteins. For example, maraviroc is specific to human immunodeficiency virus (HIV) variants that engage CCR5 as co-receptor, having no effect on those that engage CXCR4 (Scarlati et al., 1997; Westby et al., 2007). Ribavirin with pegylated interferon- α are only effective against hepatitis C virus (HCV) genotype 2 or 3, with sustained virological response (SVR) achieved in approximately 80% of individuals infected with HCV genotype 2 or 3, but less than 50% of patients infected with genotype 1 (Schinazi, Bassit, and Gavegnano, 2010). Drug specificity is also further limited for viruses that display a high prevalence of intra-patient variants or heterogeneity, such as HCV (Gonzalez-Candelas, Bracho, and Moya, 2003). Current antiviral strategies targeting viral proteins are not useful during outbreaks caused by emerging viral pathogens either, since the proteins have to first be characterized before new drugs can be developed (Schang, 2006). Alternative, broad-spectrum antiviral strategies are needed.

Viral entry is an attractive antiviral target, as drugs targeting entry can prevent infection altogether (Teissier, Penin, and Pecheur, 2011). Entry of enveloped viruses requires fusion between virion and cell membranes. Fusion is initiated by interactions between virion (glyco)proteins and cell receptors (White et al., 2008). Although the glycoproteins and (co-)receptors required for viral fusion are functionally similar, they are not conserved among different virus families (Weissenhorn, Hinz, and Gaudin, 2007). In contrast, the general mechanisms of lipid membrane fusion are well conserved among otherwise unrelated enveloped viruses (Epanand, 2003). Entry of all enveloped viruses is similarly dependent on the formation of local negative curvature for the hemifusion stalk (Chernomordik and Kozlov, 2008). The energetically costly transitions required for any viral fusion occur using only the limited energy released by virion glycoprotein attachment, binding and rearrangements (Basanez, 2002). Targeting the unique roles of envelope lipids in viral fusion could thus lead to the development of antivirals with broad-spectrum activities.

A number of important human viral pathogens, such as HIV, HCV, hepatitis B virus (HBV), herpes simplex virus type-2 (HSV-2) and influenza, all contain a host-cell derived lipid bilayer (envelope). There is an urgent need for effective strategies against these important human pathogens. The development of small molecules that disfavor the conserved formation of negative envelope curvature during fusion is an interesting antiviral strategy. Such novel small molecules should in theory have broader activities than current approaches targeting proteins.

In **chapter 3**, I described the characterization of small molecules, the rigid amphipathic fusion inhibitors, or RAFIs, which target lipid bilayers to inhibit herpes simplex virus type-1 (HSV-1) infectivity. The most potent RAFI, dUY11, primarily targeted HSV-1 virion envelopes (**Figures 3.13 to 3.16**) to inhibit fusion (**Figures 3.7 to 3.10**). Virion envelopes are a lipid bilayer with embedded glycoproteins. Viral glycoproteins are not highly conserved among distantly related viruses (Backovic and Jardetzky, 2009; Kielian, 2006; Kielian and Rey, 2006). In contrast, the envelope lipid composition is generally well-conserved, and the formation of negative curvature is required for fusion of any enveloped virus (Chernomordik and Kozlov, 2005). RAFIs thus have the potential to inhibit a broad-spectrum of viruses. Under the proposed mechanism of action, RAFIs would be expected to inhibit the infectivity of otherwise unrelated enveloped viruses, but not that of nonenveloped viruses.

I therefore tested the activities of dUY11, the most potent RAFI identified, against the infectivity of several viruses. In this chapter, I report the activities of dUY11 against the infectivity of enveloped and nonenveloped viruses. Compound dUY11 inhibited the infectivity of several otherwise unrelated enveloped viruses, including HCV and HSV-2. Consistent with the proposed target and mechanism of action, however, dUY11 was inactive against the two nonenveloped viruses tested.

4.2 Results

Under the proposed model, small molecules of appropriate molecular shape can be designed to target envelope bilayers and inhibit virion infectivity. My hypothesis is that insertion of such rigid, amphipathic small molecules into virion envelopes would prevent the lipid reorganizations necessary for the formation of the negative curvature that is required for the fusion of all enveloped viruses.

4.2.1 dUY11 inhibits the infectivity of closely related viruses

I first tested whether the target of dUY11 is conserved among closely related viruses. I evaluated the infectivity of two strains of HSV-2, a laboratory-adapted strain and a clinical isolate (333 and 186, respectively). Like that of HSV-1, the fusion of HSV-2 envelopes with plasma membranes is mediated by glycoprotein B (gB), gD, and gH/gL (Muggeridge, 2000; Turner et al., 1998). HSV-2, however, uses nectin-2 as a receptor more efficiently than HSV-1 does, and does not use 3-O-sulphated heparin sulphate (Cocchi et al., 2000; Geraghty et al., 1998; Shukla et al., 1999).

Two hundred infectious HSV-1 or HSV-2 virions were exposed to increasing concentration of dUY11 for 5 minutes at 37°C. Vero cell monolayers were then infected with the so-exposed virions and their infectivity was assessed by plaquing efficiency. dUY11 inhibited infectivity of all three HSV strains tested (HSV-1 KOS, closed circle; HSV-2 186, open square; HSV-2 333, closed triangle; **Figure 4.1**) with similar IC_{50} (IC_{50} (95% CI, μ M); 0.038 (0.035 to 0.041), 0.039 (0.033 to 0.045), or 0.044 μ M (0.039 to 0.050) for HSV-1 KOS,

HSV-2 186, or HSV-2 333, respectively; **Table 4.1**; $P > 0.05$). The target of dUY11 is therefore conserved among viruses that have relatively conserved glycoproteins, but different receptor preferences.

4.2.2 dUY11 inhibits the infectivity of otherwise unrelated enveloped viruses

I next tested the effects of dUY11 on enveloped viruses that are only distantly related. I selected vesicular stomatitis virus (VSV), Sindbis virus (SIN) and vaccinia virus (VV). VSV and SIN are two negative-sense RNA viruses with no known glycoprotein conservation with HSV-1 or -2 and which bind different cellular receptors. Sindbis glycoprotein E binds to the high-affinity laminin receptor (Wang et al., 1992), whereas the receptor for VSV G-protein has yet to be identified (Coil and Miller, 2004). Both SIN and VSV enter by clathrin-mediated endocytosis (Cureton et al., 2009; Glomb-Reinmund and Kielian, 1998), further contrasting with HSV-1 and HSV-2, which fuse to plasma membranes by pH-independent mechanisms in most cell types including Vero cells (Wittels and Spear, 1991). VV was selected as an atypical enveloped virus. Several distinct virion forms are reported, including the single-enveloped intracellular mature virus (MV), the double-enveloped extracellular enveloped virus (EV) and cell-associated virus (CEV). Intracellular naked virions are also reportedly infectious, depending on the strain (Payne and Norrby, 1978). Multiple entry pathways are proposed (Whitbeck et al., 2009), and may involve the nonfusogenic dissolution of the outer envelope of virions (Law et al., 2006; Schmidt et al., 2011).

Two hundred infectious HSV-1, VSV, SIN or VV virions (consisting of mixed infectious forms) were incubated with media containing increasing dUY11 concentration for 5 minutes at 37°C. Vero cell monolayers were then infected with the so-exposed virions and infectivity was assessed by plaquing efficiency. dUY11 inhibited the infectivity of all tested enveloped viruses (HSV-1, closed circle; VSV, open triangle; SIN, closed square; VV; closed inverted-triangle; **Figure 4.1**) and, except for VV, with similar IC_{50} (IC_{50} (95% CI, μ M); 0.038 (0.035 to 0.041), 0.005 (0.004 to 0.006), 0.011 (0.008 to 0.013), or 19 μ M (11 to 31) for HSV-1 KOS, VSV, SIN or VV, respectively; **Table 4.1**; $P > 0.05$ for all pairwise comparisons except VSV or SIN vs. HSV-1, $P < 0.05$). The target of dUY11 is therefore conserved among otherwise unrelated enveloped viruses, which fuse to different cellular membranes using unrelated glycoproteins which bind to different cell surface receptors. dUY11 was less potent against VV infectivity, with an IC_{50} up to 3,718-fold higher than the other enveloped viruses tested (IC_{50} against VV infectivity, compared to VSV; **Table 4.1**; $P < 0.001$). The higher IC_{50} against VV infectivity could result from the double-enveloped virion, for example, which may quench the drug. A nonfusogenic dissolution of the outer envelope of exposed virions could also contribute to the lower potency of dUY11 against VV (Law et al., 2006; Schmidt et al., 2011).

4.2.3 dUY11 inhibits the infectivity of hepatitis C virus

Compound dUY11 inhibited the infectivity of all the enveloped viruses I had tested (**Figure 4.1**, **Table 4.1**). I then tested another important enveloped human

pathogen, HCV. HCV likely uses several different routes of internalization requiring the E1/E2 glycoproteins and at least one of several identified receptors or co-receptors, namely scavenger receptor class B, type I (Scarselli et al., 2002), cluster of differentiation 81 (Pileri et al., 1998), and tight junction components claudin 1 (Evans et al., 2007) and occludin (Ploss et al., 2009). Like SIN and HSV-2, then, HCV binds (structurally unrelated) components of tight junctions that function in cell adhesion. Like that of SIN and VSV, HCV entry may depend on clathrin-mediated endocytosis (Blanchard et al., 2006; Coller et al., 2009). In contrast to HSV-2 and -1, which fuse to plasma membranes by pH-independent mechanisms, HCV fuses with target membranes by mechanisms that are likely pH-dependent (von Hahn and Rice, 2008).

To test the effects of dUY11 on HCV infectivity, 5 HCV genome copy equivalents per cell were exposed to increasing dUY11 concentration for 5 minutes at 37°C. Huh7.5 cells were then infected with the so-exposed virions. Viral infectivity was indirectly assessed 4 days later by the levels of expression of the HCV non-structural protein 3 (NS3) in infected cells.

Exposure to dUY11 prior to infection reduced the level of HCV NS3 at 4 days after infection (**Figure 4.2A**) in a dose dependent manner (**Figure 4.2B**), with an apparent IC_{50} of 0.221 μ M (95% CI, 0.170 to 0.286 μ M; **Table 4.1**). dUY11 therefore also inhibits the infectivity of another important enveloped human pathogen, HCV.

4.2.4 Treatment of infected cells with dUY11 inhibits the levels of Sindbis virus infectivity

dUY11 was originally described as having no effect on SIN virus replication (IC_{50} , $>497.5 \mu\text{M}$; or $>250 \mu\text{g/mL}$) (Andronova et al., 2003). dUY11 was therefore proposed to be specific against HSV replication. However, dUY11 potentially inhibited the infectivity of SIN virus when virions were directly exposed to it before infection (IC_{50} , $0.011 \mu\text{M}$ (95% CI, 0.008 to $0.013 \mu\text{M}$); **Figure 4.1**, **Table 4.1**). In the studies conducted by Andronova et al., the antiviral effects of dUY11 were assessed by treating already-infected cells, and then evaluating virus-induced cytopathic effect (CPE) microscopically. I therefore next evaluated the infectivity in cells treated with dUY11 only after infection with SIN.

Untreated Vero cells were infected with untreated SIN virions (at a multiplicity of infection (MOI) of 3 plaque-forming units (PFU) per cell). Inocula were removed 1 hour later and the infected cells were treated with media containing increasing concentrations of dUY11 continuously for 23 hours, or for only 1 hour (from 1 to 2 hours after infection). For the latter treatment, dUY11-containing media was removed after a 1-hour treatment (2 hours after infection), and the cells were washed to remove any residual drug. The cells were then overlaid with complete medium without drug. The supernatants were harvested 24 hours after infection and the levels of progeny infectivity were evaluated by plaquing efficiency.

Continuous treatment with dUY11 for 23 hours after infection of cells inhibited the levels of progeny SIN infectivity (open square, **Figure 4.3**).

Likewise, treatment of previously infected cells with dUY11 for even only 1 hour inhibited the levels of infectivity (filled squares, **Figure 4.3**). The IC_{50} against SIN infectivity was 183-fold lower when the infected cells were treated continuously for 23 hours than when they were treated for only 1 hour after infection (IC_{50} (95% CI, μM); 0.008 (0.006 to 0.012) or 1.464 μM (1.146 to 1.870) for 23- or 1-hour treatment, respectively; **Table 4.2**; $P < 0.001$). Continuous treatment of SIN-infected cells with dUY11 for 23 hours resulted in near-identical IC_{50} as direct dUY11 exposure of SIN virions before infection (IC_{50} , 0.011 μM for virion pre-exposure, **Figure 4.1** and **Table 4.1**; compared to 0.008 μM for continuous treatment of infected cells; **Figure 4.3** and **Table 4.2**; $P > 0.05$). These results suggest that progeny virions released from continuously treated cells are efficiently exposed to the drug in the extracellular medium, and rendered non-infectious. In contrast, progeny virions produced by cells treated for only 1 hour after infection would not be exposed to drug in the extracellular medium. They could, however, acquire it with pre-existing cellular factors such as membrane lipids during their assembly, for example. dUY11 localized to cell membranes (**Figure 3.4**), and assembling virions likely acquired it by budding into cellular membranes where the drug is localized.

4.2.5 dUY11 does not inhibit the infectivity of nonenveloped viruses

Under the proposed model and hypothesis, RAFIs interact with virion envelope bilayers to inhibit fusion by preventing the formation of the negative curvature required for the hemifusion stalk. Consistently, dUY11 inhibited the infectivity of

all of the enveloped viruses tested. According to the model, nonenveloped viruses, which lack the target membrane, should not be inhibited by RAFIs. I therefore next tested the antiviral activities of dUY11 on two nonenveloped viruses, poliovirus (PV) and adenovirus (AdV). PV binds to cluster of differentiation 155 (CD155) whereas AdV fiber protein binds to Coxsackie and adenovirus receptor (CAR) (Bergelson et al., 1997). Both these receptors are distantly related to HveA, in that they too belong to the immunoglobulin superfamily. PV and AdV differ in their mechanisms of cell entry. PV penetrates cells by direct RNA uncoating, whereas AdV does so by endocytosis (Tsai, 2007).

Two hundred infectious PV virions were exposed to increasing concentrations of dUY11 for 5 minutes at 37°C. Vero cell monolayers were then infected with the so-exposed virions and infectivity was assessed by plaquing efficiency. For the studies on AdV, recombinant AdV or HSV-1 virions expressing green fluorescent protein (GFP) reporter genes were pre-exposed to increasing concentrations of dUY11. HEK293 cells were then infected with the so-exposed virions and viral infectivity was assessed by GFP expression.

dUY11 did not inhibit the infectivity of PV at any tested concentration, up to 200 μ M (**Figure 4.4A**, **Table 4.1**). No dUY11 concentration inhibited GFP expression in HEK293 cells infected with GFP AdV pre-exposed to dUY11, either (filled square, **Figure 4.4B**). In contrast, 2 μ M dUY11 fully inhibited GFP expression when GFP-HSV-1 virions were exposed before infection (open circle, **Figure 4.4B**), as expected (**Figures 3.3** and **4.1**). Equal percent of cells expressed GFP when GFP HSV-1 or AdV virions were pre-exposed in the absence of drug

(5% fluorescent cells; **Figure 4.4B**). Therefore, dUY11 inhibits a step of entry conserved among otherwise unrelated enveloped viruses, but not with nonenveloped viruses.

4.3 Discussion

The novel small molecule fusion inhibitors I discovered were characterized in **chapter 3**. RAFIs interact with virion lipid bilayers and inhibit the formation of the negative curvature required for their fusion to cell membranes. In this chapter, I identified a spectrum of viruses inhibited by the most potent RAFI, dUY11. Consistently with the proposed targets, dUY11 was active against all seven enveloped viruses tested (**Figures 4.1** and **4.2**), but not against the two nonenveloped viruses tested (**Figure 4.4**). The RAFIs described in **chapter 3** are the first nucleoside derivatives that inhibit viral fusion, and the first reported broad-spectrum small molecule inhibitors of viral infectivity that target envelope bilayer curvature transition (**chapter 4**).

The fusion of otherwise unrelated enveloped viruses is similarly dependent on the formation of negative curvature (Chernomordik and Kozlov, 2005). In contrast to current antivirals, which are limited to only one or a few closely related viruses, therefore, small molecule inhibitors of viral fusion that target lipid bilayers to prevent the formation of negative curvature have the potential to have broader specificities. The mechanisms of antiviral action elucidated and the model proposed in **chapter 3** are thus further supported by the activities of dUY11 against several otherwise unrelated enveloped viruses (which

bind to unrelated receptors and have no glycoprotein sequence homology), and the lack of activity against the two nonenveloped viruses tested.

I was unable to reproduce previous findings that members of this family of compounds were inactive against SIN (dUY11 IC_{50} , $>497.5 \mu\text{M}$) (Andronova et al., 2003). However, different methods were used in those studies. Andronova et al. evaluated the development of virus-induced CPE microscopically (Andronova and Galegov, 2000). In those studies, already-infected cells were treated with dUY11 and virus-induced CPE was then evaluated by trypan blue staining. Under such treatment conditions, dUY11 did not protect the cells from virus-induced CPE resulting from primary infection. The authors therefore concluded that RAFIs were inactive against SIN. I used similar experimental conditions, by treating already-infected cells. However, I evaluated the antiviral effects by measuring levels of infectivity in the supernatants of infected cells. These treatment conditions did inhibit the levels of released progeny infectivity (**Figure 4.3**). From these results (**Figure 4.3**) and those of the infectivity assay (**Figure 4.1**), I concluded that dUY11 does in fact inhibit SIN, both directly (by exposing virions before adsorption) and by treating already-infected cells.

Current antivirals target specific viral proteins or their interactions with cellular ones, and thus promptly select for drug-resistant variants. In contrast, RAFIs target the unique function of envelope lipids in fusion, which are not encoded in their genome. Therefore, the barrier to selection for resistance may be higher than current strategies aimed at viral proteins. Moreover, the novel targets

and mechanism of action of RAFIs could make them useful even against viral strains resistant to clinical antivirals.

The largest class of clinical antivirals inhibits viral genome replication (**Table 1**). All but six of these are nucleoside or nucleotide derivatives (**Figure 1.1**), structural analogues of natural substrates of the target enzyme. RAFIs are nucleoside analogues. As other nucleoside derivatives, then, they could also inhibit HSV-1 DNA replication by targeting viral enzymes, as do clinically approved anti-HSV drugs such as acyclovir (Coen and Schaffer, 1980; Elion et al., 1977).

In this thesis, I have described the first broad-spectrum small molecule inhibitors of viral infectivity that target envelope bilayer curvature to inhibit fusion. This chapter serves as a proof-of-concept that small molecule fusion inhibitors targeting envelope lipid bilayers to prevent the formation of the negative curvature can inhibit the infectivity of otherwise unrelated enveloped viruses. Moreover, I have identified important human pathogens, for example HCV and HSV-2, which are potently inhibited by RAFIs.

4.4 References

- Andronova, V. L., and Galegov, G. A. (2000). [Comparative study of the reproduction of Sindbis virus sensitive and resistant to adamantane derivatives]. *Biull Eksp Biol Med* **129**(1), 86-9.
- Andronova, V. L., Skorobogaty, M. V., Manasova, E. V., Berlin Iu, A., Korshun, V. A., and Galegov, G. A. (2003). [Antiviral activity of some 5-arylethynyl 2'-deoxyuridine derivatives]. *Bioorg Khim* **29**(3), 290-5.
- Backovic, M., and Jardetzky, T. S. (2009). Class III viral membrane fusion proteins. *Current Opinion in Structural Biology* **19**(2), 189-196.
- Basanez, G. (2002). Membrane fusion: the process and its energy suppliers. *Cellular and Molecular Life Sciences* **59**(9), 1478-1490.
- Bergelson, J. M., Cunningham, J. A., Droguett, G., KurtJones, E. A., Krithivas, A., Hong, J. S., Horwitz, M. S., Crowell, R. L., and Finberg, R. W. (1997). Isolation of a common receptor for coxsackie B viruses and adenoviruses 2 and 5. *Science* **275**(5304), 1320-1323.
- Blanchard, E., Belouzard, S., Goueslain, L., Wakita, T., Dubuisson, J., Wychowski, C., and Rouille, Y. (2006). Hepatitis C virus entry depends on clathrin-mediated endocytosis. *Journal of Virology* **80**(14), 6964-6972.
- Chernomordik, L. V., and Kozlov, M. M. (2005). Membrane hemifusion: Crossing a chasm in two leaps. *Cell* **123**(3), 375-382.
- Chernomordik, L. V., and Kozlov, M. M. (2008). Mechanics of membrane fusion. *Nature Structural & Molecular Biology* **15**(7), 675-683.
- Cocchi, F., Menotti, L., Dubreuil, P., Lopez, M., and Campadelli-Fiume, G. (2000). Cell-to-cell spread of wild-type herpes simplex virus type 1, but not of syncytial strains, is mediated by the immunoglobulin-like receptors that mediate virion entry, nectin1 (PRR1/HveC/HIGR) and nectin2 (PRR2/HveB). *J Virol* **74**(8), 3909-17.
- Coen, D. M., and Schaffer, P. A. (1980). Two Distinct Loci Confer Resistance to Acycloguanosine in Herpes-Simplex Virus Type-1. *Proceedings of the National Academy of Sciences of the United States of America-Biological Sciences* **77**(4), 2265-2269.
- Coil, D. A., and Miller, A. D. (2004). Phosphatidylserine is not the cell surface receptor for vesicular stomatitis virus. *Journal of Virology* **78**(20), 10920-10926.
- Coller, K. E., Berger, K. L., Heaton, N. S., Cooper, J. D., Yoon, R., and Randall, G. (2009). RNA interference and single particle tracking analysis of hepatitis C virus endocytosis. *PLoS Pathog* **5**(12), e1000702.
- Cureton, D. K., Massol, R. H., Saffarian, S., Kirchhausen, T. L., and Whelan, S. P. (2009). Vesicular stomatitis virus enters cells through vesicles incompletely coated with clathrin that depend upon actin for internalization. *PLoS Pathog* **5**(4), e1000394.
- Elion, G. B., Furman, P. A., Fyfe, J. A., Demiranda, P., Beauchamp, L., and Schaeffer, H. J. (1977). Selectivity of Action of an Anti-Herpetic Agent, 9-(2-Hydroxyethoxymethyl)Guanine. *Proceedings of the National Academy of Sciences of the United States of America* **74**(12), 5716-5720.

- Epand, R. M. (2003). Fusion peptides and the mechanism of viral fusion. *Biochimica Et Biophysica Acta-Biomembranes* **1614**(1), 116-121.
- Evans, M. J., von Hahn, T., Tscherne, D. M., Syder, A. J., Panis, M., Wolk, B., Hatzioannou, T., McKeating, J. A., Bieniasz, P. D., and Rice, C. M. (2007). Claudin-1 is a hepatitis C virus co-receptor required for a late step in entry. *Nature* **446**(7137), 801-805.
- Geraghty, R. J., Krummenacher, C., Cohen, G. H., Eisenberg, R. J., and Spear, P. G. (1998). Entry of alphaherpesviruses mediated by poliovirus receptor-related protein 1 and poliovirus receptor. *Science* **280**(5369), 1618-20.
- Glomb-Reinmund, S., and Kielian, M. (1998). The role of low pH and disulfide shuffling in the entry and fusion of Semliki Forest virus and Sindbis virus. *Virology* **248**(2), 372-81.
- Gonzalez-Candelas, F., Bracho, M. A., and Moya, A. (2003). Molecular epidemiology and forensic genetics: application to a hepatitis C virus transmission event at a hemodialysis unit. *J Infect Dis* **187**(3), 352-8.
- Kielian, M. (2006). Class II virus membrane fusion proteins. *Virology* **344**(1), 38-47.
- Kielian, M., and Rey, F. A. (2006). Virus membrane-fusion proteins: more than one way to make a hairpin. *Nature Reviews Microbiology* **4**(1), 67-76.
- Law, M., Carter, G. C., Roberts, K. L., Hollinshead, M., and Smith, G. L. (2006). Ligand-induced and nonfusogenic dissolution of a viral membrane. *Proc Natl Acad Sci U S A* **103**(15), 5989-94.
- Muggeridge, M. I. (2000). Characterization of cell-cell fusion mediated by herpes simplex virus 2 glycoproteins gB, gD, gH and gL in transfected cells. *Journal of General Virology* **81**, 2017-2027.
- Payne, L. G., and Norrby, E. (1978). Adsorption and penetration of enveloped and naked vaccinia virus particles. *J Virol* **27**(1), 19-27.
- Pileri, P., Uematsu, Y., Campagnoli, S., Galli, G., Falugi, F., Petracca, R., Weiner, A. J., Houghton, M., Rosa, D., Grandi, G., and Abrignani, S. (1998). Binding of hepatitis C virus to CD81. *Science* **282**(5390), 938-941.
- Ploss, A., Evans, M. J., Gaysinskaya, V. A., Panis, M., You, H. N., de Jong, Y. P., and Rice, C. M. (2009). Human occludin is a hepatitis C virus entry factor required for infection of mouse cells. *Nature* **457**(7231), 882-886.
- Scarlatti, G., Tresoldi, E., Bjorndal, A., Fredriksson, R., Colognesi, C., Deng, H. K., Malnati, M. S., Plebani, A., Siccardi, A. G., Littman, D. R., Fenyo, E. M., and Lusso, P. (1997). In vivo evolution of HIV-1 co-receptor usage and sensitivity to chemokine-mediated suppression. *Nature Medicine* **3**(11), 1259-1265.
- Scarselli, E., Ansuini, H., Cerino, R., Roccasecca, R. M., Acali, S., Filocamo, G., Traboni, C., Nicosia, A., Cortese, R., and Vitelli, A. (2002). The human scavenger receptor class B type I is a novel candidate receptor for the hepatitis C virus. *Embo Journal* **21**(19), 5017-5025.
- Schang, L. M., St. Vincent, MR, Lacasse, JJ (2006). Five years of progress on cyclin-dependent kinases and other cellular proteins as potential targets for antiviral drugs. *Antiviral Chemistry & Chemotherapy* **17**, 293-320.

- Schinazi, R. F., Bassit, L., and Gavegnano, C. (2010). HCV drug discovery aimed at viral eradication. *Journal of Viral Hepatitis* **17**(2), 77-90.
- Schmidt, F. I., Bleck, C. K., Helenius, A., and Mercer, J. (2011). Vaccinia extracellular virions enter cells by macropinocytosis and acid-activated membrane rupture. *Embo J* **30**(17), 3647-61.
- Shukla, D., Liu, J., Blaiklock, P., Shworak, N. W., Bai, X., Esko, J. D., Cohen, G. H., Eisenberg, R. J., Rosenberg, R. D., and Spear, P. G. (1999). A novel role for 3-O-sulfated heparan sulfate in herpes simplex virus 1 entry. *Cell* **99**(1), 13-22.
- Teissier, E., Penin, F., and Pecheur, E. I. (2011). Targeting Cell Entry of Enveloped Viruses as an Antiviral Strategy. *Molecules* **16**(1), 221-250.
- Tsai, B. (2007). Penetration of nonenveloped viruses into the cytoplasm. *Annual Review of Cell and Developmental Biology* **23**, 23-43.
- Turner, A., Bruun, B., Minson, T., and Browne, H. (1998). Glycoproteins gB, gD, and gHgL of herpes simplex virus type 1 are necessary and sufficient to mediate membrane fusion in a Cos cell transfection system. *Journal of Virology* **72**(1), 873-875.
- von Hahn, T., and Rice, C. M. (2008). Hepatitis C virus entry. *Journal of Biological Chemistry* **283**(7), 3689-3693.
- Wang, K. S., Kuhn, R. J., Strauss, E. G., Ou, S., and Strauss, J. H. (1992). High-affinity laminin receptor is a receptor for Sindbis virus in mammalian cells. *J Virol* **66**(8), 4992-5001.
- Weissenhorn, W., Hinz, A., and Gaudin, Y. (2007). Virus membrane fusion. *Febs Letters* **581**(11), 2150-2155.
- Westby, M., Smith-Burchnell, C., Mori, J., Lewis, M., Mosley, M., Stockdale, M., Dorr, P., Ciaramella, G., and Perros, M. (2007). Reduced maximal inhibition in phenotypic susceptibility assays indicates that viral strains resistant to the CCR5 antagonist maraviroc utilize inhibitor-bound receptor for entry. *Journal of Virology* **81**(5), 2359-2371.
- Whitbeck, C. J., Foo, C. H., de Leon, M. P., Eisenberg, R. J., and Cohen, G. H. (2009). Vaccinia virus exhibits cell-type-dependent entry characteristics. *Virology* **385**(2), 383-391.
- White, J. M., Delos, S. E., Brecher, M., and Schornberg, K. (2008). Structures and mechanisms of viral membrane fusion proteins: Multiple variations on a common theme. *Critical Reviews in Biochemistry and Molecular Biology* **43**(3), 189-219.
- Wittels, M., and Spear, P. G. (1991). Penetration of Cells by Herpes-Simplex Virus Does Not Require a Low pH-Dependent Endocytic Pathway. *Virus Research* **18**(2-3), 271-290.

Virus	IC₅₀, μM (95% CI)
HSV-1 KOS	0.038 (0.035 to 0.041)
HSV-2 186	0.039 (0.033 to 0.045)
HSV-2 333	0.044 (0.039 to 0.050)
VSV	0.005 (0.004 to 0.006)
SIN	0.011 (0.008 to 0.013)
HCV	0.221 (0.170 to 0.286)
VV	19 (11 to 31)
PV*	>200
AdV*	>20

Table 4.1 IC₅₀ of dUY11 against enveloped and nonenveloped viruses.

Table summarizing the 50% inhibitory concentration (IC₅₀) and 95% confidence interval (CI) of dUY11 against the infectivity of HSV-1 KOS, HSV-2 186, HSV-2 333, VSV, SIN, HCV, VV, PV and AdV. The IC₅₀ and 95% CI were calculated from three or more experiments using Prism software (nonlinear regression curve fit). *No concentration tested inhibited the infectivity of poliovirus (PV) or adenovirus (AdV) by 50%. HSV-1, herpes simplex virus type-1; HSV-2, herpes simplex virus type-2; VSV, vesicular stomatitis virus; SIN, Sindbis virus; HCV, hepatitis C virus; VV, vaccinia virus.

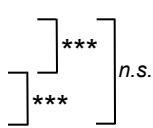
Infectivity	IC₅₀, μM (95% CI)	
Exposed SIN virions	0.011 (0.008 to 0.013)	
Released SIN progeny from cells treated for 1 hr	1.464 (1.146 to 1.870)	
Released SIN progeny from cells treated for 23 hrs	0.008 (0.006 to 0.012)	

Table 4.2 IC₅₀ of dUY11 against SIN infectivity by direct exposure of infecting virions or by treating cells for 1- or 23-hours after infection.

Table summarizing the 50% inhibitory concentration (IC₅₀) and 95% confidence interval (CI) for dUY11 against the infectivity of Sindbis (SIN) virions directly exposed before adsorption, or against the levels of progeny infectivity released from cells treated with dUY11 for 1- or 23-hours after SIN infection. The IC₅₀, 95% CI and P-values were calculated from four experiments using Prism software (unconstrained three parameter nonlinear regression curve fit for direct virion exposure, or constrained four parameter nonlinear regression curve fit for cell treatment). *n.s.*, not significant (P>0.05); ***, P<0.001.

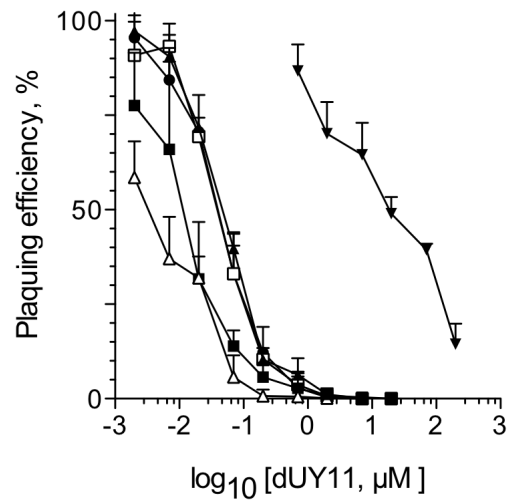


Figure 4.1 dUY11 inhibits the infectivity of otherwise unrelated enveloped viruses. Semi-logarithmic line graphs showing plaquing of HSV-1 strain KOS (●), HSV-2 strain 186 (□), HSV-2 strain 333 (▲), VSV (△), SIN (■), or VV (▼) plotted against the logarithm of dUY11 concentration. Virions (200 PFU) were incubated with 0, 0.002, 0.007, 0.02, 0.07, 0.2, 0.7, 2, 7, 20 or 70 μM dUY11 for 5 minutes at 37°C. Vero cells were then infected with the so-exposed virions to assess infectivity. Error bars, standard deviation of three or more experiments. HSV-1, herpes simplex virus type-1; HSV-2, herpes simplex virus type-2; VSV, vesicular stomatitis virus; SIN, Sindbis virus; VV, vaccinia virus.

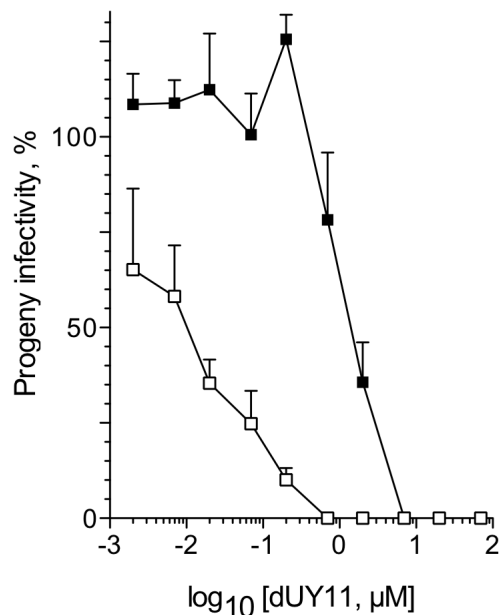


Figure 4.3 Treatment of SIN-infected cells with dUY11 inhibits the levels of progeny infectivity. Semi-logarithmic line graph showing the levels of progeny virion infectivity against the logarithm of dUY11 concentration. Vero cells were infected with SIN virus at a MOI of 3 plaque-forming units per cell. Following adsorption, cells were washed and overlaid with media supplemented with 0, 0.002, 0.007, 0.02, 0.07, 2, 7, 20 or 70 μM dUY11 for only 1 hour (■) or continuously for 23 hours (□). SIN-infected cells washed 1 hour post-treatment were overlaid with media in the absence of drug. At 24 hpi, the supernatants were harvested and the levels of progeny SIN infectivity were evaluated by plaque assay using volumes equivalent to that which produced 200 plaques in cells treated without drug. Error bars, standard deviation of four experiments. SIN, Sindbis virus. P<0.001.

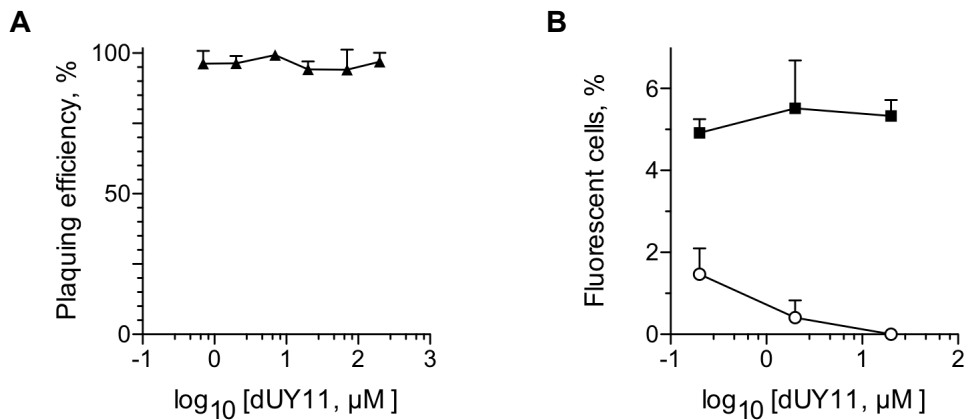


Figure 4.4 dUY11 does not inhibit the infectivity of nonenveloped viruses.

Semi-logarithmic line graphs showing the infectivity of PV (▲) (A) and GFP-expressing strains of HSV-1 (○) or AdV (■) (B) plotted against the logarithm of dUY11 concentration. Virions (200 plaque-forming units) were incubated with 0, 0.002, 0.007, 0.02, 0.07, 0.2, 0.7, 2, 7, 20 or 70 (A); or 0, 0.2, 2 or 20 (B) μM dUY11 for 5 minutes at 37°C. Vero cells were then infected with the so-exposed virions to assess infectivity by plaquing efficiency (A) or by analyzing fluorescence microscopy 18 (GFP HSV-1) or 36 (GFP AdV) hrs later (B). Error bars represent the standard deviation of three or more experiments (A) or three counts from three microscopic fields (100 magnifications) (B). GFP, green fluorescent protein; PV, poliovirus; HSV-1, herpes simplex virus type-1; AdV, adenovirus.

CHAPTER 5: RIGID AMPHIPATHIC FUSION INHIBITORS DO NOT ACT BY CLASSIC NUCLEOSIDIC ANTIVIRAL MECHANISMS

This chapter contains unpublished results and published work. (St.Vincent, MR et al., Proceedings of the National Academy of Sciences of the USA 107:17339-17344)

5.1 Introduction

Twenty-eight of the forty-eight approved antivirals target viral genome replication (**Table 1**). All but six of these are nucleoside derivatives, structural analogues of the natural substrates of the target enzyme. Following their intracellular phosphorylation to the active triphosphate forms, they are incorporated at the 3'-end of the viral DNA chain (De Clercq, 2004). Most nucleoside analogues thus compete with natural nucleotides for viral polymerases or act as chain terminators.

Drug resistance is a major limitation to current antiviral strategies targeting viral proteins such as polymerases. Antivirals targeting viral proteins promptly select for variants encoding mutations translated into structural changes in the target protein which most often affect drug binding (Menendez-Arias, 2010). Moreover, a single mutation can confer resistance to multiple drugs. For example, the M184V/I mutation confers resistance to entecavir, lamivudine and emtricitabine (McMahon et al., 2007). Resistance to all current antivirals is well-characterized, and in many cases limits clinical efficacy (Este and Cihlar, 2010).

Antivirals targeting cellular proteins are under development (Schang, 2006). These are predicted to be less constrained by the limitations of classical antivirals targeting viral proteins. For example, a number of cellular proteins are required for replication of viruses with even the smallest genomes (for which there are thus only a limited number of viral protein targets) or of only distantly related viruses (Schang, 2006). Drugs targeting cellular functions could be used against an emerging virus even before its proteins are fully characterized. Drugs targeting cellular factors required for viral replication thus have the potential for broad-spectrum activities. Moreover, the targets of such drugs are not encoded within highly-mutable viral genomes. For drugs targeting cellular proteins, the human gene encoding the targeted cellular protein is not likely to mutate in response to therapy. The inhibition of cellular molecules required for multiple viral functions would also minimize the selection for resistance (Schang, 2006). Antivirals targeting cellular proteins may thus have a higher genetic barrier to select for resistant viral mutants, a major limitation of current antivirals (Menendez-Arias, 2010). Of course, the potential for toxicities is increased for drugs targeting cellular proteins. These limitations highlight the urgent need for novel antiviral strategies.

I discovered a novel class of nucleoside derivatives, the rigid amphipathic fusion inhibitors, or RAFIs, with a unique mechanism of antiviral action. RAFIs target envelope lipid bilayers and inhibit the formation of the negative membrane curvature required for fusion. I characterized their novel antiviral mechanism and broad-spectrum properties in **chapters 3** and **4**. In this chapter, I report that

RAFIs do not act by classic nucleosidic mechanisms targeting genome replication. Unlike most other nucleoside analogues, RAFIs do not inhibit viral DNA replication, and are active against herpes simplex virus type-1 (HSV-1) strains resistant to classical nucleosidic antivirals. I also report that HSV-1 resistance to dUY11 is not readily selected for. These studies therefore highlight unique properties of RAFIs that may help to overcome some of the critical limitations of current antiviral therapies.

5.2 Results

5.2.1 dUY11 does not target viral proteins to inhibit herpes simplex virus type-1 replication

Several RAFIs were originally proposed to inhibit HSV-1 replication by nucleosidic mechanisms (Andronova et al., 2003). Their activities against HSV-1 strains resistant to acyclovir (ACV) and phosphonoformic acid (PFA; or foscarnet) were later reported (Pchelintseva et al., 2005; Skorobogatyi et al., 2006a; Skorobogatyi et al., 2006b). A non-nucleosidic mechanism targeting cellular factors was therefore proposed to be more likely (Skorobogatyi et al., 2006b). In these original studies, dUY11 was tested against wild-type or ACV- and PFA-resistant HSV-1 strains in multiple-replication cycles (48 hours after infection of cells) (Andronova et al., 2003). In **chapters 3 and 4**, I characterized the interactions of RAFIs with lipid envelopes, and described their mechanisms of action as broad-spectrum inhibitors of infectivity. I next analyzed whether RAFIS also act by targeting viral DNA replication.

5.2.1.1 dUY11 inhibits herpes simplex virus type-1 yields

As a first step to evaluate the effects of dUY11 on HSV-1 replication, I first tested dUY11 on viral yields by one-step replication assays.

Vero cell monolayers were infected with wild-type HSV-1 KOS strain at a multiplicity of infection (MOI) of 3 plaque-forming units (PFU) per cell. After a 1-hour adsorption, the inocula were removed, and the infected cells were washed and then overlaid with media containing increasing concentration of dUY11. At 24 hours post-infection (hpi), progeny virions were harvested and viral titers evaluated by standard plaquing.

Treatment of infected cells with dUY11 inhibited viral yields in those cells by nearly 100,000,000-fold (**Figure 5.1A**), with an apparent IC₅₀, IC₉₅ or IC₉₉ of 0.906, 1.382 or 1.752 μM, respectively (**Figure 5.1B**). Standard replication assays, of course, do not discriminate between differential effects the drug may have on different steps of viral replication. For example, standard replication assays would not discriminate between the effects of the drug on infection, DNA replication or progeny virion assembly or release. I thus evaluated the effects of dUY11 directly on HSV-1 DNA replication.

5.2.1.2 dUY11 does not inhibit herpes simplex virus type-1 DNA replication

dUY11 primarily targets HSV-1 virion envelopes to inhibit viral infectivity (**Figures 3.13 to 3.15, Table 3.5**). It also inhibited viral yields when added only after infection of cells with HSV-1 (**Figure 5.1**). RAFIs are nucleoside derivatives. As other nucleoside derivatives, such as the clinically approved anti-

HSV drug acyclovir (ACV) (Elion et al., 1977), then, RAFIs may too target viral enzymes to inhibit HSV-1 DNA replication. They may also target cellular proteins to inhibit gene expression, as do other antivirals under development. Roscovitine, for example, is a purine derivative that targets cyclin-dependent kinases to inhibit the initiation of transcription of HSV-1 genes (Diwan, Lacasse, and Schang, 2004). Therefore, I evaluated intracellular HSV-1 DNA levels in cells treated with dUY11 only after infection.

Vero cells were mock-infected or infected with 5 plaque-forming units (PFU) per cell of wild-type HSV-1 KOS strain. After a 1 hour adsorption, the inocula were removed, cells were washed twice and then overlaid with complete media supplemented 0 or 2 μ M dUY11 ($>IC_{99}$, **Figure 5.1**). As a control, other infected cells were treated with phosphonoformic acid (PAA). PAA targets the viral DNA polymerase by binding to its pyrophosphate binding site, thereby inhibiting viral DNA polymerization (Honest and Watson, 1977; Mao and Robishaw, 1975; Overby et al., 1974). Intracellular HSV-1 DNA levels were analyzed at 1, 5, 18 or 24 hpi by Southern blot hybridization.

Equal intracellular DNA levels were detected at 1 hpi under all three cell treatment conditions (1, bottom panel, **Figure 5.2**), indicating equal viral entry in all three conditions. Infected cells treated with 2 μ M dUY11 (11, **Figure 5.2**) had the same levels of HSV-1 DNA as in the cells infected in the absence of drug (ND, no drug; **Figure 5.2**), at all three times tested (5, 18 or 24 hpi). In contrast, HSV-1 DNA replication was inhibited by the DNA polymerase inhibitor PAA, as expected. Unlike most other nucleoside analogues, therefore, dUY11 does not

inhibit HSV-1 DNA replication. Moreover, HSV-1 DNA replication requires immediate-early (IE) and early (E) proteins (Roizman, Knipe, and Whitley, 2007). Therefore, these results also indicated that dUY11 did not inhibit IE or E gene expression.

5.2.1.3 dUY11 is active against drug-resistant herpes simplex virus type-1 strains

Most antiviral nucleoside or nucleotide analogues inhibit viral DNA replication. The ones clinically used against HSV-1 target the DNA polymerase after activation by the HSV-1 thymidine kinase (TK). Acyclovir is activated by phosphorylation, first by HSV-1 TK, and then by cellular kinases (Elion et al., 1977; Fyfe et al., 1978; Miller and Miller, 1980). Triphosphorylated ACV competes with deoxyguanosine triphosphate for the viral DNA polymerase, and acts as a chain terminator (Furman et al., 1979). The small molecule PAA also inhibits DNA replication, by targeting the pyrophosphate site of the viral DNA polymerase (Mao and Robishaw, 1975). Compounds such as ACV or PAA inhibit DNA replication and promptly select for resistant HSV-1 variants. In agreement with their mechanism of action, the mutations which confer resistance to ACV are located in either the *UL23* or *UL30* gene and gene products (which encode for TK or DNA polymerase, respectively), whereas those that confer resistance to PAA are located in the *UL30* gene (Piret and Boivin, 2011). HSV-1 strains TK⁻ and PAA^{r5}, which contain a deletion of the TK gene or a point mutation in the gene encoding the viral DNA polymerase, respectively, are resistant to ACV and PAA,

respectively (Coen and Schaffer, 1980; Fyfe et al., 1978). Unlike other nucleoside analogues, however, dUY11 did not inhibit HSV-1 DNA replication (**Figure 5.2**), indicating that RAFIs do not target DNA replication. To further test whether RAFIs targeted HSV-1 DNA polymerase, I next tested whether dUY11 is active against two mutant HSV-1 strains resistant to ACV and PAA.

Vero cell monolayers were infected at a MOI of 3 PFU per cell of wild-type HSV-1, KOS strain, or strains resistant to PAA (PAA^{r5}) or ACV (TK-). The infected wells were then overlaid with complete media supplemented with increasing concentrations of dUY11, ACV or PAA. The levels of infectivity were evaluated 23 hours later by measuring viral titers.

dUY11 inhibited viral yields produced by all three HSV-1 strains (**Figure 5.3A**). No infectious wild-type HSV-1 virions were detected in cells treated with 2 μ M dUY11 (filled square, **Figure 5.3A**), consistently with **Figure 5.1**. No infectious ACV- or PAA-resistant HSV-1 mutants were detected in cells treated with 2 μ M dUY11, either (open circle or triangle, respectively; **Figure 5.3A**). As expected, ACV inhibited the replication of both wild-type and PAA^{r5} strains, but not that of TK- (**Figure 5.3BI**). Also as expected, PAA inhibited the replication of both wild-type and TK- strains, but not that of PAA^{r5} (**Figure 5.3BII**). Therefore, dUY11 is active against HSV-1 mutants resistant to small molecules that target HSV-1 DNA polymerase.

5.2.1.4 The antiviral activities of dUY11 are not attenuated by increasing multiplicity of infection

Drug potencies depend on the number of molecules of the target proteins. The activities of drugs targeting viral proteins are therefore dependent on the MOI. Increasing the multiplicity increases the number of copies of the genes from which viral proteins are expressed, and therefore the number of molecules of the target. The potency of PAA, for example, decreases with increasing MOI, since the molecular levels of its target (the viral DNA polymerase) increases (Schang, Rosenberg, and Schaffer, 2000). The potency of antiviral agents that target viral proteins, such as PAA, is thus inversely related to the multiplicity of infection. I then next evaluated whether the potency of RAFIs depend on the levels of viral proteins by evaluating the effects of MOI on the antiviral activities of dUY11.

To this end, I selected two dUY11 test concentrations. One and two micromolar dUY11 were selected because they reduced HSV-1 titers by ~50 (IC₅₀) or 99 % (IC₉₉), respectively, in cells treated after infection (**Figure 5.1**).

Vero cells were infected at a MOI of 0.001, 0.01, 0.1, 1, 10, 30 or 100 PFU per cell for 1 hour. Following adsorption, cells were washed and overlaid for 23 hours with complete media supplemented with 2 or 1 μ M dUY11. Cells and supernatants were harvested 24 hours after infection, and viral titers were determined by standard titration.

The viral titers were reduced by up to 1,000- or 100,000,000-fold (consistently with **Figure 5.1**) when infected cells were treated with 1 or 2 μ M dUY11, respectively (**Figure 5.4**). The inhibition of the level of infectious virions

in cells treated with dUY11 was not attenuated by an increase in MOI, even to 100 PFU per cell. In contrast to drugs targeting viral proteins, therefore, an increase in MOI did not attenuate the inhibition by dUY11, consistently with RAFIs not acting by classic nucleosidic antiviral mechanisms targeting viral proteins.

5.2.2 Treatment of infected cells with dUY11 inhibits the levels of herpes simplex virus type-1 infectivity

dUY11 did not target HSV-1 proteins to inhibit DNA replication, nor IE or E gene expression (**Figures 5.2 to 5.4**). dUY11 may, however, target steps after DNA replication, such as virion assembly or release.

The lipids in virion envelopes are acquired from cellular membranes. dUY11 localized to cell membranes (**Figure 3.4**) and it inhibited the infectivity of HSV-1 virions directly exposed to it before infection (**Figure 3.3**). When infected cells were continuously treated with dUY11 only after infection, HSV-1 viral yields were inhibited (**Figure 5.1**). The inhibition of viral yields could result from RAFIs targeting steps after DNA replication. Therefore, I next evaluated the effects of dUY11 on late steps in HSV-1 replication.

5.2.2.1 Treatment of herpes simplex virus type-1 infected cells with dUY11 inhibits the levels of cell-associated and cell-free progeny infectivity

When Sindbis(SIN)-infected cells were treated only after infection, dUY11 inhibited the levels of progeny infectivity (**Figure 4.3**). I next tested if these

effects of dUY11 on the levels of progeny virion infectivity in treated cells were specific to SIN. I thus tested the effects of treating already-infected cells with dUY11 on the levels of cell-associated and cell-free progeny HSV-1 infectivity.

Vero cells were infected with 3 PFU per cell of unexposed HSV-1 virions. Inocula were removed 1 hour later and the infected cells were washed and then treated with increasing concentrations of dUY11, either continuously for 23 hours, or for only 1 hour. For the latter treatment, dUY11-containing media was removed after 1 hour (two hours after infection). Cells were then extensively washed to remove any residual compound, and then overlaid with fresh medium containing no drug for 22 hours. Supernatants and infected cells were harvested separately 24 hours after infection. The levels of cell-associated or cell-free progeny infectivity were then evaluated by plaquing assay.

The treatment of infected cells with dUY11 reduced the levels of both intracellular and extracellular progeny virion infectivity (**Figure 5.5**). The continuous treatment of already-infected cells for 23 hours with dUY11 inhibited the levels of released (open circles, **Figure 5.5**) and cell-associated (filled circles, **Figure 5.5**) progeny HSV-1 infectivity. The IC_{50} were within a 2-fold range (IC_{50} (95% CI), 0.313 μ M (0.058 to 1.700 μ M) or 0.159 μ M (0.080 to 0.315 μ M), respectively, against released or cell-associated progeny infectivity; **Table 5.1**; $P > 0.05$). Likewise, treatment of previously infected cells with dUY11 for even only 1 hour also inhibited the levels of infectious released (open squares, **Figure 5.5**) and cell-associated (filled squares, **Figure 5.5**) progeny virions, again with near-identical IC_{50} (6.681 μ M (95% CI, 4.122 to 10.827 μ M) or 6.985 μ M (95%

CI, 4.245 to 11.495 μM), respectively, against released or cell-associated progeny infectivity; **Table 5.1**; $P > 0.05$).

Similarly to the observed effects of treating cells on the levels of progeny SIN infectivity (**Figure 4.3**, **Table 4.2**), the continuous treatment of cells with dUY11 for 23 hours after infection of cells with HSV-1 more potently inhibited the levels of progeny infectivity than a 1-hour treatment. The IC_{50} was approximately 28-fold lower for continuously treated cells than for cells treated for only 1 hour after infection with HSV-1 (IC_{50} , ~ 0.24 or $6.7 \mu\text{M}$ for 23- or 1-hour treatment, respectively; **Table 5.1**; $P < 0.05$), and only 6-fold higher than direct exposure of virions before adsorption (IC_{50} $0.038 \mu\text{M}$ for exposure of infecting virions, compared to $\sim 0.24 \mu\text{M}$ for a 23-hour treatment of cells; **Table 5.1**; $P < 0.001$). These results indicate that progeny virions produced by treated cells are efficiently exposed to dUY11 in the extracellular medium (23-hour cell treatment), and that they may also acquire it during their replication (1-hour cell treatment), for example during budding. dUY11 could also inhibit the release of progeny virions.

5.2.2.2 dUY11 inhibits the release of progeny herpes simplex virus type-1 virions by 2.8-fold

dUY11 inhibited the levels of progeny HSV-1 infectivity in cells treated even for only 1 hour after infection (**Figure 5.5**), and thus which are not exposed to the drug in the extracellular medium after their release. Assembling progeny virions interact with pre-existing cellular components, such as membrane lipids, that are

incorporated into virions and which are essential for their infectivity. Indeed, dUY11 did rapidly localize to intracellular membranes in less than 30 minutes (**Figure 3.4**). dUY11 could also interfere with virion budding processes in the cells or with the release of progeny virions. I therefore next evaluated the effects of dUY11 on the release of progeny virions by monitoring the levels of HSV-1 DNA in virions released into the supernatants of infected cells.

HSV-1 virions were adsorbed onto Vero cell monolayers at a MOI of 5 PFU per cell. The cells were washed after 1 hour to remove unbound virions, and then overlaid with 0 or 7 μ M dUY11 for 23 hours. I selected a high concentration of dUY11, which fully inhibits the levels of progeny infectivity in continuously treated cells (>99%, **Figure 5.5**), to maximize the sensitivity to detect even mild effects on virion release. Supernatants containing released progeny virions were collected separately from cell-associated virions at 24 hpi. The virions were then pelleted by ultracentrifugation through a sucrose cushion. The release of progeny virions was then evaluated by Southern blot analysis of virion and total HSV-1 DNA.

Approximately 16% of the total viral DNA detected in infected and untreated cells was recovered in the released cell-free virions (middle lane; **Figure 5.6**). In contrast, only 5.9% of the total viral DNA from infected cells treated with dUY11 was recovered in the released cell-free virions (right lane; **Figure 5.6**). dUY11 therefore inhibited progeny virion release, but only by 2.8-fold. This effect can account for only a small proportion of the 100,000,000-fold

inhibition of HSV-1 yield (**Figure 5.1**), indicating that the inhibition of virion release is not the primary antiviral mechanism.

5.2.3 dUY11 does not readily select for resistant variants

The selection for genetic variants resistant to an antiviral drug is a powerful approach to identify its targets. Subsequent marker rescue studies identify the genes mutated in resistant variants. Further studies of these mutants can then provide information on the genetic barrier to the selection for resistance, in that they elucidate the number and location of mutations required to confer resistance.

I therefore undertook genetic approaches to isolate HSV-1 variants resistant to dUY11. To this end, I performed serial passages in the presence of increasing concentrations of dUY11 (multiple-cycle selection). In such studies, virus is serially passaged in the presence of an increasing concentration of the compound, or in the absence of drug as a control for genetic drifting. Mutations that confer antiviral resistance sometimes impair viral fitness. Primary drug resistance mutations are consequently often followed by the selection for compensatory mutations to improve replicative fitness. A recovery in viral titers under drug-selective pressure to wild-type levels indicates that variants that replicate in the presence of the compound have been isolated.

5.2.3.1 Standard passages in the presence of an increasing concentration of dUY11 did not readily select for resistant variants

The multiple-cycle selection for resistance was performed under my supervision by Vanessa del Fabbro (Honors student, University of Alberta, and included in this thesis with her permission). First, low passage HSV-1 was plaque-purified, and HSV-1 stocks were then prepared from non-syncytia plaques. HSV-1 was then serially passaged in the presence of an increasing concentration of dUY11. As a positive control, a parallel selection was conducted with PAA. PAA targets the virus-encoded DNA-polymerase and promptly selects for drug resistance (Schang, Phillips, and Schaffer, 1998). Parallel passages in the absence of drug-selective pressure were conducted to monitor wild-type replication.

HSV-1 was passaged ten or eight times under dUY11 or PAA selective pressure, respectively, starting at sub-inhibitory concentrations. The same low-passage, plaque-purified HSV-1 stock was used for the first passage of all three parallel studies. The virus was harvested when cytopathic effect (CPE) was generalized (4+), but before cell detachment. Infected cell number, MOI, drug concentration, time elapsed between infection and 4+ CPE, and viral titers for each parallel passage are summarized in **Table 5.2** (**Table 5.2A** and **C** for dUY11 or PAA, respectively, and **Table 5.2B** in the absence of drug).

For dUY11-selective pressure studies, we tested a sub-inhibitory concentration of 0.25 μM dUY11 for the first passage (3.5-fold below the IC_{50} of dUY11 against viral yields in continuously treated cells; IC_{50} 0.906 μM , **Figure 5.1**). In this and each of the subsequent 9 passages, 2×10^6 Vero cells were

infected with 0.1 PFU per cell, with the exception of passages 6 through 8 and 10 (**Table 5.2A**). The MOIs used for these passages were limited due to the low recovery of virus (low yields) in the previous passages. Therefore, the MOI used was 0.02, 0.03, 3×10^{-5} or 0.01 PFU per cell, respectively, for passages 6, 7, 8 or 10. The concentration of dUY11 was increased (from 0.25 to 0.50 μM at passage 2 and from 0.5 to 1 μM at passage 4) when viral titers had recovered ($\sim 2 \times 10^6$ PFU/ 10^6 cells in passages 2 and 3). Two amplification rounds were performed in the absence of drug (passages 8 and 11) in an effort to increase viral yields. All other passages (4-7 and 9-10) were performed in the presence of 1 μM dUY11. Viral replication was severely impaired in passage 4 (1.29×10^5 PFU/ 10^6 cells), when the concentration of dUY11 was increased from 0.5 to 1 μM . Viral titers never recovered to wild-type levels and low viral yields were recovered in all passages subsequent to passage 4 ($\sim 1 \times 10^8$ PFU/ 10^6 cells for wild-type; **Table 5.2B**), despite the amplification rounds in the absence of dUY11 (passages 8 and 11). The number of hours that elapsed between infection and generalized 4+ CPE varied, from approximately 50 hours to as high as 130 hours, with longer time elapsing mostly when a lower MOI had to be used (**Table 5.2A**).

For standard passages under PAA-selective pressure, or in the absence of drug, 2×10^6 Vero cells were infected at an MOI of 0.1 PFU per cell for PAA or in the absence of drug, with the exception of passages 6 through 8 and 10. For these passages in the absence of drug-selective pressure, the MOI was limited by the recovery of low viral yields under dUY11-selective pressure (**Table 5.2A**). To keep the conditions consistent with those required for the dUY11 selection, then,

an MOI of 0.02, 0.03, 3×10^{-5} or 0.01 PFU per cell was used for passages 6, 7, 8 or 10, respectively. The first two passages under PAA-selective pressure were at sub-inhibitory to IC_{50} concentration (passage 1 at 25, or 2, at 50 $\mu\text{g/mL}$), followed by two passages (3 and 4) at IC_{99} PAA (100 $\mu\text{g/mL}$). Passage 5 was performed in the presence of two times the inhibitory concentration (200 $\mu\text{g/mL}$), then three more passages (6, 7 and 8) were performed at four times the inhibitory concentration (400 $\mu\text{g/mL}$). The PAA concentration was increased (from 25 to 50 $\mu\text{g/mL}$ at passage 2; from 50 to 100 $\mu\text{g/mL}$ at passage 3, from 100 to 200 $\mu\text{g/mL}$ at passage 5 and from 200 to 400 $\mu\text{g/mL}$ at passage 6) when viral titers in the presence of PAA recovered to approximately wild-type levels (typically 1×10^7 PFU/ 10^6 cells at passages 1, 2, 4 and 5) (**Table 5.2B** and **C**). Viral titers produced by cells in the absence of drug were typically 1×10^8 PFU/ 10^6 cells (**Table 5.2B**). An average of ~70 hours elapsed between the infection of cells in the presence of PAA and 4+ CPE, or 55 hours in the absence of drug, except when MOI lower than 0.1 PFU per cell were used (**Tables 5.2B** and **C**). Selection in PAA was stopped at passage 8 because full resistance had been selected for. A total of 10 passages were performed in the absence of drug, to keep the consistency with dUY11.

The percent resistance to PAA was then determined for each passage. Vero cell monolayers (1×10^5 per well in a 6-well plate) were infected in duplicate with 200 HSV-1 virions recovered from each passage under PAA-selective pressure. Following the 1-hour adsorption, the cells were washed twice with ice-cold media. One duplicate monolayer infected with PAA-selected virus

was overlaid with complete semi-solid media alone and the other, with media supplemented with 100 $\mu\text{g}/\text{mL}$ PAA (IC_{99}). Resistance was then evaluated by monitoring plaquing. The percent PAA-resistance was calculated by dividing the number of plaques obtained in the presence of IC_{99} PAA by the number of plaques obtained in the absence of drug ($\times 100$), and plotted as a function of passage number.

Virus isolated only in passages 1, 2, 3 and 11 was evaluated for resistance to dUY11. Low viral yields were obtained in all passages subsequent to passage 4. Despite extensive efforts to amplify the virus collected in passages 4 through 10 in the presence of dUY11, no virus was produced by amplification. To determine the percent resistance to dUY11 of virus from passages 1 through 3 and 11, therefore, 200 HSV-1 virions recovered from each passage were pre-exposed to 0 or 2 μM dUY11 (IC_{99} for direct virion exposure, **Figure 3.3**). Exposing virions to dUY11 before infecting the cells is the direct approach to determine the relative percent resistance to dUY11.

Two hundred virions from each testable passage (1, 2, 3 and 11) were exposed to 0 or 2 μM dUY11 for 5 minutes at 37°C and then adsorbed onto Vero cell monolayers. Following the 1-hour adsorption, unbound virions were removed, the cells were washed and then overlaid with semi-solid media. Resistance was evaluated by monitoring plaquing. The percent dUY11-resistance was calculated by dividing the plaque number following pre-exposure to dUY11 by the plaque number obtained by pre-exposing virions to no drug ($\times 100$). The percentages were then plotted as a function of passage number.

Virus resistant to full-inhibitory PAA concentration (100 µg/mL) was detected as early as passage 2, where nearly 33% of the population was resistant (filled circle, **Figure 5.7**). By the 8th passage, more than 97% of the population was resistant to >IC₉₉ PAA, which is in close agreement with previously published studies (Honest and Watson, 1977; Schang, Phillips, and Schaffer, 1998).

In contrast, I was unable to detect dUY11-resistance. No plaques were detected when virions were pre-exposed to 2 µM dUY11 (open triangle; **Figure 5.7**). These results indicated that dUY11-resistant variants were not selected for as promptly as those resistant to antiviral agents that target the viral DNA polymerase, such as PAA.

5.3 Discussion

The novel antiviral mechanisms of the rigid amphipathic fusion inhibitors was characterized in **chapters 3** and **4**. These nucleoside derivatives target envelope bilayers to prevent the formation of the negative curvature required and conserved for the fusion of any enveloped virus (**Chapter 3**). Consequently, RAFIs have a broad antiviral spectrum, being active against a number of otherwise unrelated enveloped viruses (**Chapter 4**).

In this chapter, I expanded on those results, showing that in contrast to other nucleoside analogues, RAFIs did not inhibit HSV-1 DNA replication (**Figure 5.2**). Moreover, their antiviral activities were not attenuated by increasing the multiplicity of infection, and therefore viral protein levels (**Figure 5.4**). Also

consistently with the proposed model of action, RAFIs were active against HSV-1 variants resistant to classical nucleoside analogues such as ACV, or PAA, which target viral DNA polymerases (**Figure 5.3**). dUY11 also inhibited viral yields (**Figure 5.1**) and the levels of cell-associated and cell-free progeny HSV-1 infectivity (**Figure 5.5**) in cells treated only after infection. The release of progeny virions was also slightly reduced, but by only 2.8 fold (**Figure 5.6**), indicating that the effects of dUY11 on release is not the primary antiviral mechanism. Consistently with their unique target and mechanisms of antiviral action, resistance to RAFIs was not selected for as promptly as it is for antivirals that target viral DNA replication (**Figure 5.7**).

dUY11 was previously reported to have anti-herpetic activities, with the dose that inhibited virally-induced CPE by 50% (ID₅₀) reportedly 15.5 μM (or 7.8 μg/mL) (Andronova et al., 2003). I found that dUY11 is much more potent (IC₅₀ ~0.04 μM when virion are directly exposed, a difference of more than 400-fold; **Figure 3.3**). I also maintained already-infected cells (at a MOI of 3 PFU per cell) in drug-containing medium for only 1 hour after infection, or continuously for 23 more hours, during viral replication. The IC₅₀ against HSV-1 infectivity under these treatment conditions were ~6.7 and 0.24 μM for 1- or 23-hour treatment, respectively (**Table 5.1**). The previously reported ID₅₀ for dUY11 against HSV-1 in multiple replication cycles (evaluated 48 hours after infection of cells at a MOI of 0.1 PFU per cell) calculated by Andronova *et al.* is in close agreement with the IC₅₀ against the levels of infectious virions in cells treated after infection,

indicating that the actual inhibition measured in those studies was on the secondary infections (Andronova et al., 2003).

dUY11 was also previously reported to have antiviral activities against HSV-1 mutant strains resistant to ACV and PFA (IC_{50} , 15.6 $\mu\text{g}/\text{mL}$, or 31.0 μM) (Andronova et al., 2003). The previously reported ID_{50} for dUY11 against drug resistant HSV-1 in multiple replication cycles calculated by Andronova et al. is also in close agreement with the IC_{50} against the viral yields in one-step replication assays in cells treated only after infection with wild-type or drug-resistant strains of HSV-1 ($\sim 1.2 \mu\text{M}$ for TK-, PAA^{r5} and wild-type HSV-1; **Figures 5.1 and 5.3**). The actual inhibition measured in those studies was on the secondary infections.

There was an apparent increase in the levels of infectivity in cells treated with nanomolar concentrations (2 to 70 nM) of dUY11 (**Figure 5.5**). However, the alternating peaks in the levels of progeny infectivity are indicative of a systematic experimental error.

dUY11 also reduced the levels of viral DNA in the supernatants of infected cells by 2.8-fold (**Figure 5.6**). The inhibition of the levels of progeny infectivity and, consequently, viral yields in treated cells can at least in part be attributed to an inhibition of the release of progeny virions. It could be that progeny virions are preferentially retained at the cell surface in dUY11-treated cells. The mechanisms for this apparent increase in levels of infectious virions, or retention of cell-associated virus, are not yet known.

Current antiviral drugs target viral proteins or their interactions with cellular ones. Consequently, they promptly select for drug resistant variants. Several factors contribute to the rapid emergence of drug-resistant variants in clinically treated patients, such as the existence of quasispecies (Lauring and Andino, 2010). Low drug potency and poor patient adherence also contribute to the prompt selection for drug resistance. Some viral polymerases lack proofreading activity, thus contributing to the generation of a large heterogeneous population of genetically distinct variants within a single infected patient, any one of which could harbor a mutation that confers resistance to a particular drug (Lauring and Andino, 2010).

In contrast to nucleoside analogues targeting genome replication, RAFIs target envelope bilayers. Drugs targeting lipids should be less prone to select for resistance. Virions envelope lipids are acquired from cellular membranes, and not encoded in the highly variable viral genome. Therefore, mutations in viral genomes are not expected to affect the antiviral activities of RAFIs. In studies to characterize the barrier to resistance, I followed standard multi-cycle selection for HSV-1 variants resistant to RAFIs. Efforts to select for resistant variants to date suggest that dUY11-resistant mutants are not as readily selected for as those selected in the presence of drugs that target viral DNA polymerases.

Although it is of course not possible to conclude that viral mutants resistant to RAFIs cannot be selected for, it is more difficult to select for HSV-1 variants resistant to dUY11 than those resistant to small molecules targeting viral proteins. The higher genetic barrier to resistance may prove to be important

properties in their further development as antiviral agents. Owing to the novelty of developing small molecules that inhibit the formation of negative curvature, this antiviral strategy has never before been tested *in vivo*. It is thus not possible to predict how the higher genetic barrier to RAFI-resistance observed in cell culture would translate *in vivo*, in animal models or in clinical settings. The viability of this novel antiviral mechanism in animal models would thus be a first step to the further development of RAFIs as antiviral agents.

5.4 References

- Andronova, V. L., Skorobogatyi, M. V., Manasova, E. V., Berlin Iu, A., Korshun, V. A., and Galegov, G. A. (2003). [Antiviral activity of some 5-arylethynyl 2'-deoxyuridine derivatives]. *Bioorg Khim* **29**(3), 290-5.
- Coen, D. M., and Schaffer, P. A. (1980). Two Distinct Loci Confer Resistance to Acycloguanosine in Herpes-Simplex Virus Type-1. *Proceedings of the National Academy of Sciences of the United States of America-Biological Sciences* **77**(4), 2265-2269.
- De Clercq, E. (2004). Antiviral drugs in current clinical use. *Journal of Clinical Virology* **30**(2), 115-133.
- Diwan, P., Lacasse, J. J., and Schang, L. M. (2004). Roscovitine inhibits activation of promoters in herpes simplex virus type 1 genomes independently of promoter-specific factors. *J Virol* **78**(17), 9352-65.
- Elion, G. B., Furman, P. A., Fyfe, J. A., Demiranda, P., Beauchamp, L., and Schaeffer, H. J. (1977). Selectivity of Action of an Anti-Herpetic Agent, 9-(2-Hydroxyethoxymethyl)Guanine. *Proceedings of the National Academy of Sciences of the United States of America* **74**(12), 5716-5720.
- Este, J. A., and Cihlar, T. (2010). Current status and challenges of antiretroviral research and therapy. *Antiviral Research* **85**(1), 25-33.
- Furman, P. A., Stclair, M. H., Fyfe, J. A., Rideout, J. L., Keller, P. M., and Elion, G. B. (1979). Inhibition of Herpes-Simplex Virus-Induced DNA-Polymerase Activity and Viral-DNA Replication by 9-(2-Hydroxyethoxymethyl)Guanine and Its Triphosphate. *Journal of Virology* **32**(1), 72-77.
- Fyfe, J. A., Keller, P. M., Furman, P. A., Miller, R. L., and Elion, G. B. (1978). Thymidine Kinase from Herpes-Simplex Virus Phosphorylates the New Anti-Viral Compound, 9-(2-Hydroxyethoxymethyl)Guanine. *Journal of Biological Chemistry* **253**(24), 8721-8727.
- Honess, R. W., and Watson, D. H. (1977). Herpes-Simplex Virus-Resistance and Sensitivity to Phosphonoacetic Acid. *Journal of Virology* **21**(2), 584-600.
- Lauring, A. S., and Andino, R. (2010). Quasispecies theory and the behavior of RNA viruses. *PLoS Pathog* **6**(7), e1001005.
- Mao, J. C. H., and Robishaw, E. E. (1975). Mode of Inhibition of Herpes-Simplex Virus DNA-Polymerase by Phosphonoacetate. *Biochemistry* **14**(25), 5475-5479.
- McMahon, M. A., Jilek, B. L., Brennan, T. P., Shen, L., Zhou, Y., Wind-Rotolo, M., Xing, S. F., Bhat, S., Hale, B., Hegarty, R., Chong, C. R., Liu, J. O., Siliciano, R. F., and Thio, C. L. (2007). Brief report - The HBV drug entecavir - Effects on HIV-1 replication and resistance. *New England Journal of Medicine* **356**(25), 2614-2621.
- Menendez-Arias, L. (2010). Molecular basis of human immunodeficiency virus drug resistance: An update. *Antiviral Research* **85**(1), 210-231.
- Miller, W. H., and Miller, R. L. (1980). Phosphorylation of acyclovir (acycloguanosine) monophosphate by GMP kinase. *J Biol Chem* **255**(15), 7204-7.

- Overby, L. R., Robishaw, E. E., Schleich, Jb, Rueter, A., Shipkowi, NI, and Mao, J. C. H. (1974). Inhibition of Herpes-Simplex Virus Replication by Phosphonoacetic Acid. *Antimicrobial Agents and Chemotherapy* **6**(3), 360-365.
- Pchelintseva, A. A., Skorobogatyj, M. V., Petrunina, A. L., Andronova, V. L., Galegov, G. A., Astakhova, I. V., Ustinov, A. V., Malakhov, A. D., and Korshun, V. A. (2005). Synthesis and evaluation of anti-HSV activity of new 5-alkynyl-2'-deoxyuridines. *Nucleosides Nucleotides & Nucleic Acids* **24**(5-7), 923-926.
- Piret, J., and Boivin, G. (2011). Resistance of herpes simplex viruses to nucleoside analogues: mechanisms, prevalence, and management. *Antimicrob Agents Chemother* **55**(2), 459-72.
- Roizman, B., Knipe, D. M., and Whitley, R. (2007). The replication of Herpes simplex virus. In "Fields' virology, 5th ed." (D. M. Knipe, P. M. Howley, D. E. Griffin, R. A. Lamb, M. A. Martin, B. Roizman, and S. E. Straus, Eds.), pp. 2501-2601. Lippincott-Williams & Wilkins, Philadelphia. PA.
- Schang, L. M., Phillips, J., and Schaffer, P. A. (1998). Requirement for cellular cyclin-dependent kinases in herpes simplex virus replication and transcription. *Journal of Virology* **72**(7), 5626-5637.
- Schang, L. M., Rosenberg, A., and Schaffer, P. A. (2000). Roscovitine, a specific inhibitor of cellular cyclin-dependent kinases, inhibits herpes simplex virus DNA synthesis in the presence of viral early proteins. *J Virol* **74**(5), 2107-20.
- Schang, L. M., St. Vincent, MR, Lacasse, JJ (2006). Five years of progress on cyclin-dependent kinases and other cellular proteins as potential targets for antiviral drugs. *Antiviral Chemistry & Chemotherapy* **17**, 293-320.
- Skorobogatyi, M. V., Pchelintseva, A. A., Petrunina, A. L., Stepanova, I. A., Andronova, V. L., Galegov, G. A., Malakhov, A. D., and Korshun, V. A. (2006a). 5-Alkynyl-2'-deoxyuridines, containing bulky aryl groups: evaluation of structure-anti-HSV-1 activity relationship. *Tetrahedron* **62**(6), 1279-1287.
- Skorobogatyi, M. V., Ustinov, A. V., Stepanova, I. A., Pchelintseva, A. A., Petrunina, A. L., Andronova, V. L., Galegov, G. A., Malakhov, A. D., and Korshun, V. A. (2006b). 5-Arylethynyl-2'-deoxyuridines, compounds active against HSV-1. *Organic & Biomolecular Chemistry* **4**(6), 1091-1096.

Infectivity	IC ₅₀ , μ M (95% CI)
Exposed HSV-1 virions	0.038 (0.036 to 0.042)
Released HSV-1 progeny from cells treated for 1 hr	6.681 (4.122 to 10.827)
Cell-associated HSV-1 progeny from cells treated for 1 hr	6.985 (4.245 to 11.495)
Released HSV-1 progeny from cells treated for 23 hrs	0.313 (0.058 to 1.700)
Cell-associated HSV-1 progeny from cells treated for 23 hrs	0.159 (0.080 to 0.315)

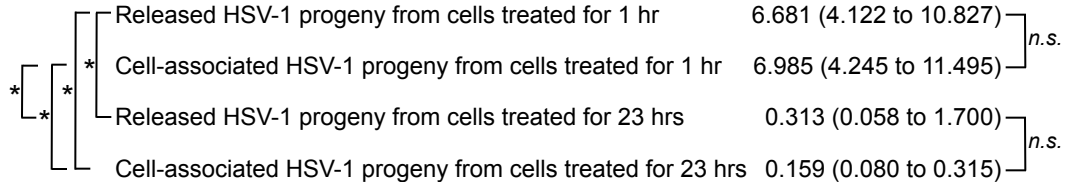


Table 5.1 IC₅₀ of dUY11 against HSV-1 infectivity by direct exposure of infecting virions or by treating cells for 1- or 23-hours after infection.

Table summarizing IC₅₀ and 95% confidence interval (CI) for dUY11 against the infectivity of HSV-1 virions directly exposed before adsorption, or against the levels of released or cell-associated progeny infectivity from cells treated with dUY11 for 1 or 23 hours after HSV-1 infection. The IC₅₀, 95% CI and P-values were calculated from three experiments using Prism software (four parameter nonlinear regression curve fit). *n.s.*, not significant (P>0.05); *, P<0.05. HSV-1, herpes simplex virus type-1.

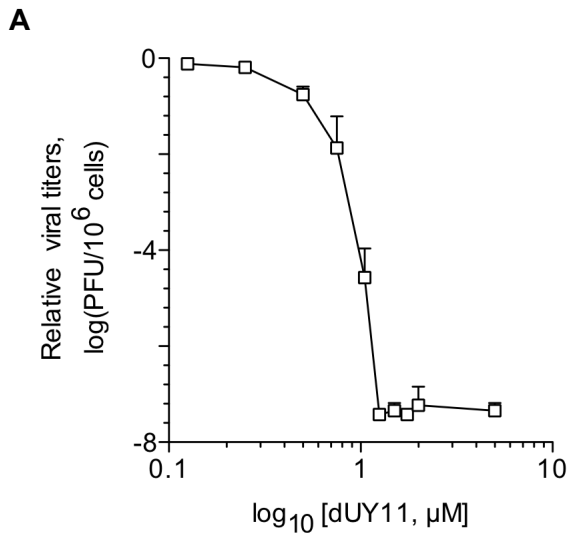
A	Passage number	Cell number	MOI (PFU/cell)	dUY11 (μM)	Time to harvest (hpi)	Viral titer (PFU/10^6 cells)
	1	2×10^6	0.1	0.25	41.5	1.18×10^7
	2	2×10^6	0.1	0.50	60	1.88×10^6
	3	2×10^6	0.1	0.50	79	2.40×10^6
	4	2×10^6	0.1	1.00	62	1.29×10^5
	5	2×10^6	0.1	1.00	133	1.59×10^4
	6	2×10^6	0.02	1.00	98	7.00×10^4
	7	2×10^6	0.03	1.00	77	3.40×10^1
	8	2×10^6	3×10^{-5}	0	112	1.67×10^8
	9	2×10^6	0.1	1.00	51	1.67×10^4
	10	2×10^6	0.01	1.00	90	2.87×10^4

B	Passage number	Cell number	MOI (PFU/cell)	Time to harvest (hpi)	Viral titer (PFU/10^6 cells)
	1	2×10^6	0.1	41.0	4.83×10^7
	2	2×10^6	0.1	61.5	8.30×10^7
	3	2×10^6	0.1	56.0	2.45×10^8
	4	2×10^6	0.1	49.0	3.85×10^8
	5	2×10^6	0.1	60.5	2.84×10^8
	6	2×10^6	0.02	62.5	1.64×10^8
	7	2×10^6	0.03	53.75	7.15×10^7
	8	2×10^6	3×10^{-5}	90.0	3.16×10^7
	9	2×10^6	0.1	51.0	2.09×10^8
	10	2×10^6	0.01	66.0	6.05×10^7

C	Passage number	Cell number	MOI (PFU/cell)	PAA (μg/mL)	Time to harvest (hpi)	Viral titer (PFU/10^6 cells)
	1	2×10^6	0.1	25	41.0	3.08×10^7
	2	2×10^6	0.1	50	81.5	9.25×10^5
	3	2×10^6	0.1	100	81.0	2.62×10^5
	4	2×10^6	0.1	100	65.5	1.43×10^7
	5	2×10^6	0.1	200	60.5	6.72×10^7
	6	2×10^6	0.1	400	98.0	7.55×10^5
	7	2×10^6	0.1	400	53.75	1.09×10^7
	8	2×10^6	0.1	400	64.0	3.16×10^7

Table 5.2 Viral titers did not recover under dUY11 selection pressure.

Tables summarizing the viral titers at full cytopathic effect (CPE) in the presence of dUY11 (**A**) or phosphonoacetic acid (PAA) (**C**), or in the absence of drug (**B**). Plaque-purified HSV-1 strain KOS was passaged in medium containing an increasing concentration of dUY11 or PAA, or in the absence of drug. The number of cells infected, the concentration of dUY11 or PAA used, the MOI and the viral titer at harvest times (full CPE; cell rounding in the absence of detachment) are indicated (**A,B,C**). Viral titers after each passage was evaluated by standard plaque assay.



B

Percent inhibitory concentration	IC, μM (95% CI)
IC ₅₀	0.906 (0.877 to 0.936)
IC ₉₅	1.382 (1.285 to 1.487)
IC ₉₉	1.752 (1.575 to 1.948)

Figure 5.1 dUY11 inhibits HSV-1 yield with an apparent IC₅₀ of 0.906 μM. Logarithmic line graph showing HSV-1 titer against dUY11 concentration (**A**) and table summarizing inhibitory concentration (IC) of dUY11 against viral yield (**B**). Vero cells were infected with HSV-1 KOS at a multiplicity of infection of 3 plaque-forming units per cell for 1 hour. Infected cells were washed and overlaid with media supplemented with 0, 0.125, 0.25, 0.5, 0.75, 1, 1.25, 1.5, 1.75, 2, or 5 μM dUY11 continuously for 23 hours. At 24 hpi, cells and supernatants were harvested and viral titers evaluated by plaqueing (**A**). The concentration of dUY11 which inhibited viral yields by 50, 95 or 99% (IC₅₀, IC₉₅ and IC₉₉, respectively) were calculated using Prism software (nonlinear regression curve fit). Error bars, standard deviation of twelve experiments.

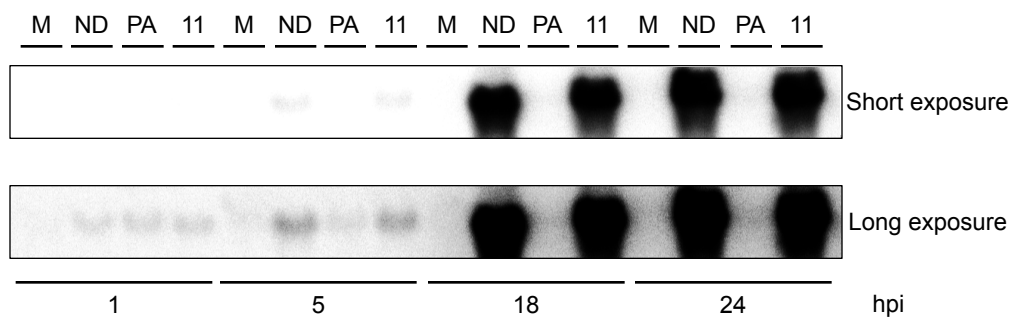


Figure 5.2 dUY11 does not inhibit HSV-1 DNA replication. Southern blot analysis showing intracellular viral DNA levels from cells infected in the absence of drug, or in the presence of phosphonoacetic acid or dUY11 at 1, 5, 18 or 24 hrs post-infection (hpi). Vero cells were mock infected (**M**) or infected with HSV-1 KOS at a multiplicity of infection of 5 plaque-forming units per cell, washed and overlaid with medium containing no drug (**ND**), 400 μM phosphonoacetic acid (**PA**) or 2 μM dUY11 (**11**). Cells were harvested at 1, 5, 18 or 24 hpi, DNA was isolated, resolved by agarose gel electrophoresis, transferred onto a nitrocellulose membrane, and hybridized with the radiolabeled JK fragment from the HSV-1 EcoRI library. The hybridized membrane is shown at short (top panel) and long (bottom panel) exposures.

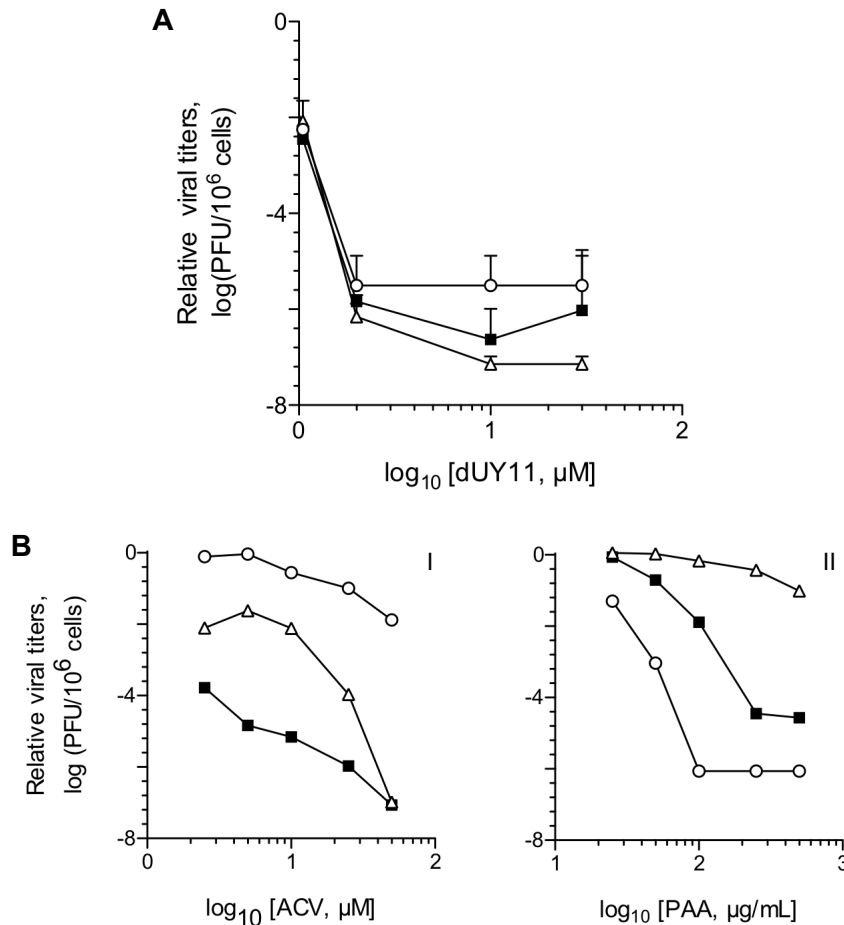


Figure 5.3 dUY11 inhibits the levels of infectivity in cells infected by HSV-1 strains resistant to drugs that target viral DNA replication.

Semi-logarithmic line graphs showing viral titers at 24 h against the logarithm of the concentration of dUY11, acyclovir (ACV) or phosphonocetic acid (PAA). Vero cells were infected with wild-type (■, KOS), PAA resistant (△, PAA^{r5}) or ACV resistant (○, TK-) HSV-1 virus at a multiplicity of infection of 3 plaque-forming units per cell for 1 hour at 37°C. After removing inocula, infected cells were washed and overlaid with complete medium supplemented with (A) 0, 0.5, 1.05, 2 or 10 μM dUY11; (B) 0, 2.5, 5, 10, 25 or 50 μM ACV (I), or 0, 25, 50, 100, 250 or 500 μg/ml PAA (II). Cells and supernatants were harvested at 24 hpi and viral replication was evaluated by plaque assay. Viral yields were calculated by dividing viral titers in the presence of drug by viral titers in the absence of drug. The error bars represent the ranges of two experiments (A).

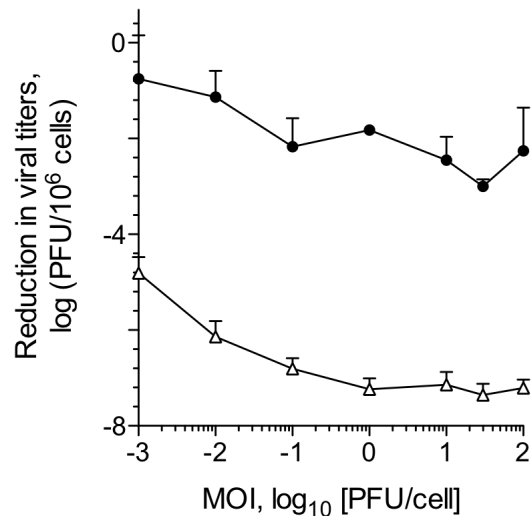


Figure 5.4 The antiviral effects of dUY11 are not attenuated by increasing multiplicity of infection. Logarithmic line graph showing relative viral titers at 24 hours post-infection (hpi) plotted against multiplicity of infection (MOI). Vero cells were infected for 1 h with 0.001, 0.01, 0.1, 1, 10, 30 or 100 plaque-forming unit per cell, washed and overlaid with media supplemented with 1 (●) or 2 μM (△) dUY11, or in the absence of drug. Cells and supernatants were harvested at 24 hpi and viral replication was evaluated by plaque assay. Viral yields were calculated for each MOI by dividing viral titers in the presence of dUY11 by viral titers in the absence of drug. The error bars represent the ranges of two experiments.

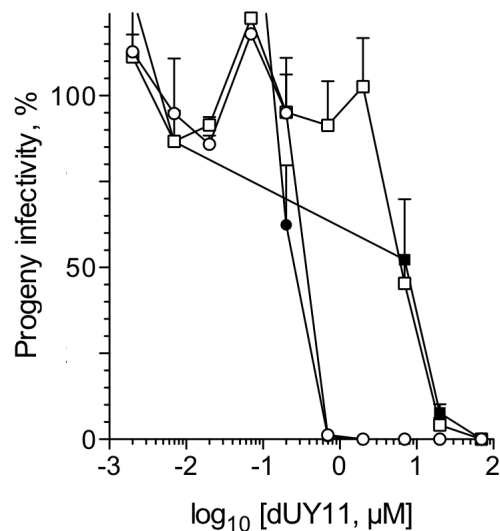


Figure 5.5 Treatment of HSV-1 infected cells with dUY11 inhibits the levels of cell-free and cell-associated progeny infectivity. Semi-logarithmic line

graph showing progeny virion infectivity against the logarithm of dUY11 concentration. Vero cells were infected with HSV-1 KOS at a multiplicity of infection of 3 plaque-forming units per cell for 1 hour. Infected cells were washed and overlaid with media supplemented with 0, 0.002, 0.007, 0.02, 0.07, 2, 7, 20 or 70 μM dUY11 for 1 hour (**squares**) or continuously for 23 hours (**circles**). HSV-1 infected cells washed 1 hour post-treatment were overlaid with media in the absence of drug. At 24 hpi, intracellular (**filled symbols**) and released (**open symbols**) progeny virions were harvested separately. The levels of infectivity were evaluated by plaque assay using volumes equivalent to that which produced 200 plaques in cells treated without drug. Error bars represent the ranges of two experiments. The percent of progeny virion infectivity produced from infected cells treated with 0.002 to 0.07 μM dUY11 was increased nearly 4-fold, and thus omitted for clarity.

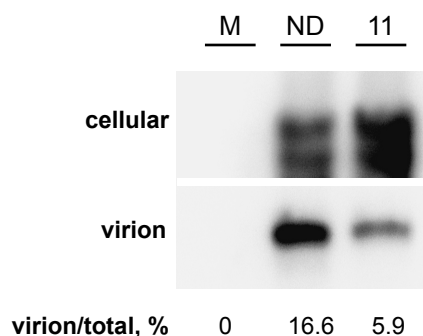


Figure 5.6 dUY11 inhibits the release of progeny virions by only 2.8 fold. Southern blot analysis showing the levels of viral DNA in cells and in released extracellular virions. Vero cells were mock-infected (**M**; left lane) or infected with HSV-1 KOS at a multiplicity of infection of 5 plaque-forming units per cell. After a 1-hour adsorption, cells were washed and infected cells were overlaid with media supplemented with no drug (**ND**; center lane) or 7 μ M dUY11 (**11**; right lane). At 24 hpi, cell-associated and released progeny virions were harvested separately. Virions were purified from the medium through a 20% sucrose cushion and virion pellets were lysed. The levels of viral DNA in cell-associated (**cellular**; top panel) and extracellular (**virion**, bottom panel) virions were analysed by Southern blot hybridization. DNA levels from released extracellular virions are expressed as percent of total viral DNA, calculated by dividing the DNA level in released extracellular virions by the total recovered DNA.

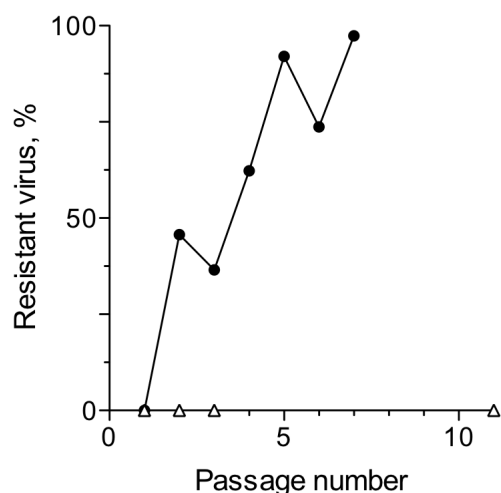


Figure 5.7 No dUY11-resistant variants were detected after 10 passages in selective media. Line graph showing the percentage of dUY11- and phosphonoacetic acid (PAA)-resistant virus against passage number. Plaque-purified HSV-1 strain KOS was passaged in medium containing an increasing concentration of dUY11 or PAA, or in the absence of drug. To determine % resistance to PAA, Vero cells were then infected with 200 HSV-1 virions from each passage, washed, and overlaid with semi-solid medium containing no drug or 100 $\mu\text{g}/\text{mL}$ PAA (\bullet). To determine % resistance to dUY11, 200 HSV-1 virions isolated from each passage were exposed to no drug, or to 2 μM dUY11 (Δ) for 5 minutes at 37°C. Vero cells were infected for the so-exposed virions for 1 hour, washed, and overlaid with semi-solid medium containing no drug. Resistance was evaluated by monitoring plaquing. Percent resistance was calculated by dividing the number of plaques in the presence of drug by the number of plaques in the absence of drug ($\times 100$). PAA selection was discontinued at passage 8. The % resistance to dUY11 for passages 4 through 10 could not be determined due to low viral yields.

CHAPTER 6: HERPES SIMPLEX VIRUS TYPE-2 VIRIONS PRE-EXPOSED TO RIGID AMPHIPATHIC FUSION INHIBITORS ARE NOT INFECTIOUS TO MICE

This chapter contains unpublished data.

6.1 Introduction

Herpes simplex virus type 2 (HSV-2) is the most prevalent agent of genital herpes, a common sexually transmitted disease (STD) (Xu et al., 2006). HSV-1 also produces a subset of cases of genital infections (Kalinyak, Fleagle, and Docherty, 1977). Following primary infection, HSV-1 and -2 establish lifelong latent infections, with periodic recurrences (Colberg-Poley, Isom, and Rapp, 1981). HSV-1 or -2 infection rates are beginning to decrease in some countries, such as the United States (Xu et al., 2010), and barrier methods to prevent transmission (e.g. condoms) are available. Nonetheless, genital herpes remains a highly prevalent STD (Fife et al., 2006). Moreover, several studies have shown that infection with HSV-2 enhances the risk for sexual transmission of other diseases, such as HIV (for examples, see (Freeman et al., 2006; Renzi et al., 2003; Schacker et al., 1998; Wald and Link, 2002). Current antiviral drugs do not stop the spread or new genital herpes infections, or other viral STDs. Novel antiviral agents are therefore needed.

Microbicides could contribute to controlling the spread of STDs, but their development presents unique challenges relative to other antiviral strategies

(Hendrix, Cao, and Fuchs, 2009). Microbicides must remain active in the presence of vaginal fluids, seminal fluids, cervical mucous and acidic vaginal pH. Viscosity, distribution and retention of topically administered products to ensure good coating of the target epithelia (vagina or rectum) are fundamental for their efficacy (Morris and Lacey, 2010). An ideal microbicide should be odorless, colorless, not systemically absorbed, and acceptable to the users. They must be suitable for use in the developed and underdeveloped world. Stability, low cost and ease of application, as well as easy delivery mechanisms (i.e. vaginal rings, films) are all important factors (Buckheit et al., 2010).

Attempts at developing microbicides have yet to be successful, and multiple advanced clinical trials on antiviral microbicides have failed. Several non-specific surfactants such as nonoxynol-9 appeared initially promising. Unfortunately, the lack of specificity of all such agents resulted in toxicities on the vaginal and rectal epithelium and, consequently, inefficacy (Phillips and Zacharopoulos, 1998). They all failed to prevent transmission (Roddy et al., 1998; Van Damme et al., 2002), and in some cases, they even increased it (Cone et al., 2006; Phillips and Zacharopoulos, 1998).

Other microbicides aim at inhibiting viral entry by non-specific or specific mechanisms. For example, the anionic polymer (Carraguard) and cellulose sulfate (Ushercell) were under development as microbicides (Balzarini and Van Damme, 2007). Unfortunately, two phase 3 clinical trials indicated they are ineffective (Ramjee et al., 2008; Scordi-Bello et al., 2005; Skoler-Karpoff et al., 2008; Van Damme et al., 2008). Viral fusion inhibitors are also under development, such as

the modified enfuvirtide C52-L (Veazey et al., 2005). However, such peptidomimetics are clinically limited by their instability. These limitations would be expected to be enhanced in a microbicide, which must remain active intravaginally or intrarectally for several hours.

Agents targeting viral replication are also being considered for microbicide development. The first vaginal gel (1% tenofovir formulation) was recently found to reduce the transmission of HIV, with an estimated overall reduction of HIV infection by 39%, and up to 54% in women with high gel adherence (Karim et al., 2010). However, there are reservations regarding the prophylactic development of drugs targeting viral proteins used therapeutically, as such strategies are predicted to introduce additional drug-resistant selective pressures (Wilson et al., 2008). Exposure of an infected individual to the topical microbicide may add to the selective pressures, and resistant mutants may be selected for more rapidly. These resistant mutants would not be sensitive to the microbicide agent, and such strategies may thus increase the transmission of drug-resistant variants.

I have discovered a novel family of inhibitors of infectivity, the rigid amphipathic fusion inhibitors, or RAFIs. In **chapters 3, 4 and 5**, I characterized their novel mechanisms of action in cultured cells. RAFIs inhibit infectivity by preventing the first steps of infection (fusion). They also inhibit the infectivity produced by cells treated after infection. RAFIs may therefore have the potential for therapeutic and prophylactic uses. However, the inhibition of negative

curvature formation is a novel antiviral approach. Consequently, the viability of this antiviral strategy to inhibit infection *in vivo* was untested.

As a first step to address the viability of RAFIs as antiviral microbicides, I tested whether virions exposed to dUY11 were infectious to animals. In pilot studies, therefore, I evaluated whether HSV-2 virions pre-exposed to a high concentration of dUY11 were infectious to mice. In this chapter, I report that even three lethal doses of HSV-2 exposed to dUY11 before infecting the mice were not infectious to them, as evaluated by clinical signs of infection and evaluation of virus replication. These findings indicate that the novel antiviral mechanisms of RAFIs are also effective against infection of mice.

6.2 Results

6.2.1 Evaluation of the infectivity to mice of herpes simplex virus type-2 exposed to dUY11 before infection

The viability of the novel antiviral strategy of RAFIs in animals was yet unknown. I therefore performed preliminary studies to evaluate whether HSV-2 virions exposed to RAFI were infectious to mice. I selected a commonly used model, intravaginal infection of mice with HSV-2 (Parr et al., 1994). This small animal model has been extensively used to evaluate potential microbicides, vaccines and antivirals (Keller et al., 2005; Mcdermott et al., 1984). Previous reports indicated that 1,000 plaque-forming units (PFU) of HSV-2 strain 186 is a lethal dose for approximately 50% of mice (LD₅₀) in diestrus and proestrus

(Bernstein et al., 2003). In the first study, therefore, progesterone-treated mice were inoculated with 1,000 PFU of HSV-2.

The studies in cell cultures had identified dUY11 as the most potent RAFI (**Figure 3.2, Table 3.1**). dUY11 inhibited the infectivity of the two HSV-2 strains I tested (**Figure 4.1**). Moreover, dUY11 was not cytotoxic and only mildly cytostatic at 150 μ M (**Figure 3.5, Tables 3.2 and 3.3**), although it formed aggregates at concentrations higher than 70 μ M.

I tested dUY11 at the highest possible stable concentration of 70 μ M, initially dissolved in dimethyl sulfoxide (DMSO) and then further diluted in DMEM.

6.2.1.1 One lethal dose for 50% of mice of herpes simplex virus type-2 exposed to dUY11 is not infectious to mice

In an initial study, I exposed one LD₅₀ (1,000 PFU) of HSV-2 virions to 70 μ M dUY11 or DMSO diluted in DMEM, to then evaluate their infectivity to mice. Female BALB/C mice were synchronized by sub-cutaneous injection of 3 mg per kg of sterile Depo-Provera (Kaushic et al., 2003). Six days later, randomized groups of 5 animals were anesthetized prior to infection. Aliquots of infectious HSV-2 virions (containing a total of 1×10^4 PFU each of strain 186) pre-warmed to 37°C were exposed to 70 μ M dUY11 or DMSO vehicle at 37°C for a minimum of 5 minutes. Each animal was then infected intravaginally with 1,000 PFU (1xLD₅₀) of the so-exposed HSV-2 virions. Infection was assessed daily by monitoring weight, clinical signs, and shedding of infectious virus.

Clinical signs were scored using the 5-point scale (**Table 2.1**) established by Gillgrass et al. (2003), with minor modifications. A score of 0 was assigned to healthy mice with no sign of infection. A score of 0+ was assigned if mild redness and swelling of external vagina was observed, whereas a score of 1 was assigned if these signs were accompanied by localized hair loss. A score of 2 was assigned if moderate redness and swelling of external genitalia was observed, whereas a score of 2+ was assigned if these signs were accompanied by localized hair loss. A score of 3 was assigned if redness and inflammation of the external vagina were severe, accompanied by hair loss in the genital area. A score of 4 was assessed if localized genital ulcerations accompanied severe inflammation, redness and hair loss in the genital area and surrounding tissue. A score of 5 was assigned to animals with severe genital ulceration extending to surrounding tissue, or to animals with neurological symptoms, including hind-limb paralysis. Mice were euthanized when they developed clinical signs of terminal illness, defined as disseminated infection, ulcerated secondary infection, bacterial contamination of skin lesions, hind-limb paralysis, or more than 10% of body weight loss in a 24-hour period.

6.2.1.1.1 Evaluation of herpes simplex virus type-2 infection

Viral replication in mice infected with virions exposed to dUY11 or DMSO vehicle before infection was monitored by standard titration of vaginal lavages. One LD₅₀ of HSV-2 strain 186 exposed to DMSO was sufficient to infect all 5 control animals, as expected. Consequently, all five shed infectious virus (black

bar, **Figure 6.1A**). Four shed detectable virus on the first day after infection, and none by 8 days post-infection (dpi). The average peak titer for the group of control animals was $\sim 10^4$ PFU per animal on days 4 and 5 after infection (filled square, **Figure 6.1B**).

No animal infected with $1xLD_{50}$ HSV-2 virions exposed to dUY11 before intravaginal infection shed any detectable virus (open bar, **Figure 6.1A**) at any time until 11 days after infection (open square, **Figure 6.1B**), when the study was terminated.

All 5 mice infected with $1xLD_{50}$ HSV-2 exposed to DMSO before infection displayed obvious clinical signs (black bar, **Figure 6.1C**). All five showed mild signs of clinical infection (scores of 1) on the first day after infection. Two animals displayed either no or only mild signs of clinical infection thereafter. A score of 3 or higher was assessed for three of the five animals at 8 dpi. Three mice infected with $1xLD_{50}$ HSV-2 exposed to DMSO before infection had to be euthanized due to advanced clinical illness (filled square, **Figure 6.1D**) on day 8 or 9 (one or two mice, respectively).

No animal infected with $1xLD_{50}$ HSV-2 exposed to dUY11 before infection showed any obvious clinical sign of infection at any time (open bar, **Figure 6.1C**). No animal scored higher than 0 at any time up to 11 dpi, when the study was terminated. All five animals infected with $1xLD_{50}$ HSV-2 pre-exposed to dUY11 survived (open square, **Figure 6.1D**). None had to be euthanized until 11 dpi, when the study was terminated.

Therefore, our first study indicated 1xLD₅₀ HSV-2 exposed to a high concentration of dUY11 before infecting the animals was not infectious to mice.

6.2.1.2 Three lethal doses for 50% of mice of herpes simplex virus type-2 exposed to dUY11 are not infectious to mice

One LD₅₀ of HSV-2 pre-exposed to dUY11 was not infectious to mice (**Figure 6.1**). I next evaluated the infectivity of three LD₅₀ (3xLD₅₀) exposed to dUY11 to mice.

Female BALB/C mice were synchronized by progesterone administration, as described in **section 6.2.1.1**. Six days later, randomized groups of 5 animals each were anesthetized prior to infection. Aliquots of infectious HSV-2 virions (containing a total of 2.5×10^4 PFU each of strain 186) pre-warmed to 37°C were exposed to 70 µM dUY11 or DMSO vehicle at 37°C for a minimum of 5 minutes. Each anesthetized mouse was then infected intravaginally with 3xLD₅₀ (3,000 PFU) of the so-exposed HSV-2 virions. Infection was assessed daily by monitoring weight, clinical signs and shedding of infectious virus, as described in **section 6.2.1.1**.

6.2.1.2.1 Evaluation of herpes simplex virus type-2 infection

Viral replication in mice infected with virions exposed to dUY11 or DMSO vehicle before infection was monitored by standard titration of vaginal lavages. All 5 animals infected with 3xLD₅₀ HSV-2 exposed to DMSO vehicle before infection shed infectious virus, as expected (black bar, **Figure 6.2A**). All shed

detectable levels of virus at 2 dpi (the first sampling day) and continued to shed detectable virus until 6 dpi (filled square, **Figure 6.2B**). Two animals still shed detectable virus at 7 dpi and one at 8 dpi. One animal survived past 8 dpi, shedding no detectable virus until the end of the study. The average peak virus shedding was approximately $\sim 10^4$ PFU per animal at days 2 through 4.

No mouse infected with $3 \times LD_{50}$ HSV-2 virions exposed to dUY11 before infection shed any detectable virus (open bar, **Figure 6.2A**) at any time for up to 14 days after infection (open square, **Figure 6.2B**), when the study was terminated.

All 5 animals infected with $3 \times LD_{50}$ HSV-2 exposed to DMSO vehicle displayed clinical signs of infection (black bar, **Figure 6.2C**). All five showed mild signs of clinical infection (scores of 1) on the first examination day (2 dpi) and advanced clinical signs (scores of 2 or higher) at some time during the study. Clinical signs of disease advanced in all five animals after 4 dpi, when virus shedding decreased, as expected when animals start to show neurological signs, indicating that the infection has moved from the skin to the central nervous system. Advanced clinical signs included disseminated infection to secondary sites and bacterial contamination of ulcerations (**Figure 6.3**), and neurological implications. All animals infected with virus exposed to vehicle had to be euthanized due to terminal illness (filled square, **Figure 6.2D**), as expected for the inoculum. Two animals were euthanized at 7 dpi, two at 8 dpi and the fifth, at 10 dpi.

No animal infected with 3xLD₅₀ HSV-2 exposed to dUY11 before infection showed any obvious clinical sign of infection at any time during the study (open bar, **Figures 6.2C** and **6.3**). No animal was scored higher than 0 at any time for up to 14 dpi. All five mice infected with 3xLD₅₀ HSV-2 pre-exposed to dUY11 survived (open square, **Figure 6.2D**). None of the five animals were euthanized until day 14, when the study was terminated.

In summary, 3xLD₅₀ HSV-2 pre-exposed to a high concentration of dUY11 was not infectious to mice.

6.3 Discussion

RAFIs act by unique non-nucleosidic mechanisms (**Chapters 3** and **5**). They target the virion envelope bilayer to prevent the formation of the negative curvature required for fusion of all enveloped viruses. I showed that exposure of infectious virions to these novel compounds inhibited their infectivity to cultured cells (**Chapters 4** and **5**). In this chapter, I expand on those results, showing that HSV-2 virions exposed to a high concentration of dUY11 are not infectious to mice either (**Figures 6.1** to **6.3**).

Drugs targeting molecules of cellular origin, such as envelope lipids, are less characterized as antivirals than classic drugs targeting proteins. Therefore, the viability of such compounds as an antiviral strategy to prevent infection of animals was untested.

As a first step to evaluate its viability, I have shown that HSV-2 virions exposed to a high concentration of dUY11 in DMEM before infecting mice are non-infectious to them when introduced vaginally.

In my studies, however, the animals were exposed only once to a high dUY11 concentration in a liquid formulation (with the pre-exposed virions). The effects of direct exposure of the vagina to RAFI in a relevant formulation have yet to be evaluated. As for all microbicide agents, a formulation with an appropriate viscosity will be required to prevent infection *in vivo*. The appropriate viscosity to coat the mucosal surface with effective concentrations of RAFI is needed for infecting virions to be exposed to RAFI molecules. Studies aimed at evaluating the efficacy of RAFIs in the presence of vaginal fluids, cervical mucous, or at vaginal pH are also important, since such treatment conditions could counteract the antiviral activities of dUY11. The ability to remain active under such treatment conditions is a critical characteristic for any agent pursued as a potential microbicide (Buckheit et al., 2010). The minimal effective dose, pharmacokinetics and responses to direct RAFI application into mouse vagina have yet to be investigated. Moreover, microbicides are sometimes used several times per day. The effects of repeated exposure and multiple dosing must therefore be evaluated. The intravaginal mouse model would be useful for such studies (Catalone et al., 2004).

Previous attempts at developing microbicides used non-specific agents, which lacked specificity or efficacy. Agents targeting lipids aimed at destabilizing virion envelopes. Some compounds modulated membrane fluidity with

cholesterol-like, cholesterol-binding molecules, or cholesterol regulating drugs (Barman and Nayak, 2007; Brugh, 1977; Harada, 2005; Kim et al., 1978; Pal, Barenholz, and Wagner, 1981). However, they also disturb the stability or fluidity of cellular membranes, which are critical to cell membrane integrity. The best studied membrane destabilizing agent is nonoxynol-9. Unfortunately nonoxynol-9, like all of these agents, is non-specific. Such agents have antiviral activities that are directly correlated with cytotoxicity, mucosal injuries, or induction of inflammatory responses. All of these side effects actually enhance susceptibility to infection (Cone et al., 2006; Phillips and Zacharopoulos, 1998). Antiviral drugs targeting viral proteins are thus now being pursued as prophylactic microbicides. However, the selection for drug resistance remains a major concern for microbicidal strategies targeting viral proteins.

Targeting the formation of negative envelope bilayer curvature to inhibit viral fusion may address some of the concerns and limitations of existing microbicide strategies. RAFIs target envelope curvature transitions unique to virions and are thus specific, at least in cultured cells. Moreover, their target is conserved among otherwise unrelated enveloped viruses, several of which are responsible for important STDs. RAFIs have the potential to have broad specificities, a highly desirable characteristic for microbicides. RAFIs are specific for envelope functions not encoded within mutable viral genomes. They may thus prove useful in prophylactic and therapeutic interventions without posing additional drug-resistant selective risks. Further *in vivo* studies on the potential of RAFIs as antiviral compounds are therefore warranted.

6.4 References

- Balzarini, J., and Van Damme, L. (2007). Microbicide drug candidates to prevent HIV infection. *Lancet* **369**(9563), 787-797.
- Barman, S., and Nayak, D. P. (2007). Lipid raft disruption by cholesterol depletion enhances influenza A virus budding from MDCK cells. *J Virol* **81**(22), 12169-78.
- Bernstein, D. I., Stanberry, L. R., Sacks, S., Ayisi, N. K., Gong, Y. H., Ireland, J., Mumper, R. J., Holan, G., Matthews, B., McCarthy, T., and Bournel, N. (2003). Evaluations of unformulated and formulated dendrimer-based microbicide candidates in mouse and guinea pig models of genital herpes. *Antimicrobial Agents and Chemotherapy* **47**(12), 3784-3788.
- Brugh, M. (1977). Butylated Hydroxytoluene Protects Chickens Exposed to Newcastle-Disease Virus. *Science* **197**(4310), 1291-1292.
- Buckheit, R. W., Watson, K. M., Morrow, K. M., and Ham, A. S. (2010). Development of topical microbicides to prevent the sexual transmission of HIV. *Antiviral Research* **85**(1), 142-158.
- Catalone, B. J., Kish-Catalone, T. M., Budgeon, L. R., Neely, E. B., Ferguson, M., Krebs, F. C., Howett, M. K., Labib, M., Rando, R., and Wigdahl, B. (2004). Mouse model of cervicovaginal toxicity and inflammation for preclinical evaluation of topical vaginal microbicides. *Antimicrobial Agents and Chemotherapy* **48**(5), 1837-1847.
- Colberg-Poley, A. M., Isom, H. C., and Rapp, F. (1981). Involvement of an Early Human Cytomegalo-Virus Function in Reactivation of Quiescent Herpes-Simplex Virus Type-2. *Journal of Virology* **37**(3), 1051-1059.
- Cone, R. A., Hoen, T., Wong, X. X., Abusuwwa, R., Anderson, D. J., and Moench, T. R. (2006). Vaginal microbicides: detecting toxicities in vivo that paradoxically increase pathogen transmission. *Bmc Infectious Diseases* **6**, -.
- Fife, K. H., Fortenberry, J. D., Ofner, S., Katz, B. P., Morrow, R. A., and Orr, D. P. (2006). Incidence and prevalence of herpes simplex virus infections in adolescent women. *Sexually Transmitted Diseases* **33**(7), 441-444.
- Freeman, E. E., Weiss, H. A., Glynn, J. R., Cross, P. L., Whitworth, J. A., and Hayes, R. J. (2006). Herpes simplex virus 2 infection increases HIV acquisition in men and women: systematic review and meta-analysis of longitudinal studies. *Aids* **20**(1), 73-83.
- Gillgrass, A. E., Ashkar, A. A., Rosenthal, K. L., and Kaushic, C. (2003). Prolonged exposure to progesterone prevents induction of protective mucosal responses following intravaginal immunization with attenuated herpes simplex virus type 2. *Journal of Virology* **77**(18), 9845-9851.
- Harada, S. (2005). The broad anti-viral agent glycyrrhizin directly modulates the fluidity of plasma membrane and HIV-1 envelope. *Biochemical Journal* **392**, 191-199.
- Hendrix, C. W., Cao, Y. J., and Fuchs, E. J. (2009). Topical Microbicides to Prevent HIV: Clinical Drug Development Challenges. *Annual Review of Pharmacology and Toxicology* **49**, 349-375.

- Kalinyak, J. E., Fleagle, G., and Docherty, J. J. (1977). Incidence and Distribution of Herpes-Simplex Virus Type-1 and Type-2 from Genital Lesions in College-Women. *Journal of Medical Virology* **1**(3), 175-181.
- Karim, Q. A., Karim, S. S. A., Frohlich, J. A., Grobler, A. C., Baxter, C., Mansoor, L. E., Kharsany, A. B. M., Sibeko, S., Mlisana, K. P., Omar, Z., Gengiah, T. N., Maarschalk, S., Arulappan, N., Mlotshwa, M., Morris, L., Taylor, D., and Grp, C. T. (2010). Effectiveness and Safety of Tenofovir Gel, an Antiretroviral Microbicide, for the Prevention of HIV Infection in Women. *Science* **329**(5996), 1168-1174.
- Kaushic, C., Ashkar, A. A., Reid, L. A., and Rosenthal, K. L. (2003). Progesterone increases susceptibility and decreases immune responses to genital herpes infection. *Journal of Virology* **77**(8), 4558-4565.
- Keller, M. J., Tuyama, A., Carlucci, M. J., and Herold, B. C. (2005). Topical microbicides for the prevention of genital herpes infection. *Journal of Antimicrobial Chemotherapy* **55**(4), 420-423.
- Kim, K. S., Moon, H. M., Sapienza, V., Carp, R. I., and Pullarkat, R. (1978). Inactivation of Cytomegalovirus and Semliki Forest Virus by Butylated Hydroxytoluene. *Journal of Infectious Diseases* **138**(1), 91-94.
- Mcdermott, M. R., Smiley, J. R., Leslie, P., Brais, J., Rudzroga, H. E., and Bienenstock, J. (1984). Immunity in the Female Genital-Tract after Intravaginal Vaccination of Mice with an Attenuated Strain of Herpes-Simplex Virus Type-2. *Journal of Virology* **51**(3), 747-753.
- Morris, G. C., and Lacey, C. J. (2010). Microbicides and HIV prevention: lessons from the past, looking to the future. *Curr Opin Infect Dis* **23**(1), 57-63.
- Pal, R., Barenholz, Y., and Wagner, R. R. (1981). Depletion and Exchange of Cholesterol from the Membrane of Vesicular Stomatitis-Virus by Interaction with Serum-Lipoproteins or Poly(Vinylpyrrolidone) Complexed with Bovine Serum-Albumin. *Biochemistry* **20**(3), 530-539.
- Parr, M. B., Kepple, L., Mcdermott, M. R., Drew, M. D., Bozzola, J. J., and Parr, E. L. (1994). A Mouse Model for Studies of Mucosal Immunity to Vaginal Infection by Herpes-Simplex Virus Type-2. *Laboratory Investigation* **70**(3), 369-380.
- Phillips, D. M., and Zacharopoulos, V. R. (1998). Nonoxynol-9 enhances rectal infection by herpes simplex virus in mice. *Contraception* **57**(5), 341-348.
- Ramjee, G., Doncel, G. F., Sanjay, M., Tolley, E. E., and Dickson, K. (2008). Microbicides 2008 conference: From discovery to advocacy. *AIDS research and Therapy* **5**(19), 1-14.
- Renzi, C., Douglas, J. M., Jr., Foster, M., Critchlow, C. W., Ashley-Morrow, R., Buchbinder, S. P., Koblin, B. A., McKirnan, D. J., Mayer, K. H., and Celum, C. L. (2003). Herpes simplex virus type 2 infection as a risk factor for human immunodeficiency virus acquisition in men who have sex with men. *J Infect Dis* **187**(1), 19-25.
- Roddy, R. E., Zekeng, L., Ryan, K. A., Tamoufe, U., Weir, S. S., and Wong, E. L. (1998). A controlled trial of nonoxynol 9 film to reduce male-to-female transmission of sexually transmitted diseases. *New England Journal of Medicine* **339**(8), 504-510.

- Schacker, T., Ryncarz, A. J., Goddard, J., Diem, K., Shaughnessy, M., and Corey, L. (1998). Frequent recovery of HIV-1 from genital herpes simplex virus lesions in HIV-1-infected men. *Jama* **280**(1), 61-6.
- Scordi-Bello, I. A., Mosoian, A., He, C. J., Chen, Y. B., Cheng, Y., Jarvis, G. A., Keller, M. J., Hogarty, K., Waller, D. P., Profy, A. T., Herold, B. C., and Klotman, M. E. (2005). Candidate sulfonated and sulfated topical microbicides: Comparison of anti-human immunodeficiency virus activities and mechanisms of action. *Antimicrobial Agents and Chemotherapy* **49**(9), 3607-3615.
- Skoler-Karppoff, S., Ramjee, G., Ahmed, K., Altini, L., Plagianos, M. G., Friedland, B., Govender, S., De Kock, A., Cassim, N., Palanee, T., Dozier, G., Maguire, R., and Lahteenmaki, P. (2008). Efficacy of Carraguard for prevention of HIV infection in women in South Africa: a randomised, double-blind, placebo-controlled trial. *Lancet* **372**(9654), 1977-1987.
- Van Damme, L., Govinden, R., Mirembe, F. M., Guedou, F., Solomon, S., Becker, M. L., Pradeep, B. S., Krishnan, A. K., Alary, M., Pande, B., Ramjee, G., Deese, J., Crucitti, T., and Taylor, D. (2008). Lack of effectiveness of cellulose sulfate gel for the prevention of vaginal HIV transmission. *New England Journal of Medicine* **359**(5), 463-472.
- Van Damme, L., Ramjee, G., Alary, M., Vuylsteke, B., Chandeying, V., Rees, H., Sirivongrangson, P., Mukenge-Tshibaka, L., Ettiegne-Traore, V., Uaheowitchai, C., Karim, S. S. A., Masse, B., Perriens, J., Laga, M., and Grp, C.-S. (2002). Effectiveness of COL-1492, a nonoxynol-9 vaginal gel, on HIV-1 transmission in female sex workers: a randomised controlled trial. *Lancet* **360**(9338), 971-977.
- Veazey, R. S., Klasse, P. J., Schader, S. M., Hu, Q. X., Ketas, T. J., Lu, M., Marx, P. A., Dufour, J., Colonno, R. J., Shattock, R. J., Springer, M. S., and Moore, J. P. (2005). Protection of macaques from vaginal SHIV challenge by vaginally delivered inhibitors of virus-cell fusion. *Nature* **438**(7064), 99-102.
- Wald, A., and Link, K. (2002). Risk of human immunodeficiency virus infection in herpes simplex virus type 2-seropositive persons: a meta-analysis. *J Infect Dis* **185**(1), 45-52.
- Wilson, D. P., Coplan, P. M., Wainberg, M. A., and Blower, S. M. (2008). The paradoxical effects of using antiretroviral-based microbicides to control HIV epidemics. *Proc Natl Acad Sci U S A* **105**(28), 9835-40.
- Xu, F., Sternberg, M. R., Gottlieb, S. L., Berman, S. M., Markowitz, L. E., Forhan, S. E., and Taylor, L. D. (2010). Seroprevalence of herpes simplex virus type 2 among persons aged 14-49 years- United States, 2005-2008. *Morbidity & Mortality Weekly Report* **59**(15), 456-459.
- Xu, F. J., Sternberg, M. R., Kottiri, B. J., McQuillan, G. M., Lee, F. K., Nahmias, A. J., Berman, S. M., and Markowitz, L. E. (2006). Trends in herpes simplex virus type 1 and type 2 seroprevalence in the United States. *Jama-Journal of the American Medical Association* **296**(8), 964-973.

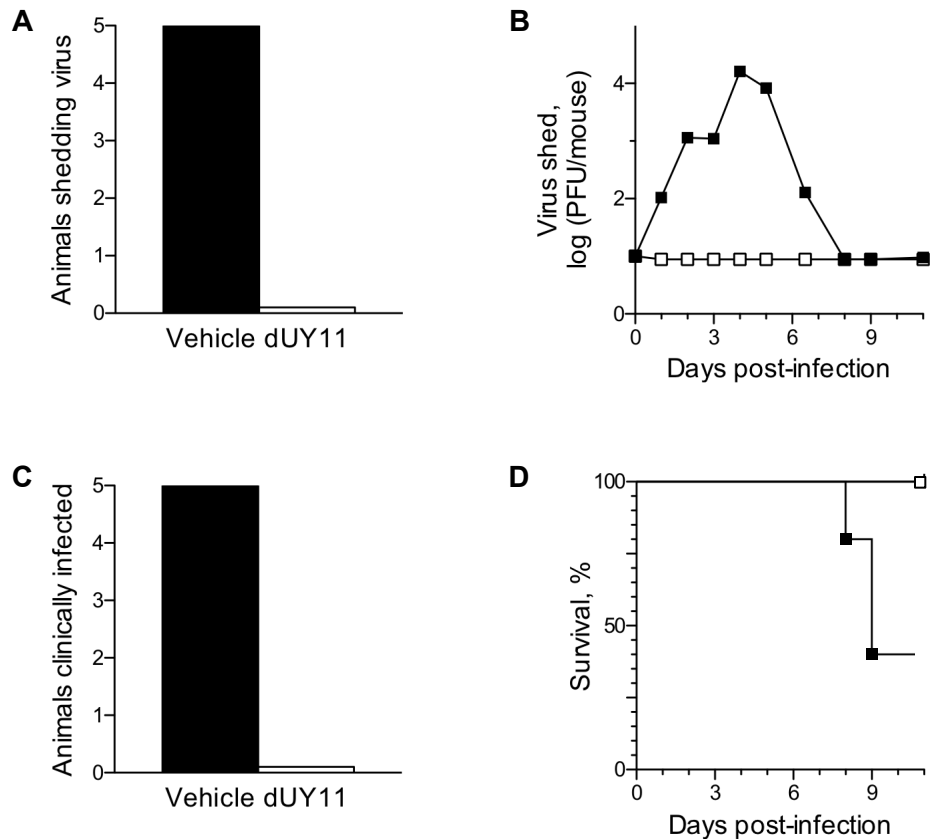


Figure 6.1 One LD₅₀ of HSV-2 virions pre-exposed to a high dose of dUY11 is not infectious to mice. Bar or line graphs showing number of animals shedding infectious virus (**A**), average virus shedding (**B**), number of animals displaying clinical signs (**C**) or alive (**D**). Groups of 5 synchronized female BALB/C mice were vaginally infected with 1,000 infectious HSV-2 strain 186 virions (1xLD₅₀) exposed for 5 minutes at 37°C to 0 (filled bars and squares) or 70 μM dUY11 (open bars and squares). Mice were monitored daily for weight, shedding of infectious virus (by standard titration of vaginal lavages) (**A,B**), and clinical signs (**C**). Mice were euthanized when they developed clinical signs of terminal illness (disseminated infection, bacterial contamination of skin lesions, hind-limb paralysis, or more than 10% of body weight loss in a 24-hour period) (**D**).

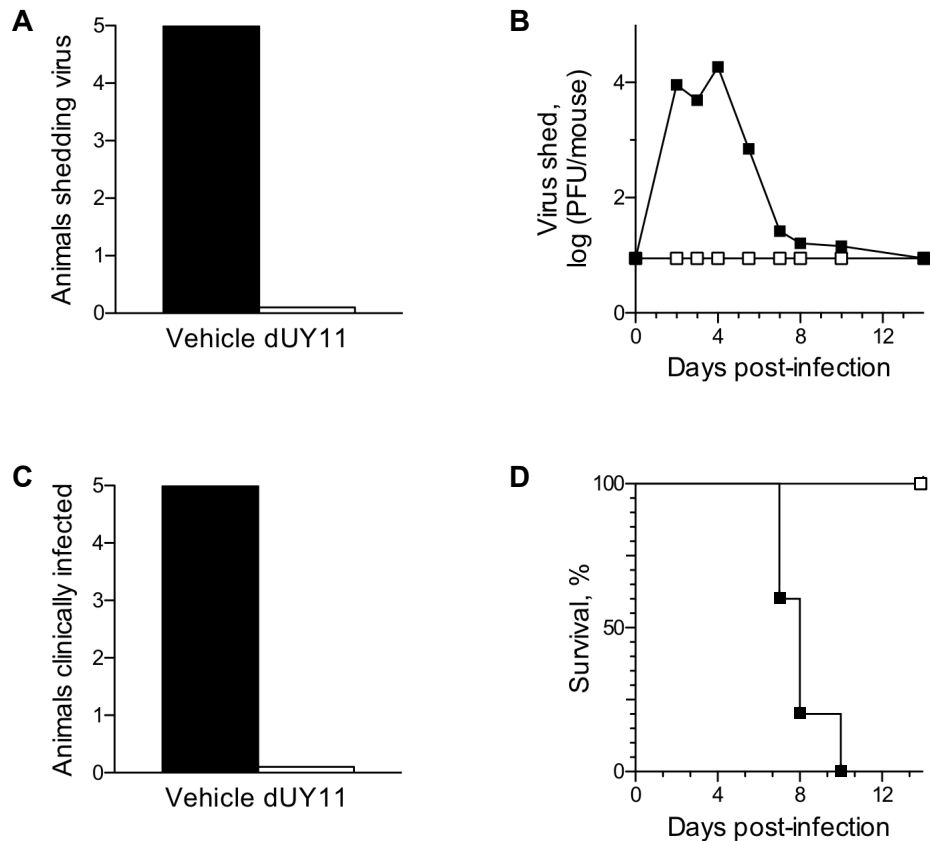


Figure 6.2 Three LD₅₀ of HSV-2 virions pre-exposed to a high dose of dUY11 are not infectious to mice. Bar or line graphs showing number of animals shedding infectious virus (**A**), average virus shedding (**B**), number of animals displaying clinical signs (**C**) or alive (**D**). Groups of 5 synchronized female BALB/C mice were vaginally infected with 3,000 infectious HSV-2 strain 186 virions (3xLD₅₀) exposed for 5 minutes at 37°C to 0 (filled bars and squares) or 70 μM dUY11 (open bars and squares). Mice were monitored daily for weight, shedding of infectious virus (by standard titration of vaginal lavages) (**A,B**), and clinical signs (**C**). Mice were euthanized when they developed clinical signs of terminal illness (disseminated infection, bacterial contamination of skin lesions, hind-limb paralysis, or more than 10% of body weight loss in a 24-hour period) (**D**).

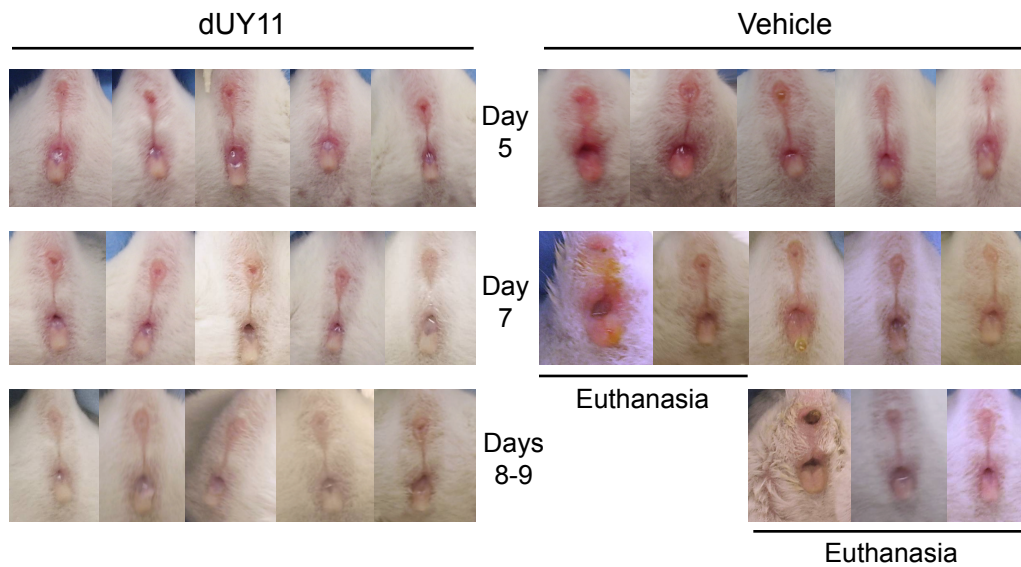


Figure 6.3 Mice infected with 3xLD₅₀ of HSV-2 pre-exposed to a high dose of dUY11 show no clinical signs. Photographic images of the vagina and perineal region of HSV-2 infected mice. Groups of 5 synchronized female BALB/C mice were vaginally infected with 3,000 infectious HSV-2 strain 186 virions (3xLD₅₀) exposed for 5 minutes at 37°C to 0 (**vehicle**, right) or 70 μM dUY11 (**dUY11**, left). Mice were monitored and photographed daily.

CHAPTER 7: DISCUSSION

In my Doctoral thesis, I describe the discovery and characterization of the first family of broad-spectrum small molecule inhibitors of the infectivity of enveloped viruses, including HCV, HSV-2, and drug-resistant HSV-1 strains. The rigid amphipathic fusion inhibitors (RAFIs) I have characterized have a novel antiviral mechanism. They are the first nucleoside analogues described to target bilayers and inhibit the formation of the negative envelope curvature required for the fusion of all enveloped viruses.

For my studies, I used mostly dUY11, the most potent RAFI identified to date, and HSV-1, a commonly used model in antiviral drug discovery (Schang, 2006). Structurally, the molecular shape, amphipathicity and rigidity were all required for their antiviral activities. Exposure of virions directly before adsorption onto cultured cells or by treating already-infected cells inhibited infectivity. Treating virions with RAFIs before infection inhibited the expression of a RFP reporter driven by a VP16-inducible promoter, indicating that RAFIs inhibited entry. However, virion exposure did not inhibit high-affinity binding, nor did it disrupt cellular or virion membranes. RAFIs inhibited the transition from lamellar to inverted-hexagonal phase (i.e., from flat to negative curvature) in model bilayer systems. The active interactions of RAFIs with virions required fluid envelopes, and the inhibition of infectivity of pre-exposed virions was independent of the cell type infected. These findings are all consistent with RAFIs interacting with virion bilayers to inhibit the formation of negative envelope

curvature required for their fusion to cell membranes (**Chapter 3**). The mechanism of antiviral action of RAFIs was further supported by dUY11 being active against the seven otherwise unrelated enveloped viruses tested, which bind to unrelated receptors and have no glycoprotein sequence homology, but not the two nonenveloped viruses tested (**Chapter 4**). Although RAFIs are nucleoside derivatives, dUY11 did not inhibit HSV-1 DNA replication. It did, however, inhibit the levels of progeny virion infectivity in already-infected and then treated cells, including those infected by PAA- or ACV-resistant HSV-1 strains. In contrast to most nucleoside derivatives, dUY11 did not promptly select for resistant variants either. Therefore, RAFIs do not act by classical nucleosidic antiviral mechanisms (**Chapter 5**). In pilot studies using small groups of mice, HSV-2 virions exposed to a high concentration of dUY11 were not infectious to mice (**Chapter 6**). Therefore, the inhibition of infectivity of virions exposed to RAFIs is not limited to cultured cells.

I have thus described the first nucleoside derivatives that inhibit viral fusion, and the first small molecule inhibitors of viral infectivity that target envelope bilayer curvature. My studies also provide an exciting proof-of-concept that such antiviral approaches are viable. Moreover, I have identified potent compounds that merit further development as potential antiviral agents.

7.1 Mechanisms of action of rigid amphipathic fusion inhibitors

According to my hypothesis and the proposed model, RAFIs interact with virion envelope lipids to prevent the formation of the negative curvature required for

viral fusion. The fusion of virion envelopes to cell membranes occurs through intermediate structures according to the principles of the widely accepted “hemifusion stalk” model (Chernomordik and Kozlov, 2005). To form the hemifusion stalk intermediate, the external leaflet of virion envelopes must transition from positive to negative curvature (Chernomordik and Kozlov, 2008). This energetically demanding lipid intermediate requires envelope lipids to diffuse and tilt, and their acyl chains splay and stretch, at the neck of the stalk (Kozlovsky and Kozlov, 2002) (**Figure 1.3**).

In agreement with the hemifusion stalk model, the fusion of vesicles can be modulated by the exogenous addition of natural lipids with different molecular shapes. Cone shaped lipids (with hydrophilic headgroups of smaller cross-section than their hydrophobic tails) adopt configurations with the headgroups bent towards each other (inverted-hexagonal phase; **Table 1.6**), and promote negative membrane curvature. In agreement with the general principles of the hemifusion stalk model, therefore, the exogenous addition of natural cone-shaped lipids such as phosphatidylethanolamine (PE) or oleic acid (OA) promote fusion when added into the outer leaflets of fusing vesicles. Conversely, inverted-cone shaped lysophospholipids (with hydrophilic headgroups of larger cross-section than their hydrophobic tail) promote positive curvature (where the lipid headgroups are bent away from each other, or so-called micellar phases; **Table 1.6**), and thus disfavor the formation of the negative membrane curvature required for fusion.

Consistently with the hemifusion stalk model, the exogenous addition of inverted-cone shaped lipids, such as lysophosphatidylcholine (LPC), into the outer leaflets

of vesicles inhibits their fusion (Basanez, Goni, and Alonso, 1998; Yeagle et al., 1994). Molecules that disfavor the formation of negative curvature inhibit viral fusion, too (Chernomordik and Kozlov, 2003). The exogenous addition of LPC to the external leaflet of virion envelopes inhibits the fusion of influenza (Chernomordik et al., 1999; Gunther-Ausborn, Praetor, and Stegmann, 1995), rabies virus (Gaudin, 2000), tick-borne encephalitis virus (Stiasny and Heinz, 2004), Sendai virus (Yeagle et al., 1994) and baculovirus (Vogel, Leikina, and Chernomordik, 1993), for example, by modulating envelope curvature (Gaudin, 2000; Stiasny and Heinz, 2004). Lysophospholipids (which adopt micellar configurations) are also virucidal, or detergents that lyse virion envelopes (Hilmarsson, Kristmundsdottir, and Thormar, 2005).

RAFIs are synthetic small molecules that also have a hydrophilic region of larger cross-section than their hydrophobic one. RAFIs too disfavored the formation of negative membrane curvature (**Figures 3.11** and **3.12**). In contrast to micellar-forming lipids, however, RAFIs did not lyse virions (**Figure 3.7**). SAR studies indicated that the molecular shape (with a hydrophilic region of larger cross-section than the hydrophobic one), amphipathicity and rigidity were all important structural requirements (**Figure 3.2** and **Table 3.1**). The introduction of polarity and flexibility in the linker or core hydrophobic moiety, such as in dUY7 or dUY9 for example, which reduce amphipathicity and rigidity, also decreased the antiviral activities (**Figure 3.2** and **Table 3.1**). Modifications of the molecular shape or rigidity would be expected to prevent the proper positioning of the compounds into envelopes, or to reduce their ability to prevent the lipid

reorganizations (diffusion, tilting, stretching and splaying of envelope lipids) required for hemifusion stalk formation (further discussed in **section 7.5**). Consistently, dUY11 targets virion envelopes (**Figure 3.14**) and its active interactions with virions required fluid envelopes (**Figure 3.15**). These findings are all most consistent with RAFIs interacting with virion bilayers to inhibit the formation of negative curvature required for the hemifusion stalk.

The antiviral activities of nucleoside analogues containing small alkynyl substituents were studied before, but analogues with large polyaryl substituents were not. The first 5-alkynyl-2'-deoxyuridine (5-phenylethynyl-2'-deoxyuridine) was tested nearly 30 years ago by Dr. Erik De Clercq and co-workers (De Clercq et al., 1982; De Clercq et al., 1983). The activities of such small 5-alkynyl-2'-deoxyuridine were evaluated against viral genome replication. Alkynyl side chain derivatives, such as elongated, branched or further substituted modifications, including a phenylethynyl substituent, all lacked antiviral activities (De Clercq et al., 1983). Such 2'-deoxyuridine derivatives with small, flexible mono-phenyl substituents therefore appeared prospectless, and were not further pursued as antivirals. In contrast to those compounds, however, the 2'-deoxyuridine analogues with aromatic substituents described in this thesis are potent antivirals. These compounds contain large, rigid, polycyclic substituents with a hydrophilic region of larger cross-section than their hydrophobic one. Their molecular shape and rigidity are thus unique from those compounds originally investigated by Dr De Clercq's group. Moreover, I evaluated and characterized the activities of RAFIs as inhibitors of infectivity, not as inhibitors of genome replication.

The 5-arylethynyl-2'-deoxyuridines characterized as fusion inhibitors in this thesis were originally synthesized because of their fluorescence as DNA labels (Korshun et al., 1998; Korshun et al., 1997; Malakhov et al., 2000; Skorobogatyi et al., 2006a). Two 2'-deoxyuridine analogues with bulky, polycyclic 5-arylethynyl substituents (dUY4 and dUY11) belonging to this family of fluorescent DNA probes were then reported to have selective anti-herpetic activities (selectivity index (SI) of 10 or 32, respectively, for dUY4 or dUY11) (Andronova et al., 2003; Pchelintseva et al., 2005). Another 6 members showed moderate selective activity, with SIs between 8 and 10 (Skorobogatyi et al., 2006b; Skorobogatyi et al., 2006c). The 5-arylethynyl-2'-deoxyuridines with polycyclic substituents therefore showed limited potential as small molecule antivirals. Considering these are nucleoside derivatives designed to be incorporated into DNA to label it (and thus are known substrates for DNA polymerases), a classic nucleosidic mechanism as inhibitors of viral genome replication was proposed (Andronova et al., 2003; Pchelintseva et al., 2005).

The initial studies reported that the dose of dUY11 and dUY2 required to inhibit HSV-1 (strain L₂)-induced cytopathicity by 50% (ID₅₀) was 7.8 or 15.6 µg/mL (15.5 or 34.5 µM), respectively (Andronova et al., 2003). The dose of dUY11 required to inhibit HSV-1 cytopathicity by 95% (ID₉₅) was reportedly 31 µM (Andronova et al., 2003). The ID₅₀ and ID₉₅ calculated by Andronova et al. (2003) were evaluated 48 hours after infection of Vero cells at a multiplicity of infection (MOI) of 0.1 plaque-forming units (PFU) per cell. The concentration which caused the death of no more than 50% of cells (CD₅₀) was reported to be

>250 $\mu\text{g/mL}$, or >497 μM , measured by trypan blue exclusion 72 hours after compound addition (Andronova et al., 2003). dUY11 was therefore characterized as having a SI of 32, expressed as the $\text{CD}_{50}/\text{ID}_{50}$ ratio (Andronova et al., 2003).

I found that dUY11 was a much more potent antiviral than reported in those original studies. When I exposed HSV-1 virions directly to dUY11 before infection, the IC_{50} and IC_{95} against infectivity (IC_{50} , 0.038 μM ; IC_{95} , 2.16 μM , **Figure 3.3**) were ~400- or 15-fold lower, respectively, than the ID_{50} and ID_{95} calculated by Andronova et al. at 48 hpi (2003). Moreover, CD_{50} was not reached at any dUY11 concentration at which it was stable in DMEM (up to 70 μM), even when the compound was replenished every 24 hours (**Figure 3.5, Table 3.3**). Despite extensive efforts, I was not able to obtain dUY11 in stable solutions at any concentration above 70 μM , for any time under any condition. The SI calculated from my experiments was therefore larger than 1,800.

I also maintained already-infected Vero cells (at a MOI of 3 PFU per cell) in dUY11-containing medium continuously for 23 hours. The IC_{50} against the levels of infectivity in cells continuously treated (IC_{50} ~0.24 μM , **Table 5.1**) was only 4-fold less than the IC_{50} determined when I measured viral yields 24 hours after infection (IC_{50} , 0.9 μM , **Figure 5.1**), and only 6-fold higher than the IC_{50} against HSV-1 when virions were directly exposed before infection (IC_{50} , ~0.24 μM for continuous treatment of cells, compared to 0.038 μM for direct exposure of virions; **Table 5.1**; $P < 0.001$). Moreover, the IC_{50} and IC_{95} against HSV-1 determined by measuring viral yield (0.906 or 1.382 μM for IC_{50} or IC_{95} , respectively, **Figure 5.1**) were approximately 17- or 22-fold lower, respectively,

than those calculated by Andronova et al. (ID₅₀, 15.5; ID₉₅, 31 μM) (2003). Although I infected at a higher MOI (3 compared to 0.1 PFU per cell used by Andronova et al.) and evaluated a different parameter at a different time (24 hpi compared to 48 hpi by Andronova et al.), the IC₅₀ and IC₉₅ were similar (2003). Therefore, the actual inhibition measured in such studies were most likely on the secondary infections (Andronova et al., 2003). The differences in the IC₅₀ reported against HSV-1 are thus a consequence of the different methods used to evaluate the antiviral effects of RAFIs. Andronova et al. reported the IC₅₀ of these fusion inhibitors by visually estimating the viral yields in RAFI-treated cells. I determined the IC₅₀ by directly measuring the effects of RAFIs on HSV-1 infectivity, a more relevant parameter considering these compounds are fusion inhibitors.

I also treated already-infected cells (at a MOI of 3 PFU per cell) with dUY11 for only 1 hour after infection, or continuously for 23 more hours. When already-infected cells were treated for only 1 hour after infection rather than for 23 hours, the IC₅₀ against the levels of infectivity increased 28-fold (IC₅₀ ~6.8 μM for 1h treatment, compared to ~0.24 μM for 23h treatment; **Table 5.1**; P<0.05), or 179-fold when compared to direct virion exposure (IC₅₀ ~6.8 μM for a 1h treatment, compared to 0.038 μM for virion exposure; **Table 5.1**; P<0.001). Not surprisingly, the levels of infectivity produced by cells continuously treated with dUY11 (and thus continuously exposed to it) are lower than those in cells treated for only 1 hour after infection. Progeny virions released from cells continuously treated with dUY11 are exposed to extracellular drug in the medium, and thus

rendered non-infectious. In contrast, progeny virions produced by cells treated with dUY11 for only 1 hour are not exposed to it in the extracellular medium. The precise mechanisms whereby RAFIs inhibit the levels of progeny infectivity in treated cells is yet unknown (further discussed in **section 7.5**). A likely explanation is that assembling virions acquire it with preexisting cellular factors, such as membrane lipids, by budding from cellular membranes where RAFIs are localized.

Under such a scenario, RAFIs redistribute to sites of virion budding. Consistently, dUY11 did rapidly localize to plasma and intracellular membranes after even only a 30-minute treatment of cells (**Figure 3.4**). Cellular membranes are constantly being remodeled, and even with only a brief cell treatment of 1 hour, the drug is redistributed to intracellular membranes. Normal cellular processes, for example clathrin-dependent and -independent endocytosis, pinocytosis and phagocytosis (Conner and Schmid, 2003), also redistribute regions of the plasma membrane intracellularly. Membrane biogenesis, remodeling, selective lipid distribution or trafficking to new sites in replicating cells would be expected to redistribute RAFIs to other pre-existing or even newly forming membranes (Fagone and Jackowski, 2009).

Assembling herpes viruses interact with several cell membranes before they are released from infected cells (Mettenleiter, Klupp, and Granzow, 2009). The newly-formed capsids first bud from the nucleus into the inner nuclear membrane. They then most likely fuse with the outer nuclear membrane (envelopment-deenvelopment-reenvelopment model), losing their previous

envelope. Tegument-associated capsids then undergo a second budding process into cytoplasmic membrane vesicles derived from the *trans*-Golgi network (TGN). These membranes are the sites from which assembling HSV-1 and HSV-2 virions bud to acquire their final envelope, and serve as the vesicles that then transport progeny virions to the cell surface for release. The inhibition of the levels of infectious progeny virions in RAFI treated cells thus requires the compounds to be localized to the TGN.

The fusion of cellular vesicles, including those transporting progeny virions, at the plasma membrane are not likely to be inhibited by RAFIs. An inhibition of fusion of intracellular vesicles would be toxic to cells, and dUY11 was not cytotoxic and was only mildly cytostatic at high concentrations (**Figure 3.5**). The release of extracellular virions was reduced in treated cells by only 2.8-fold (**Figure 5.6**), indicating that most progeny virions are released into the extracellular medium, which requires the fusion of cellular vesicles with the plasma membrane. The apparent selectivity for extracellular viral fusion can be explained by several important differences between viral and cellular fusion, discussed in **section 7.2**.

My hypothesis is that the antiviral activities of RAFIs result from their abilities to interfere with the envelope lipid reorganizations required for the formation of the hemifusion stalk. The antiviral activities of RAFIs are thus dependent on their molecular shape (hydrophilic region of larger cross-section than the hydrophobic one), not their chemical compositions. Two chemically distinct nucleoside derivatives, ddUY11 and aUY11, were synthesized (by our

collaborators) based on derivatizations of the lead compound dUY11. Both ddUY11 and aUY11 maintain the molecular shape of dUY11, but are chemically distinct. Relative to dUY11, they either lack a 3'-hydroxyl (ddUY11), or the furanose also contains a 2'-hydroxyl in the beta configuration (aUY11) (**Figure 3.1II**). Yet despite their distinct chemical structures, dUY11, ddUY11 and aUY11 all inhibited HSV-1 infectivity with similar IC_{50} (0.038, 0.062, or 0.129 μ M for dUY11, ddUY11 and aUY11, respectively; **Table 3.1**). There is no relation between the antiviral activities of RAFIs and any potential cytotoxic or cytostatic effects. For example, dUY11 is the most active RAFI and has no cytotoxic effect (**Table 3.3**). ddUY11 and aUY11 are similarly active (IC_{50} , 0.062 or 0.129 μ M for ddUY11 and aUY11, respectively; **Table 3.1**). Of these, only ddUY11 was (microscopically) observed to be cytotoxic (20 μ M; **Figure 3.2I**). Therefore, these three chemically distinct molecules similarly inhibit viral infectivity, while only one of them was cytotoxic.

7.2 Selectivity of rigid amphipathic fusion inhibitors for viral fusion

Specificity for viral functions is an important property for the safety of any drug. RAFIs are designed to target lipid bilayers to affect mechanistic details unique to the fusion of virion envelopes with cell membranes. Fusion of a metabolically inert vesicle membrane to the external leaflet of a cell membrane is unique to virions. The lipid targets of RAFIs are of cellular origin, and at least one RAFI (dUY11) distributed to cellular membranes (**Figure 3.4**), without any obvious cytotoxic effect. It does not affect cell doubling time (**Table 3.2**), for example.

There are several important differences between virion-to-cell and cell-to-cell fusion, which may explain the apparent selectivity of RAFIs for only viral fusion. The two membranes differ in the mechanisms available to overcome the energy barriers for fusion (as discussed further below). An increase in the energy barrier for fusion would thus inhibit viral fusion, while allowing cellular fusion to proceed.

Fusion is an energetically costly process. There are kinetic barriers for the formation of each lipid intermediate, and fusion requires persistent energy input (Chernomordik and Kozlov, 2003). The apposing membranes must overcome the hydration repulsion that separates them, the elastic deformation of the membrane leaflets (bending), the disruption of bilayers for stalk formation, and the expansion of the fusion pore (Chernomordik and Kozlov, 2008). The kinetic barriers for fusion are reduced in part by the diffusion of the neutral lipids within the hydrophobic membrane core, by the differential packing of different shaped lipids in each leaflet, and the characteristic properties of lipids to tilt, and of their acyl chains to splay and stretch (Kozlovsky and Kozlov, 2002).

Previous studies reported that molecules which disfavor the formation of negative curvature (larger hydrophilic heads than their hydrophobic region) only inhibit fusion when localized to the outer leaflets of vesicles (Chernomordik, 1996; Stiasny and Heinz, 2004). In agreement with these reports, then, the addition of RAFIs to the external leaflet of virion envelopes would impose an increase in the energy barrier to fusion by disfavoring the formation of negative curvature. Metabolically inert virions cannot overcome this increase in energy

barrier to fusion. Virion envelopes have access only to the limited energy released by virion glycoprotein binding and refolding (Basanez, 2002). For cellular fusion, in contrast, several mechanisms are available to overcome increases in the energy barriers to fusion. These include the modulation of membrane curvature by protein cages or coats, by energy dependent lipid-binding or modifying enzymes, and by membrane bending proteins, for example (Zimmerberg and Kozlov, 2006). Other important differences between cellular and viral fusion include the different leaflets that act as fusion sites, and the different leaflets exposed to RAFIs. All of these could contribute to the apparent selectivity of RAFIs for only viral fusion.

The exogenous addition of RAFIs to extracellular virions likely localize only to their external leaflets (the one exposed to the environment). RAFIs are highly unlikely to passively translocate across the hydrophobic core of the envelope bilayer; their polar hydrophilic region is much too large. Therefore, RAFIs most likely localize only to outer leaflets of extracellular virions. The external leaflets of cell membranes are also the only ones exposed to extracellular compounds. In cells, however, normal cellular processes that internalize particles consequently also redistribute regions of the plasma membrane. Such processes could thus internalize RAFIs, which did indeed localize to intracellular membranes (**Figure 3.4**). However, membrane inversion occurs during endocytosis. The external leaflet of the plasma membrane thus becomes the luminal (or inner) leaflet of cellular vesicles. In the absence of their relocation to the cytoplasmic leaflet, RAFIs would thus remain in the luminal leaflet of intracellular vesicles or organelles. Molecules with hydrophilic heads of larger

cross-section than their hydrophobic ones (which promote positive curvature) only inhibit fusion when localized to the external leaflet of fusing vesicles. Therefore, RAFIs localized to the luminal (inner) leaflets of intracellular vesicles would not be expected inhibit their fusion.

Alternatively, RAFIs may be actively translocated to the cytoplasmic leaflet of cellular membranes by as yet unknown mechanisms. Some cellular translocases, for example the P-glycoprotein MDR1, are known to have broad substrate specificity (van Helvoort et al., 1996). Moreover, multiple members of the solute carrier superfamily transport nucleoside and nucleotide analogues across membranes (Pastor-Anglada et al., 2005), and the RAFIs too, are nucleoside analogues. The potential localization of RAFIs to the cytoplasmic leaflets of intracellular vesicles would disfavor the formation of the hemifusion stalk, thus increasing the energy barrier to cellular fusion too. In contrast to virion envelopes, however, fusing cellular vesicles have access to several energy-dependent mechanisms to minimize or overcome the increases in energy barrier to fusion.

Energy-dependent proteins and lipid-binding or modifying proteins all function to bend membranes in cellular fusion (Kozlov, McMahon, and Chernomordik, 2010). For example, the enzymatic remodeling or translocation of lipids facilitate membrane deformations by generating lipids of particular geometries or by creating mismatches in the area between the two leaflets, respectively (McMahon and Gallop, 2005; Sheetz and Singer, 1974; Zimmerberg and Kozlov, 2006). The membrane stresses resulting from mismatches between

two leaflets, for example, are relieved by membrane bending toward the leaflet with excess material, and by relocation or extraction of excess material from that leaflet (Bettache et al., 2003). Lipid remodeling and translocation therefore modify the normal relative depletion in lipids to favor the membrane curvature required for fusion (Burger, 2000).

Another factor that may contribute to the selectivity of RAFIs for virion envelopes over cell membranes is the different leaflet that acts as the fusion site. Virion envelopes fuse with the external leaflets of cell membranes, which are enriched in lipids with relatively larger hydrophilic heads (Janmey and Kinnunen, 2006). In contrast, most cellular fusion events occur at the cytoplasmic leaflet, which are enriched with cone shaped lipids that favor the formation of the hemifusion stalk (Cooke and Deserno, 2006). This asymmetry of membrane lipids, with an enrichment in facilitators of negative curvature at cellular vesicle fusion sites, could also contribute to overcoming the energy barriers for fusion.

Virion envelopes, in contrast to cellular membranes, lack proteins that function to modulate membrane curvature or stress. Further contrasting from cell membranes, the chemical composition of envelopes is static, in that the lipids cannot be enzymatically remodeled or translocated between leaflets, either (Lenard and Rothman, 1976). The energy for viral fusion is provided exclusively by virion glycoproteins. The modulation of envelope lipid reorganizations may thus increase the barrier for fusion beyond that released by glycoprotein refolding.

Virion and most cell membranes also differ in topology. Virions envelopes have a positive curvature relative to most cell membranes. Extracellular

microvesicles, or exosomes, would be one exception. Exosomes, like virions, are extracellular vesicles (40 to 100 nm in diameter) with a positive curvature. They are released from most cell types by direct fusion of multivesicular bodies with plasma membranes (Ostrowski et al., 2010). Exosome secretion has been identified in nearly all cell types, highlighting their importance in many physiological processes and pathological states (Mathivanan and Simpson, 2009). Exosomes associate with target cell membranes through ligand-receptor interactions and can be internalized by direct fusion (Thery, Ostrowski, and Segura, 2009). Receptor-mediated endocytosis is proposed for exosomal uptake, for example by clathrin-mediated endocytosis in dendritic cells (Morelli et al., 2004), or by phagocytosis in macrophages (Feng et al., 2010). Like all physiological fusion events, the uptake of exosomes by membrane invagination is an energy-driven process facilitated by several proteins and enzymes that function to bend membranes, for example Rab GTPases (Simons and Raposo, 2009), F-BAR domain containing proteins (Frost et al., 2008) and lipid translocases (Devaux et al., 2008). Therefore, cellular processes such as exocytosis and exosome uptake are not likely to be constrained by increases in fusion energy barriers (a measurable effect discussed in **section 7.5**).

7.3 Broad-spectrum activities of rigid amphipathic fusion inhibitors

The entry of all enveloped viruses is similarly dependent on the formation of the negative envelope curvature for fusion (Chernomordik and Kozlov, 2005). The energetically costly lipid reorganizations occur using only the limited energy

released by binding and rearrangements of virion glycoproteins, rendering it unique among biological fusions (Basanez, 2002). Virion glycoproteins from unrelated viruses share no sequence homology and bind to unrelated receptors and co-receptors to merge their envelope bilayer with the target cell membrane. In contrast to current strategies aimed at disrupting viral proteins or their interactions with cellular ones, antivirals targeting conserved steps in viral fusion thus have the potential for broad-spectrum activities.

The small molecule inhibitors of infectivity, RAFIs, discovered and described in this thesis, target lipid bilayers to prevent the formation of negative membrane curvature. This novel antiviral mechanism is further supported by the activities of dUY11 against several otherwise unrelated enveloped viruses (that bind to unrelated receptors and have no glycoprotein sequence homology), and the lack of activity against the two nonenveloped viruses tested (**Table 4.1**). Also consistently with the proposed mechanism of antiviral action, RAFIs are active against HSV-1 variants resistant to classical nucleoside analogues, such as ACV, or other small molecule compounds which target DNA polymerases (**Figure 5.3**). RAFIs have the potential to inhibit a broad spectrum of enveloped viruses, including variants resistant to clinical drugs.

Both dUY2 and dUY11 were previously reported to have antiviral activities against HSV-1 mutant strains resistant to acyclovir (ACV; HSV/ACV^R), phosphonoformic acid (PFA; HSV/PFA^R), or both (HSV/(ACV+PFA)^R). The IC₅₀ of dUY11 was reported to be 31.2 µg/ml (62.1 µM) against HSV/ACV^R or 15.6 µg/ml (31 µM) against HSV/PFA^R and HSV/(ACV+PFA)^R (Andronova et al.,

2003). The antiviral activities of several more members of this family of nucleoside analogues against ACV- and PFA-resistant HSV-1 strains were also reported. The ID₅₀ of dUY4, dUY5, dUY6, dUY7, dUY8, dUY9 and aY12 (measured 48 hours after infection of Vero cells at a MOI of 0.1 PFU per cell) were reported to be 7.4, 16.9, >385.5, 67.7, 26.0, 116.9, or 111.1 μM, respectively, against HSV-1/ACV^R (Pchelintseva et al., 2005; Skorobogatyi et al., 2006b; Skorobogatyi et al., 2006c).

Consistently with these previous reports, dUY11 was active against ACV- and PAA-resistant HSV-1 strains (~1.2 μM for TK-, PAA^r and wild-type HSV-1; **Figure 5.3**). The previously reported ID₅₀ for dUY11 against drug resistant HSV-1 in multiple HSV-1 replication cycles calculated by Andronova et al. is also in close agreement with the IC₅₀ against the levels of progeny infectivity in cells treated only after infection with drug-resistant strains of HSV-1. The actual inhibition measured in such studies was on secondary infections, and the antiviral activities of RAFIs against such variants have not yet been evaluated by directly exposing virions before adsorption. RAFIs are novel nucleoside derivatives that do not act by classic mechanisms targeting viral genome replication, and direct exposure of even drug-resistant virions would be expected to inhibit their infectivity (a measurable effect discussed in **section 7.5**).

The antiviral activities of RAFIs were previously reported to be specific against HSV-1. dUY11 was reported to be inactive against Sindbis (SIN; IC₅₀, >497.5 μM) (Andronova et al., 2003). Despite extensive efforts, however, I was unable to reproduce these results. In fact, dUY11 is highly potent against the

infectivity of several unrelated enveloped viruses, including SIN (**Table 4.1**). dUY11 inhibited SIN infectivity when virions were directly exposed to it before infection (IC_{50} 0.011 μ M, **Table 4.1**), and by treating SIN-infected cells (IC_{50} 0.008 μ M, **Table 4.2**; $P < 0.001$). When already-infected cells were treated for only 1 hour after infection, the IC_{50} of dUY11 against the levels of progeny SIN infectivity increased 183-fold (IC_{50} ~1.5 or 0.008 μ M for 1 or 23-hour treatment, respectively; **Table 4.2**). These findings are consistent with the potent effects of dUY11 against HSV-1 infectivity when virions were directly exposed to the drug before infection or in continuously treated cells, compared to their exposure in cells treated for only 1 hour after infection (**Figure 5.5** and **Table 5.1**). These results further support the model that progeny virions released from cells continuously treated with dUY11 are directly exposed to it in the extracellular medium, and thus rendered non-infectious. In contrast, progeny virions released from infected cells treated with dUY11 for only 1 hour after infection must acquire the drug (likely by budding into cellular membranes where RAFIs are localized).

The differences in the IC_{50} of dUY11 against the levels of HSV-1 or SIN progeny infectivity in treated cells most likely reflect the differences in the potency of dUY11 against each virus. The IC_{50} of dUY11 against the levels of progeny infectivity in infected cells treated for only 1 hour after infection was 4.5-fold higher for HSV-1 than for SIN (IC_{50} , ~6.8 or 1.5 μ M for HSV-1 or SIN, respectively; **Tables 5.1** and **4.2**). Consistently, the IC_{50} of dUY11 against the infectivity of HSV-1 was 3.5-fold higher than against SIN (IC_{50} , 0.038 or 0.011

μM against HSV-1 or SIN virions, respectively; **Table 4.1**; $P < 0.001$) when virions were directly exposed before adsorption. These differences in IC_{50} against the levels of SIN or HSV-1 infectivity in cells treated may thus simply reflect the intrinsic differences in the IC_{50} of dUY11 against the infectivity each virus. There are of course other important differences in the replication cycles of SIN and HSV-1. For example, progeny SIN virions bud into the plasma membrane (Leung, Ng, and Chu, 2011), whereas assembling HSV-1 virions acquire their final envelopes by budding into *trans*-Golgi membranes (Mettenleiter, Klupp, and Granzow, 2009). The differences in the IC_{50} of dUY11 against the levels of progeny HSV-1 or SIN virion infectivity may reflect the intracellular distribution of RAFIs to sites of progeny assembly and budding (further discussed in **section 7.5**).

There are slight differences in the IC_{50} of dUY11 against the infectivity of the other enveloped viruses I tested, too (**Table 4.1**). The IC_{50} of dUY11 against the two HSV-2 strains was within the range of error to the IC_{50} against HSV-1 (6 nM, **Table 4.1**; $P < 0.05$). A 3.4-, 7.6- or 489-fold difference in IC_{50} was calculated against SIN, vesicular stomatitis virus (VSV), or vaccinia virus (VV), respectively, compared to HSV-1. With VV being a particular exception (for reasons discussed below), these minor differences in potency may reflect differences in virion morphology or size (**Table 7.1**). HSV-1 and HSV-2 are spherical and approximately 200 nm in diameter (Wildy, Russell, and Horne, 1960). SIN virions are also spherical, but considerably smaller with a diameter of 70 nm (Brown, Waite, and Pfefferkorn, 1972). VSV virions, in contrast, are

bullet-shaped and approximately 70 x 180 nm (Bradish and Kirkham, 1966).

Smaller vesicles have a more positive curvature, and membrane curvature affects the bending energies and fusion pore kinetics (Zhang and Jackson, 2010).

Therefore, differences in morphology or size are expected to differentially influence the mechanistic details of the lipid reorganizations required for the formation of the negatively curved hemifusion stalk, and consequently, the sensitivity to increases in the energy barrier to fusion imposed by RAFIs.

Experiments with protein-free liposomes have revealed that fusion kinetics depend on vesicle size, with the smallest liposomes being the most fusogenic (Malinin, Frederik, and Lentz, 2002). Yet, dUY11 was more potent against SIN (the smallest spherical virion tested) than HSV-1 and HSV-2 (the largest spherical virions tested), and most potent against VSV (a bullet-shaped virion). The differences in IC_{50} against the infectivity of otherwise unrelated enveloped viruses could reflect differences in the free energy released following virion glycoprotein binding to cell surface receptors and refolding. There are reported differences in the number of glycoproteins that participate in fusion, depending on the virus. For example, one to three influenza HA trimers are estimated to be required for hemifusion, and up to six are required for fusion pore expansion (Blumenthal et al., 1996; Danieli et al., 1996). For HIV, in contrast, a single gp120-gp41 heterotrimer is proposed to be sufficient for fusion (Yang et al., 2005). The effect of varying the number of fusogenic glycoproteins participating on fusion kinetics is a measurable one, and is further discussed in **section 7.5**.

The differences in the IC_{50} of dUY11 against the infectivity of unrelated viruses could also reflect the differences in the lipid composition of each virus. The composition and saturation of lipids in membranes are critical determinants of lipid packing and membrane curvature stress, which in turn influence the kinetics of membrane fusion (Chernomordik, 1996). The lipid composition of membranes, including virion envelopes, is a well-documented factor which influences the lipid reorganizations required for the formation of the negatively-curved hemifusion stalk (Chernomordik, 1996; Haque, McIntosh, and Lentz, 2001), and consequently, the energy barriers to fusion. The exogenous addition of natural lipids to modulate membrane curvature to promote or inhibit fusion provides one such example. Alterations in virion lipid composition by overexpressing lipid translocating enzymes in infected cells are also documented. For example, the lipid composition of HIV vectors was modulated by overexpressing the phospholipid floppase ABCB4, which mediates the transport of PC from the inner to the outer membrane leaflet (van Til et al., 2008). Virus produced from cells overexpressing ABCB4 was enriched in PC and cholesterol but contained less sphingomyelin (SM), and viral titers were reduced 5.9 fold (van Til et al., 2008).

All biological membranes, including virion envelopes, contain variable proportions of many lipids, including glycerophospholipids, sphingolipids and cholesterol. The lipid species of otherwise unrelated enveloped viruses are well-conserved (**Appendices 1 and 2**), but even only minor differences in their relative enrichment would influence fusion kinetics. Gangliosides, for example, are

complex lipids with a strong amphiphilic character due to their large saccharidic headgroup and double-tailed hydrophobic moiety, and have a hydrophilic headgroup of larger cross-section than their hydrophobic region. They are components of all animal cell membranes but are particularly abundant in the plasma membranes of neurons (Sonnino et al., 2007). The heterogeneity in ganglioside structure results in a large variability in their physicochemical properties, such as the geometry of the lipid headgroup, hydrogen bond network at the lipid-water interface, carbohydrate-water or neighboring lipid interactions and transition temperatures. Some species such as GD1a and GM1 exhibit dual effects on lamellar to inverted-hexagonal phase transition temperature, depending on their proportion in lipid mixtures (Perillo et al., 1994). Both GD1a and GM1 promoted the transition of dioleoylphosphatidylethanolamine bilayers from a lamellar to inverted-hexagonal phase when present at <1 mol %, but increased the transition temperature between 1 and 2 mol %, or inhibited it when present above 3 mol % (Perillo et al., 1994). Therefore, even only slight differences in the proportion of lipids in the envelopes of unrelated viruses could differentially regulate their sensitivity to RAFIs.

It may be that some viruses have an increased proportion of cone-shaped lipids in their external leaflet, for example, which would favor the formation of negative curvature. Such viruses would have a lower energy barrier to fusion than those containing an increased proportion of inverted-cone shaped lipids, which disfavor the negative curvature required for hemifusion stalk. This too is a measurable effect, further discussed in **section 7.5**.

Among the enveloped viruses I tested, VV was the only one the infectivity of which was not potently inhibited by exposure to dUY11 (IC₅₀, 19 μM; **Table 4.1**). VV virions are generally described as brick-shaped particles with rounded-edges and a dimension of 320-380 nm by 260-340 nm (Malkin, McPherson, and Gershon, 2003). VV is also characterized by the existence of at least two infectious and enveloped forms, the intracellular mature virus (MV, surrounded by one membrane) and the extracellular enveloped virus (EEV, an MV particle surrounded by a second lipid bilayer) (Roberts and Smith, 2008), in addition to infectious intracellular naked virions (Payne, 1980; Payne and Norrby, 1978) or cell-associated virions with ruptured membranes (Roberts and Smith, 2008). The infectivity of virions which lack the target membrane (naked VV), or which contain a second envelope that may be shed by nonfusogenic mechanisms (Law et al., 2006; Schmidt et al., 2011), are all expected to contribute to the reduced potency of RAFIs against VV.

7.4 Other potential small molecules targeting envelope lipids

The work presented in this thesis demonstrates that small molecules targeting virion lipids to inhibit their infectivity can be developed. Active RAFIs are amphipathic, with a hydrophilic region resembling the shape of polar headgroups of membrane lipids and a larger cross-section than their planar, rigid hydrophobic region.

All RAFIs identified to date are nucleoside derivatives. The novelty of small molecule nucleoside analogues as fusion inhibitors may have resulted in

similar compounds being overlooked when evaluating potential antivirals. Other nucleoside analogues may also act by similar mechanisms. Some families of nucleoside derivatives are reported to have unusual properties somewhat similar to the RAFIs I discovered. For example, members belonging to the family of bicyclic furanopyrimidine nucleoside analogues (BCNAs) were initially reported as highly potent and selective inhibitors of VSV by TK-dependent mechanisms (McGuigan et al., 1999). SAR studies then revealed that 2',3'-dideoxy derivatives bearing an alkyl side chain displayed antiviral activities against HCMV (McGuigan et al., 2000). The importance of alkyl side chain length was also evaluated in SAR studies. Octyl to dodecyl side chains showed potent antiviral activities, which decreased with a chain length shorter than C8 or longer than C12 (McGuigan et al., 2004). The potent activity of fully deoxygenated (2',3',5'-trideoxy) alkyl furanopyrimidines (that cannot be phosphorylated) against HCMV indicated a non-nucleosidic antiviral mechanism was more likely (Bidet et al., 2004; McGuigan et al., 2004). Time-of-addition studies performed by McGuigan et al. revealed that 5'-trideoxy alkyl furanopyrimidines with a nonyl side chain target a step prior to DNA synthesis (2004). When added 2 hours after infection (the earliest time tested), the compound inhibited virus yield by 3 logs. However, when its addition was delayed (24 or 48 hours), the compound inhibited virus yield by only 2 or 1 log, respectively. The activities of ganciclovir and cidofovir (which target the DNA polymerase), in contrast, showed no reduction in activity when addition was delayed to as late as 48 hours after infection of cells, as expected (McGuigan et al., 2004). These findings were taken as proof that

these agents act by novel, non-nucleosidic mechanisms. The compounds were reported to be inactive against two closely-related viruses, HSV-1 and HSV-2 (McGuigan et al., 2004). The activities of these unusual BCNAs against HSV-1 and HSV-2, however, were measured by treating already-infected cells and recording viral CPE in treated cells when it reached 100% completion in untreated control cells (De Clercq et al., 1986). Evaluating such parameters would not detect the effects of compounds that target virion bilayers to inhibit infectivity, if indeed some BCNA analogues act by mechanisms similar to RAFIs. Moreover, there are some structural similarities between this series of BCNA derivatives and the molecular shape of RAFIs (**Figure 7.1A** and **B**), particularly in the hydrophilic regions of the amphipathic molecules. Like RAFIs, the hydrophilic regions of these compounds have a larger cross-section than their hydrophobic one. However, the non-polar (phenyl) linker joining the hydrophilic region and the hydrocarbon chain has rotational flexibility. Similarly, dUY4 and dUY6 have rotational flexibility (**Figure 3.1VI**), and they are still moderately active (IC_{50} , ~8 or 32 μ M, respectively; **Table 3.1**, **Figure 3.2V**). The activities of BCNAs against HSV-1 and HSV-2 should be evaluated by pre-exposing virions before infection and then monitoring plaquing efficiency. Of course, targets distinct from those of RAFIs are also possible, and the precise antiviral mechanisms of these unusual BCNAs remain to be elucidated.

Other classes of nucleoside analogues with lipophilic properties critical to their antiviral activities have also been reported. Alkoxyalkyl lipid conjugates of acyclic nucleoside phosphonates (ANPs) are being investigated for improved oral

bioavailability and reduced nephrotoxicities (Hostetler, 2009). To improve pharmacokinetic and antiviral activities, it was proposed that ANPs could be modified to mimic partially metabolized phospholipids by converting them to hexadecyloxypropyl (HDP) and octadecyloxyethyl (ODE) esters (Painter and Hostetler, 2004). To increase cellular uptake and, consequently, their metabolism into diphosphates, it was proposed that ANP derivatives resembling lysophospholipid analogs would cross cellular membranes into the cytoplasm more rapidly (De Clercq and Holy, 2005). Current clinical studies of HDP-cidofovir (CMX001) include two phase 2 trials, one in stem cell transplant recipients seropositive for HCMV and another, for the prevention of adenovirus disease following hematopoietic stem cell transplantation (Chimerix Inc.). They are also being pursued in the development of drugs to treat poxvirus infections (Lanier et al., 2010b).

It is perhaps striking the number of ANPs initially reported to be inactive, but which show broad-spectrum activities as their HDP ester (Choo et al., 2007; Hostetler et al., 2006; Prichard et al., 2008). The esterification of ANPs resulted in large increases in potency and an expansion of their range of antiviral activity against even drug-resistant variants. For example, adefovir was reported to be inactive against HIV (Balzarini, 1993), but both HDP- and ODE-adefovur are highly active against HIV with low nanomolar EC_{50} values *in vitro* (Hostetler et al., 2006). HDP-tenofovir was reported to be ~300-fold more active than tenofovir against the replication of 27 wild-type HIV isolates, including all major subtypes of HIV-1 and HIV-2, as well as 29 NRTI-resistant isolates (Lanier et al., 2010a).

HDP-tenofovir (CMX157) directly associates with HIV virions when these are exposed only 1 minute before infection, and it was equally potent at reducing viral p24 levels when HIV_{III_B} virions were pre-exposed to the drug from 1 to 120 minutes before infection (Lanier et al., 2009). Lanier et al. also evaluated the number of CMX157 molecules that interact with HIV virions. HIV-1 was incubated with 500 nM CMX157 (or tenofovir as a control) for 2 hours, pelleted to remove unbound compound, and then lysed. The supernatants were then analyzed by liquid chromatography-mass spectrometry. Approximately 30,000 CMX157 molecules were associated with each virion, compared to 100 tenofovir molecules per virion (Lanier et al., 2009). This group concluded that the enhanced potencies and broad-specificities of HDP- and ODE-ANPs against wild-type and NRTI-resistant HIV strains result from their enhanced delivery, uptake and conversion to active diphosphates in infected cells (Hostetler, 2009; Lanier et al., 2010a; Lanier et al., 2009). CMX157 has some characteristics similar to RAFIs, namely their broad-specificity against even drug-resistant variants, the short exposure time required to inhibit viral replication, and their molecular shape (**Figure 7.1C**). Like RAFIs, these compounds too are amphipathic, with a hydrophilic region consisting of a nucleoside analogue and of larger cross-section than the hydrophobic one. The hydrophobic region of CMX157, however, has flexibility and a polar linker joins it to the hydrophilic region. dUY8, for example, similarly has rotational flexibility in its polar linker and its hydrophobic region (**Figure 3.1VI**; IC₅₀, 6 μM; **Table 3.1**), which is bulkier than CMX157. The activities of these compounds on lamellar to inverted-hexagonal phase transition

should be evaluated, to determine if they too disfavor the formation of membranes with negative curvature. Alternatively, the enhanced potencies and broad-spectrum activities of HDP- and ODE-ANPs compared to the parent compounds could result from their enhanced targeting to infected cells, as has been suggested.

All RAFIs identified to date are nucleoside derivatives. However, non-nucleoside scaffolds may also be used. Amphipathic compounds containing an appropriate hydrophobic moiety attached to a hydrophilic moiety of adequate shape and rigidity may also act as RAFIs.

A publication by Wolf et al. described non-nucleoside derivatives with properties similar to those I described during my PhD studies (2010). These were rhodamine derivatives with broad-spectrum activities against all of the enveloped viruses tested, but not the nonenveloped ones. The direct exposure of Nipah virus-enveloped pseudotyped VSV to the lead compound, LJ001, before adsorption inhibited entry at a step after binding but before virus-cell fusion (IC_{50} , 1 μ M). In fusion assays, LJ001 inhibited virus-cell, virus-liposome, but not cell-cell, fusion. The compounds intercalated into virion envelopes to irreversibly inactivate virions, while leaving intact envelope proteins. The authors reported that the compounds were not toxic to cells either (at 10 μ M for 4 days). It was proposed that the novel antiviral compounds exploit the lack of biogenic reparative capacity of virion envelopes (Wolf et al., 2010). LJ001 was then proposed to be activated by ambient light to generate singlet oxygen within membranes, since its antiviral activity was lost when virions were pre-exposed in the dark, or in the presence of vitamin E (an antioxidant) or dimethylanthracene (a singlet oxygen quencher)

(Vigant et al., 2010). The authors hypothesized that LJ001 selectively inactivates virions by generating reactive oxygen species in membranes, which only cells, but not metabolically inert virions, can repair. The mechanism whereby ambient light generates ROS in metabolically inert LJ001-exposed virions remains to be elucidated. The molecular shape of LJ001 is, however, strikingly similar to active RAFIs (**Figure 7.1D**). It is also amphipathic, with a hydrophilic region of larger cross-section than its rigid and hydrophobic one. The effects of this compound on lamellar to inverted-hexagonal phase transition should be evaluated, as it may be a RAFI.

Other novel strategies are also being pursued in the development of compounds that selectively target envelope bilayers to inhibit early steps in viral replication (Teissier, Penin, and Pecheur, 2011). Examples of such membranotropic broad-spectrum antivirals include cosalane (Zhan, Li, and Liu, 2010) and arbidol (Teissier et al., 2011). The precise antiviral mechanisms of these compounds have not yet been fully elucidated. Cosalane associates with virion membranes and is active against HIV and some herpes viruses *in vitro* (Casimiro-Garcia et al., 2000). It is proposed to inhibit several steps of viral replication but, due to its hydrophobic properties, major efforts are focused on maximizing bioavailability and tissue clearance (Zhan, Li, and Liu, 2010).

Arbidol is another non-nucleosidic small molecule with antiviral properties targeting early steps in viral replication. It is an indole derivative clinically used in Russia since 1990 against influenza A and B (Boriskin et al., 2008). Arbidol inhibits a broad range of enveloped viruses, including influenza A,

B and C viruses (Leneva et al., 2009), respiratory syncytial virus (Shi et al., 2007) and hepatitis B virus (HBV) (Chai et al., 2006). Arbidol also inhibited the fusion of HCV pseudoparticles (containing envelope proteins of HCV genotypes 1a, 1b or 2a) with liposomes in a dose- and time-dependent manner (Pecheur et al., 2007). The pretreatment of cells for 48 to 24 hours with arbidol (15 μ M) protected Huh7.5.1 cells from infection with JFH-1 (1,000- or 100-fold reduction in virus yields for 48 or 24 hour pretreatment, respectively) (Boriskin, Pecheur, and Polyak, 2006).

Arbidol has an affinity for hydrophobic environments (Pecheur et al., 2007) and rapidly incorporates into model membranes (Villalain, 2010). Using surface plasmon resonance, Teissier et al. showed that arbidol stably associates with dimyristoylphosphatidylcholine lipid membranes and nuclear magnetic resonance experiments revealed that it directly interacts with the phospholipid membrane (Teissier et al., 2011). Moreover, arbidol has a dual binding capacity, in that it also interacts with the indole rings of proteins incorporated into lipid membranes (Teissier et al., 2011). It is thus hypothesized that arbidol inhibits fusion by stabilizing the interactions between virion glycoproteins and envelope lipids to prevent the conformational changes that lead to membrane merger (Teissier et al., 2011). However, the precise details of its mechanisms of antiviral action remain to be elucidated.

An unrelated series of compounds have also been described as inhibitors of viral fusion, by modulating membrane fluidity. It is known that membrane fluidity is important for infectivity. For example, a 5% decrease in the fluidity of

the HIV-1 envelope reduced HIV-1 infectivity by 56%, whereas a 5% increase in its fluidity enhanced infectivity 2.4-fold (Harada et al., 2005). Glycyrrhizin, an active component of licorice roots, has broad-spectrum antiviral activities against a number of enveloped viruses including HSV-1, VSV, VZV, SARS, influenza and HIV (Baba and Shigeta, 1987; Cinatl et al., 2003; Ito et al., 1988; Wolkerstorfer et al., 2009). Single-round infection experiments revealed that the EC₅₀ of glycyrrhizin was 0.2 mg/ml (0.24 mM) when HIV virions were adsorbed onto cells in the presence of glycyrrhizin, and electron spin resonance studies indicated that the fluidity of HIV virions was suppressed when these were incubated with glycyrrhizin at 37°C for 1 hour (Harada, 2005). Glycyrrhizin also restricted the anisotropic movement of acyl chains, measured by electron-spin resonance of 5-doxyl stearic acid (DSA). Pretreating cells with 1 mg/ml (1.19 mM) glycyrrhizin, however, enhanced the infectivity of NL43-luciferase HIV by up to 40%, depending on the cell type (Harada, 2005). The authors concluded that glycyrrhizin increases the rigidity of both plasma and virion membranes. Its pro- and anti-infectivity activities were thus proposed to result from direct modulation of lipid bilayer membrane fluidity to promote (when cells were treated) or prevent (when virions were exposed) access of fusion proteins and their receptors, thus modulating fusion.

The chemical structures of cosalane, arbidol and glycyrrhizin (**Figure 7.1E, F and G**) are distinct from those of active RAFIs. These compounds nonetheless highlight that compounds selectively targeting envelope bilayers are gaining interest from an antiviral perspective (Teissier, Penin, and Pecheur, 2011).

Targeting envelope bilayers to inhibit cell entry could help overcome some of the limitations of current antivirals, as discussed in **section 7.6**.

7.5 Future considerations

The studies described in my PhD thesis identify and characterize a novel family of small molecules that target envelope bilayers and disfavor the formation of the negative curvature required for the fusion of envelope viruses. Studies to further characterize the inhibition of infectivity by targeting envelope bilayers, or secondary antiviral mechanisms (such as the inhibition of progeny virion release; **Figure 5.6**) are warranted.

Under the proposed model, RAFIs interact with virion envelope lipids. dUY11 exposure did not lyse virions (**Figure 3.7**). It may still have more subtle effects on vesicle integrity. The effects of virion exposure to RAFIs on morphology could be evaluated by electron microscopy or cryo-electron tomography, to evidence any gross deformations or disruption in virion morphology (Grunewald et al., 2003). The effects of RAFIs on membrane integrity could be evaluated by content leakage of RAFI-exposed lipid vesicles encapsulating fluorescent dyes, such as sulforhodamine B (Guo, MacKay, and Szoka, 2003). Moreover, the effects of RAFIs on the fusion kinetics of vesicles with different sizes or lipid compositions should also be evaluated. Assays that evaluate lipid and content mixing simultaneously are now available (van den Bogaart and Jahn, 2011). Such studies could be used to evaluate if the apparent

differences in IC_{50} against enveloped viruses can be at least in part attributed to virion size or composition.

Under the proposed mechanism of antiviral action, RAFIs increase the energy barrier to fusion. The kinetic barriers for fusion are in part reduced by diffusion of the neutral lipids within the hydrophobic membrane core, and by the characteristic properties of lipids to tilt, and of the acyl chains to splay and stretch (Kozlovsky and Kozlov, 2002). To evaluate the effects of RAFIs on such lipid reorganizations, the effects of RAFIs on acyl chain movements could be measured by spin-label electron spin resonance in membranes containing DSA.

The mechanisms whereby the treatment of infected cells reduces the levels of infectivity remain to be elucidated. One possibility was that less progeny virions were released from treated cells. Indeed, the release of progeny HSV-1 virions was reduced, albeit by only 2.8-fold (**Figure 5.6**). To determine the specificity of this effect, the release of progeny virions from cells infected by other enveloped viruses should be tested too. For example, the effects of dUY11 on the release of progeny SIN virions could be tested.

RAFIs may reduce progeny virion release by inhibiting intracellular budding events. For HSV-1 or -2, the inhibition of release could occur at intracellular organelles, at the plasma membrane, or perhaps at both. An increased retention of virions within intracellular membranes may be differentiated from retention at plasma membranes by the differential ultracentrifugation of synchronized, infected RAFI-treated cells (Harley, Dasgupta, and Wilson, 2001).

The effects of RAFIs on cellular fusion and fission should be further investigated, since specificity is important for any drug under development. Many intracellular and physiological events require the fusion of cells, or the fusion and fission of cell membranes. The fission and fusion of mitochondria, for example, are required for their integrity, electrical function and protection, to name a few (Berman, Pineda, and Hardwick, 2008). Cell division also requires extensive fission and fusion of intracellular vesicular compartments, and fission of the plasma membrane (Barr and Gruneberg, 2007; Prekeris and Gould, 2008). If RAFIs inhibit cellular fusion or fission events, an increase in cells delayed in the mitotic phase of the cell cycle is expected. dUY11 was slightly cytostatic at high concentrations (150 μ M; **Figure 3.5, Table 3.2**). The effects of RAFIs on mitotic progression could be evaluated in synchronized RAFI-treated cells by flow cytometry, to measure 2N or 4N DNA content at various times after cell treatment (Wiebusch et al., 2008).

Like virions, exosomes are extracellular vesicles of positive curvature. Exosomes use energy-driven processes to fuse to cell membranes and deliver their cargo to target cells. RAFIs are therefore not expected to inhibit exosomal fusion. Despite the differences in the mechanisms available to exosomes or virion envelopes to overcome increases in energy barriers to fusion, the similarities between the two processes warrant further investigations. Exosomes and virions are both extracellular vesicles of positive curvature, and they both fuse to the external leaflets of cell membranes.

RAFIs inhibit the formation of negative membrane curvature, an intermediate step that is required and conserved for fusion of all enveloped viruses. Consequently, RAFIs are active against all of the enveloped viruses tested, including HSV-2, HCV and HSV-1 variants resistant to classical antivirals that inhibit DNA replication (**Chapters 4 and 5**). The potential broad-spectrum activities of small molecules such as RAFIs would make them useful against emerging enveloped viral pathogens too. For example, they could have been useful in the recent influenza pandemic or the SARS outbreak. Under such circumstances, no viral proteins or interactions with cellular proteins would have to be characterized before the use of broad-spectrum drugs such as RAFIs against an emerging virus (Teissier, Penin, and Pecheur, 2011).

Since the completion of my PhD research, dUY11 and aUY11 have both been tested against H1N1 influenza A (A/Puerto Rice/8/34). Both RAFIs inhibited the plaquing of influenza A when virions were directly exposed before infection (IC_{50} , ~200 nM; Che Colpitts, unpublished results). A number of other important human viral pathogens contain a host-cell derived lipid bilayer (envelope), such as HIV and HBV, as well as variants resistant to clinical drugs. The activities of RAFIs against the infectivity of these too should be evaluated.

Genetic studies may aid in the further elucidation of RAFI-mediated inhibition of fusion. We have not yet been successful in selecting for RAFI-resistant HSV-1 mutants (**Figure 5.7**), but they may still be selected for. Viral factors that increase fusion efficiency could counteract the activities of RAFIs. Fusogenic viral mutant strains may be isolated, for example, to overcome the

increased energy barrier imposed by RAFI insertion into envelope bilayers. Resistant variants harboring mutations in virion glycoproteins could overcome increases in fusion energy barriers by releasing additional free energy during the conformational changes triggered by receptor binding, or by increasing the number of virion proteins participating in fusion. Resistance to the HIV fusion inhibitor enfuvirtide has been correlated to the affinity of envelope binding to receptor and co-receptor, to receptor density and to fusion kinetics, for example (Reeves et al., 2002). The extent and rate of fusion increases with increasing surface density of hemagglutinin (HA), for example (Clague, Schoch, and Blumenthal, 1991; Danieli et al., 1996). Mutant strains with higher numbers of glycoproteins expressed at the virion surface to participate in fusion could thus provide one possible mechanism of resistance (such that increased energy is available for the formation of the fusion intermediates) (Dutch, Joshi, and Lamb, 1998).

Overcoming the energy barriers imposed by RAFIs by increasing the protein density could be tested using HA. Stoichiometric studies on membrane fusion initiated by HA suggest that the formation of the hemifusion intermediate requires the concerted action of at least three HA trimers (Danieli et al., 1996), whereas pore expansion is predicted to require as many as 9 additional HA trimers outside of the membrane contact zone (Leikina et al., 2004). Following the method described by Günther-Ausborn et al., R18-labeled HA-virosomes could be used to test whether increasing the free energy by increasing the levels of fusogenic HA can rescue the inhibition of fusion by dUY11 (2000). In this

system, HAs from two different strains (X-47 recombinant and the A/Shangdong) with optimal fusion at pH 5.7 or 5.1, respectively, are coreconstituted into virosomes at various ratios such that the HA surface density remains constant, but the number of active fusogenic proteins is varied. Thus, this system enables the evaluation of a defined number of active fusogenic proteins, while keeping the total protein density constant by controlling the pH during the fusion reaction.

Another possibility is the isolation of viral populations with altered lipid composition. Virion envelopes enriched with cone shaped lipids in their outer leaflets may rescue the effects of RAFIs by promoting the negative membrane curvature required for fusion. Such an effect could be tested by the exogenous addition of PE or PA, for example, into RAFI-exposed virions.

The role of specific virion proteins, for example HIV Gag and nef, in modulating envelope lipid composition by associating with specific cellular lipid microdomains has been characterized (Brugger et al., 2007; Patil, Gautam, and Bhattacharya, 2010). Viral populations with altered lipid compositions could arise from preferential interactions between virion (glyco)proteins with lipids that favor the negative curvature to promote fusion. Virions budding from membrane regions enriched with such lipids could also be selected for. Such resistant variants would be most interesting, since no such mechanism of resistance has yet been characterized. Moreover, the determining factors that regulate envelope lipid composition are yet unknown, and these studies may provide some insight into the mechanisms whereby cellular lipids are sorted into virion envelopes.

RAFI targets are among the first steps in the viral replication cycle (fusion), and they act extracellularly. Such properties are highly desirable characteristics for agents pursued as microbicides to prevent transmission of STIs, such as HIV (Buckheit et al., 2010). The novel mechanism of antiviral action of RAFIs could thus be useful in the development of prophylactic agents, since they may prevent infection by direct exposure of infecting virions. To date, the infectivity of RAFI-exposed HSV-2 to animals has only been evaluated in small groups of mice, by preexposing virions to a high concentration of dUY11 before infecting the animals. These studies indicated that under these specific treatment conditions, HSV-2 virions are not infectious to mice (**Chapter 6**). To evaluate the potential of this novel antiviral strategy *in vivo*, studies in mice would have to be expanded to larger groups. The potential uses of such compounds, for example as microbicides, should be tested next. The compounds would then be applied topically before infection, in a formulation appropriate for microbicides aiming to prevent infection by sexually transmitted diseases. Time of application (before infection), repeated drug exposure, and effective drug concentration all remain to be investigated (Buckheit et al., 2010).

RAFIs may have the potential for therapeutic use, too. In cultured cells, dUY11 localized to cellular membranes (**Figure 3.4**), and it inhibited the levels of progeny SIN and HSV-1 infectivity in cells treated only after infection (**Figures 4.3 and 5.5**, respectively). The external leaflet of the plasma membrane is more than 10,000 times larger than that of a virion envelope (with most eukaryotic cells having a diameter of 10 to 30 μm , in comparison to even large viruses of 100 nm

diameter). The differences in surface area between virion and cellular membranes are even greater when considering the total surface area of cytoplasmic membranes, too (~10 times that of the surface area of the plasma membrane) (Janmey, 1998). This phenomenon would of course be enhanced when considering an entire organism, whereby RAFIs could redistribute to membranes of cells from many organs. Such a quenching by cellular membranes could be expected to reduce the concentration of RAFIs in target (infected) cells, or may require the administration of high or repeated doses. The feasibility of a therapeutic approach should be investigated *in vivo*, using established small animal models (such as mice, rats or rabbits) to evaluate the pharmacokinetics and pharmacodynamics of RAFIs (Andes and Craig, 2002). Dosing regimens (repeats, dosing), routes of administration (intravenous or oral) and the metabolism of RAFIs should also be evaluated. RAFIs should be tested as substrates for cellular solute carrier transporters, for example the concentrative or equilibrative nucleoside transporters, which could function in their uptake, efflux or elimination (Izzedine, Launay-Vacher, and Deray, 2005).

The addition of a new investigational compound to current therapies has become the standard approach to the clinical development of antiviral drugs. Therefore, studies aimed at evaluating the synergistic or antagonistic effects of RAFIs in model systems may also be pursued. For example, the efficacy of RAFIs could be tested with ribavirin and pegylated- IFN against HCV, first *in vitro*, and then *in vivo*. The addition of a new investigational compound to currently approved drug regimens may reveal potential drug-drug interactions too.

7.6 Perspective

In addition to identifying potent, selective, broad-spectrum antiviral compounds, the work described in my Doctoral thesis serves as an important proof-of-concept that small molecule fusion inhibitors targeting envelope bilayer curvature are a viable antiviral strategy. This novel approach may help to overcome some of the limitations of current clinical antivirals. RAFIs act extracellularly (and do not require intracellular metabolism), and they selectively inhibit functions specific to virion envelopes, two important properties for the development of drugs that are safe. The target of RAFIs is not encoded in the highly mutable viral genome either, and drug-resistance has not yet been detected. RAFIs thus have a higher barrier to selection for resistance than current strategies targeting proteins. Moreover, RAFIs target viral functions conserved among all enveloped viruses, and they thus inhibit a broad range of viruses, including important human pathogens such as HCV. The novel antiviral mechanisms of action of RAFIs to selectively target viral fusion renders them particularly suitable for their further development as a new class of prophylactic or therapeutic broad-spectrum antivirals.

7.7 References

- Andes, D., and Craig, W. A. (2002). Animal model pharmacokinetics and pharmacodynamics: a critical review. *Int J Antimicrob Agents* **19**(4), 261-8.
- Andronova, V. L., Skorobogaty, M. V., Manasova, E. V., Berlin Iu, A., Korshun, V. A., and Galegov, G. A. (2003). [Antiviral activity of some 5-arylethynyl 2'-deoxyuridine derivatives]. *Bioorg Khim* **29**(3), 290-5.
- Baba, M., and Shigeta, S. (1987). Antiviral Activity of Glycyrrhizin against Varicella-Zoster Virus In Vitro. *Antiviral Research* **7**(2), 99-107.
- Barr, F. A., and Gruneberg, U. (2007). Cytokinesis: placing and making the final cut. *Cell* **131**(5), 847-60.
- Basanez, G. (2002). Membrane fusion: the process and its energy suppliers. *Cellular and Molecular Life Sciences* **59**(9), 1478-1490.
- Basanez, G., Goni, F. M., and Alonso, A. (1998). Effect of single chain lipids on phospholipase C-promoted vesicle fusion. A test for the stalk hypothesis of membrane fusion. *Biochemistry* **37**(11), 3901-3908.
- Berman, S. B., Pineda, F. J., and Hardwick, J. M. (2008). Mitochondrial fission and fusion dynamics: the long and short of it. *Cell Death and Differentiation* **15**(7), 1147-1152.
- Bettache, N., Baisamy, L., Baghdiguian, S., Payrastra, B., Mangeat, P., and Bienvenue, A. (2003). Mechanical constraint imposed on plasma membrane through transverse phospholipid imbalance induces reversible actin polymerization via phosphoinositide 3-kinase activation. *J Cell Sci* **116**(Pt 11), 2277-84.
- Bidet, O., McGuigan, C., Snoeck, R., Andrei, G., De Clercq, E., and Balzarini, J. (2004). Non-nucleoside structures retain full anti-HCMV potency of the dideoxy furanopyrimidine family. *Antivir Chem Chemother* **15**(6), 329-32.
- Blumenthal, R., Sarkar, D. P., Durell, S., Howard, D. E., and Morris, S. J. (1996). Dilatation of the influenza hemagglutinin fusion pore revealed by the kinetics of individual cell-cell fusion events. *Journal of Cell Biology* **135**(1), 63-71.
- Boriskin, Y. S., Leneva, I. A., Pecheur, E. I., and Polyak, S. J. (2008). Arbidol: a broad-spectrum antiviral compound that blocks viral fusion. *Curr Med Chem* **15**(10), 997-1005.
- Boriskin, Y. S., Pecheur, E. I., and Polyak, S. J. (2006). Arbidol: a broad-spectrum antiviral that inhibits acute and chronic HCV infection. *Virology* **3**, 56.
- Bradish, C. J., and Kirkham, J. B. (1966). The morphology of vesicular stomatitis virus (Indiana C) derived from chick embryos or cultures of BHK21/13 cells. *J Gen Microbiol* **44**(3), 359-71.
- Brown, D. T., Waite, M. R., and Pfefferkorn, E. R. (1972). Morphology and morphogenesis of Sindbis virus as seen with freeze-etching techniques. *J Virol* **10**(3), 524-36.
- Brugger, B., Krautkramer, E., Tibroni, N., Munte, C. E., Rauch, S., Leibrecht, I., Glass, B., Breuer, S., Geyer, M., Krausslich, H. G., Kalbitzer, H. R.,

- Wieland, F. T., and Fackler, O. T. (2007). Human immunodeficiency virus type 1 Nef protein modulates the lipid composition of virions and host cell membrane microdomains. *Retrovirology* **4**, 70.
- Buckheit, R. W., Watson, K. M., Morrow, K. M., and Ham, A. S. (2010). Development of topical microbicides to prevent the sexual transmission of HIV. *Antiviral Research* **85**(1), 142-158.
- Burger, K. N. J. (2000). Greasing membrane fusion and fission machineries. *Traffic* **1**(8), 605-613.
- Casimiro-Garcia, A., De Clercq, E., Pannecouque, C., Witvrouw, M., Stup, T., Turpin, J. A., Buckheit, R. W., and Cushman, M. (2000). Synthesis and Anti-HIV Activity of Cosalane Analogues Incorporating Nitrogen in the Linker Chain. *Bioorganic & Medicinal Chemistry* **8**(1), 191-200.
- Chai, H., Zhao, C., Zhao, Y., and Gong, P. (2006). Synthesis and in vitro anti-hepatitis B virus activities of some ethyl 5-hydroxy-1H-indole-3-carboxylates. *Bioorg Med Chem* **14**(8), 2552-8.
- Chernomordik, L. (1996). Non-bilayer lipids and biological fusion intermediates. *Chemistry and Physics of Lipids* **81**(2), 203-213.
- Chernomordik, L. V., and Kozlov, M. M. (2003). Protein-lipid interplay in fusion and fission of biological membranes. *Annual Review of Biochemistry* **72**, 175-207.
- Chernomordik, L. V., and Kozlov, M. M. (2005). Membrane hemifusion: Crossing a chasm in two leaps. *Cell* **123**(3), 375-382.
- Chernomordik, L. V., and Kozlov, M. M. (2008). Mechanics of membrane fusion. *Nature Structural & Molecular Biology* **15**(7), 675-683.
- Chernomordik, L. V., Leikina, E., Kozlov, M. M., Frolov, V. A., and Zimmerberg, J. (1999). Structural intermediates in influenza haemagglutinin-mediated fusion. *Molecular Membrane Biology* **16**(1), 33-42.
- Choo, H., Beadle, J. R., Kern, E. R., Prichard, M. N., Keith, K. A., Hartline, C. B., Trahan, J., Aldern, K. A., Korba, B. E., and Hostetler, K. Y. (2007). Antiviral activities of novel 5-phosphono-pent-2-en-1-yl nucleosides and their alkoxyalkyl phosphonoesters. *Antimicrobial Agents and Chemotherapy* **51**(2), 611-615.
- Cinatl, J., Morgenstern, B., Bauer, G., Chandra, P., Rabenau, H., and Doerr, H. W. (2003). Glycyrrhizin, an active component of liquorice roots, and replication of SARS-associated coronavirus. *Lancet* **361**(9374), 2045-2046.
- Clague, M. J., Schoch, C., and Blumenthal, R. (1991). Delay time for influenza virus hemagglutinin-induced membrane fusion depends on hemagglutinin surface density. *J Virol* **65**(5), 2402-7.
- Conner, S. D., and Schmid, S. L. (2003). Regulated portals of entry into the cell. *Nature* **422**(6927), 37-44.
- Cooke, I. R., and Deserno, M. (2006). Coupling between lipid shape and membrane curvature. *Biophysical Journal* **91**(2), 487-495.
- Danieli, T., Pelletier, S. L., Henis, Y. I., and White, J. M. (1996). Membrane fusion mediated by the influenza virus hemagglutinin requires the

- concerted action of at least three hemagglutinin trimers. *Journal of Cell Biology* **133**(3), 559-569.
- De Clercq, E., Balzarini, J., Descamps, J., Huang, G. F., Torrence, P. F., Bergstrom, D. E., Jones, A. S., Serafinowski, P., Verhelst, G., and Walker, R. T. (1982). Antiviral, antimetabolic, and cytotoxic activities of 5-substituted 2'-deoxycytidines. *Molecular Pharmacology* **21**(1), 217-223.
- De Clercq, E., Descamps, J., Balzarini, J., Giziewicz, J., Barr, P. J., and Robins, M. J. (1983). Nucleic acid related compounds. 40. Synthesis and biological activities of 5-alkynyluracil nucleosides. *J Med Chem* **26**(5), 661-6.
- De Clercq, E., and Holy, A. (2005). Acyclic nucleoside phosphonates: a key class of antiviral drugs. *Nat Rev Drug Discov* **4**(11), 928-40.
- De Clercq, E., Holy, A., Rosenberg, I., Sakuma, T., Balzarini, J., and Maudgal, P. C. (1986). A novel selective broad-spectrum anti-DNA virus agent. *Nature* **323**(6087), 464-7.
- Devaux, P. F., Herrmann, A., Ohlwein, N., and Kozirov, M. M. (2008). How lipid flippases can modulate membrane structure. *Biochimica Et Biophysica Acta-Biomembranes* **1778**(7-8), 1591-1600.
- Dutch, R. E., Joshi, S. B., and Lamb, R. A. (1998). Membrane fusion promoted by increasing surface densities of the paramyxovirus F and HN proteins: comparison of fusion reactions mediated by simian virus 5 F, human parainfluenza virus type 3 F, and influenza virus HA. *J Virol* **72**(10), 7745-53.
- Fagone, P., and Jackowski, S. (2009). Membrane phospholipid synthesis and endoplasmic reticulum function. *J Lipid Res* **50 Suppl**, S311-6.
- Feng, D., Zhao, W. L., Ye, Y. Y., Bai, X. C., Liu, R. Q., Chang, L. F., Zhou, Q., and Sui, S. F. (2010). Cellular Internalization of Exosomes Occurs Through Phagocytosis. *Traffic* **11**(5), 675-687.
- Frost, A., Perera, R., Roux, A., Spasov, K., Destaing, O., Egelman, E. H., De Camilli, P., and Unger, V. M. (2008). Structural basis of membrane invagination by F-BAR domains. *Cell* **132**(5), 807-17.
- Gaudin, Y. (2000). Rabies virus-induced membrane fusion pathway. *Journal of Cell Biology* **150**(3), 601-611.
- Grunewald, K., Desai, P., Winkler, D. C., Heymann, J. B., Belnap, D. M., Baumeister, W., and Steven, A. C. (2003). Three-dimensional structure of herpes simplex virus from cryo-electron tomography. *Science* **302**(5649), 1396-8.
- Gunther-Ausborn, S., Praetor, A., and Stegmann, T. (1995). Inhibition of Influenza-Induced Membrane-Fusion by Lysophosphatidylcholine. *Journal of Biological Chemistry* **270**(49), 29279-29285.
- Gunther-Ausborn, S., Schoen, P., Bartoldus, I., Wilschut, J., and Stegmann, T. (2000). Role of hemagglutinin surface density in the initial stages of influenza virus fusion: lack of evidence for cooperativity. *J Virol* **74**(6), 2714-20.

- Guo, X., MacKay, J. A., and Szoka, F. C., Jr. (2003). Mechanism of pH-triggered collapse of phosphatidylethanolamine liposomes stabilized by an ortho ester polyethyleneglycol lipid. *Biophys J* **84**(3), 1784-95.
- Haque, M. E., McIntosh, T. J., and Lentz, B. R. (2001). Influence of lipid composition on physical properties and PEG-mediated fusion of curved and uncurved model membrane vesicles: "Nature's own" fusogenic lipid bilayer. *Biochemistry* **40**(14), 4340-4348.
- Harada, S. (2005). The broad anti-viral agent glycyrrhizin directly modulates the fluidity of plasma membrane and HIV-1 envelope. *Biochemical Journal* **392**, 191-199.
- Harada, S., Yusa, K., Monde, K., Akaike, T., and Maeda, Y. (2005). Influence of membrane fluidity on human immunodeficiency virus type 1 entry. *Biochemical and Biophysical Research Communications* **329**(2), 480-486.
- Harley, C. A., Dasgupta, A., and Wilson, D. W. (2001). Characterization of herpes simplex virus-containing organelles by subcellular fractionation: Role for organelle acidification in assembly of infectious particles. *Journal of Virology* **75**(3), 1236-1251.
- Hilmarsson, H., Kristmundsdottir, T., and Thormar, H. (2005). Virucidal activities of medium- and long-chain fatty alcohols, fatty acids and monoglycerides against herpes simplex virus types 1 and 2: comparison at different pH levels. *Acta Pathologica, Microbiologica et Immunologica Scandinavica* **113**(1), 58-65.
- Hostetler, K. Y. (2009). Alkoxyalkyl prodrugs of acyclic nucleoside phosphonates enhance oral antiviral activity and reduce toxicity: Current state of the art. *Antiviral Research* **82**(2), A84-A98.
- Hostetler, K. Y., Aldern, K. A., Wan, W. B., Ciesla, S. L., and Beadle, J. R. (2006). Alkoxyalkyl esters of (S)-9-[3-Hydroxy-2-(phosphonomethoxy)propyl] adenine are potent inhibitors of the replication of wild-type and drug-resistant human immunodeficiency virus type 1 in vitro. *Antimicrobial Agents and Chemotherapy* **50**(8), 2857-2859.
- Ito, M., Sato, A., Hirabayashi, K., Tanabe, F., Shigeta, S., Baba, M., Declercq, E., Nakashima, H., and Yamamoto, N. (1988). Mechanism of Inhibitory Effect of Glycyrrhizin on Replication of Human Immunodeficiency Virus (Hiv). *Antiviral Research* **10**(6), 289-298.
- Izzedine, H., Launay-Vacher, V., and Deray, G. (2005). Renal tubular transporters and antiviral drugs: an update. *Aids* **19**(5), 455-62.
- Janmey, P. A. (1998). The cytoskeleton and cell signaling: component localization and mechanical coupling. *Physiol Rev* **78**(3), 763-81.
- Janmey, P. A., and Kinnunen, P. K. (2006). Biophysical properties of lipids and dynamic membranes. *Trends Cell Biol* **16**(10), 538-46.
- Korshun, V. A., Manasova, E. V., Balakin, K. V., Malakhov, A. D., Perepelov, A. V., Sokolova, T. A., and Berlin, Y. A. (1998). New fluorescent nucleoside derivatives - 5-alkynylated 2'-deoxyuridines. *Nucleosides & Nucleotides* **17**(9-11), 1809-1812.

- Korshun, V. A., Prokhorenko, I. A., Gontarev, S. V., Skorobogaty, M. V., Balakin, K. V., Manasova, E. V., Malakhov, A. D., and Berlin, Y. A. (1997). New pyrene derivatives for fluorescent labeling of oligonucleotides. *Nucleosides & Nucleotides* **16**(7-9), 1461-1464.
- Kozlov, M. M., McMahon, H. T., and Chernomordik, L. V. (2010). Protein-driven membrane stresses in fusion and fission. *Trends Biochem Sci* **35**(12), 699-706.
- Kozlovsky, Y., and Kozlov, M. M. (2002). Stalk model of membrane fusion: Solution of energy crisis. *Biophysical Journal* **82**(2), 882-895.
- Lanier, E. R., Ptak, R. G., Lampert, B. M., Keilholz, L., Hartman, T., Buckheit, R. W., Mankowski, M. K., Osterling, M. C., Almond, M. R., and Painter, G. R. (2010a). Development of Hexadecyloxypropyl Tenofovir (CMX157) for Treatment of Infection Caused by Wild-Type and Nucleoside/Nucleotide-Resistant HIV. *Antimicrobial Agents and Chemotherapy* **54**(7), 2901-2909.
- Lanier, R., Lampert, B., Robertson, A., Almond, M., and Painter, G. (2009). Hexadecyloxypropyl tenofovir associates directly with HIV and subsequently inhibits viral replication in untreated cells. In "16th Conference on Retroviruses and Opportunistic Infections", Montreal, Canada.
- Lanier, R., Trost, L., Tippin, T., Lampert, B., Robertson, A., Foster, S., Rose, M., Painter, W., O'Mahony, R., Almond, M., and Painter, G. (2010b). Development of CMX001 for the Treatment of Poxvirus Infections. *Viruses* **2**(12), 2740-2762.
- Law, M., Carter, G. C., Roberts, K. L., Hollinshead, M., and Smith, G. L. (2006). Ligand-induced and nonfusogenic dissolution of a viral membrane. *Proc Natl Acad Sci U S A* **103**(15), 5989-94.
- Leikina, E., Mittal, A., Cho, M. S., Melikov, K., Kozlov, M. M., and Chernomordik, L. V. (2004). Influenza hemagglutinins outside of the contact zone are necessary for fusion pore expansion. *J Biol Chem* **279**(25), 26526-32.
- Lenard, J., and Rothman, J. E. (1976). Transbilayer Distribution and Movement of Cholesterol and Phospholipid in Membrane of Influenza-Virus. *Proceedings of the National Academy of Sciences of the United States of America* **73**(2), 391-395.
- Leneva, I. A., Russell, R. J., Boriskin, Y. S., and Hay, A. J. (2009). Characteristics of arbidol-resistant mutants of influenza virus: implications for the mechanism of anti-influenza action of arbidol. *Antiviral Res* **81**(2), 132-40.
- Leung, J., Ng, M., and Chu, J. (2011). Replication of Alphaviruses: A Review on the Entry Process of Alphaviruses into Cells. *Advances in Virology* **2011**(1), 1-9.
- Malakhov, A. D., Malakhova, E. V., Kuznitsova, S. V., Grechishnikova, I. V., Skorobogaty, M. V., Korshun, V. A., and Berlin, Y. A. (2000). Synthesis and Fluorescent Properties of 5-(1-pyrenylethynyl)-2'-deoxyuridine-

- containing oligodeoxynucleotides. *Russian journal of Bioorganic Chemistry* **26**(1), 39-50.
- Malinin, V. S., Frederik, P., and Lentz, B. R. (2002). Osmotic and curvature stress affect PEG-induced fusion of lipid vesicles but not mixing of their lipids. *Biophysical Journal* **82**(4), 2090-2100.
- Malkin, A. J., McPherson, A., and Gershon, P. D. (2003). Structure of intracellular mature vaccinia virus visualized by in situ atomic force microscopy. *J Virol* **77**(11), 6332-40.
- Mathivanan, S., and Simpson, R. J. (2009). ExoCarta: A compendium of exosomal proteins and RNA. *Proteomics* **9**(21), 4997-5000.
- McGuigan, C., Barucki, H., Blewett, S., Carangio, A., Erichsen, J. T., Andrei, G., Snoeck, R., De Clercq, E., and Balzarini, J. (2000). Highly potent and selective inhibition of varicella-zoster virus by bicyclic furopyrimidine nucleosides bearing an aryl side chain. *Journal of Medicinal Chemistry* **43**(26), 4993-4997.
- McGuigan, C., Pathirana, R. N., Snoeck, R., Andrei, G., De Clercq, E., and Balzarini, J. (2004). Discovery of a new family of inhibitors of human cytomegalovirus (HCMV) based upon lipophilic alkyl furano pyrimidine dideoxy nucleosides: Action via a novel non-nucleosidic mechanism. *Journal of Medicinal Chemistry* **47**(7), 1847-1851.
- McGuigan, C., Yarnold, C. J., Jones, G., Velazquez, S., Barucki, H., Brancale, A., Andrei, G., Snoeck, R., De Clercq, E., and Balzarini, J. (1999). Potent and selective inhibition of varicella-zoster virus (VZV) by nucleoside analogues with an unusual bicyclic base. *Journal of Medicinal Chemistry* **42**(22), 4479-4484.
- McMahon, H. T., and Gallop, J. L. (2005). Membrane curvature and mechanisms of dynamic cell membrane remodelling. *Nature* **438**(7068), 590-596.
- Mettenleiter, T. C., Klupp, B. G., and Granzow, H. (2009). Herpesvirus assembly: an update. *Virus Res* **143**(2), 222-34.
- Morelli, A. E., Larregina, A. T., Shufesky, W. J., Sullivan, M. L. G., Stolz, D. B., Papworth, G. D., Zahorchak, A. F., Logar, A. J., Wang, Z. L., Watkins, S. C., Falo, L. D., and Thomson, A. W. (2004). Endocytosis, intracellular sorting, and processing of exosomes by dendritic cells. *Blood* **104**(10), 3257-3266.
- Ostrowski, M., Carmo, N. B., Krumeich, S., Fanget, I., Raposo, G., Savina, A., Moita, C. F., Schauer, K., Hume, A. N., Freitas, R. P., Goud, B., Benaroch, P., Hacoheh, N., Fukuda, M., Desnos, C., Seabra, M. C., Darchen, F., Amigorena, S., Moita, L. F., and Thery, C. (2010). Rab27a and Rab27b control different steps of the exosome secretion pathway. *Nat Cell Biol* **12**(1), 19-30; sup pp 1-13.
- Painter, G. R., and Hostetler, K. Y. (2004). Design and development of oral drugs for the prophylaxis and treatment of smallpox infection. *Trends in Biotechnology* **22**(8), 423-427.
- Pastor-Anglada, M., Cano-Soldado, P., Molina-Arcas, M., Lostao, M. P., Larrayoz, I., Martinez-Picado, J., and Casado, F. J. (2005). Cell entry and export of nucleoside analogues. *Virus Res* **107**(2), 151-64.

- Patil, A., Gautam, A., and Bhattacharya, J. (2010). Evidence that Gag facilitates HIV-1 envelope association both in GPI-enriched plasma membrane and detergent resistant membranes and facilitates envelope incorporation onto virions in primary CD4+ T cells. *Virology* **7**, 3.
- Payne, L. G. (1980). Significance of extracellular enveloped virus in the in vitro and in vivo dissemination of vaccinia. *J Gen Virol* **50**(1), 89-100.
- Payne, L. G., and Norrby, E. (1978). Adsorption and penetration of enveloped and naked vaccinia virus particles. *J Virol* **27**(1), 19-27.
- Pchelintseva, A. A., Skorobogatyj, M. V., Petrunina, A. L., Andronova, V. L., Galegov, G. A., Astakhova, I. V., Ustinov, A. V., Malakhov, A. D., and Korshun, V. A. (2005). Synthesis and evaluation of anti-HSV activity of new 5-alkynyl-2'-deoxyuridines. *Nucleosides Nucleotides & Nucleic Acids* **24**(5-7), 923-926.
- Pecheur, E. I., Lavillette, D., Alcaras, F., Molle, J., Boriskin, Y. S., Roberts, M., Cosset, F. L., and Polyak, S. J. (2007). Biochemical mechanism of hepatitis C virus inhibition by the broad-spectrum antiviral arbidol. *Biochemistry* **46**(20), 6050-9.
- Perillo, M. A., Scarsdale, N. J., Yu, R. K., and Maggio, B. (1994). Modulation by gangliosides of the lamellar-inverted micelle (hexagonal II) phase transition in mixtures containing phosphatidylethanolamine and dioleoylglycerol. *Proc Natl Acad Sci U S A* **91**(21), 10019-23.
- Prekeris, R., and Gould, G. W. (2008). Breaking up is hard to do - membrane traffic in cytokinesis. *J Cell Sci* **121**(Pt 10), 1569-76.
- Prichard, M. N., Hartline, C. B., Harden, E. A., Daily, S. L., Beadle, J. R., Valiaeva, N., Kern, E. R., and Hostetler, K. Y. (2008). Inhibition of Herpesvirus Replication by Hexadecyloxypropyl Esters of Purine- and Pyrimidine-Based Phosphonmethoxyethyl Nucleoside Phosphonates. *Antimicrobial Agents and Chemotherapy* **52**(12), 4326-4330.
- Reeves, J. D., Gallo, S. A., Ahmad, N., Miamidian, J. L., Harvey, P. E., Sharron, M., Pohlmann, S., Sfakianos, J. N., Derdeyn, C. A., Blumenthal, R., Hunter, E., and Doms, R. W. (2002). Sensitivity of HIV-1 to entry inhibitors correlates with envelope/coreceptor affinity, receptor density, and fusion kinetics. *Proc Natl Acad Sci U S A* **99**(25), 16249-54.
- Roberts, K. L., and Smith, G. L. (2008). Vaccinia virus morphogenesis and dissemination. *Trends Microbiol* **16**(10), 472-9.
- Schang, L. M. (2006). Herpes simplex viruses in antiviral drug discovery. *Current Pharmaceutical Design* **12**(11), 1357-1370.
- Schmidt, F. I., Bleck, C. K., Helenius, A., and Mercer, J. (2011). Vaccinia extracellular virions enter cells by macropinocytosis and acid-activated membrane rupture. *Embo J* **30**(17), 3647-61.
- Sheetz, M. P., and Singer, S. J. (1974). Biological membranes as bilayer couples. A molecular mechanism of drug-erythrocyte interactions. *Proc Natl Acad Sci U S A* **71**(11), 4457-61.
- Shi, L., Xiong, H., He, J., Deng, H., Li, Q., Zhong, Q., Hou, W., Cheng, L., Xiao, H., and Yang, Z. (2007). Antiviral activity of arbidol against influenza A

- virus, respiratory syncytial virus, rhinovirus, coxsackie virus and adenovirus in vitro and in vivo. *Arch Virol* **152**(8), 1447-55.
- Simons, M., and Raposo, G. (2009). Exosomes - vesicular carriers for intercellular communication. *Current Opinion in Cell Biology* **21**(4), 575-581.
- Skorobogatyi, M. V., Malakhov, A. D., Pchelintseva, A. A., Turban, A. A., Bondarev, S. L., and Korshun, V. A. (2006a). Fluorescent 5-alkynyl-2'-deoxyuridines: High emission efficiency of a conjugated perylene nucleoside in a DNA duplex. *Chembiochem* **7**(5), 810-816.
- Skorobogatyi, M. V., Pchelintseva, A. A., Petrunina, A. L., Stepanova, I. A., Andronova, V. L., Galegov, G. A., Malakhov, A. D., and Korshun, V. A. (2006b). 5-Alkynyl-2'-deoxyuridines, containing bulky aryl groups: evaluation of structure-anti-HSV-1 activity relationship. *Tetrahedron* **62**(6), 1279-1287.
- Skorobogatyi, M. V., Ustinov, A. V., Stepanova, I. A., Pchelintseva, A. A., Petrunina, A. L., Andronova, V. L., Galegov, G. A., Malakhov, A. D., and Korshun, V. A. (2006c). 5-Arylethynyl-2'-deoxyuridines, compounds active against HSV-1. *Organic & Biomolecular Chemistry* **4**(6), 1091-1096.
- Sonnino, S., Mauri, L., Chigorno, V., and Prinetti, A. (2007). Gangliosides as components of lipid membrane domains. *Glycobiology* **17**(1), 1R-13R.
- Stiasny, K., and Heinz, F. X. (2004). Effect of membrane curvature-modifying lipids on membrane fusion by tick-borne encephalitis virus. *Journal of Virology* **78**(16), 8536-8542.
- Teissier, E., Penin, F., and Pecheur, E. I. (2011). Targeting Cell Entry of Enveloped Viruses as an Antiviral Strategy. *Molecules* **16**(1), 221-250.
- Teissier, E., Zandomenighi, G., Loquet, A., Lavillette, D., Lavergne, J. P., Montserret, R., Cosset, F. L., Bockmann, A., Meier, B. H., Penin, F., and Pecheur, E. I. (2011). Mechanism of inhibition of enveloped virus membrane fusion by the antiviral drug arbidol. *PLoS One* **6**(1), e15874.
- Thery, C., Ostrowski, M., and Segura, E. (2009). Membrane vesicles as conveyors of immune responses. *Nat Rev Immunol* **9**(8), 581-93.
- van den Bogaart, G., and Jahn, R. (2011). Inside insight to membrane fusion. *Proc Natl Acad Sci U S A* **108**(29), 11729-30.
- van Helvoort, A., Smith, A. J., Sprong, H., Fritzsche, I., Schinkel, A. H., Borst, P., and van Meer, G. (1996). MDR1 P-glycoprotein is a lipid translocase of broad specificity, while MDR3 P-glycoprotein specifically translocates phosphatidylcholine. *Cell* **87**(3), 507-17.
- van Til, N. P., Heutinck, K. M., van der Rijt, R., Paulusma, C. C., van Wijland, M., Markusic, D. M., Elferink, R. P., and Seppen, J. (2008). Alteration of viral lipid composition by expression of the phospholipid floppase ABCB4 reduces HIV vector infectivity. *Retrovirology* **5**, 14.
- Vigant, F., Lee, J., Akyol-Ataman, Z., Robinson, L., Jung, M., and Lee, B. (2010). *11th annual symposium on antiviral drug resistance, Hersey, Pennsylvania.*

- Villalain, J. (2010). Membranotropic effects of arbidol, a broad anti-viral molecule, on phospholipid model membranes. *J Phys Chem B* **114**(25), 8544-54.
- Vogel, S. S., Leikina, E. A., and Chernomordik, L. V. (1993). Lysophosphatidylcholine Reversibly Arrests Exocytosis and Viral Fusion at a Stage between Triggering and Membrane Merger. *Journal of Biological Chemistry* **268**(34), 25764-25768.
- Wiebusch, L., Neuwirth, A., Grabenhenrich, L., Voigt, S., and Hagemeyer, C. (2008). Cell cycle-independent expression of immediate-early gene 3 results in G1 and G2 arrest in murine cytomegalovirus-infected cells. *J Virol* **82**(20), 10188-98.
- Wildy, P., Russell, W. C., and Horne, R. W. (1960). The morphology of herpes virus. *Virology* **12**, 204-22.
- Wolf, M. C., Freiberg, A. N., Zhang, T. H., Akyol-Ataman, Z., Grock, A., Hong, P. W., Li, J. R., Watson, N. F., Fang, A. Q., Aguilar, H. C., Porotto, M., Honko, A. N., Damoiseaux, R., Miller, J. P., Woodson, S. E., Chantasirivisal, S., Fontanes, V., Negrete, O. A., Krogstad, P., Dasgupta, A., Moscona, A., Hensley, L. E., Whelan, S. P., Faull, K. F., Holbrook, M. R., Jung, M. E., and Lee, B. (2010). A broad-spectrum antiviral targeting entry of enveloped viruses. *Proceedings of the National Academy of Sciences of the United States of America* **107**(7), 3157-3162.
- Wolkerstorfer, A., Kurz, H., Bachhofner, N., and Szolar, O. H. (2009). Glycyrrhizin inhibits influenza A virus uptake into the cell. *Antiviral Res* **83**(2), 171-8.
- Yang, X. Z., Kurteva, S., Ren, X. P., Lee, S., and Sodroski, J. (2005). Stoichiometry of envelope glycoprotein trimers in the entry of human immunodeficiency virus type 1. *Journal of Virology* **79**(19), 12132-12147.
- Yeagle, P. L., Smith, F. T., Young, J. E., and Flanagan, T. D. (1994). Inhibition of Membrane-Fusion by Lysophosphatidylcholine. *Biochemistry* **33**(7), 1820-1827.
- Zhan, P., Li, Z., and Liu, X. (2010). Cosalane and its analogues: a unique class of anti-HIV agents. *Mini Rev Med Chem* **10**(10), 966-76.
- Zhang, Z., and Jackson, M. B. (2010). Membrane Bending Energy and Fusion Pore Kinetics in Ca²⁺-Triggered Exocytosis. *Biophysical Journal* **98**(11), 2524-2534.
- Zimmerberg, J., and Kozlov, M. M. (2006). How proteins produce cellular membrane curvature. *Nature Reviews Molecular Cell Biology* **7**(1), 9-19.

Family	Genus	Species	Genome	Virion Size, nm	Morphology	Membrane budding site
Enveloped						
<i>Retroviridae</i>	<i>Lentivirus</i>	HIV	(+)ssRNA; 9.8 kb	180	~spherical	plasma membrane
<i>Flaviviridae</i>	<i>Hepacivirus</i>	HCV	(+)ssRNA; 9.6 kb	55-65	spherical	endoplasmic reticulum
<i>Orthomyxoviridae</i>	<i>Influenzavirus A</i>	influenza A	segmented (-)ssRNA	80-120	~spherical	plasma membrane
<i>Herpesviridae</i>	<i>Simplexvirus</i>	HSV	dsDNA; 150 kb	150-200	spherical	inner nuclear membrane; trans-Golgi
<i>Rhabdoviridae</i>	<i>Vesiculovirus</i>	VSV	(-)ssRNA; 11 kb	70x180	bullet	plasma membrane
<i>Togaviridae</i>	<i>Alphavirus</i>	SIN	(+)ssRNA; 12 kb	70	spherical	plasma membrane
<i>Hepadnaviridae</i>	<i>Orthohepadnavirus</i>	HBV	~dsDNA*; 3.2 kb	40	spherical	pre-Golgi
<i>Poxviridae</i>	<i>Orthopoxvirus</i>	VV	dsDNA; 190 kb	350x250	~rectangular	infectious-form dependent
Non-enveloped						
<i>Picornaviridae</i>	<i>Enterovirus</i>	PV	(+)ssRNA; 7.5 kb	30	icosahedral	NA
<i>Adenoviridae</i>	<i>Mastadenovirus</i>	HAdV-5	dsDNA; 35 kb	100	icosahedral	NA

Table 7.1 Virion properties of some enveloped and nonenveloped viruses. HIV-1, human immunodeficiency virus; HCV, hepatitis C virus; HSV, herpes simplex virus; VSV, vesicular stomatitis virus; SIN, Sindbis virus; HBV, hepatitis B virus; PV, poliovirus; HAdV-5, human adenovirus serotype 5; VV, vaccinia virus; ss, single stranded; ds, double stranded; *, the genome of HBV is mostly double-stranded and circular; NA, not applicable.

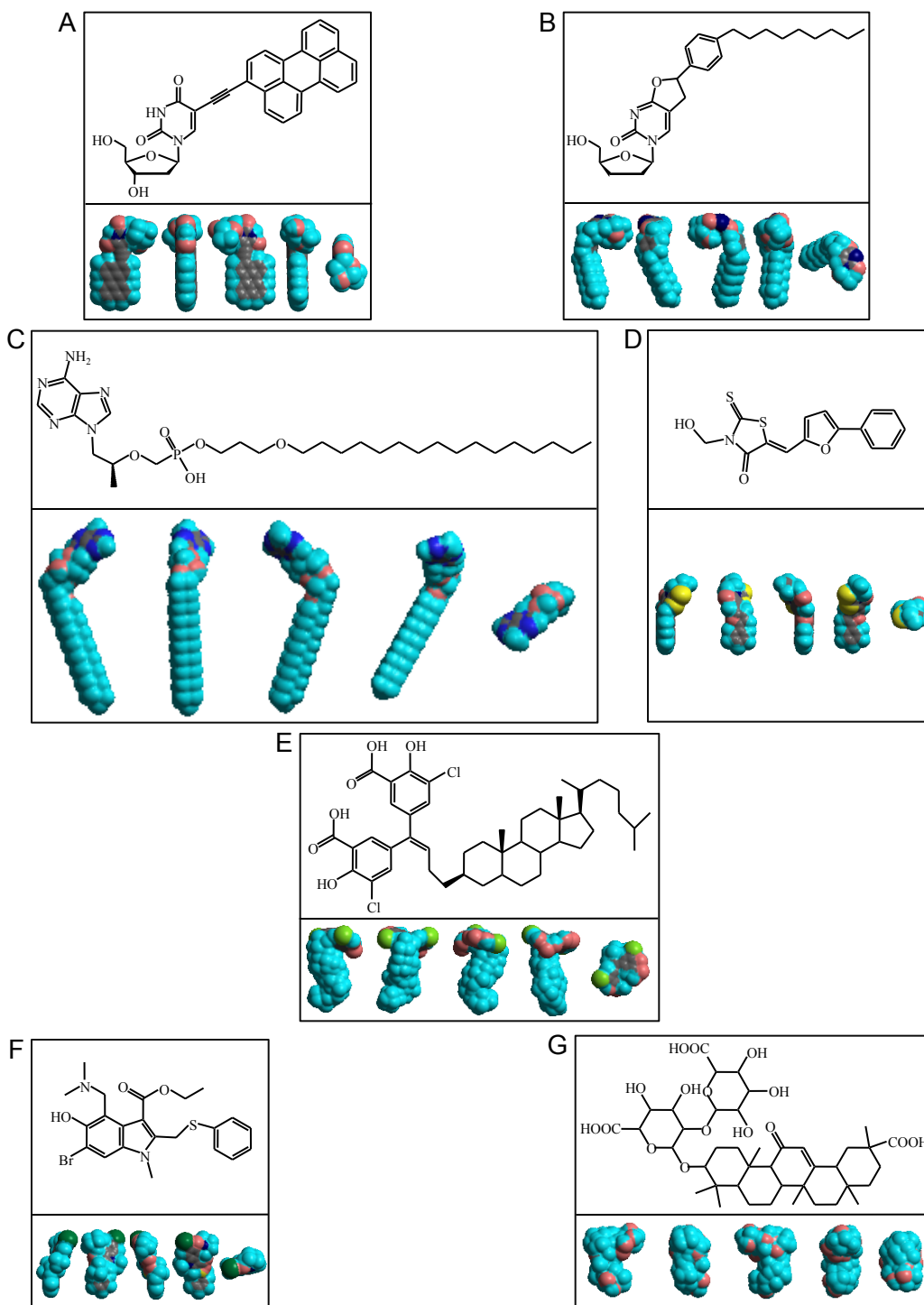


Figure 7.1 Small molecules targeting virion envelopes. Chemical structures and three-dimensional space-filling models displayed in 5 orthogonal planes of the rigid amphipathic fusion inhibitor dUY11 (**A**), and BCNA (**B**), CMX157 (**C**), and LJ001 (**D**), which display some similarities to the molecular shape of dUY11; or cosalane (**E**), arbidol (**F**), and glycyrrhizin (**G**), which have molecular shapes distinct from dUY11. Grey, carbon; teal, hydrogen; pink, oxygen; blue, nitrogen; red, phosphate; dark green, bromine; yellow, sulphur; light green, chlorine.

Host Cell/ Virus Family and Species	Percent of Total Phospholipid, mol %										CH/PL molar ratio	Reference
	PC	PE	PS	PI	SM	LPE	LPC	PA	Other			
Herpesviridae												
Uninfected HFF	34.1	21.6	29.6	5.8	-	-	-	3.0	5.8 ^a	-	Liu et al., 2011	
HCMV-infected HFF	33.1	22.4	28.9	4.0	-	-	-	4.6	6.8 ^a	-	Liu et al., 2011	
HCMV from HFF	33.7	48.6	8.1	2.9	-	-	-	1.7	5.1 ^a	-	Liu et al., 2011	
Uninfected BHK-21 cells (PM)	71.7	13.9	2.5	4.3	7.6	-	-	-	-	-	van Genderen et al., 1995	
HSV-1 from BHK-21	55.8	13.0	7.1	8.2	15.9	-	-	-	-	-	van Genderen et al., 1995	
Vero cells infected with HSV	58.4	26.3	2.7	10.8	1.8	-	-	-	-	-	van Genderen et al., 1994	
HSV-1 from Vero	51.2	29.8	4.6	11.3	3.1	-	-	-	-	-	van Genderen et al., 1994	
BHK-21 cells infected with HSV	65.0	21.7	2.0	2.7	9.0	-	-	-	-	-	van Genderen et al., 1994	
HSV-1 from BHK-21	49.3	18.2	4.8	3.2	24.6	-	-	-	-	-	van Genderen et al., 1994	
Uninfected RK (ON)	PC+PI: 66.3	16.5	4.2	p.e.	6.3	-	-	-	6.7 ^b	-	Ben-Porat and Kaplan, 1971	
Uninfected RK (IN)	PC+PI: 50.5	22.3	2.7	p.e.	21.2	-	-	-	3.3 ^b	-	Ben-Porat and Kaplan, 1971	
Infected RK (ON)	PC+PI: 62.3	21.7	3.2	p.e.	8.6	-	-	-	4.2 ^b	-	Ben-Porat and Kaplan, 1971	
Infected RK (IN)	PC+PI: 50.5	21.5	3.7	p.e.	20.8	-	-	-	3.5 ^b	-	Ben-Porat and Kaplan, 1971	
PRV from RK	PC+PI: 51.2	21.0	3.5	p.e.	21.0	-	-	-	3.3 ^b	-	Ben-Porat and Kaplan, 1971	
Poxviridae												
Uninfected whole RK13 cells	42.8	35.8	5.8	7.0	9.8	-	-	-	0.8 ^c	-	Sodeik et al., 1993	
VV strain IHD-J from RK13 (INV)	36.0	25.6	3.7	15.2	5.7	-	-	-	11.9 ^c	-	Sodeik et al., 1993	
VV strain IHD-J from RK13 (EEV)	29.8	33.9	9.5	5.8	13.4	-	-	-	7.6 ^c	-	Sodeik et al., 1993	
Whole infected HeLa cells	52.7	19.6	4.8	12.1	5.6	-	0.8	-	5.6	-	Stern & Dales, 1974	
VV strain IHD-J from HeLa	48.9	12.4	4.6	12.1	4.7	-	1.0	-	15.3	-	Stern & Dales, 1974	
Whole L2 cells	44.5	25.3	5.2	10.5	7.6	-	0.5	-	5.4	-	Stern & Dales, 1974	
VV strain IHD-J from L2	34.2	14.2	4.5	18.7	2.2	-	0.7	-	24.1	-	Stern & Dales, 1974	
Whole BHK-21 cells	46.0	19.0	6.7	10.0	8.1	-	1.0	-	8.9	-	Stern & Dales, 1974	
VV strain IHD-J from BHK-21	35.7	PE+PS: 14.4	p.e.	13.7	2.6	-	1.3	-	29.6	-	Stern & Dales, 1974	

Host Cell/ Virus Family and Species	Percent of Total Phospholipid, mol %					CH/PL					Reference
	PC	PE	PS	PI	SM	LPE	LPC	PA	Other	molar ratio	
<i>Hepadnaviridae</i>											
huGK-14 cells	52.0	29.7	1.7	5.5	6.7	-	ND	-	4.6 ^d	-	Satoh et al., 1990
HBV from huGK-14	83.6	7.2	ND	5.3	2.9	-	1.0	-	ND	-	Satoh et al., 1990
Human hepatoma PLC/PRF/5 cells	50.2	31.0	2.5	5.3	7.1	-	ND	-	3.9 ^d	-	Satoh et al., 1990
HBV from PLC/PRF/5	85.7	7.3	ND	3.9	3.1	-	ND	-	ND	-	Satoh et al., 1990
<i>Orthomyxoviridae</i>											
Uninfected whole MDCK cells	62.5	20.1	4.2	5.2	7.7	-	-	-	-	-	van Meer & Simons, 1986
FPV from MDCK (apical)	9.6	44.8	22.4	2.8	20.5	-	-	-	-	-	van Meer & Simons, 1986
FPV from BHK-21	38.5	28.6	6.7	8.2	18.0	-	-	-	-	-	van Meer & Simons, 1986
Uninfected whole MDCK cells	34.8	36.4	7.2	9.0	12.6	-	-	-	-	-	van Meer & Simons, 1982
FPV from MDCK	2.4	58.4	16.8	1.3	21.3	-	-	-	-	-	van Meer & Simons, 1982
FPV from polarized MDCK	2.4	55.9	20.8	2.1	19.0	-	-	-	-	-	van Meer & Simons, 1982
FPV from depolarized MDCK	3.4	55.6	15.4	1.7	24.1	-	-	-	-	-	van Meer & Simons, 1982
InfA strain WSN from MDBK cells	12.0	38.0	16.0	3.0	31.0	-	-	-	-	-	Rothman et al., 1976
InfA strain WSN from rhesus MK cells	23.7	26.3	9.2	5.4	35.4	-	-	-	-	0.73	Klenk, Rott & Becht, 1972
InfA strain A0/PR8 from ECE	32.8	11.7	8.8	3.85	24.0	3.5 ^e	4.65 ^b	7.85	2.55 ^f	-	Blough & Weinstein., 1967
Uninfected whole CKC	44.0 ^g	16.0	4.0	5.0	SM+LPE: 17.0	p.e.	-	2.0	12.0 ^f	-	Kates et al., 1961
InfA strain Melbourne from CKC	36.0 ^g	8.0	5.0	5.0	SM+LPE: 14.0	p.e.	-	12.0	20.0 ^f	-	Kates et al., 1961
Uninfected whole CEC	48.0 ^g	18.0	6.0	PI+LPC ^b : 6.0	SM+LPE: 20.0	p.e.	-	-	2.0 ^f	-	Kates et al., 1961
InfA strain Melbourne from CEC	28.0 ^g	22.0	7.0	PI+LPC ^b : 6.0	SM+LPE: 35.0	p.e.	-	-	2.0 ^f	-	Kates et al., 1961

Host Cell/ Virus Family and Species	Percent of Total Phospholipid, mol %									CH/PL molar ratio	Reference	
	PC	PE	PS	PI	SM	LPE	LPC	PA	Other			
<i>Paramyxoviridae</i>												
NDV Clone-30 from CEC	22.7	26.8	PS+PI:15.5	p.e.	23.0	4.2	3.5	2.8	2.1 ^a	1.02	Muñoz-Barroso et al., 1997	
Uninfected whole CEF	42.0	36.0	PS+PI: 12.0	p.e.	9.0	-	-	-	3	0.17	Quigley et al., 1971	
Uninfected CEF (PM)	35.0	31.0	PS+PI: 13.0	p.e.	20.0	-	-	-	2	0.51	Quigley et al., 1971	
NDV from CEF	26.0	33.0	PS+PI: 10.0	p.e.	26.0	-	-	-	4	-	Quigley et al., 1971	
NDV strain Blacksburg from ECE	11.6	34.6	12.0		6.5	18.0	3.1	1.7	7.0	3.0 ^f	-	Blough & Lawson, 1968
Sendai virus strain Cantel from ECE	37.3	26.8	12.0		5.5	8.8	1.6	-	-	8.9 ^d	1.00	Barnes et al., 1987
Sendai virus from CEF	27.0	31.0	PS+PI: 14.0	p.e.	24.0	-	-	-	5	-	Quigley et al., 1971	
Sendai from ECE	8.0 ^g	37.0	15.0		6.4	11.8	2.0	1.8 ^b	10	7.6 ^f	-	Blough & Lawson, 1968
Uninfected HaK cells (PM)	46.8	13.0	5.0		11.7	24.4	-	-	-	-	0.51	Klenk & Choppin, 1970
SV5 strain W3 from HaK	43.8	17.1	5.0		8.5	25.8	-	-	-	-	0.60	Klenk & Choppin, 1970
Uninfected MDBK cells	57.2	24.5	5.6		5.9	6.7	-	-	-	-	0.25	Klenk & Choppin, 1970
Uninfected MDBK cells (PM)	44.5	27.2	2.2		2.9	22.8	-	-	-	-	0.75	Klenk & Choppin, 1970
SV5 strain W3 from MDBK cells	23.8	40.9	2.0		5.2	27.3	-	-	-	-	0.84	Klenk & Choppin, 1970
Whole MK cells	46.4	32.5	5.0		11.4	4.9	-	-	-	-	0.15	Klenk & Choppin, 1969
MK cell PM	32.1	38.8	17.2		ND	11.8	-	-	-	-	0.81	Klenk & Choppin, 1969
SV5 strain W3 from MK	25.2	40.3	17.9		2.9	12.2	-	-	-	-	0.89	Klenk & Choppin, 1969
Whole BHK21-F cells	63.0	17.0	9.4		5.7	6.9	-	-	-	-	0.15	Klenk & Choppin, 1969
BHK21-F cell PM	49.5	11.2	5.1		10.0	24.2	-	-	-	-	0.68	Klenk & Choppin, 1969
SV5 strain W3 from BHK21-F	38.5	15.6	5.2		10.5	30.0	-	-	-	-	0.64	Klenk & Choppin, 1969

Host Cell/ Virus Family and Species	Percent of Total Phospholipid, mol %										CH/PL molar ratio	Reference
	PC	PE	PS	PI	SM	LPE	LPC	PA	Other			
<i>Rhabdoviridae</i>												
Uninfected whole BHK-21 CCL10 cells	31.3 ^h	12.5 ⁱ	4.7	5.7	5.7	-	-	0.8	1.6 ^j	0.46		Kalvodova et al., 2009
Uninfected BHK-21 CCL10 (PM)	14.4 ^h	10.4 ⁱ	8.1	1.9	8.6	-	-	0.3	1.5 ^j	0.93		Kalvodova et al., 2009
VSV from BHK-21 CCL10	11.4 ^h	14.6 ⁱ	9.8	1.0	11.5	-	-	0.1	0.2 ^j	0.90		Kalvodova et al., 2009
Uninfected BHK-21 cells (PM)	43	27.3	6.3	6.7	13.9	-	-	1.9	1.0	0.49		Luan et al., 1995
VSV from BHK-21 cells	28.5	27.0	13.3	4.1	21.6	-	-	4.3	1.4	0.83		Luan et al., 1995
Uninfected BHK-21 cells (PM)	71.7	13.9	2.5	4.3	7.6	-	-	-	-	-		van Genderen et al., 1995
VSV from BHK-21	41.4	22.2	10.8	4.8	20.8	-	-	-	-	-		van Genderen et al., 1995
Uninfected whole MDCK cells	62.5	20.1	4.2	5.2	7.7	-	-	-	-	-		van Meer & Simons, 1986
VSV from MDCK (basolateral)	28.9	33.5	18.9	3.2	15.6	-	-	-	-	-		van Meer & Simons, 1986
VSV from BHK-21 (no polarized PM)	38.3	27.1	7.0	10.1	17.6	-	-	-	-	-		van Meer & Simons, 1986
Uninfected whole MDCK cells	34.8	36.4	7.2	9.0	12.6	-	-	-	-	-		van Meer & Simons, 1982
VSV from MDCK	9.2	51.4	16.3	3.2	19.9	-	-	-	-	-		van Meer & Simons, 1982
VSV from polarized MDCK	11.3	38.4	17.2	6.9	26.4	-	-	-	-	-		van Meer & Simons, 1982
VSV from depolarized MDCK	7.7	52.9	15.2	2.3	22.0	-	-	-	-	-		van Meer & Simons, 1982
VSV strain San Juan-infected CEF (PM)	45.3	27.3	6.4	7.3	12.3	-	-	-	1.7 ^f	-		Pessin & Glaser, 1980
VSV strain San Juan from CEF	35.4	30.5	10.9	7.0	16.0	-	-	-	0.3 ^f	-		Pessin & Glaser, 1980
VSV serotype Indiana from BHK-21	29.0	32.0	20.0	-	20.0	-	-	-	-	0.71		Pal et al., 1980
BHK-21 cells (PM)	-	-	-	-	-	-	-	-	-	0.54		Patzer et al., 1978
VSV serotype Indiana from BHK-21	24	31.0	18.0	1.9	24.0	-	0.9	0.3	-	0.72		Patzer et al., 1978
VSV serotype New Jersey from BHK-21	-	-	-	-	-	-	-	-	-	0.81		Patzer et al., 1978

Host Cell/ Virus Family and Species	Percent of Total Phospholipid, mol %										CH/PL molar ratio	Reference
	PC	PE	PS	PI	SM	LPE	LPC	PA	Other			
Rhabdoviridae												
Uninfected whole L-cells	34.8	28.4	PS+PI: 16.0	p.e.	8.9	-	2.3	2.4	8.6 ^k	0.25	McSharry & Wagner, 1971	
Uninfected L-cells (PM)	51.0	22.6	PS+PI: 7.0	p.e.	16.2	-	<0.1	<0.1	3.3 ^k	0.58	McSharry & Wagner, 1971	
VSV serotype Indiana from L-cells	16.4	33.1	PS+PI: 17.3	p.e.	20.9	-	1.5	5.9	4.8 ^f	0.64	McSharry & Wagner, 1971	
VSV serotype New Jersey from L-cells	15.9	31.3	PS+PI: 15.4	p.e.	22.0	-	3.7	4.4	7.3 ^f	1.23	McSharry & Wagner, 1971	
Uninfected whole CEC	51.7	23.6	PS+PI: 11.2	p.e.	7.2	-	<0.1	2.9	0.70 ^k	0.27	McSharry & Wagner, 1971	
Uninfected CEC (PM)	37.8	30.5	PS+PI: 10.1	p.e.	11.9	-	<0.1	3.8	<0.2 ^k	1.01	McSharry & Wagner, 1971	
VSV serotype Indiana from CEC	18.4	37.0	PS+PI: 17.0	p.e.	23.9	-	<0.1	3.7	<0.1 ^f	0.60	McSharry & Wagner, 1971	
VSV serotype New Jersey from CEC	21.9	36.0	PS+PI: 16.9	p.e.	23.6	-	<0.1	2.0	<0.2 ^k	0.63	McSharry & Wagner, 1971	
Uninfected BHK-21 cells (PM)	34.2	35.3	8.2	0.8	14.3	0.8	0.5	4.1	0.9 ^l	-	Blough et al., 1977	
Rabies strain Flury HEP from BHK-21	23.4	35.1	7.8	0.2	31.3	-	1.5	tr	0.2 ^l	0.48	Blough et al., 1977	
Uninfected Nil2 fibroblasts	49.1	20.0	6.4	6.1	9.2	3.2	1.3	1.6	3.3 ^d	0.31	Portoukalian et al., 1977	
Rabies virus from Nil2	20.5	33.0	17.5	0.3	26.8	1.4	0.5	ND	-	0.77	Portoukalian et al., 1977	
Uninfected whole BHK-21 cells	20.3	30.5	PS+PI: 9.6	p.e.	16.0	-	4.2	-	9.6 ^f	0.20	Schleisinger et al., 1973	
Rabies virus strain ERA from BHK-21	21.7	20.2	PS+PI: 19.8	p.e.	19.8	-	8.3	-	13.2 ^f	0.92	Schleisinger et al., 1973	
Bunyaviridae												
Uninfected BHK-21 cells	49.8	22.8	6.6	5.7	6.9	-	0.7	0.6	4.5 ^m	-	Renkonen et al., 1972	
Uukuniemi virus from BHK-21	41.9	23.4	11.6	3.3	15.1	-	1.1	1.2	1.5 ^m	-	Renkonen et al., 1972	
Flaviviridae												
Huh7.5 cells	41.3	29.3	9.0	12.7	7.4	-	-	-	0.3 ^a	0.26 ⁿ	Merz et al., 2011	
HCV genotype Jc1E2 ^{FLAG} from Huh7.5	56.9	7.5	0.9	2.7	30.8	-	-	-	1.1 ^a	0.65 ⁿ	Merz et al., 2011	

Host Cell/ Virus Family and Species	Percent of Total Phospholipid, mol %										CH/PL molar ratio	Reference
	PC	PE	PS	PI	SM	LPE	LPC	PA	Other			
<i>Togaviridae</i>												
Uninfected whole BHK-21 CCL10 cells	31.3 ^h	12.5 ⁱ	4.7	5.7	5.7	-	-	0.8	1.6 ^j	0.46	Kalvodova et al., 2009	
Uninfected BHK-21 CCL10 (PM)	14.4 ^h	10.4 ⁱ	8.1	1.9	8.6	-	-	0.3	1.5 ^j	0.93	Kalvodova et al., 2009	
SFV from BHK-21 CCL10	14.1 ^h	11.2 ⁱ	10.6	0.8	12.9	-	-	0.2	0.4 ^j	0.84	Kalvodova et al., 2009	
Uninfected BHK-21 (clone Wi-2)	49.8	22.8 ^o	6.6	5.7	6.9	-	0.7	0.6	4.5 ^m	-	Renkonen et al., 1972	
SFV from BHK-21 (clone Wi-2)	42.4	23.2 ^o	13.4	1.6	16.0	-	0.5	1.3	0.6 ^m	-	Renkonen et al., 1972	
Uninfected BHK-21 (clone C13) cell (PM)	40.0	21.0	7.1	3.2	17.0	-	3.5	5.7	-	0.58	Renkonen et al., 1971	
Infected BHK-21 (clone C13) cell (PM)	44.0	21.0	6.2	4.4	14.0	-	2.9	4.3	-	0.48	Renkonen et al., 1971	
SFV from BHK-21 (clone C13)	34.0	26.0	12.0	0.9	21.0	-	1.2	4.1	-	0.97	Renkonen et al., 1971	
SFV from BHK-21 (clone Wi-2)	33.0	23.0	13.0	1.5	21.0	-	1.0	5.6	-	0.99	Renkonen et al., 1971	
Whole CEC	39.6	30.3	8.0	7.0	10.9	-	-	-	-	0.3	Hirschberg & Robbins, 1974	
PM from CEC	35.8	28.4	9.2	13.0	8.7	-	-	-	-	0.6	Hirschberg & Robbins, 1974	
SIN virus from CEC	29.9	28.5	17.9	1.0	27.3	-	-	-	-	0.8	Hirschberg & Robbins, 1974	
Uninfected whole BHK-21 cells	55.4	23.3	8.7	9.1	3.5	-	-	-	-	0.25	David, 1971	
Uninfected BHK21 cell (PM)	26.3	32.7	20.6	3.5	16.5	-	-	-	-	0.73	David, 1971	
SIN from BHK-21	26.2	35.4	20.3	ND	18.2	-	-	-	-	-	David, 1971	
Uninfected whole CEC	56.3	20.5	10.8	9.6	3.2	-	-	-	-	0.21	David, 1971	
Uninfected CEC PM	43.5	23.8	11.1	18.8	3.3	-	-	-	-	0.55	David, 1971	
SIN from CEC	26.4	32.1	20.8	ND	20.5	-	-	-	-	-	David, 1971	
SIN virus from CEF	21.0	33.0	PS+PI: 15.0	p.e.	29.0	-	-	-	2.0	-	Quigley et al., 1971	
Uninfected whole CEF	50.0 ^g	26.0	-	-	11.0	-	-	-	-	-	Pfefferkorn et al., 1963	
SIN from CEF	38.0 ^g	25.0	-	-	25.0	-	-	-	-	3.0	Pfefferkorn et al., 1963	
Uninfected BHK/13S cells	37.1	25.0	7.7	8.9	5.3	-	4.8	-	6.5 ^d	0.17	Bardeletti & Gautheron, 1976	
Rubella from BHK/13S	44.2	19.0	9.1	9.2	6.9	-	5.8	-	4.4 ^d	0.26	Bardeletti & Gautheron, 1976	

Host Cell/ Virus Family and Species	Percent of Total Phospholipid, mol %					LPE	LPC	PA	Other	CH/PL molar ratio	Reference
	PC	PE	PS	PI	SM						
<i>Togaviridae</i>											
Uninfected whole CFC	51.2	20.1 ^o	6.6	7.5	6.3	-	-	-	9.1 ^p	-	Heydrick et al., 1971
VEE virus from CFC	35.4	28.1 ^o	16.9	1.8	13.1	-	-	-	3.7 ^p	-	Heydrick et al., 1971
Uninfected whole L-cells	47.8	16.1 ^o	2.9	3.9	9.3	-	-	-	20.1 ^p	-	Heydrick et al., 1971
VEE virus from L-cells	23.3	29.1 ^o	14.7	0.5	26.2	-	-	-	5.1 ^p	-	Heydrick et al., 1971
<i>Coronaviridae</i>											
Uninfected Sac(-) whole cells	71.8	16.8	3.8	5.9	1.8	-	-	-	-	-	van Genderen et al., 1995
MHV strain A59 from Sac(-)	71.7	10.8	5.7	10.1	4.2	-	-	-	-	-	van Genderen et al., 1995
Uninfected PK/1	30.0	13.1	2.5	3.8	SM+LPC: 50.5	-	p.e.	-	-	0.02	Pike and Garwes, 1977
TGEV strain FS _{772/70} from PK/1	38.9	12.2	2.2	3.4	SM+LPC: 43.3	-	p.e.	-	-	0.01	Pike and Garwes, 1977
Uninfected APT/2	69.1	9.9	ND	2.3	SM+LPC: 18.7	-	p.e.	-	-	0.02	Pike and Garwes, 1977
TGEV strain FS _{772/70} from APT/2	70.5	5.5	ND	2.2	SM+LPC: 21.8	-	p.e.	-	-	0.01	Pike and Garwes, 1977
<i>Retroviridae</i>											
Uninfected whole MT-4 cells	43.5 ^q	29.9 ^o	10.4	5.1	10.9 ^r	-	-	-	-	0.27	Lorizate et al., 2009
HIV-1 strain NL4-3 from MT-4	17.6 ^q	36.1 ^o	22.1	0.9	23.3 ^r	-	-	-	-	0.78	Lorizate et al., 2009
Uninfected whole 293T cells	65.4 ^q	17.7 ^o	6.0	7.6	3.2 ^r	-	-	-	-	0.33	Lorizate et al., 2009
HIV-1 NL4-3 from 293T	41.4 ^q	27.1 ^o	13.0	2.0	16.4 ^r	-	-	-	-	0.89	Lorizate et al., 2009
Uninfected H9 (PM)	21.8	23.6 ^o	13.5	11.7 ^s	20.8 ^r	-	-	NA	7.1 ^t	-	Chan et al., 2008
HIV-1 from H9	27.8	21.6 ^o	13.4	7.4 ^s	25.8 ^r	-	-	NA	5.9 ^t	-	Chan et al., 2008
MDM clone 4 (PM)	24.0	21.3 ^o	11.0	8.4 ^s	31.6 ^r	-	-	NA	3.7 ^t	-	Chan et al., 2008
HIV-1 _{MN} from MDM clone 4	21.6	17.9 ^o	10.5	9.7 ^s	35.0 ^r	-	-	NA	5.3 ^t	-	Chan et al., 2008
Uninfected whole MT-4 cells	43.0	32.9 ^o	7.4	-	10.4 ^r	-	-	-	-	0.39	Brugger et al., 2006
HIV-1 strain NL4-3 from MT-4 cells	16	35.2 ^o	15.5	-	33.1 ^r	-	-	-	-	0.83	Brugger et al., 2006

Host Cell/ Virus Family and Species	Percent of Total Phospholipid, mol %									CH/PL molar ratio	Reference
	PC	PE	PS	PI	SM	LPE	LPC	PA	Other		
<i>Retroviridae</i>											
Uninfected H9 cells (PM)	47.5	23.3	10.3	4.9	9.6	-	-	0.59	3.44 ^u	0.48	Aloia et al., 1993
HIV-1 strain RF infected H9 cells (PM)	50.5	24.9	6.4	4.7	7.1	-	-	0.33	6.07 ^u	0.37	Aloia et al., 1993
HIV-1 strain RF from H9 cells	29.8	24.6	9.0	0.4	24.1	-	-	1.21	8.25 ^u	0.96	Aloia et al., 1993
HIV-2-L infected H9 cells (PM)	50.5	24.5	6.3	5.5	8.3	-	-	0.47	4.49 ^u	0.34	Aloia et al., 1993
HIV-2-L from H9 cells	27.6	27.3	15.5	1.1	23.0	-	-	1.21	4.81 ^u	0.88	Aloia et al., 1993
HIV-LK013	-	-	-	-	-	-	-	-	-	0.84	Aloia et al., 1993
HIV-F7529	-	-	-	-	-	-	-	-	-	0.91	Aloia et al., 1993
HIV-4105	-	-	-	-	-	-	-	-	-	0.92	Aloia et al., 1993
HIV-OT	-	-	-	-	-	-	-	-	-	0.77	Aloia et al., 1993
SIV-B670	-	-	-	-	-	-	-	-	-	0.79	Aloia et al., 1993
HIV-HZ321	-	-	-	-	-	-	-	-	-	1.27	Aloia et al., 1993
HIV-BK	-	-	-	-	-	-	-	-	-	1.25	Aloia et al., 1993
HIV from Hut78 cells	23.8	24.6	15.1	2.1	28.3	-	-	0.9	5.0 ^u	0.88	Aloia et al., 1988
HTLV-III _B	-	-	-	-	-	-	-	-	-	1.20	Aloia et al., 1993
HTLV-III _{RF}	-	-	-	-	-	-	-	-	-	1.20	Aloia et al., 1993
HTLV-III _{MN}	-	-	-	-	-	-	-	-	-	1.60	Aloia et al., 1993
HTLV-III _B from H9 cells	35.0	26.0	24.0	6.0	13.0	-	-	-	-	1.2	Crews et al., 1988
HTLV-III _{MN} from H9 cells	32.0	43.0	4.0	11.0	11.0	-	-	-	-	1.6	Crews et al., 1988
HTLV-III _{RF} from H9 cells	30.0	30.0	14.0	16.0	11.0	-	-	-	-	1.2	Crews et al., 1988
HTLV-1	-	-	-	-	-	-	-	-	-	1.2	Crews et al., 1988
Uninfected REF (PM)	26.5	21.7 ^o	11.3	14.8 ^s	21.8 ^r	-	-	NA	4.0 ^t	-	Chan et al., 2008
MLV from REFs	19.0	23.3 ^o	15.7	10.6 ^s	28.1 ^r	-	-	NA	3.4 ^t	-	Chan et al., 2008

Host Cell/ Virus Family and Species	Percent of Total Phospholipid, mol %									CH/PL molar ratio	Reference	
	PC	PE	PS	PI	SM	LPE	LPC	PA	Other			
Retroviridae												
FLV	-	-	-	-	-	-	-	-	-	-	1.2	Crews et al., 1988
RLV	-	-	-	-	-	-	-	-	-	-	1.3	Crews et al., 1988
Gibbon ape leukemia virus	-	-	-	-	-	-	-	-	-	-	1.1	Crews et al., 1988
SSV	-	-	-	-	-	-	-	-	-	-	1.0	Crews et al., 1988
ALV strain RAV-2 from CEF	20.0	30.0	PS+PI: 16.0 p.e.		33.0	-	-	-	1.0	-		Quigley et al., 1971
ASV strain B77 from CEF	21.0	29.0	PS+PI: 17.0 p.e.		30.0	-	-	-	3.0	-		Quigley et al., 1971
RSV strain Schmidt-Ruppin infected CEF (PM)	39.3	31.2	7.9	3.2	15.5	-	-	-	2.9	0.48		Pessin & Glaser, 1980
RSV strain Schmidt-Ruppin from CEF	24.8	34.8	15.5	2.2	22.6	-	-	-	0.1	0.8		Pessin & Glaser, 1980
Whole uninfected QC	59.0	22.0	PS+PI: 9.0 p.e.		5.0	-	-	-	3.0 ^v	-		Quigley et al., 1972
QC (PM)	49.0	20.0	PS+PI: 15.0 p.e.		13.0	-	-	-	3.0 ^v	-		Quigley et al., 1972
RSV strain Schmidt-Ruppin from QC	30.0	26.0	PS+PI: 17.0 p.e.		22.0	-	-	-	6.0 ^v	-		Quigley et al., 1972
Whole uninfected CEF	46.0	31.0	PS+PI: 10.0 p.e.		10.0	-	-	-	4.0 ^v	0.17		Quigley et al., 1971
Uninfected CEF (PM)	37.0	26.0	PS+PI: 14.0 p.e.		20.0	-	-	-	2.0 ^v	0.51		Quigley et al., 1971
RSV strain Schmidt-Ruppin from CEF	20.0	33.0	PS+PI: 12.0 p.e.		29.0	-	-	-	4.0 ^v	0.88		Quigley et al., 1971
Arteriviridae												
Uninfected BHK-21 cells (PM)	71.7	13.9	2.5	4.3	7.6	-	-	-	-	-		van Genderen et al., 1995
Equine arteritis virus from BHK-21	54.9	13.9	5.1	7.1	19.5	-	-	-	-	-		van Genderen et al., 1995

	Lauric C12:0	Myristic C14:0	C14:1	C15:0	Palmitic C16:0	Palmitoleic C16:1	C16:2	C17:0	Stearic C18:0	Oleic C18:1	Linoleic C18:2	C18:3
<i>Hepadnaviridae</i>												
PC from huGK-14 cells	-	1.3	-	-	31.5	21.3	-	-	4.4	41.1	-	-
PC of HBV from huGK-14	-	1.4	-	-	28.1	15.7	-	-	4.4	50.0	-	-
PE from huGK-14 cells	-	0.5	-	-	18.1	11.8	-	-	20.9	44.9	-	-
PE of HBV from huGK-14	-	1.7	-	-	13.3	8.5	-	-	19.0	54.0	-	-
<i>Orthomyxoviridae</i>												
Influenza strain A ₀ /PR8/34 (total PL)	tr ^a	1.6	-	-	15.1	5.2	-	-	14.8	15.8	4.3	0.9
PC from Influenza strain A ₀ /PR8/34	-	4.0	-	-	30.1	2.4	-	-	13.9	26.8	10.7	ND
SM from Influenza strain A ₀ /PR8/34	-	1.7	-	-	43.3	0.7	-	-	9.3	9.3	tr ^a	tr ^a
PE from Influenza strain A ₀ /PR8/34	-	tr ^a	-	-	16.7	1.6	-	-	19.2	45.3	10.2	tr ^a
PS from Influenza strain A ₀ /PR8/34	-	2.9	-	-	15.4	1.2	-	-	34.2	20.9	9.2	1.8
Influenza strain B/LEE/40 (total PL)	ND	tr ^a	-	-	20.9	0.8	-	-	16.9	17.0	4.2	2.8
PC from Influenza strain B/LEE/40	-	tr ^a	-	-	38.7	tr	-	-	15.4	28.7	6.5	0.7
SM from Influenza strain B/LEE/40	-	ND	-	-	44.4	0.6	-	-	11.1	5.5	2.1	tr ^a
PE from Influenza strain B/LEE/40	-	2.3	-	-	14.7	0.8	-	-	11.2	35	9.8	1.8
PS from Influenza strain B/LEE/40	-	ND	-	-	13.0	0.9	-	-	32.7	26.1	1.0	ND
pL of uninfected CEE	1.5	3.5	-	-	23.2	3.1	-	-	17.3	17.1	3.9	1.1
nL of uninfected CEE	ND	2.8	-	-	22.3	5.9	-	-	8.5	35.5	12.3	0.6
pL of Influenza strain A ₀ /PR8/34 from CEE	tr	1.6	-	-	15.1	5.2	-	-	14.8	15.8	4.3	0.9
nL of Influenza strain A ₀ /PR8/34 from CEE	ND	4.1	-	-	28.5	6.6	-	-	18.8	22.0	4.6	tr
pL of Influenza strain A ₂ /Jap/305/57 from CEE	1.0	3.1	-	-	17.5	1.1	-	-	9.7	20.5	7.0	tr
nL of Influenza strain A ₂ /Jap/305/57 from CEE	5.8	16.8	-	-	23.7	3.2	-	-	6.2	10.3	0.9	0.8
pL of Influenza strain B/Lee/40 from CEE	ND	tr	-	-	20.9	0.8	-	-	16.9	17.0	4.2	2.8
nL of Influenza strain B/Lee/40 from CEE	14.2	14.8	-	-	25.0	1.1	-	-	16.9	9.6	6.5	4.8

	Arachidic				Arachidonic									
	C20:0	C20:1	C20:2	C20:3	C20:4	C20:5	C21:5	C22:0	C22:1	C22:3	C22:4	C22:5	C22:6	
PC from huGK-14 cells	-	-	-	-	0.4	-	-	-	-	-	-	-	-	
PC of HBV from huGK-14	-	-	-	-	0.4	-	-	-	-	-	-	-	-	
PE from huGK-14 cells	-	-	-	-	3.8	-	-	-	-	-	-	-	-	
PE of HBV from huGK-14	-	-	-	-	3.7	-	-	-	-	-	-	-	-	
Influenza strain A ₀ /PR8/34 (total PL)	9.4	-	-	-	4.2	-	-	13.7	tr ^a	-	-	-	-	
PC from Influenza strain A ₀ /PR8/34	0.8	-	-	-	5.3	-	-	0.9	ND	-	-	-	-	
SM from Influenza strain A ₀ /PR8/34	3.1	-	-	-	2.7	-	-	15.1	0.6	-	-	-	-	
PE from Influenza strain A ₀ /PR8/34	1.9	-	-	-	4.1	-	-	ND	ND	-	-	-	-	
PS from Influenza strain A ₀ /PR8/34	2.3	-	-	-	3.6	-	-	1.6	ND	-	-	-	-	
Influenza strain B/LEE/40 (total PL)	3.9	-	-	-	13.4	-	-	7.3	ND	-	-	-	-	
PC from Influenza strain B/LEE/40	2.8	-	-	-	7.0	-	-	ND	ND	-	-	-	-	
SM from Influenza strain B/LEE/40	7.6	-	-	-	3.1	-	-	12.1	ND	-	-	-	-	
PE from Influenza strain B/LEE/40	ND	-	-	-	24.4	-	-	ND	ND	-	-	-	-	
PS from Influenza strain B/LEE/40	tr ^a	-	-	-	10.3	-	-	tr ^a	ND	-	-	-	-	
pL of uninfected CEE	0.9	ND	-	-	12.9	-	-	1.2	ND	-	-	-	-	
nL of uninfected CEE	0.9	ND	-	-	4.0	-	-	tr	ND	-	-	-	-	
pL of Influenza strain A ₀ /PR8/34 from CEE	8.4	tr	-	-	4.2	-	-	13.7	tr	-	-	-	-	
nL of Influenza strain A ₀ /PR8/34 from CEE	6.1	ND	-	-	4.9	-	-	4.4	ND	-	-	-	-	
pL of Influenza strain A ₂ /Jap/305/57 from CEE	5.0	ND	-	-	14.4	-	-	9.6	ND	-	-	-	-	
nL of Influenza strain A ₂ /Jap/305/57 from CEE	3.1	ND	-	-	14.1	-	-	4.7	ND	-	-	-	-	
pL of Influenza strain B/Lee/40 from CEE	3.9	ND	-	-	13.4	-	-	7.3	ND	-	-	-	-	
nL of Influenza strain B/Lee/40 from CEE	1.9	ND	-	-	1.6	-	-	2.0	ND	-	-	-	-	

	C22 polyene	Lignoceric C24:0	C24:1	C24:4	other	saturated	unsaturated mono poly	saturated/ unsaturated	Reference
PC from huGK-14 cells	-	-	-	-	-	37.2	62.4 0.4	0.59	Satoh <i>et al.</i> , 1990
PC of HBV from huGK-14	-	-	-	-	-	33.9	65.7 0.4	0.51	Satoh <i>et al.</i> , 1990
PE from huGK-14 cells	-	-	-	-	-	39.5	56.7 3.8	0.65	Satoh <i>et al.</i> , 1990
PE of HBV from huGK-14	-	-	-	-	-	34.0	62.5 3.7	0.51	Satoh <i>et al.</i> , 1990
Influenza strain A ₀ /PR8/34 (total PL)	8.4	6.8	ND	-	0.6 ^b	61.4	21.0 17.8	1.58	Blough, 1971
PC from Influenza strain A ₀ /PR8/34	4.9	tr ^a	ND	-	-	49.7	29.2 20.9	0.99	Blough, 1971
SM from Influenza strain A ₀ /PR8/34	0.8	13	0.9	-	-	85.5	11.5 3.5	5.70	Blough, 1971
PE from Influenza strain A ₀ /PR8/34	1.1	ND	ND	-	-	37.8	46.9 15.4	0.61	Blough, 1971
PS from Influenza strain A ₀ /PR8/34	5.8	1.1	ND	-	-	57.5	22.1 20.4	1.35	Blough, 1971
Influenza strain B/LEE/40 (total PL)	3.0	9.0	ND	-	0.9 ^b	58.0	17.8 23.4	1.41	Blough, 1971
PC from Influenza strain B/LEE/40	ND	tr ^a	ND	-	-	56.9	28.7 14.2	1.33	Blough, 1971
SM from Influenza strain B/LEE/40	ND	11.4	2.1	-	-	86.6	8.2 5.2	6.46	Blough, 1971
PE from Influenza strain B/LEE/40	ND	ND	ND	-	-	28.2	35.8 36.0	0.39	Blough, 1971
PS from Influenza strain B/LEE/40	12.8	1.8	ND	-	-	47.5	27.0 24.1	0.93	Blough, 1971
pL of uninfected CEE	6.5	1.6	-	ND	6.3 ^b	49.2	20.2 24.4	1.10	Tiffany & Blough, 1969
nL of uninfected CEE	3.7	2.8	-	ND	0.5 ^b	37.3	41.4 20.6	0.60	Tiffany & Blough, 1969
pL of Influenza strain A ₀ /PR8/34 from CEE	8.4	6.8	-	tr	0.6 ^b	60.4	21.0 17.8	1.56	Tiffany & Blough, 1969
nL of Influenza strain A ₀ /PR8/34 from CEE	ND	tr	-	ND	ND	61.9	28.6 9.5	1.62	Tiffany & Blough, 1969
pL of Influenza strain A ₂ /Jap/305/57 from CEE	1.1	8.1	-	1.8 ^c	ND	54.0	21.6 24.3	1.18	Tiffany & Blough, 1969
nL of Influenza strain A ₂ /Jap/305/57 from CEE	5.6	1.0	-	ND	3.9 ^b	61.3	13.5 21.4	1.76	Tiffany & Blough, 1969
pL of Influenza strain B/Lee/40 from CEE	ND	9.0	-	ND	3.8 ^b	58.0	17.8 20.4	1.52	Tiffany & Blough, 1969
nL of Influenza strain B/Lee/40 from CEE	ND	0.5	-	ND	1.1 ^b	75.3	10.7 12.9	3.19	Tiffany & Blough, 1969

	Lauric C12:0	Myristic C14:0	C14:1	C15:0	Palmitic C16:0	Palmitoleic C16:1	C16:2	C17:0	Stearic C18:0	Oleic C18:1	Linoleic C18:2	C18:3
<i>Orthomyxoviridae</i>												
Influenza strain A ₀ /PR8/34 from ECE	ND	1.6	-	-	15.1	5.2	-	-	14.8	15.8	4.3	0.9
Influenza strain A ₀ /PR8/34 from ECE	-	0.7	-	-	16.2	6.7	-	-	14.3	13.2	2.8	1.1
Whole CKC	-	0.9	-	0.5 ^d	23.0	1.4	-	1.2 ^e	17.0	21.0	27.0	-
Influenza strain Melbourne from CKC	-	0.7	-	0.9 ^d	23.0	1.3	-	1.6 ^e	21.0	21.0	24.0	-
Whole CEC	-	0.3	-	tr ^d	38.0	1.1	-	tr ^e	10.0	28.0	8.7	-
Influenza strain Melbourne from CEC	-	0.3	-	tr ^d	32.0	1.2	-	tr ^e	13.0	29.0	9.4	-
<i>Paramyxoviridae</i>												
NDV strain Clone-30 from CEC (total PL)	-	-	-	3.5	19.9	1.0	-	3.6	17.5	22	11.7	-
PE of NDV Clone-30 from CEC	-	-	-	1.6	14.2	0.3	-	3.2	16.8	27.6	11.8	-
PC of NDV Clone-30 from CEC	-	-	-	0.8	29.0	0.3	-	0.13	8.0	15.3	12.1	-
PS + PI of NDV Clone-30 from CEC	-	-	-	0.34	12.0	ND	-	0.77	38.1	23.4	10.1	-
pL of NDV strain Milano	1.7	2.6	-	-	17.3	1.6	-	-	16.7	21.1	6.7	tr
nL of NDV strain Milano	3.3	28.2	-	-	13.3	5.6	-	-	9.8	11.2	4.9	1.5
pL of NDV strain Sato-Japan	0.8	3.0	-	-	19.3	1.0	-	-	13.6	15.7	6.0	0.7
nL of NDV strain Sato-Japan	2.4	3.6	-	-	17.6	3.4	-	-	9.5	25.2	10.0	2.9
pL of NDV strain Blacksburg (B1) from ECE	tr	tr	-	-	11.9	tr	-	-	14.6	20.0	6.9	ND
nL of NDV strain Blacksburg (B1) from ECE	2.7	4.1	-	-	28.1	4.6	-	-	22.1	20.4	6.9	0.7

	Arachidic				Arachidonic									
	C20:0	C20:1	C20:2	C20:3	C20:4	C20:5	C21:5	C22:0	C22:1	C22:3	C22:4	C22:5	C22:6	
Influenza strain A ₀ /PR8/34 from ECE	8.4	-	-	-	4.2	-	-	13.7	ND	-	-	-	-	
Influenza strain A ₀ /PR8/34 from ECE	10.0	-	-	-	3.2	-	-	15.5	-	-	-	-	-	
Whole CKC	-	0.9	-	0.3	7.6	-	-	-	-	-	-	-	-	
Influenza strain Melbourne from CKC	-	tr	-	tr	6.2	-	-	-	-	-	-	-	-	
Whole CEC	-	0.6	-	0.9	7.3	-	-	-	-	-	-	-	-	
Influenza strain Melbourne from CEC	-	1.6	-	0.9	5.8	-	-	-	-	-	-	-	-	
NDV strain Clone-30 from CEC (total PL)	1.0	-	-	6.5	-	-	1.3 ^f	-	1.0	-	-	-	5.3	
PE of NDV Clone-30 from CEC	0.6	-	-	7.0	-	-	1.3 ^f	-	0.3	-	-	-	6.3	
PC of NDV Clone-30 from CEC	0.1	-	-	2.1	-	-	2.3 ^f	-	1.1	-	-	-	4.2	
PS + PI of NDV Clone-30 from CEC	1.8	-	-	ND	-	-	ND	-	1.2	-	-	-	2.1	
pL of NDV strain Milano	2.6	ND	-	-	9.7	-	-	3.9	ND	-	-	-	-	
nL of NDV strain Milano	0.8	ND	-	-	2.0	-	-	13.3	ND	-	-	-	-	
pL of NDV strain Sato-Japan	2.6	0.6	-	-	12.2	-	-	7.6	4.1	-	-	-	-	
nL of NDV strain Sato-Japan	1.2	ND	-	-	5.0	-	-	1.7	tr	-	-	-	-	
pL of NDV strain Blacksburg (B1) from ECE	7.0	ND	-	-	ND	-	-	23.8	ND	-	-	-	-	
nL of NDV strain Blacksburg (B1) from ECE	1.3	ND	-	-	5.9	-	-	ND	tr	-	-	-	-	

	C22 polyene	Lignoceric C24:0	C24:1	C24:4	other	saturated	unsaturated mono poly	saturated/ unsaturated	Reference
Influenza strain A ₀ /PR8/34 from ECE	8.4	6.8	ND	-	0.6	60.4	21.0 17.8	1.56	Blough & Tiffany, 1968
Influenza strain A ₀ /PR8/34 from ECE	8.9	7.3	-	-	-	64.0	19.9 16.0	1.78	Blough & Weinstein, 1967
Whole CKC	-	-	-	-	-	43.5	22.4 34.9	0.76	Kates <i>et al.</i> , 1961
Influenza strain Melbourne from CKC	-	-	-	-	-	47.2	22.3 30.2	0.90	Kates <i>et al.</i> , 1961
Whole CEC	4.7	-	-	-	-	48.9	29.1 21.6	0.96	Kates <i>et al.</i> , 1961
Influenza strain Melbourne from CEC	7.5	-	-	-	-	46.9	30.2 23.6	0.87	Kates <i>et al.</i> , 1961
NDV strain Clone-30 from CEC (total PL)	-	-	-	-	-	45.5	24.0 24.8	0.93	Muñoz-Barroso <i>et al.</i> , 1997
PE of NDV Clone-30 from CEC	-	-	-	-	-	36.4	28.2 26.4	0.67	Muñoz-Barroso <i>et al.</i> , 1997
PC of NDV Clone-30 from CEC	-	-	-	-	-	38.0	16.7 20.7	1.02	Muñoz-Barroso <i>et al.</i> , 1997
PS + PI of NDV Clone-30 from CEC	-	-	-	-	-	53.0	24.6 12.2	1.44	Muñoz-Barroso <i>et al.</i> , 1997
pL of NDV strain Milano	9.3	2.9	-	2.2	1.8	47.7	22.7 27.9	0.94	Tiffany & Blough, 1969
nL of NDV strain Milano	1.1	2.9	-	1.2	1.3	71.6	16.8 10.7	2.60	Tiffany & Blough, 1969
pL of NDV strain Sato-Japan	8.6	2.9	-	ND	1.6	49.8	21.4 27.5	1.02	Tiffany & Blough, 1969
nL of NDV strain Sato-Japan	8.8	6.9	-	ND	2.0	42.9	28.6 26.7	0.78	Tiffany & Blough, 1968
pL of NDV strain Blacksburg (B1) from ECE	6.5	9.3	-	ND	-	66.6	20.0 13.4	1.99	Tiffany & Blough, 1968
nL of NDV strain Blacksburg (B1) from ECE	ND	2.1	-	tr	tr	60.4	25.0 13.5	1.57	Tiffany & Blough, 1968

	Lauric C12:0	Myristic C14:0	C14:1	C15:0	Palmitic C16:0	Palmitoleic C16:1	C16:2	C17:0	Stearic C18:0	Oleic C18:1	Linoleic C18:2	C18:3
<i>Paramyxoviridae</i>												
BHK21-F cell PM	-	0.5	-	-	21	2.0	-	-	22.2	40.7	11.2	ND
SV5 strain W3 from BHK21-F	-	ND	-	-	26.2	3.3	-	-	17.4	38.0	4.7	ND
MK cell PM	-	1.3	-	-	20.3	5.0	-	-	21.7	33.8	11.1	ND
SV5 strain W3 from MK	-	1.0	-	-	20.0	4.4	-	-	22.6	46.3	2.7	ND
Whole adult HaK cells	-	1.2	-	-	18.9	3.8	-	-	17.6	43.5	11.6	ND
Adult HaK cell PM	-	0.5	-	-	24.2	2.5	-	-	21.2	31.9	16.9	ND
SV5 strain W3 from adult HaK	-	3.5	-	-	28.5	4.1	-	-	16.2	33.9	6.2	ND
Whole MDBK cells	-	2.5	-	-	14.8	3.8	-	-	11.6	41.7	3.1	1.5
MDBK cell PM	-	1.5	-	-	17.0	4.1	-	-	15.3	47.7	2.5	1.5
SV5 strain W3 from MDBK	-	1.5	-	-	17.8	3.3	-	-	11.6	35.5	1.5	2.6
Whole MK cells (total PL)	-	1.9	-	-	15	8.1	-	-	15.7	40.0	9.0	-
PC from whole MK	-	1.5	-	-	19.5	9.5	-	-	12.7	42.5	8.0	-
PE from whole MK	-	ND	-	-	7.4	3.5	-	-	28.1	46.3	5.1	-
MK cell PM (total PL)	-	1.3	-	-	20.3	5.0	-	-	21.7	33.8	11.1	-
SV5 strain W3 from MK (total PL)	-	1.0	-	-	20.0	4.4	-	-	22.6	46.3	2.7	-
PC of SV5 strain W3 from MK	-	1.5	-	-	29.1	7.6	-	-	14.4	40.5	2.1	-
PE of SV5 strain W3 from MK	-	1.1	-	-	17.3	3.5	-	-	20.6	56.0	1.5	-
BHK21-F cells (total PL)	-	1.5	-	-	21.9	4.6	-	-	14.5	50.0	7.5	-
PC from whole BHK21-F	-	0.5	-	-	20.1	4.4	-	-	13.9	51.3	8.1	-
PE from whole BHK21-F	-	0.8	-	-	19.4	6.3	-	-	20.9	44.2	5.4	-
BHK21-F cell PM (total PL)	-	0.5	-	-	21.0	2.0	-	-	22.2	40.7	11.2	-
SV5 strain W3 from BHK21-F (total PL)	-	-	-	-	26.2	3.3	-	-	17.4	38.0	4.7	-
Whole adult HaK cells (total PL)	-	1.2	-	-	18.9	3.8	-	-	17.6	43.5	11.6	-
Adult HaK cell PM (total PL)	-	0.5	-	-	24.2	2.5	-	-	21.1	31.9	16.9	-

	Arachidic				Arachidonic									
	C20:0	C20:1	C20:2	C20:3	C20:4	C20:5	C21:5	C22:0	C22:1	C22:3	C22:4	C22:5	C22:6	
BHK21-F cell PM	ND	-	-	-	2.4	-	-	-	-	-	-	-	-	
SV5 strain W3 from BHK21-F	ND	-	-	-	10.2	-	-	-	-	-	-	-	-	
MK cell PM	ND	-	-	-	6.8	-	-	-	-	-	-	-	-	
SV5 strain W3 from MK	ND	-	-	-	5.6	-	-	-	-	-	-	-	-	
Whole adult HaK cells	ND	-	-	-	3.4	-	-	-	-	-	-	-	-	
Adult HaK cell PM	ND	-	-	-	2.9	-	-	-	-	-	-	-	-	
SV5 strain W3 from adult HaK	ND	-	-	-	11.4	-	-	-	-	-	-	-	-	
Whole MDBK cells	6.1	-	-	-	7.8	-	-	-	-	-	-	-	-	
MDBK cell PM	3.9	-	-	-	3.1	-	-	-	-	-	-	-	-	
SV5 strain W3 from MDBK	10.5	-	-	-	6.7	-	-	-	-	-	-	-	-	
Whole MK cells (total PL)	-	-	-	-	10.3	-	-	-	-	-	-	-	-	
PC from whole MK	-	-	-	-	6.3	-	-	-	-	-	-	-	-	
PE from whole MK	-	-	-	-	9.6	-	-	-	-	-	-	-	-	
MK cell PM (total PL)	-	-	-	-	6.8	-	-	-	-	-	-	-	-	
SV5 strain W3 from MK (total PL)	-	-	-	-	5.6	-	-	-	-	-	-	-	-	
PC of SV5 strain W3 from MK	-	-	-	-	4.8	-	-	-	-	-	-	-	-	
PE of SV5 strain W3 from MK	-	-	-	-	-	-	-	-	-	-	-	-	-	
BHK21-F cells (total PL)	-	-	-	-	ND	-	-	-	-	-	-	-	-	
PC from whole BHK21-F	-	-	-	-	2.8	-	-	-	-	-	-	-	-	
PE from whole BHK21-F	-	-	-	-	3.0	-	-	-	-	-	-	-	-	
BHK21-F cell PM (total PL)	-	-	-	-	2.4	-	-	-	-	-	-	-	-	
SV5 strain W3 from BHK21-F (total PL)	-	-	-	-	10.2	-	-	-	-	-	-	-	-	
Whole adult HaK cells (total PL)	-	-	-	-	3.4	-	-	-	-	-	-	-	-	
Adult HaK cell PM (total PL)	-	-	-	-	2.9	-	-	-	-	-	-	-	-	

	Lignoceric					saturated	unsaturated	saturated/ unsaturated	Reference	
	C22 polyene	C24:0	C24:1	C24:4	other					mono
BHK21-F cell PM	-	-	-	-	-	43.7	42.7	14.9	0.76	Klenk & Choppin, 1970
SV5 strain W3 from BHK21-F	-	-	-	-	-	43.6	41.3	14.9	0.78	Klenk & Choppin, 1970
MK cell PM	-	-	-	-	-	43.3	38.8	17.9	0.76	Klenk & Choppin, 1970
SV5 strain W3 from MK	-	-	-	-	-	43.6	50.7	8.3	0.74	Klenk & Choppin, 1970
Whole adult HaK cells	-	-	-	-	-	37.7	47.3	15.0	0.60	Klenk & Choppin, 1970
Adult HaK cell PM	-	-	-	-	-	45.9	34.4	19.8	0.85	Klenk & Choppin, 1970
SV5 strain W3 from adult HaK	-	-	-	-	-	48.2	38.0	17.6	0.87	Klenk & Choppin, 1970
Whole MDBK cells	-	-	-	-	5.9 ^g	35.0	45.5	18.3	0.55	Klenk & Choppin, 1970
MDBK cell PM	-	-	-	-	2.1 ^g	37.7	51.8	9.2	0.62	Klenk & Choppin, 1970
SV5 strain W3 from MDBK	-	-	-	-	5.4 ^g	41.4	38.8	16.2	0.75	Klenk & Choppin, 1970
Whole MK cells (total PL)	-	-	-	-	-	32.6	48.1	19.3	0.48	Klenk & Choppin, 1969
PC from whole MK	-	-	-	-	-	33.7	52.0	14.3	0.51	Klenk & Choppin, 1969
PE from whole MK	-	-	-	-	-	35.5	49.8	14.7	0.55	Klenk & Choppin, 1969
MK cell PM (total PL)	-	-	-	-	-	43.3	38.8	17.9	0.76	Klenk & Choppin, 1969
SV5 strain W3 from MK (total PL)	-	-	-	-	-	43.6	50.7	8.3	0.74	Klenk & Choppin, 1969
PC of SV5 strain W3 from MK	-	-	-	-	-	45.0	48.1	6.9	0.82	Klenk & Choppin, 1969
PE of SV5 strain W3 from MK	-	-	-	-	-	39.0	59.5	1.5	0.64	Klenk & Choppin, 1969
BHK21-F cells (total PL)	-	-	-	-	-	37.9	54.6	7.5	0.61	Klenk & Choppin, 1969
PC from whole BHK21-F	-	-	-	-	-	34.5	55.7	10.9	0.52	Klenk & Choppin, 1969
PE from whole BHK21-F	-	-	-	-	-	41.1	50.5	8.4	0.70	Klenk & Choppin, 1969
BHK21-F cell PM (total PL)	-	-	-	-	-	43.7	42.7	13.6	0.78	Klenk & Choppin, 1969
SV5 strain W3 from BHK21-F (total PL)	-	-	-	-	-	43.6	41.3	14.9	0.78	Klenk & Choppin, 1969
Whole adult HaK cells (total PL)	-	-	-	-	-	37.7	47.3	15.0	0.60	Klenk & Choppin, 1969
Adult HaK cell PM (total PL)	-	-	-	-	-	45.8	34.4	19.8	0.84	Klenk & Choppin, 1969

	Lauric C12:0	Myristic C14:0	C14:1	C15:0	Palmitic C16:0	Palmitoleic C16:1	C16:2	C17:0	Stearic C18:0	Oleic C18:1	Linoleic C18:2	C18:3
<i>Paramyxoviridae</i>												
Uninfected allantoic fluid from ECE	tr ^a	0.8 ^h	-	tr	27.0 ⁱ	-	-	1.4	18.4	28.1	13.8	tr ^a
Sendai virus strain Cantel from ECE (total PL)	tr ^a	4.5 ^h	tr ^a	tr	22.3 ⁱ	1.0	-	0.5	15.4	22.8	7.7	tr ^a
CL of Sendai virus strain Cantel from ECE	tr ^a	2.2 ^h	tr ^a	0.5	28.9 ⁱ	1.3	-	3.9	15.5	6.4	1.7	1.0
PI of Sendai virus strain Cantel from ECE	tr ^a	1.3 ^h	tr ^a	1.8	21.5 ⁱ	1.4	-	1.8	8.7	2.7	0.7	tr ^a
PS of Sendai virus strain Cantel from ECE	tr ^a	0.7 ^h	tr ^a	1.0	18.8 ⁱ	1.0	-	0.6	24.7	19.4	4.1	tr ^a
PE of Sendai virus strain Cantel from ECE	tr ^a	0.8 ^h	tr ^a	0.9	20.5 ⁱ	0.6	-	0.5	21.9	21.7	5.5	ND
PC of Sendai virus strain Cantel from ECE	tr ^a	1.4 ^h	tr ^a	1.3	27.0 ⁱ	4.7	-	0.6	12.9	18.9	5.3	tr ^a
SM of Sendai virus strain Cantel from ECE	tr ^a	1.9 ^h	tr ^a	2.2	28.3 ⁱ	1.4	-	1.0	13.9	7.0	1.6	tr ^a
Sendai virus strain murine from ECE	tr	tr	-	-	24.2	1.0	-	-	12.7	22.3	10.5	-
<i>Rhabdoviridae</i>												
VSV from LM-K cells	-	4.48	-	-	19.8	6.08	-	-	20.39	10.06	35.48	-
VSV serotype Indiana from BHK-21 cells	-	1.6	-	-	15.0	5.1	-	ND	14.1	44.5	5.1	ND
VSV (total PL)	tr	1.4	0.3	-	20.0	4.5	0.5	0.6	17.8	39.7	2.0	1.9
PE from VSV	0.4 ^j	3.4 ^j	5.2 ^j	-	10.1 ^j	4.0 ^j	3.4 ^j	3.0 ^j	14.9 ^j	35.6 ^j	1.5	2.2
PE from inner leaflet (65.5% of total)	0.2	1.8	5.5	-	8.9	3.6	3.9	1.1	15.9	36.9	1.5	2.5
PE from outer leaflet (34.5% of total)	0.7	6.3	4.5	-	12.6	4.6	2.5	6.5	12.9	33	1.6	1.5
PC from VSV	tr	1.5	0.6	-	27.9	8.3	0.6	1.7	11.2	40.2	1.1	2.6
SM from VSV	tr	1.8	0.6	-	10.8	3.5	tr	2.1	31	37.7	0.8	1.1

	Arachidic				Arachidonic								
	C20:0	C20:1	C20:2	C20:3	C20:4	C20:5	C21:5	C22:0	C22:1	C22:3	C22:4	C22:5	C22:6
Uninfected allantoic fluid from ECE	tr ^a	tr ^a	-	0.5	4.6	tr ^a	-	tr ^a	-	-	-	tr ^a	1.69
Sendai virus strain Cantel from ECE (total PL)	0.5	0.9	tr ^a	tr ^a	9.9	tr ^a	-	1.6	tr	-	1.9	1.0	0.5
CL of Sendai virus strain Cantel from ECE	tr ^a	0.9	0.9	tr ^a	7.3	1.5	-	tr ^a	ND	-	1.3	0.5	tr ^a
PI of Sendai virus strain Cantel from ECE	1.2	1.0	ND	24.0	4.6	tr ^a	-	2.8	0.5	-	2.1	tr ^a	1.3
PS of Sendai virus strain Cantel from ECE	1.8	2.7	tr ^a	tr ^a	2.2	tr ^a	-	tr ^a	0.7	-	tr ^a	tr ^a	1.1
PE of Sendai virus strain Cantel from ECE	0.7	0.6	tr ^a	tr ^a	6.2	ND	-	tr ^a	tr ^a	-	1.2	0.8	1.2
PC of Sendai virus strain Cantel from ECE	tr ^a	1.5	tr ^a	tr ^a	6.1	tr	-	tr ^a	tr ^a	-	1.4	1.4	3.9
SM of Sendai virus strain Cantel from ECE	0.7	2.1	ND	0.5	1.1	0.5	-	1.1	tr ^a	-	0.6	tr ^a	tr ^a
Sendai virus strain murine from ECE	3.9	-	-	-	12.2	-	-	8.0	-	-	-	-	ND
<i>Rhabdoviridae</i>													
VSV from LM-K cells	-	-	-	-	2.76	-	-	-	-	-	-	-	-
VSV serotype Indiana from BHK-21 cells	-	2.9	ND	0.5	2.2	ND	-	-	-	-	ND	0.5	0.3
VSV (total PL)	0.3	-	-	-	-	-	-	1.6	-	-	-	-	-
PE from VSV	0.2 ^j	-	-	-	-	-	-	1.0 ^j	-	-	-	-	-
PE from inner leaflet (65.5% of total)	0.2	-	-	-	-	-	-	1.1	-	-	-	-	-
PE from outer leaflet (34.5% of total)	0.1	-	-	-	-	-	-	0.9	-	-	-	-	-
PC from VSV	tr	-	-	-	-	-	-	0.2	-	-	-	-	-
SM from VSV	tr	-	-	-	-	-	-	0.7	-	-	-	-	-

		Lignoceric					saturated	unsaturated	saturated/	Reference
	C22 polyene	C24:0	C24:1	C24:4	other		mono	poly	unsaturated	
Uninfected allantoic fluid from ECE	-	tr ^a	0.6	ND	-	47.6	29.7	20.6	0.95	Barnes <i>et al.</i> , 1987
Sendai virus strain Cantel from ECE (total PL)	-	6.0	tr ^a	3.6	-	50.8	24.7	24.7	1.03	Barnes <i>et al.</i> , 1987
CL of Sendai virus strain Cantel from ECE	-	9.3	1.8	3.6	-	60.3	10.5	17.9	2.12	Barnes <i>et al.</i> , 1987
PI of Sendai virus strain Cantel from ECE	-	11.0	tr ^a	5.4	0.9 ^k	51.0	5.6	38.0	1.17	Barnes <i>et al.</i> , 1987
PS of Sendai virus strain Cantel from ECE	-	11.0	tr ^a	3.8	tr ^{a,k}	58.6	23.8	11.2	1.67	Barnes <i>et al.</i> , 1987
PE of Sendai virus strain Cantel from ECE	-	7.3	0.6	3.5	0.5 ^k	53.0	23.5	18.5	1.26	Barnes <i>et al.</i> , 1987
PC of Sendai virus strain Cantel from ECE	-	4.6	tr ^a	2.7	0.5 ^k	48.4	25.1	20.9	1.05	Barnes <i>et al.</i> , 1987
SM of Sendai virus strain Cantel from ECE	-	17.4	1.5	9.7	-	65.3	12.0	14.0	2.51	Barnes <i>et al.</i> , 1987
Sendai virus strain murine from ECE	-	5.1	-	-	-	53.9	23.3	22.7	1.17	Blough & Lawson, 1968
<i>Rhabdoviridae</i>										
VSV from LM-K cells	-	-	-	0.95	-	44.7	16.1	39.2	0.81	Anderson <i>et al.</i> , 1987
VSV serotype Indiana from BHK-21 cells	p.e.	-	0.5	-	6.2 ^l	31.1	58.8	8.6	0.46	Pal <i>et al.</i> , 1980
VSV (total PL)	9.6 ^m	-	-	-	-	41.7	44.5	14.0	0.71	Fong & Brown, 1978
PE from VSV	14.8 ^{j,m}	-	-	-	-	33.0	44.8	21.9	0.49	Fong & Brown, 1978
PE from inner leaflet (65.5% of total)	16.7 ^m	-	-	-	-	29.2	46.0	24.6	0.41	Fong & Brown, 1978
PE from outer leaflet (34.5% of total)	12.3 ^m	-	-	-	-	40.0	42.1	17.9	0.67	Fong & Brown, 1978
PC from VSV	4.2 ^m	-	-	-	-	42.5	49.1	8.5	0.74	Fong & Brown, 1978
SM from VSV	10.1 ^m	-	-	-	-	46.4	41.8	12.0	0.86	Fong & Brown, 1978

	Lauric C12:0	Myristic C14:0	C14:1	C15:0	Palmitic C16:0	Palmitoleic C16:1	C16:2	C17:0	Stearic C18:0	Oleic C18:1	Linoleic C18:2	C18:3
<i>Rhabdoviridae</i>												
VSV strain Indiana (total PL)	-	ND	-	-	24.9	10.2	-	-	16.8	37.7	1.1	4.3
PE of VSV strain Indiana PE	-	0.5	-	-	11.9	10.7	-	-	5.0	55.8	1.1	1.2
PS + PI of VSV strain Indiana PS + PI	-	0.4	-	-	6.1	8.4	-	-	27.9	43.8	1.2	1.0
PC of VSV strain Indiana PC	-	1.7	-	-	29.2	14.0	-	-	5.3	46.6	1.0	1.8
SM of VSV strain Indiana SM	-	ND	-	-	75.9	0.7	-	-	4.7	7.0	ND	ND
Whole CEC	ND	1.5	-	-	26.7	4.5	-	-	21.0	23.0	11.8	-
CEC PM	4.2	1.9	-	-	23.0	3.7	-	-	22.0	22.8	11.7	-
VSV Indiana serotype from CEC	ND	2.1	-	-	22.2	3.8	-	-	30.3	21.3	7.8	-
Whole BHK21	tr	1.2	-	-	15.8	6.2	-	-	16.7	48.7	2.5	-
BHK21 cell PM	6.5	3.2	-	-	25.8	5.0	-	-	19.0	34.5	1.9	-
VSV Indiana serotype from BHK21	tr	8.4	-	-	26.2	7.0	-	-	17.8	33.2	2.7	-
Whole L-cells	-	tr ⁿ	-	-	13.3	tr ⁿ	-	-	19.6	44.5	2.3	-
L-cell PM	-	tr ⁿ	-	-	15.0	tr ⁿ	-	-	29.4	38.9	2.4	-
VSV strain Indiana from L-cells	-	tr ⁿ	-	-	23.6	2.3	-	-	25.0	29.6	8.2	-
VSV strain New Jersey from L-cells	-	tr ⁿ	-	-	19.3	tr ⁿ	-	-	24.0	38.7	2.5	-
Whole CEC	-	tr ⁿ	-	-	21.1	tr ⁿ	-	-	22.4	25.4	5.3	-
CEC PM	-	tr ⁿ	-	-	19.4	tr ⁿ	-	-	21.9	32.2	3.9	-
VSV strain Indiana from CEC	-	tr ⁿ	-	-	21.6	2.7	-	-	22.9	18.1	2.3	-
PM from BHK21 cells	0.8	1.5	-	-	8.5	4.4	-	-	14.2	39.9	7.6	tr ^o
Rabies virus strain HEP from BHK21	0.3	1.2	-	-	20.3	3.2	-	-	20.1	35.6	1.4	ND
Uninfected Nil2 fibroblasts	-	-	-	-	12.0	4.0	-	-	18.0	43.0	17.0	-
Rabies from Nil2	-	-	-	-	20.0	ND	-	-	22.0	25.0	5.0	-

	Arachidic				Arachidonic								
	C20:0	C20:1	C20:2	C20:3	C20:4	C20:5	C21:5	C22:0	C22:1	C22:3	C22:4	C22:5	C22:6
VSV strain Indiana (total PL)	-	-	-	-	2.3	-	-	-	-	-	-	4.4	4.4
PE of VSV strain Indiana PE	-	-	-	-	4.1	-	-	1.2	-	-	-	3.3	2.9
PS + PI of VSV strain Indiana PS + PI	-	-	-	-	1.3	-	-	1.0	-	-	-	2.7	1.9
PC of VSV strain Indiana PC	-	-	-	-	ND	-	-	ND	-	-	-	ND	ND
SM of VSV strain Indiana SM	-	-	-	-	ND	-	-	1.8	-	-	-	ND	ND
Whole CEC	-	-	-	-	11.2	-	-	-	-	-	-	-	-
CEC PM	-	-	-	-	10.5	-	-	-	-	-	-	-	-
VSV Indiana serotype from CEC	-	-	-	-	12.6	-	-	-	-	-	-	-	-
Whole BHK21	-	-	-	-	8.6	-	-	-	-	-	-	-	-
BHK21 cell PM	-	-	-	-	4.8	-	-	-	-	-	-	-	-
VSV Indiana serotype from BHK21	-	-	-	-	4.5	-	-	-	-	-	-	-	-
Whole L-cells	tr ⁿ	-	-	-	6.4	-	-	tr ⁿ	-	-	-	-	-
L-cell PM	tr ⁿ	-	-	-	4.3	-	-	tr ⁿ	-	-	-	-	-
VSV strain Indiana from L-cells	tr ⁿ	-	-	-	5.4	-	-	tr ⁿ	-	-	-	-	-
VSVstrain New Jersey from L-cells	-	-	-	-	5.5	-	-	-	-	-	-	-	-
Whole CEC	-	-	-	-	11.6	-	-	-	-	-	-	-	-
CEC PM	-	-	-	-	8.4	-	-	-	-	-	-	-	-
VSV strain Indiana from CEC	tr ⁿ	-	-	-	12.4	-	-	tr ⁿ	-	-	-	-	-
PM from BHK21 cells	ND	0.4	-	-	13.1	-	-	0.7	ND	3.7	1.4	0.5	0.6
Rabies virus strain HEP from BHK21	ND	0.7	-	-	7.4	-	-	ND	ND	ND	ND	2.8	2.6
Uninfected Nil2 fibroblasts	ND	-	-	1.0	2.0	-	-	-	-	-	-	-	-
Rabies from Nil2	ND	-	-	6.0	16.0	-	-	-	-	-	-	-	-

		Lignoceric				other	saturated	unsaturated	saturated/ unsaturated	Reference
		C22 polyene	C24:0	C24:1	C24:4					
VSV strain Indiana (total PL)	-	0.5	2.3	-	-	42.2	50.2	16.5	0.63	Patzer <i>et al.</i> , 1978
PE of VSV strain Indiana PE	-	ND	ND	-	-	18.6	66.5	12.6	0.23	Patzer <i>et al.</i> , 1978
PS + PI of VSV strain Indiana PS + PI	-	ND	1.0	-	-	35.4	53.2	8.1	0.58	Patzer <i>et al.</i> , 1978
PC of VSV strain Indiana PC	-	ND	ND	-	-	36.2	60.6	2.8	0.57	Patzer <i>et al.</i> , 1978
SM of VSV strain Indiana SM	-	1.3	7.0	-	-	83.7	14.7	ND	5.69	Patzer <i>et al.</i> , 1978
Whole CEC	-	-	-	-	-	49.2	27.5	23.0	0.97	David, 1971
CEC PM	-	-	-	-	-	51.1	26.5	22.2	1.05	David, 1971
VSV Indiana serotype from CEC	-	-	-	-	-	54.6	25.1	20.4	1.20	David, 1971
Whole BHK21	-	-	-	-	-	33.7	54.9	11.1	0.51	David, 1971
BHK21 cell PM	-	-	-	-	-	54.5	39.5	6.7	1.18	David, 1971
VSV Indiana serotype from BHK21	-	-	-	-	-	52.4	40.2	7.2	1.10	David, 1971
Whole L-cells	-	tr ⁿ	-	-	-	32.9	44.5	8.7	0.62	McSharry & Wagner, 1971
L-cell PM	-	tr ⁿ	-	-	-	44.4	38.9	6.7	0.97	McSharry & Wagner, 1971
VSV strain Indiana from L-cells	-	tr ⁿ	-	-	-	48.6	31.9	13.6	1.07	McSharry & Wagner, 1971
VSVstrain New Jersey from L-cells	-	2.9	-	-	-	46.2	38.7	8.0	0.99	McSharry & Wagner, 1971
Whole CEC	-	3.0	-	-	-	46.5	25.4	16.9	1.10	McSharry & Wagner, 1971
CEC PM	-	tr ⁿ	-	-	-	41.3	32.2	12.3	0.93	McSharry & Wagner, 1971
VSV strain Indiana from CEC	-	5.0	-	-	-	49.5	20.8	14.7	1.39	McSharry & Wagner, 1971
PM from BHK21 cells	-	2.8	ND	-	ND	28.5	44.7	26.9	0.40	Blough <i>et al.</i> , 1977
Rabies virus strain HEP from BHK21	-	ND	1.9	-	2.4	41.9	41.4	14.2	0.75	Blough <i>et al.</i> , 1977
Uninfected Nil2 fibroblasts	-	-	-	-	-	30.0	47.0	20.0	0.45	Portoukalian <i>et al.</i> , 1977
Rabies from Nil2	-	-	-	-	-	42.0	25.0	27.0	0.81	Portoukalian <i>et al.</i> , 1977

	Lauric C12:0	Myristic C14:0	C14:1	C15:0	Palmitic C16:0	Palmitoleic C16:1	C16:2	C17:0	Stearic C18:0	Oleic C18:1	Linoleic C18:2	C18:3
<i>Togaviridae</i>												
PC from whole BHK21 cells	-	-	-	-	22.0	9.0	-	-	6.8	46.0	12.0	-
PS from whole BHK21 cells	-	-	-	-	5.6	2.4	-	-	31.0	44.0	10.0	-
PI from whole BHK21 cells	-	-	-	-	8.7	2.8	-	-	37.0	20.0	3.7	-
PE from whole BHK21 cells	-	-	-	-	4.6	3.0	-	-	15.0	41.0	12.0	-
PC from BHK21 cell PM	-	-	-	-	31.0	6.4	-	-	7.9	45.0	5.6	-
PS from BHK21 cell PM	-	-	-	-	4.4	2.8	-	-	29.0	53.0	5.5	-
PI from BHK21 cell PM	-	-	-	-	6.7	2.3	-	-	38.0	30.0	2.9	-
PE from BHK21 cell PM	-	-	-	-	5.1	2.4	-	-	8.3	50.0	8.3	-
SM from BHK21 cell PM	-	-	-	-	69.0	tr	-	-	tr	tr	-	-
PC of SFV from BHK21	-	-	-	-	38.0	6.3	-	-	8.7	38.0	5.7	-
PS of SFV from BHK21	-	-	-	-	5.3	4.1	-	-	34.0	46.0	7.0	-
PI of SFV from BHK21	-	-	-	-	7.9	3.0	-	-	42.0	16.0	4.2	-
PE of SFV from BHK21	-	-	-	-	4.3	1.6	-	-	5.2	43.0	10.0	-
SM of SFV from BHK21	-	-	-	-	74.0	1.6	-	-	0.7	tr	-	-
Whole BHK21 Clone Wi2	-	-	-	-	21.0	-	-	-	8.0	48.0	12.0	-
BHK21-Wi2 PM	-	-	-	-	26.0	-	-	-	12.0	46.0	9.0	-
SFV from BHK21-Wi2	-	-	-	-	23.0	-	-	-	15.0	42.0	8.0	-
Whole CEC	ND	1.5	-	-	26.7	4.5	-	-	21.0	23.0	11.8	-
CEC PM	4.2	1.9	-	-	23.0	3.7	-	-	22.0	22.8	11.7	-
Sindbis from CEC	9.3 ^p	4.4	-	-	30.0	6.8	-	-	21.4	22.0	1.0	-
Whole BHK21 cells	tr	1.2	-	-	15.8	6.2	-	-	16.7	48.7	2.5	-
BHK21 cell PM	6.5	3.2	-	-	25.8	5.0	-	-	19.0	34.5	1.9	-
Sindbis from BHK21	3.1	6.6	-	-	26.5	5.3	-	-	20.2	32.4	1.9	-

	Arachidic				Arachidonic								
	C20:0	C20:1	C20:2	C20:3	C20:4	C20:5	C21:5	C22:0	C22:1	C22:3	C22:4	C22:5	C22:6
PC from whole BHK21 cells	-	-	-	-	-	-	-	-	-	-	-	-	-
PS from whole BHK21 cells	-	-	-	-	-	-	-	-	-	-	-	-	-
PI from whole BHK21 cells	-	-	-	-	-	-	-	-	-	-	-	-	-
PE from whole BHK21 cells	-	-	-	-	-	-	-	-	-	-	-	-	-
PC from BHK21 cell PM	-	-	-	-	-	-	-	-	-	-	-	-	-
PS from BHK21 cell PM	-	-	-	-	-	-	-	-	-	-	-	-	-
PI from BHK21 cell PM	-	-	-	-	-	-	-	-	-	-	-	-	-
PE from BHK21 cell PM	-	-	-	-	-	-	-	-	-	-	-	-	-
SM from BHK21 cell PM	-	-	-	-	-	-	-	9.7	-	-	-	-	-
PC of SFV from BHK21	-	-	-	-	-	-	-	-	-	-	-	-	-
PS of SFV from BHK21	-	-	-	-	-	-	-	-	-	-	-	-	-
PI of SFV from BHK21	-	-	-	-	-	-	-	-	-	-	-	-	-
PE of SFV from BHK21	-	-	-	-	-	-	-	-	-	-	-	-	-
SM of SFV from BHK21	-	-	-	-	-	-	-	3.7	-	-	-	-	-
Whole BHK21 Clone Wi2	-	2.0	-	-	-	-	-	-	-	-	-	-	-
BHK21-Wi2 PM	-	2.0	-	-	-	-	-	-	-	-	-	-	-
SFV from BHK21-Wi2	-	2.0	-	-	-	-	-	-	-	-	-	-	-
Whole CEC	-	-	-	-	11.2	-	-	-	-	-	-	-	-
CEC PM	-	-	-	-	10.5	-	-	-	-	-	-	-	-
Sindbis from CEC	-	-	-	-	2.4	-	-	-	-	-	-	-	-
Whole BHK21 cells	-	-	-	-	8.6	-	-	-	-	-	-	-	-
BHK21 PM	-	-	-	-	4.8	-	-	-	-	-	-	-	-
Sindbis from BHK21	-	-	-	-	3.4	-	-	-	-	-	-	-	-

	C22 polyene	Lignoceric C24:0	C24:1	C24:4	other	saturated	unsaturated mono poly	saturated/ unsaturated	Reference
PC from whole BHK21 cells	-	-	-	-	0.9	28.8	55.0 12.9	0.42	Laine <i>et al.</i> , 1972
PS from whole BHK21 cells	-	-	-	-	4.9	36.6	46.4 14.9	0.60	Laine <i>et al.</i> , 1972
PI from whole BHK21 cells	-	-	-	-	25.0	45.7	22.8 28.7	0.89	Laine <i>et al.</i> , 1972
PE from whole BHK21 cells	-	-	-	-	14.0	19.6	44.0 26.0	0.28	Laine <i>et al.</i> , 1972
PC from BHK21 cell PM	-	-	-	-	1.8	38.9	51.4 7.4	0.66	Laine <i>et al.</i> , 1972
PS from BHK21 cell PM	-	-	-	-	3.6	33.4	55.8 9.1	0.51	Laine <i>et al.</i> , 1972
PI from BHK21 cell PM	-	-	-	-	18	44.7	32.3 20.9	0.84	Laine <i>et al.</i> , 1972
PE from BHK21 cell PM	-	-	-	-	11.0	13.4	54.4 19.3	0.18	Laine <i>et al.</i> , 1972
SM from BHK21 cell PM	-	tr	22.0	-	-	83.9	15.6 ND	5.38	Laine <i>et al.</i> , 1972
PC of SFV from BHK21	-	-	-	-	1.2	46.7	44.3 6.9	0.91	Laine <i>et al.</i> , 1972
PS of SFV from BHK21	-	-	-	-	2.5	39.3	50.1 9.5	0.66	Laine <i>et al.</i> , 1972
PI of SFV from BHK21	-	-	-	-	27.0	49.9	19.0 31.2	0.99	Laine <i>et al.</i> , 1972
PE of SFV from BHK21	-	-	-	-	23.0	9.5	44.6 33.0	0.12	Laine <i>et al.</i> , 1972
SM of SFV from BHK21	-	5.5	14.0	-	-	78.7	22.0 ND	3.58	Laine <i>et al.</i> , 1972
Whole BHK21 Clone Wi2	-	-	-	-	tr	29.0	50.0 12.0	0.47	Renkonen <i>et al.</i> , 1971
BHK21-Wi2 PM	-	-	-	-	tr	38.0	48.0 9.0	0.67	Renkonen <i>et al.</i> , 1971
SFV from BHK21-Wi2	-	-	-	-	tr	38.0	44.0 8.0	0.73	Renkonen <i>et al.</i> , 1971
Whole CEC	-	-	-	-	-	49.2	27.5 23.0	0.97	David, 1971
CEC PM	-	-	-	-	-	51.1	26.5 22.2	1.05	David, 1971
Sindbis from CEC	-	-	-	-	-	65.1	28.8 3.4	2.02	David, 1971
Whole BHK21 cells	-	-	-	-	-	33.7	54.9 11.1	0.51	David, 1971
BHK21 PM	-	-	-	-	-	54.5	39.5 6.7	1.18	David, 1971
Sindbis from BHK21	-	-	-	-	-	56.4	37.7 5.3	1.31	David, 1971

	Lauric C12:0	Myristic C14:0	C14:1	C15:0	Palmitic C16:0	Palmitoleic C16:1	C16:2	C17:0	Stearic C18:0	Oleic C18:1	Linoleic C18:2	C18:3
<i>Togaviridae</i>												
Uninfected whole BHK21/13S cells	0.8	1.4	-	tr	21.7	2.5	-	2.1	19.6	35.0	14.0	-
Rubella virus from BHK21/13S	0.5	3.0	-	9.9	26.4	2.4	-	7.0	14.5	15.9	6.6	-
<i>Retroviridae</i>												
PM of RSV (strain Schmidt-Ruppin)-infected CEF	-	-	-	p.e.	21.8	7.4	-	p.e.	17.7	32.6	2.7	p.e.
RSV strain Schmidt-Ruppin from CEF	-	-	-	p.e.	17.3	5.8	-	p.e.	17.3	29.3	2.3	p.e.

	Arachidic				Arachidonic								
	C20:0	C20:1	C20:2	C20:3	C20:4	C20:5	C21:5	C22:0	C22:1	C22:3	C22:4	C22:5	C22:6
Uninfected whole BHK21/13S cells	-	-	-	-	3.0	-	-	-	-	-	-	-	-
Rubella virus from BHK21/13S	-	ND	-	-	ND	-	-	-	-	-	-	-	-
PM of RSV (strain Schmidt-Ruppin)-infected CEF	p.e.	-	p.e.	-	4.2	-	-	2.4	-	-	p.e.	-	p.e.
RSV strain Schmidt-Ruppin from CEF	p.e.	-	p.e.	-	6.1	-	-	3.1	-	-	p.e.	-	p.e.

	C22 polyenes	Lignoceric C24:0	C24:1	C24:4	other	saturated	unsaturated mono poly	saturated/ unsaturated	Reference
Uninfected whole BHK21/13S cells	-	-	-	-	-	45.6	37.5 17.0	0.84	Voiland & Bardeletti, 1980
Rubella virus from BHK21/13S	-	-	-	-	8.8 ^q	68.0	18.3 6.6	2.73	Voiland & Bardeletti, 1980
PM of RSV (strain Schmidt-Ruppin)-infected CEF -	-	1.0	1.2	-	8.2 ^r	42.9	42.0 6.9	0.88	Pessin & Glaser, 1980
RSV strain Schmidt-Ruppin from CEF	-	1.6	2.0	-	12.7 ^r	39.3	39.6 8.4	0.82	Pessin & Glaser, 1980

APPENDICES

Appendix 1. The lipid composition of virion envelopes and cell membranes

Appendix 1 is a table summarizing a literary review of the studies evaluating the lipid composition of enveloped viruses, presenting the percent of total phospholipids (PL, mol %) of phosphatidylcholine (PC), phosphatidylethanolamine (PE), phosphatidylserine (PS), phosphatidylinositol (PI), sphingomyelin (SM), lysophosphatidylethanolamine (LPE), lysophosphatidylcholine (LPC), phosphatidic acid (PA), and the cholesterol (CH) to PL molar ratio (CH/PL).

The table includes DNA viruses from the *herpesviridae* family, human cytomegalovirus (HCMV) (Liu et al., 2011), herpes simplex virus type-1 (HSV-1) (van Genderen et al., 1994; van Genderen et al., 1995) and pseudorabies virus (PRV) (Ben-Porat and Kaplan, 1971); the *poxviridae* family, vaccinia virus (VV) (Sodeik et al., 1993; Stern and Dales, 1974); and the *hepadnaviridae* family, hepatitis B virus (HBV) (Satoh et al., 1990); negative-sense single stranded (ss) RNA viruses from the *orthomyxoviridae* family, including Fowl plague virus (FPV) (van Meer and Simons, 1982; van Meer and Simons, 1986) and influenza A virus (InfA) (Blough et al., 1967; Kates et al., 1961; Klenk, Becht, and Rott, 1972; Rothman et al., 1976); the *paramyxoviridae* family, Newcastle disease virus (NDV) (Blough and Lawson, 1968; Munoz-Barroso et al., 1997; Quigley, Rifkin, and Reich, 1971), Sendai virus (Barnes, Pehowich, and Allen, 1987; Blough, 1971; Quigley, Rifkin, and Reich, 1971) and Simian virus 5 (SV5) (Klenk and

Choppin, 1969; Klenk and Choppin, 1970); the *rhabdoviridae* family, vesicular stomatitis virus (VSV) (Kalvodova et al., 2009; Luan, Yang, and Glaser, 1995; McSharry and Wagner, 1971; Pal, Petri, and Wagner, 1980; Patzer et al., 1978; Pessin and Glaser, 1980; van Genderen et al., 1995; van Meer and Simons, 1982; van Meer and Simons, 1986) and rabies virus (Blough, Tiffany, and Aaslestad, 1977; Portoukalian et al., 1977; Schleisinger, Wells, and Hummeler, 1973); and the *bunyaviridae*, Uukuniemi virus (Renkonen et al., 1972); the positive-sense ssRNA from the *flaviviridae* family, hepatitis C virus (HCV) (Merz et al., 2011); and the *togaviridae* family, Semliki Forest virus (SFV) (Kalvodova et al., 2009; Renkonen et al., 1971; Renkonen et al., 1972), Sindbis virus (SIN) (David, 1971; Hirschberg and Robbins, 1974; Pfefferkorn and Salmonhu.H, 1963; Quigley, Rifkin, and Reich, 1971), Rubella virus (Bardeletti and Gautheron, 1976) and Venezuelan equine encephalitis (VEE) (Heydrick, Comer, and Wachter, 1971); the *coronaviridae* mouse hepatitis virus (MHV) (van Genderen et al., 1995) and transmissible gastroenteritis virus (TGEV) (Pike and Garwes, 1977); the *retroviridae* family, human immunodeficiency virus (HIV) (Aloia et al., 1988; Aloia, Tian, and Jensen, 1993; Brugger et al., 2006; Chan et al., 2008; Lorizate et al., 2009), human T-lymphotropic virus (HTLV) (Aloia, Tian, and Jensen, 1993; Crews et al., 1988), murine leukemia virus (MLV) (Chan et al., 2008), feline leukemia virus (FLV) (Crews et al., 1988), Rauscher leukemia virus (RLV) (Crews et al., 1988), Gibbon ape leukemia virus (Crews et al., 1988), simian sarcoma virus (SSV) (Crews et al., 1988), avian leucosis virus (ALV) (Quigley, Rifkin, and Reich, 1971), avian sarcoma virus (ASV) (Quigley, Rifkin, and Reich,

1971) and Rous-Sarcoma virus (RSV) (Pessin and Glaser, 1980; Quigley, Rifkin, and Reich, 1971; Quigley, Rifkin, and Reich, 1972), and equine arteritis virus (EAV) (van Genderen et al., 1995).

When reported in the original research, the cell line and virus strain used to analyze envelope and cell membrane lipid composition are listed. Cells include human foreskin fibroblasts (HFF), baby hamster kidney (BHK-21), rabbit kidney (RK), hamster fibroblasts (Nil2), human hepatoma (huGK-14; Huh7.5), Mardin-Darby canine kidney (MDCV), Mardin-Darby bovine kidney (MDBV), rhesus monkey kidney (MK), embryonated chicken egg (ECE), calf kidney cells (CKC), chicken embryo cells (CEC), chicken embryo fibroblast (CEF), Syrian hamster kidney (HaK), african green monkey (BGM), chicken fibroblast cells (CFC), primary pig kidney (PK/1), secondary adult pig thyroid (APT/2), T-cell derived (H9), monocyte-derived macrophage (MDM), OKT4⁺ leukemic (Hut78), rat embryo fibroblast (REF), mouse fibroblast (L cell), human cervical carcinoma (HeLa) and quail cells (QC).

a, identified as phosphatidylglycerol; *b*, identified as lysolecithin; *c*, identified as acyl-bis(monoacylglycerol) phosphate; *d*, identified as cardiolipin (CL); *e*, identified as lysocephalin; *f*, identified as uncharacterized; *g*, identified as lecithin; *h*, identified as PC and PC O-mixture; *i*, identified as PE and PE O-mixture; *j*, identified as diacylglycerol (17:0-17:0) and phosphatidylglycerol (17:0-17:0); *k*, identified as CL and uncharacterized mixture; *l*, identified as lysobisphosphatidic acid (LBA); *m*, identified as CL and LBA mixture; *n*, identified as cholesterol (CH) and CH-ester mixture; *o*, identified as PE and

plasmogen-PE mixture; *p*, identified as glycerophosphate (GP), cyclic GP, GP glycerol and uncharacterized mixture; *q*, identified as aPC and ePC mixture; *r*, identified as SM and dihydroSM mixture; *s*, identified as a phosphatidylinositol (PI), phosphatidylinositol phosphate (PIP) and phosphatidylinositol bisphosphate (PIP₂) mixture; *t*, identified as ceramide (Cer) and Glu-Cer mixture; *u*, identified as lysophospholipids and uncharacterized mixture; *v*, identified as PA, PG and diphosphatidylglycerol mixture.

Definition of other symbols and abbreviations

-, not reported; ND, not detected; NA, not available; tr, trace; p.e., presented elsewhere as a mixture; PM, plasma membrane; ON, outer nuclear fraction; IN, inner nuclear fraction; INV, intracellular naked virus; EEV, extracellular enveloped virus; and HEP, high egg passage.

Appendix 2. The fatty acid composition of virion envelopes and cell membranes

Appendix 2 is table summarizing a literary review of the studies evaluating the fatty acid composition of enveloped viruses. The table lists the percentage fatty acid of total phospholipids (PLs, unless otherwise indicated), phosphatidylcholine (PC), cardiolipin (CL), phosphatidylethanolamine (PE), phosphatidylserine (PS), phosphatidylinositol (PI), sphingomyelin (SM), the sum of saturated or unsaturated (monoenoic and polyenoic) fatty acids and the ratio of saturated to unsaturated fatty acids.

The table lists the double-stranded (ds) DNA virus hepatitis B (HBV) (Sato et al., 1990); the negative-sense single stranded (ss) RNA virus from the *orthomyxoviridae* family, influenza A virus (Blough, 1971; Blough and Tiffany, 1969; Blough et al., 1967; Kates et al., 1961; Tiffany and Blough, 1969b); the *paramyxoviridae* Newcastle disease virus (NDV) (Munoz-Barroso et al., 1997; Tiffany and Blough, 1969a), Simian virus 5 (SV5) (Klenk and Choppin, 1969; Klenk and Choppin, 1970) and Sendai virus (Barnes, Pehowich, and Allen, 1987; Blough and Lawson, 1968); the *rhabdoviridae* vesicular stomatitis virus (VSV) (Anderson, Daya, and Reeve, 1987; Barnes, Pehowich, and Allen, 1987; Blough and Lawson, 1968; Blough, Tiffany, and Aaslestad, 1977; David, 1971; Fong and Brown, 1978; McSharry and Wagner, 1971; Pal, Petri, and Wagner, 1980; Patzer et al., 1978) and rabies virus (Blough, Tiffany, and Aaslestad, 1977; Portoukalian et al., 1977); the positive-sense ssRNA viruses from the *togaviridae* family, Semliki Forest virus (SFV) (Laine et al., 1972; Renkonen et al., 1971), Sindbis virus (SIN) (David, 1971) and Rubella virus (Voiland and Bardeletti, 1980), and the *retroviridae* Rous-Sarcoma virus (RSV) (Pessin and Glaser, 1980).

When reported in the original research, the cell line and virus strain used to analyze envelope and cellular membrane fatty acid composition are listed. These include human hepatoma cells (huGK-14), embryonated chicken egg (ECE), calf kidney cells (CKC), chicken embryo cells (CEC), baby hamster kidney (BHK-21), rhesus monkey kidney (MK), Syrian hamster kidney (HaK), Mardin-Darby bovine kidney (MDBV), thymidine-kinase deficient mouse

fibroblast (LM-K), mouse fibroblasts (L), hamster fibroblasts (Nil2) or chicken embryo fibroblast (CEF).

a, <0.5% of total; *b*, uncharacterized; *c*, identified as C24:polyenes; *d*, identified as C₁₅-branched + n-C₁₅; *e*, identified as C₁₇-branched + n-C₁₇; *f*, specified as 21:5 n-3; *g*, identified as <C20:4; *h*, identified as C14:0, C14:0 3-OH and C14:0 2-OH mixture; *i*, identified as C16:0 and C16:0 2-OH mixture; *j*, calculated as 65% (inner PE) + 35% (outer PE); *k*, identified as C11:0; *l*, 0.4% C13:0 + 3.4% C15:1 + 2.4% C17:1; *m*, identified as C20-C22 polyenes; *n*, <0.1% of total; *o*, <0.3% of total; *p*, average of 3 experiments (19.0 %, 4.0%, 5.1%); *q*, consists of 2.1% hydroxyacid + 6.7 % C19:0; *r*, consists primarily of C15:0, C17:0, C18:0, C18:3, C20:0, C20:2, C22:4 and C22:6.

Definition of other symbols and abbreviations

-, not reported; ND, not detected; tr, trace; pL, polar lipids; nL, neutral lipids; p.e., presented elsewhere as a mixture; PM, plasma membrane.

References

- Aloia, R. C., Jensen, F. C., Curtain, C. C., Mobley, P. W., and Gordon, L. M. (1988). Lipid-Composition and Fluidity of the Human Immunodeficiency Virus. *Proceedings of the National Academy of Sciences of the United States of America* **85**(3), 900-904.
- Aloia, R. C., Tian, H. R., and Jensen, F. C. (1993). Lipid-Composition and Fluidity of the Human-Immunodeficiency-Virus Envelope and Host-Cell Plasma-Membranes. *Proceedings of the National Academy of Sciences of the United States of America* **90**(11), 5181-5185.
- Anderson, R., Daya, M., and Reeve, J. (1987). An Evaluation of the Contribution of Membrane-Lipids to Protection against Ultraviolet-Radiation. *Biochimica Et Biophysica Acta* **905**(1), 227-230.
- Bardeletti, G., and Gautheron, D. C. (1976). Phospholipid and Cholesterol Composition of Rubella-Virus and Its Host-Cell BHK 21 Grown in Suspension Cultures. *Archives of Virology* **52**(1-2), 19-27.
- Barnes, J. A., Pehowich, D. J., and Allen, T. M. (1987). Characterization of the Phospholipid and Fatty-Acid Composition of Sendai Virus. *Journal of Lipid Research* **28**(2), 130-137.
- Ben-Porat, T., and Kaplan, A. S. (1971). Phospholipid Metabolism of Herpesvirus-Infected and Uninfected Rabbit Kidney Cells. *Virology* **45**(1), 252-&.
- Blough, H. A. (1971). Fatty Acid Composition of Individual Phospholipids of Influenza Virus. *Journal of General Virology* **12**(SEP), 317-&.
- Blough, H. A., and Lawson, D. E. M. (1968). Lipids of Paramyxoviruses - a Comparative Study of Sendai and Newcastle Disease Viruses. *Virology* **36**(2), 286-&.
- Blough, H. A., and Tiffany, J. M. (1969). Incorporation of Branched-Chain Fatty Acids into Myxoviruses. *Proceedings of the National Academy of Sciences of the United States of America* **62**(1), 242-&.
- Blough, H. A., Tiffany, J. M., and Aaslestad, H. G. (1977). Lipids of Rabies Virus and BHK-21 Cell-Membranes. *Journal of Virology* **21**(3), 950-955.
- Blough, H. A., Weinstein, D. B., Lawson, D. E. M., and Kodicek, E. (1967). Effect of Vitamin A on Myxoviruses .2. Alterations in Lipids of Influenza Virus. *Virology* **33**(3), 459-&.
- Brugger, B., Glass, B., Haberkant, P., Leibrecht, I., Wieland, F. T., and Krasslich, H. G. (2006). The HIV lipidome: A raft with an unusual composition. *Proceedings of the National Academy of Sciences of the United States of America* **103**(8), 2641-2646.
- Chan, R., Uchil, P. D., Jin, J., Shui, G. H., Ott, D. E., Mothes, W., and Wenk, M. R. (2008). Retroviruses Human Immunodeficiency Virus and Murine Leukemia Virus Are Enriched in Phosphoinositides. *Journal of Virology* **82**(22), 11228-11238.
- Crews, F. T., McElhaney, M. R., Klepner, C. A., and Lippa, A. S. (1988). Lipids Are Major Components of Human Immunodeficiency Virus (HIV) - Modification of HIV Lipid-Composition, Membrane Organization, and

- Protein Conformation by AI-721. *Drug Development Research* **14**(1), 31-44.
- David, A. E. (1971). Lipid Composition of Sindbis Virus. *Virology* **46**(3), 711-&.
- Fong, B. S., and Brown, J. C. (1978). Asymmetric Distribution of Phosphatidylethanolamine Fatty Acyl Chains in Membrane of Vesicular Stomatitis-Virus. *Biochimica Et Biophysica Acta* **510**(2), 230-241.
- Heydrick, F. P., Comer, J. E., and Wachter, R. F. (1971). Phospholipid Composition of Venezuelan Equine Encephalitis Virus. *Journal of Virology* **7**(5), 642-&.
- Hirschberg, C., and Robbins, P. W. (1974). Glycolipids and Phospholipids of Sindbis Virus and Their Relation to Lipids of Host-Cell Plasma-Membrane. *Virology* **61**(2), 602-608.
- Kalvodova, L., Sampaio, J. L., Cordo, S., Ejsing, C. S., Shevchenko, A., and Simons, K. (2009). The Lipidomes of Vesicular Stomatitis Virus, Semliki Forest Virus, and the Host Plasma Membrane Analyzed by Quantitative Shotgun Mass Spectrometry. *Journal of Virology* **83**(16), 7996-8003.
- Kates, M., Tyrrell, D. A. J., James, A. T., and Allison, A. C. (1961). Lipids of Influenza Virus and Their Relation to Those of Host Cell. *Biochimica Et Biophysica Acta* **52**(3), 455-&.
- Klenk, H. D., Becht, H., and Rott, R. (1972). Structure of Influenza-Virus Envelope. *Virology* **47**(3), 579-&.
- Klenk, H. D., and Choppin, P. W. (1969). Lipids of Plasma Membranes of Monkey and Hamster Kidney Cells and of Parainfluenza Virions Grown in These Cells. *Virology* **38**(2), 255-&.
- Klenk, H. D., and Choppin, P. W. (1970). Plasma Membrane Lipids and Parainfluenza Virus Assembly. *Virology* **40**(4), 939-&.
- Laine, R., Kettunen, M. L., Gahmberg, C. G., Renkonen, O., and Kaariain.L (1972). Fatty Chains of Different Lipid Classes of Semliki Forest Virus and Host-Cell Membranes. *Journal of Virology* **10**(3), 433-+.
- Liu, S. T. H., Sharon-Friling, R., Ivanova, P., Milne, S. B., Myers, D. S., Rabinowitz, J. D., Brown, H. A., and Shenk, T. (2011). Synaptic vesicle-like lipidome of human cytomegalovirus virions reveals a role for SNARE machinery in virion egress. *Proceedings of the National Academy of Sciences of the United States of America* **108**(31), 12869-12874.
- Lorizate, M., Brugger, B., Akiyama, H., Glass, B., Muller, B., Anderluh, G., Wieland, F. T., and Krausslich, H. G. (2009). Probing HIV-1 Membrane Liquid Order by Laurdan Staining Reveals Producer Cell-dependent Differences. *Journal of Biological Chemistry* **284**(33), 22238-22247.
- Luan, P., Yang, L., and Glaser, M. (1995). Formation of Membrane Domains Created during the Budding of Vesicular Stomatitis-Virus - a Model for Selective Lipid and Protein Sorting in Biological-Membranes. *Biochemistry* **34**(31), 9874-9883.
- McSharry, J. J., and Wagner, R. R. (1971). Lipid Composition of Purified Vesicular Stomatitis Viruses. *Journal of Virology* **7**(1), 59-&.
- Merz, A., Long, G., Hiet, M. S., Brugger, B., Chlanda, P., Andre, P., Wieland, F., Krijnse-Locker, J., and Bartenschlager, R. (2011). Biochemical and

- Morphological Properties of Hepatitis C Virus Particles and Determination of Their Lipidome. *Journal of Biological Chemistry* **286**(4), 3018-3032.
- Munoz-Barroso, I., Cobaleda, C., Zhadan, G., Shnyrov, V., and Villar, E. (1997). Dynamic properties of Newcastle Disease Virus envelope and their relations with viral hemagglutinin-neuraminidase membrane glycoprotein. *Biochimica Et Biophysica Acta-Biomembranes* **1327**(1), 17-31.
- Pal, R., Petri, W. A., and Wagner, R. R. (1980). Alteration of the Membrane Lipid-Composition and Infectivity of Vesicular Stomatitis-Virus by Growth in a Chinese-Hamster Ovary Cell Sterol Mutant and in Lipid-Supplemented Baby Hamster-Kidney Clone 21 Cells. *Journal of Biological Chemistry* **255**(16), 7688-7693.
- Patzer, E. J., Moore, N. F., Barenholz, Y., Shaw, J. M., and Wagner, R. R. (1978). Lipid Organization of the Membrane of Vesicular Stomatitis-Virus. *Journal of Biological Chemistry* **253**(13), 4544-4550.
- Pessin, J. E., and Glaser, M. (1980). Budding of Rous-Sarcoma Virus and Vesicular Stomatitis-Virus from Localized Lipid Regions in the Plasma-Membrane of Chicken-Embryo Fibroblasts. *Journal of Biological Chemistry* **255**(19), 9044-9050.
- Pfefferkorn, E. R., and Salmonhu.H (1963). Purification and Partial Chemical Analysis of Sindbis Virus. *Virology* **20**(3), 433-&.
- Pike, B. V., and Garwes, D. J. (1977). Lipids of Transmissible Gastroenteritis Virus and Their Relation to Those of 2 Different Host-Cells. *Journal of General Virology* **34**(MAR), 531-535.
- Portoukalian, J., Bugand, M., Zwingelstein, G., and Precausta, P. (1977). Comparison of Lipid-Composition of Rabies Virus Propagated in Nil-2 Cells Maintained in Monolayer Versus Spinner Culture. *Biochimica Et Biophysica Acta* **489**(1), 106-118.
- Quigley, J. P., Rifkin, D. B., and Reich, E. (1971). Phospholipid Composition of Rous Sarcoma Virus, Host Cell Membranes and Other Enveloped Rna Viruses. *Virology* **46**(1), 106-+.
- Quigley, J. P., Rifkin, D. B., and Reich, E. (1972). Lipid Studies of Rous-Sarcoma Virus and Host-Cell Membranes. *Virology* **50**(2), 550-&.
- Renkonen, O., Kaaraine.L, Simons, K., and Gahmberg, C. G. (1971). Lipid Class Composition of Semliki Forest Virus and of Plasma Membranes of Host Cells. *Virology* **46**(2), 318-+.
- Renkonen, O., Kaariain.L, Petterss.R, and Okerblom, N. (1972). Phospholipid Composition of Uukuniemi Virus, a Non-Cubical Tick-Borne Arbovirus. *Virology* **50**(3), 899-901.
- Rothman, J. E., Tsai, D. K., Dawidowicz, E. A., and Lenard, J. (1976). Transbilayer Phospholipid Asymmetry and Its Maintenance in Membrane of Influenza-Virus. *Biochemistry* **15**(11), 2361-2370.
- Satoh, O., Umeda, M., Imai, H., Tunoo, H., and Inoue, K. (1990). Lipid-Composition of Hepatitis-B Virus Surface-Antigen Particles and the Particle-Producing Human Hepatoma-Cell Lines. *Journal of Lipid Research* **31**(7), 1293-1300.

- Schleisinger, H. R., Wells, H. J., and Hummeler, K. (1973). Comparison of Lipids of Intracellular and Extracellular Rabies Viruses. *Journal of Virology* **12**(5), 1028-1030.
- Sodeik, B., Doms, R. W., Ericsson, M., Hiller, G., Machamer, C. E., Vanthof, W., Vanmeer, G., Moss, B., and Griffiths, G. (1993). Assembly of Vaccinia Virus - Role of the Intermediate Compartment between the Endoplasmic-Reticulum and the Golgi Stacks. *Journal of Cell Biology* **121**(3), 521-541.
- Stern, W., and Dales, S. (1974). Biogenesis of Vaccinia - Concerning the Origin of Envelope Phospholipids. *Virology* **62**(2), 293-306.
- Tiffany, J. M., and Blough, H. A. (1969a). Fatty Acid Composition of 3 Strains of Newcastle Disease Virus. *Virology* **37**(3), 492-&.
- Tiffany, J. M., and Blough, H. A. (1969b). Myxovirus Envelope Proteins - a Directing Influence on Fatty Acids of Membrane Lipids. *Science* **163**(3867), 573-574.
- van Genderen, I. L., Brandimarti, R., Torrissi, M. R., Campadelli, G., and Vanmeer, G. (1994). The Phospholipid-Composition of Extracellular Herpes-Simplex Virions Differs from That of Host-Cell Nuclei. *Virology* **200**(2), 831-836.
- van Genderen, I. L., Godeke, G. J., Rottier, P. J. M., and Vanmeer, G. (1995). The Phospholipid-Composition of Enveloped Viruses Depends on the Intracellular Membrane through Which They Bud. *Biochemical Society Transactions* **23**(3), 523-526.
- van Meer, G., and Simons, K. (1982). Viruses Budding from Either the Apical or the Basolateral Plasma-Membrane Domain of Mdk Cells Have Unique Phospholipid Compositions. *Embo Journal* **1**(7), 847-852.
- van Meer, G., and Simons, K. (1986). The Function of Tight Junctions in Maintaining Differences in Lipid-Composition between the Apical and the Basolateral Cell-Surface Domains of Mdk Cells. *Embo Journal* **5**(7), 1455-1464.
- Voiland, A., and Bardeletti, G. (1980). Fatty acid composition of rubella virus and BHK21/13S infected cells. *Arch Virol* **64**(4), 319-28.